PREDICTING CHANGES TO OYSTER LIFESPANS IN A WARMING CLIMATE USING GEOHISTORICAL RECORDS

A Dissertation

Presented to the Faculty of the Graduate School

of Cornell University

In Partial Fulfillment of the Requirements for the Degree of

Doctor of Philosophy

by

Stephen Robert Durham

August 2017

PREDICTING CHANGES TO OYSTER LIFESPANS IN A WARMING CLIMATE USING GEOHISTORICAL RECORDS

Stephen Robert Durham, Ph. D.

Cornell University 2017

The threat of anthropogenic impacts to nature has been growing for centuries and has reached a point where many scientists believe we are causing a sixth mass extinction and that status quo carbon emission levels will lead to dangerous climate change. This realization has sparked increasing efforts to restore and conserve ecosystems and the biodiversity they support. Given that the history of anthropogenic environmental deterioration long predates most efforts at monitoring or record keeping, however, there has been increasing appreciation of the conservation value of geohistorical records—sources of data on the characteristics of species, communities and ecosystems in the distant past, such as fossils—though their use in conservation and restoration practice is still uncommon.

This dissertation aimed to assess the perspectives on geohistorical data among oyster restoration professionals in the United States, and then to produce a case study of conservation-relevant geohistorical data for the eastern oyster, *Crassostrea virginica*, one of the most ecologically and economically important shellfish species in North America. Chapter 1 demonstrates the overall interest among oyster restoration professionals in geohistorical data and identifies commonalities among the data types needed for oyster restoration and those available from geohistorical records. Chapter 2 develops a method for estimating lifespans of oysters using Mg/Ca profiles from laser ablation-inductively coupled plasma-mass spectrometry analysis of their shells.

Finally, Chapter 3 uses this method to estimate lifespan differences between modern *C. virginica* populations in South Carolina and fossil counterparts that inhabited a warmer interglacial period in the past. It is shown that lifespans for *C. virginica* were shorter in the warmer climate, and that these differences were consistent with predictions of the metabolic theory of ecology. We end by using the relationship between oyster lifespan and temperature to suggest possible oyster lifespan reductions under future warming scenarios based on current climate model predictions and highlighting some implications of these results for managing, conserving, and restoring oyster populations for the future.

BIOGRAPHICAL SKETCH

Stephen Durham is originally from Guilford, Connecticut. His interest in paleontology started at a young age, nurtured by *Jurassic Park* movies and visits to the Yale Peabody Museum of Natural History in nearby New Haven. He began pursuing this interest seriously starting as an undergraduate at Dartmouth College. He volunteered as a research assistant at the Peabody Museum in the summer of 2006, worked as an assistant in geobiology and paleontology labs at Dartmouth in 2007 and 2008, and was accepted to a National Science Foundation Research Experiences for Undergraduates program in biodiversity conservation at the University of North Carolina Wilmington in 2008. That summer was formative for Stephen and set his career interests on a path towards the young field of conservation paleobiology.

Soon after graduating from Dartmouth College in 2009 with a B.A. in biology, Stephen moved to Ithaca, NY to work at the Paleontological Research Institution (PRI), and began his doctoral program at Cornell University the following year, in the Fall of 2011. While at Cornell, Stephen was awarded a National Science Foundation Graduate Research Fellowship and participated in several projects in addition to his dissertation work, including surveying ecologists' perspectives on long-term data, investigating the application of benthic index metrics to mollusk assemblages, and studying the impact of the Deepwater Horizon oil spill on oyster body sizes in Louisiana using buried oyster shells. Throughout his time in Ithaca, Stephen contributed to outreach and collections work at PRI and its Museum of the Earth, giving lectures, helping members of the public identify and learn about fossils, and assisting with curating and rehousing some of the institution's fossil invertebrate collection, which is among the largest in the United States.

This work is dedicated to my family, who has always believed in me and encouraged me to pursue my interest in paleontology. It is especially in memory of my grandparents, whose pride in their grandson was one of my surest sources of inspiration and confidence throughout my youth and early adulthood. I miss you.

ACKNOWLEDGMENTS

I gratefully acknowledge financial support during my doctoral research program from the Cornell Graduate Fellowship, two teaching assistantships through the Department of Earth and Atmospheric Sciences, a Graduate Research Fellowship from the National Science Foundation, and a contract position working on the NSF-funded PaleoNiches project at the Paleontological Research Institution. I received research support during my PhD program from the Paleontological Research Institution, the Geological Society of America, the Paleontological Society, Conchologists of America, and the Atkinson Center's Sustainable Biodiversity Fund to help me complete my dissertation and other research endeavors. Travel assistance to attend a field course and present my research at professional meetings was generously provided by the Mario Einaudi Center for International Studies, the Cornell Graduate School, the Department of Earth and Atmospheric Sciences S. Kaufman Travel Fund, and the Geological Society of America.

My sincere gratitude also goes to the many people who, through roles large and small, made it possible for me to complete this project. First, I would like to thank the members of my committee: Gregory Dietl, Warren Allmon, Matthew Hare, David Gillikin, and John Wehmiller. Your patient support, encouragement, and generosity with your time and knowledge have been essential to getting me across the finish line and giving me the experience and training to successfully do scientific research. I look forward to continuing to learn from your examples as I take my next steps on the road from student to colleague.

I would especially like to thank Warren Allmon, who through his leadership at the Paleontological Research Institution gave me many opportunities beyond those available to the typical student of paleontology, and Gregory Dietl, whose mentorship

and friendship since my undergraduate days have been a profound influence on my life and its direction. In particular, thank you Greg for always leading by example, and teaching me that sometimes “there ain’t no way but the hard way, so get used to it.” I cannot thank you both enough for your unflagging belief in my potential and the doors you have opened for me.

I also gratefully acknowledge the help of Linda Ivany of Syracuse University and her students Emily Judd and David Moss, who welcomed me into the lab on multiple occasions and trained me to mill oyster samples for stable isotope analysis, and John Handley for multiple discussions of data analysis and for inviting me to Rochester, NY to give a talk at the Rochester Academy of Science. I also would not have gotten this far in my academic career if not for the mentorship of Patricia Kelley and Christy Visaggi and her husband Simon Kline during and after the summer of 2008. Thank you for encouraging me to pursue my PhD.

Thanks is also due to the other friends and students who have supported me through my graduate career. These include several current and former staff members at the Paleontological Research Institution: Leon Apgar, Maureen Bickley, Kelly Cronin, Brian Gollands, Richard Kissel, Alicia Michael, Paula Mikkelsen, Judith Nagel-Myers, Leslie Skibinski, and Alex Wall. Also, thank you Jonathan Hendricks, for your good humor, mentorship, understanding, and encouragement starting in my very first summer at PRI and continuing through my eighth. To the other graduate students who have overlapped with me in our small paleo program—Ursula Smith, Mary Kosloski, Dana Friend, Jansen Smith, and Brendan Anderson—thanks for sharing the journey. Working with you on projects from fieldwork to organizing symposia made the last six years much more enjoyable. To Carlie Peitsch, PRI’s post-doc for the last two years, I always enjoyed our discussions. Your enthusiasm for science is infectious and, even if you didn’t know it, was just what I needed on some

days. I am also grateful for the many talented students and PRI volunteers that helped out with tasks in the lab from sample processing and data collection to fieldwork, for this and other projects, including Neil Adams, Peter Balzani, Eleanor Bent, Thomas Butler, Chenga Drury, Daniel Farthing, Maddie Gaetano, Julia Hoshino, Jessica LaMay, Whitney Lapic, Limin Li, Emma Mosier, Taina Moynihan, Barbara Skoblick, Colin Sweeney, William Tifft, Annalee Tweitmann, and Michael Zelko.

Finally, finishing my doctorate would not have been possible without my amazing family. To my parents, who raised me to work hard, and did the same to give me every opportunity to succeed, thank you. Kelley and Chris, thanks for being caring and inspirational siblings, and to my twin brother Tim—whose coding prowess saved days of my life during this project—thank you for being a valued sounding board and best friend literally from the beginning. Last but certainly not least, thank you to my beautiful wife Beth, who supported me in every sense of the word through the last six years. I know it hasn't always been easy, but thank you for indulging my frequent late nights, working weekends, absences for conferences and fieldwork, and often stressed and grumpy moods.

TABLE OF CONTENTS

LIST OF FIGURES

LIST OF TABLES

CHAPTER 1

PERSPECTIVES ON GEOHISTORICAL DATA AMONG OYSTER RESTORATION PROFESSIONALS IN THE UNITED STATES[1]

Abstract

Conservation paleobiology aims to apply data from geohistorical records, such as fossils and their associated sediments, to the conservation of biodiversity and ecosystem services. Integrating geohistorical data into conservation/restoration practice, however, has proved difficult. To better understand how geohistorical data can be more effectively integrated into the conservation/restoration of an ecologically, economically, and culturally important group—oysters—a web-based survey was conducted to assess the awareness and understanding of geohistorical data and perspectives on their use in restoration among oyster researchers and restoration practitioners in the United States. The 97 survey responses not only demonstrate overall willingness to use geohistorical data in oyster restoration but also highlight knowledge gaps. For instance, although many respondents understood some uses for geohistorical data, e.g., providing baseline information, few respondents mentioned others, such as reconstructing historical ranges of variation of ecosystem attributes. Respondents were also generally not aware of the full range of restoration metrics that can be measured from geohistorical records. The responses further suggested how geohistorical information might both reinforce and expand the information currently available to oyster restoration professionals. For instance, only half of respondents indicated that their baseline information predates the 20th century, but geohistorical

[1] Reprinted from *Journal of Shellfish Research*, Vol. 34 (2), Durham, S. R., Dietl, G. P., Perspectives on geohistorical data among oyster restoration professionals in the United States, Pages 227-239, Copyright (2015), with permission. Available from http://dx.doi.org/10.2983/035.034.0204.

records of oysters can provide data on timescales ranging from decades to millennia. Finally, it is argued that to raise awareness of this underutilized information and address respondents' doubts about the completeness, precision/accuracy, and relevance of geohistorical data in a rapidly changing, human-dominated world, increased collaboration between conservation paleobiologists and conservation/restoration scientists is needed.

1.1 Introduction

Conservation paleobiology is a rapidly expanding field (Dietl & Flessa 2011; CPW 2012) that aims to provide conservation scientists and restoration practitioners with information on species, communities, and ecosystems from geohistorical records—"the organic remains, biogeochemical signals, and associated sediments of the geological record" (NRC 2005, p. 11). These records are the only source of data on what happens to living organisms under environmental conditions the Earth is not experiencing today (Dietl & Flessa 2011; Dietl et al. 2015). This information is useful for reconstructing biotic responses to many kinds of disturbance in the past, such as climate change, that can serve as "natural experiments" to improve both understanding of species, community, or ecosystem dynamics and predictions of future responses to similar disturbances (Willis et al. 2010a, see Dietl et al. 2015 for other valuable uses).

Despite their promise, however, the application of geohistorical data in many conservation and restoration fields is still rare, and paleobiologists have found it challenging to integrate their data into the conservation toolkit (Willis & Birks 2006; Flessa 2009; Davies et al. 2014). For instance, doubts about the completeness or accuracy of geohistorical data are common among scientists in other fields (NRC 2005; Willis & Birks 2006; Dietl & Flessa 2011), and often stems from

misunderstandings and lack of familiarity with geohistorical data (Dietl & Flessa 2011).

With the goal of promoting the integration of geohistorical data into conservation and restoration, a survey was designed to assess what researchers and restoration professionals working with a declining but ecologically, economically, and culturally important group—oysters—know and do not know about geohistorical data, and how they could be used for restoration. The purpose of asking practitioners directly about the applications of geohistorical data to oyster restoration was to raise awareness of their availability, better understand how they might best contribute to restoration, and evaluate the potential for collaboration between oyster restoration practitioners and conservation paleobiologists.

Why oysters?

The survey was designed for oyster researchers and restoration professionals because oysters form important estuarine habitats that also have significant economic and cultural value through the goods and services they offer human society, such as provision of food, habitat, and foraging ground for other economically important species, shoreline stabilization, and support of fisheries and the cultural heritage of coastal communities (e.g., Kurlansky 2006; Grabowski & Peterson 2007). Oyster reef habitats are also declining globally. Beck et al. (2011) used data from sources such as surveys, harvest records, and aerial photographs—some dating back 130 years—to determine that oyster reefs are at less than 10% of their historical abundance in 63% of ecoregions worldwide, and less than 1% of their historical abundance in 28% of ecoregions. Primary causes of this decline include pollution, disease, and overharvesting by humans (Beck et al. 2011). Finally, oyster reefs produce geohistorical records that can yield useful information for their restoration and

management. These records develop as death assemblages beneath the surface of the living oyster reef, growing as each new generation of oysters settles on the structure and as sediment and the shells of dead oysters accumulate over centuries (Hargis & Haven 1999).

1.2 Materials and methods

To evaluate the knowledge of restoration professionals about geohistorical data and perspectives on their use in oyster restoration a web survey was hosted on the servers of the Paleontological Research Institution in Ithaca, NY, from June 20 to July 31, 2013 that was composed of 17 questions focused on professional background, perspectives on geohistorical data, and general demographic information (Appendix 1.1). The first category included questions about oyster species of interest, which states and countries respondents' work affected, how many years of experience respondents had in the field, the publications respondents used for their work, the details of their specific work/research related to oyster restoration, and how respondents defined restoration success. The second category included questions about respondents' use of baseline information—the "reference conditions against which current changes can be assessed" (Dietl & Flessa 2011, p. 30)—and their opinions about geohistorical information. Respondents were asked to identify the baselines they used in their work according to recognized Chesapeake Bay cultural periods—prehuman, before 8000 BCE; hunter-gatherer, 8000 BCE to 1200 CE; agricultural, 1200 CE to 1600 CE; market colonial establishment, 1600 CE to 1700 CE; market-colonial development, 1700 CE to 1900 CE; global market 1, 1900 CE to 1950 CE; and/or global market 2, 1950 CE to present (Lotze et al. 2006). Other questions in this section assessed respondents awareness of the universal metrics (UM), universal environmental variables (UEV), and restoration variables (RV) (NOAA FOHC 2013)

that can be assessed in the past using geohistorical records, determined if and how they would use such data, and identified applications of geohistorical data to oyster restoration of which respondents were already aware. Finally, the questions in the third category asked respondents for information about their race, sex, education, job type, and workplace. A variety of question types were used, from multiple-choice to short, written responses. See Appendix 1.2 for detailed information on how the survey population was selected, the survey was administered, responses were categorized, and the data were analyzed. A table of the survey responses and categorizations can be downloaded at http://hdl.handle.net/ 1813/39030.

1.3 Results

Demographics

During the survey period, 97 responses were received (out of 396 professionals contacted; 26% response rate) from researchers and restoration professionals in the United States. Respondents were 37% female and 60% male (n = 36 and n = 58, respectively; three respondents skipped the question) and most self-identified as white (92%, n = 89). Asian and Hispanic respondents were each 2% (n = 2) of the response population (one other and three nonresponses were 1% and 3%, respectively). A majority of respondents self-identify as researchers (56%, n = 54) and/or fisheries/resource managers (27%, n = 26) with 8% (n = 8) working as policy developers and 27% (n = 26) responding other (one respondent skipped the question; responses to this question were not mutually exclusive). Most work in academia (41%, n = 40) and state or federal government agencies (41%, n = 40), and 19% (n = 18) work for non-governmental organizations. Others work in environmental consulting (3%, n = 3), industry (2%, n = 2), and other (2%, n = 2; one respondent skipped the question; responses to this question were not mutually exclusive). Respondents overall

were very well educated, with 75% holding graduate degrees (52%, n = 50 doctorates and 23%, n = 22 masters degrees) and 23% (n = 22) with bachelors degrees.

Professional background

Respondents worked predominantly with one or more of three oyster species: *Crassostrea virginica* (Gmelin, 1791; 90%, n = 87), *Ostrea lurida* (Carpenter, 1864; 12%, n = 12), and *Crassostrea gigas* (Thunberg, 1793; 5%, n = 5). The respondents' work affected 22 coastal states in four regions [Figure A1.2-1; 36%, n = 35 Northeast; 45%, n = 44 Southeast; 9%, n = 9 Northwest and Southwest; and 9%, n = 9 work affected multiple regions; see Appendix 1.2 for a description of response categorization; regions are based on the National Oceanic and Atmospheric Administration (NOAA) Damage Assessment, Remediation, and Restoration Program (DARRP); NOAA ORR 2013]. Respondents' years of experience (binned into 5-y intervals) ranged from less than 5 years (14%, n = 14) to more than 25 years (21%, n = 20). The most common experience level among respondents was 5–10 years (25%, n = 24). The majority of respondents' work involved research (62%, n = 60) and restoration (58%, n = 56) with many fewer respondents involved in administration (7%, n=7), aquaculture (3%, n=3), and education (3%, n = 3); responses to this question were not mutually exclusive; see Appendix 1.2 for a description of response categorization.

When asked to name at least three publications they read and publish in, 78% (n = 286) of publications mentioned in responses were peer-reviewed books and journals and 22% (n = 81) were non-peer-reviewed gray literature, such as technical reports and conference proceedings from government and nongovernmental organizations (see Appendix 1.2 for a description of response categorization). The most frequently mentioned source was the Journal of Shellfish Research (58%, n =

56). When respondents were asked to define restoration success, responses varied in emphasis and detail, but the majority required structural criteria to be met (86%, n = 83), meaning aspects of the physical organization of the habitat, such as oyster density and reef areal extent (Burrows et al. 2005). Fewer responses mentioned goals related to functional aspects of oyster reef habitat (36%, n = 35), the ecological processes and products the habitat supports and provides, such as water filtration and foraging and breeding grounds for associated fauna (Burrows et al. 2005). Few respondents discussed success criteria involving ecosystem services (11%, n = 11)—predominantly functional characteristics but with explicit mention of their benefits to human society—or stakeholder consensus (4%, n = 4)—the ability of a restoration project to satisfy multiple interests (Figure 1.1; see Appendix 1.2 for a description of response categorization).

Perspectives on geohistorical data

When asked the ages of baselines that apply to their work, 15% (n = 15) of respondents indicated that baselines do not apply to their work, and of those who did identify baseline ages, 53% (n = 43) did not predate 1900 CE, and 90% (n = 73) date to 1700 CE or younger. Only 4% (n = 3) of respondents who use baselines use information that predates all human influence (>8000 y ago; Figure 1.2).

Overall, respondents indicated that geohistorical data have potential to inform oyster restoration projects: the majority of respondents said geohistorical data can be sometimes informative for oyster restoration (61%, n = 59), and 36% (n = 35) said they can be very informative for oyster restoration. No respondents thought that geohistorical data are not informative for oyster restoration, although 3% (n = 3) were unsure (Figure 1.3A).

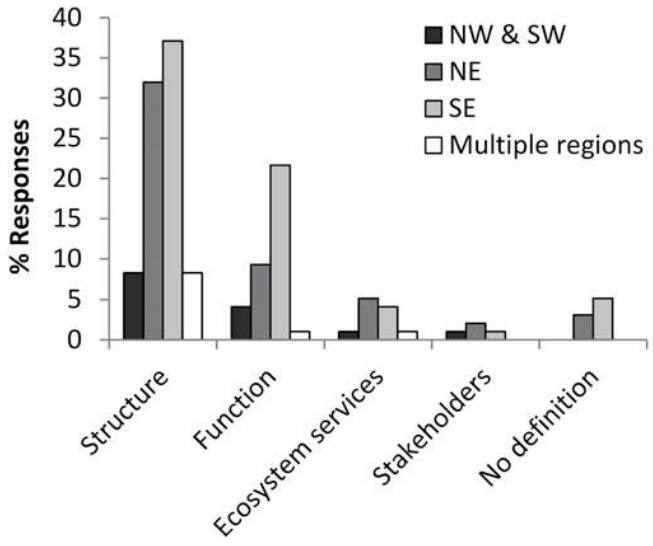

Figure 1.1 | Percent of respondents from each DARRP region that mentioned each category of success criteria in their answers to Question 7. Respectively, structure and function categories refer to oyster reef habitat characteristics that make up the physical organization of the habitat, such as oyster abundance and density and water currents, and the ecological processes and products the habitat supports and provides, such as water filtration and foraging and breeding grounds for associated fauna (sensu Burrows et al. 2005). The ecosystem services category encompassed responses explicitly mentioning habitat characteristics benefitting human society. The stakeholder consensus category refers to responses that included incorporation of multiple interests as a success criterion for restoration.

Most short-answer responses were exclusively positive about the use of geohistorical data in oyster restoration (55%, n = 53) or expressed both positive and negative views on their utility (22%, n = 21). Fewer replies solely discussed reasons that geohistorical data may not be useful in oyster restoration (18%, n = 17; Figure 1.3B; two responses were neither positive nor negative, and four respondents did not answer the question). A majority of respondents recognized the potential of geohistorical data to improve baselines (76%, n = 74) and understanding of the historical range of variation (HRV)—"the variation of ecological characteristics and processes over scales of time and space that are appropriate for a given management

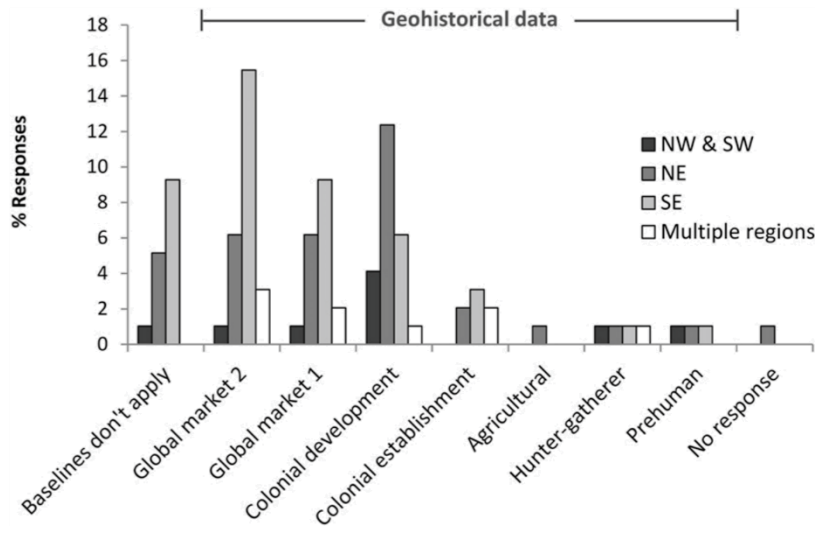

Figure 1.2 | Earliest baseline used by respondents from each DARRP region. Age bins are cultural periods for Chesapeake Bay, MD defined by Lotze et al. (2006): prehuman, before 8000 BCE; hunter-gatherer, 8000 BCE to 1200 CE; agricultural, 1200 CE to 1600 CE; market-colonial establishment, 1600 CE to 1700 CE; market-colonial development, 1700 CE to 1900 CE; global market 1, 1900 CE to 1950 CE; and global market 2, 1950 CE to present. The line above the histogram emphasizes that various types of geohistorical records are capable of providing baseline information of almost any age.

application" (Wiens et al. 2012, p. 5)—of oyster reef ecosystems (9%, n=9). Some respondents further discussed the applicability of geohistorical baselines to planning and managing restoration projects (37%, n = 36), such as selecting appropriate sites and improving targets and success criteria, or to conducting basic research into the responses of oyster reefs to past environmental conditions and disturbances (9%, n = 9) or anthropogenic and nonanthropogenic change (8%, n = 8; Figure 1.3C). The majority of negative comments (n = 38) expressed concern that the world has changed so significantly that geohistorical data are less relevant to current conservation and restoration (87%, n = 33), and 16% (n = 6) discussed reservations about the completeness and biased nature of geohistorical records (Figure 1.3C; one respondent mentioned both criticisms; see Appendix 1.2 for a description of response categorization).

Most respondents were unaware of successful applications of geohistorical data to oyster restoration practice (64%, n = 62), but 35% (n = 34) of respondents said that they did know of successful case studies. Interestingly, of those responses that were sufficiently detailed (68%, n = 23), only about half discussed data that were geohistorical (57%, n = 13). Others discussed nongeohistorical data such as time-

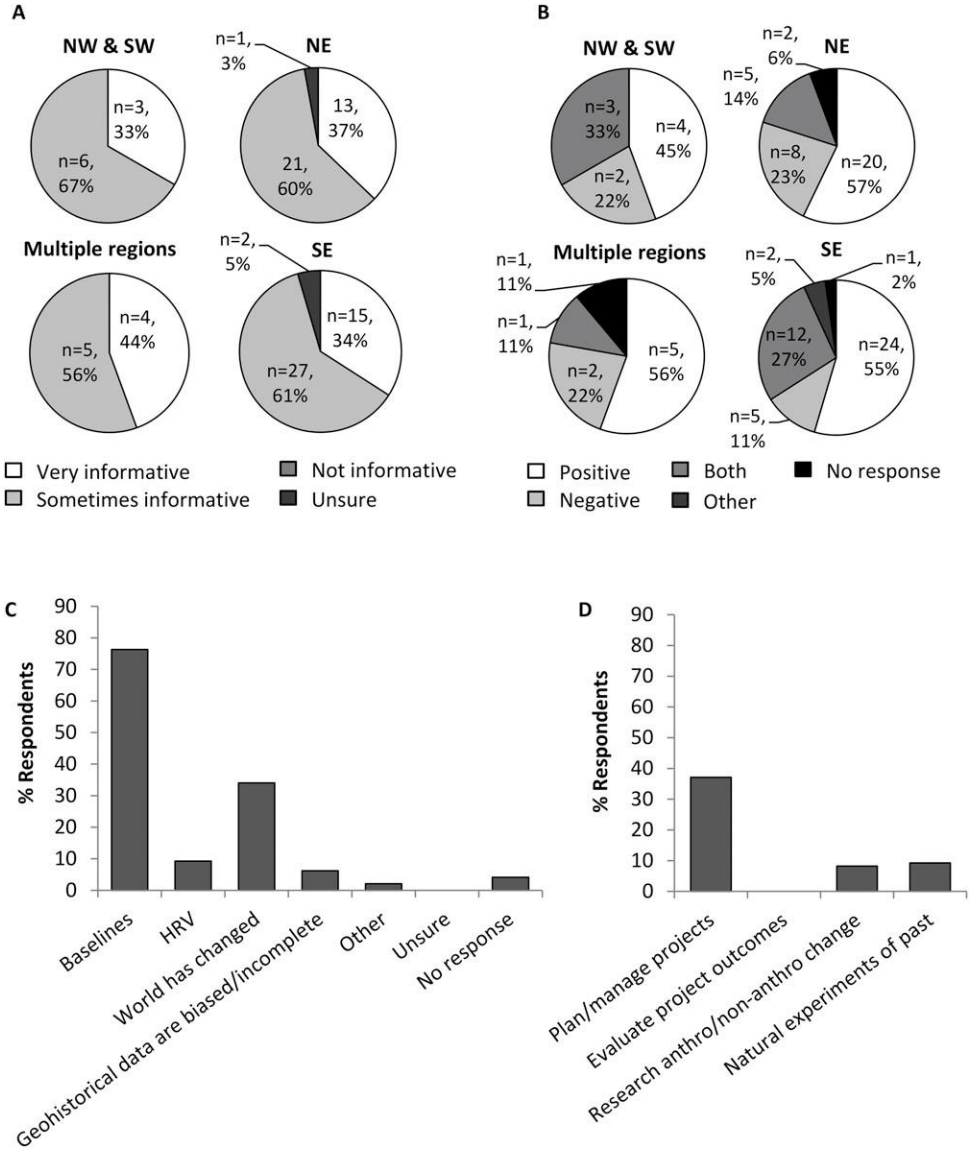

Figure 1.3 | What respondents think about applying geohistorical data in restoration: (A) responses to Question 9a by DARRP region; (B) character of responses (positive, negative, etc.) to Question 9b by DARRP region; (C) percent of responses to Question 9b falling into each general response category; (D) percent of positive responses to Question 9b that discussed one or more specific categories of uses for geohistorical data.

series data from monitoring live populations or historical records such as fisheries landings data or photographs (see Appendix 1.2 for a description of response categorization)

Most respondents were aware that paleobiologists can measure universal oyster restoration metrics such as reef areal dimension (62%, n = 60), oyster size-frequency distribution (58%, n = 56), and oyster density (51%, n = 49) using death assemblages and fossils. Many respondents also chose unsure (33%, n = 32), however, and fewer chose other restoration variables and universal environmental variables such as predation and competition (29%, n = 28), dissolved oxygen (20%, n = 19), salinity (44%, n = 43), and water temperature (41%, n = 40; Figure 1.4; NOAA FOHC 2013). Most respondents chose four to six metrics (59%, n = 44) and 84% (n = 63) selected six or fewer.

When asked how they would use geohistorical data on the NOAA metrics if they had them, most respondents indicated they would use the data to produce baseline information (73%, n = 71) or investigate the HRV of various aspects of oyster reef ecosystems (5%, n = 5). Many respondents would use baseline and/or HRV information to plan or manage restoration projects (41%, n = 40) or to investigate the responses of oyster reefs to past environmental conditions and disturbances (10%, n = 10) or to anthropogenic and nonanthropogenic change (3%, n = 3; Figure 1.5; see Appendix 1.2 for a description of response categorization). One respondent (1%) discussed using geohistorical data to retroactively evaluate the status of “completed” restoration projects.

1.3 Discussion

The largely positive reactions to the use of geohistorical data in oyster restoration by professionals who vary in experience, expertise, and geographic location indicate willingness to use these data in the oyster restoration community. Further, qualitative comparisons of responses between DARRP regions show similar patterns for all questions (e.g., Figures 1.1–1.4), except those with obvious

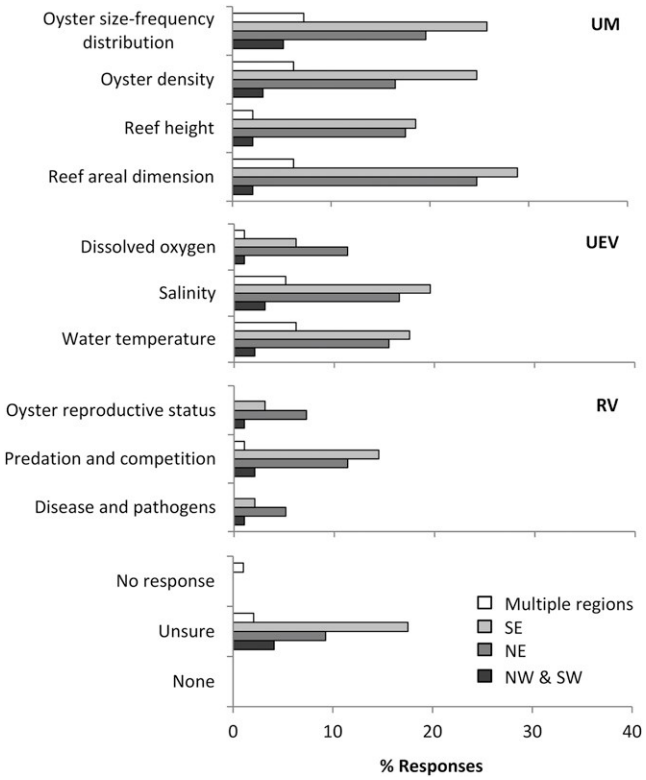

Figure 1.4 | Percent of responses to Question 11a by DARRP region. Data are grouped based on the universal metrics (UM), universal environmental variables (UEV), and restoration variables (RV) defined by NOAA FOHC (2013).

regional differences, such as oyster species of interest, suggesting that geohistorical data could be integrated to benefit restoration in all oyster-producing regions of the United States. Finally, the responses indicate where collaborations might begin by

highlighting information gaps that paleobiologists could potentially fill and demonstrating the knowledge within the oyster restoration community about geohistorical data and methods.

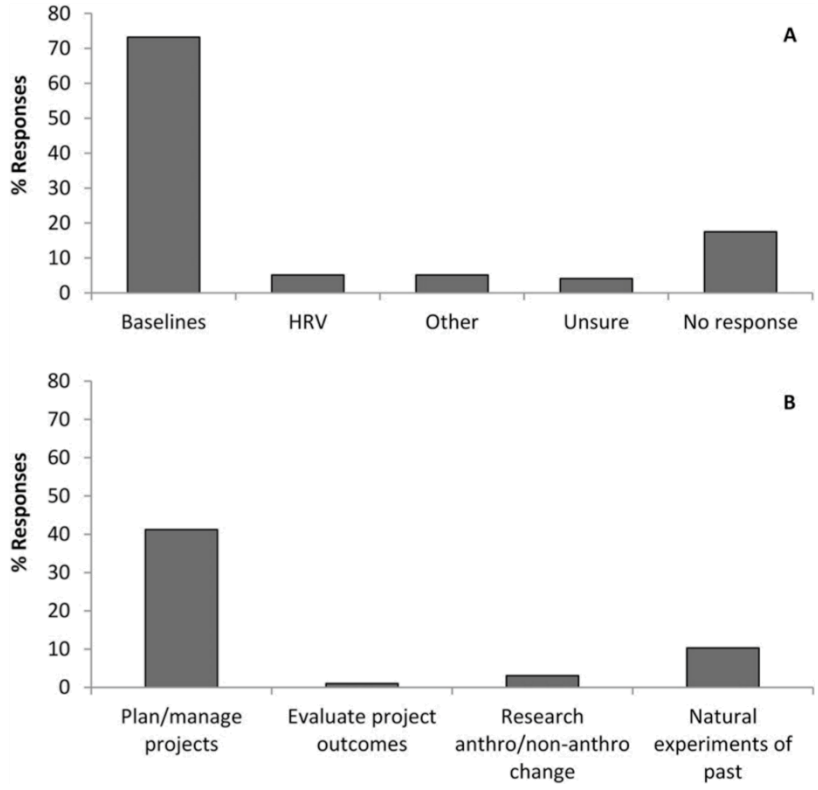

Figure 1.5 | Percent of responses to Question 11b falling into (A) general and (B) specific categories of uses for geohistorical data.

What oyster restoration professionals knew about geohistorical data

Despite the overall positive reactions to the potential of geohistorical data, the short-answer responses revealed a broader spectrum of views on their utility. Some responses expressed skepticism about the use of geohistorical data, for instance: "I'm not sure how geohistorical data on these [NOAA metrics] would affect a present-day project, except as interesting history." Others were enthusiastic: "[Geohistorical data] are extremely important. Although most coastal systems are far from their pristine

states, much can be gained by understanding the physical and chemical changes in an area through time, and relating those to population dynamics of a species." Responses like these illustrate the familiarity of respondents with geohistorical data and concepts, and if/how respondents would apply them in their own work. For instance, the majority of respondents (76%, Figure 1.3C) valued the baseline information accessible from geohistorical records, but only 68% (n = 50) of respondents that mentioned baselines also discussed an application for them, possibly indicating uncertainty about what exactly to do with geohistorical data.

The responses that discussed using geohistorical data to reconstruct the HRV of oyster reef ecosystem attributes indicated a more sophisticated understanding of geohistorical applications relative to those who only mentioned baseline concepts, because those respondents necessarily thought beyond the use of geohistorical data for describing environments at single points in the past. In fact, the HRV itself is a target in management and restoration of certain systems, such as forests, floodplains, and rivers (Wiens et al. 2012). Geohistorical data could help oyster restoration professionals develop similar HRV-based restoration and monitoring criteria for the dynamic estuarine habitats of oysters.

What oyster restoration professionals did not know about geohistorical data

Some responses also suggested that geohistorical data are generally not well understood by many oyster restoration professionals. For instance, geohistorical data were misidentified in several descriptions of applied studies (10 out of 23 respondents that gave sufficiently detailed answers discussed uses of historical accounts or survey records although the term geohistorical record was defined on the survey page). Furthermore, more NOAA metrics are often measurable from geohistorical records than the four to six selected by most respondents. Many universal metrics can either be

measured from preserved shells, such as size, or inferred from them, such as degree of clustering and general growing environment on reefs (Kent 1992). Proxies also can be used to determine universal environmental variables in the past, such as temperature (e.g., Schöne et al. 2004), and restoration variables, such as predation (Alexander & Dietl 2003; Walker 2007).

Further, the most common criticism of the utility of geohistorical data for restoration—that the world has changed permanently, so information from the past is of limited utility for restoration—takes for granted the extent to which the current knowledge of the degraded state of most oyster habitats depends on studies of the history of these systems. For instance, studies have demonstrated historical degradation in terms of structural characteristics such as abundance and body size (e.g., Kirby & Miller 2005; Beck et al. 2011) and functional characteristics such as water filtration (e.g., zu Ermgassen et al. 2013). Historical and geohistorical studies can also identify the long-term causes of change and their relative importance (Jackson et al. 2001; Kirby & Miller 2005). Thus, geohistorical data can provide critical information for identifying and managing the causes and biotic consequences of environmental change.

A second criticism, that geohistorical records are biased and incomplete, is a common reason for distrusting geohistorical data (NRC 2005; Jackson & Hobbs 2009; Dietl & Flessa 2011; Davies et al. 2014). It is true that geohistorical records do not exist for every habitat type in all time periods, and they tend to be biased in both content—for instance organisms with mineralized hard parts such as vertebrates and mollusks are generally better represented than soft-bodied taxa—and distribution in space and time, due to unevenness in the preservation of sedimentary environments and sampling effort by paleobiologists (NRC 2005). Even relatively sparse records can be informative, however, if they are well situated geographically and temporally to

answer specific questions (NRC 2005; Dietl & Flessa 2011). Sometimes, certain types of bias can even be advantageous. For instance, time averaging of geohistorical records—the accumulation of bones, shells, and other material of different ages into the same sediment layer over time by biotic and abiotic burial and mixing processes, such as bioturbation and waves—can "smooth out" much of the variability characteristic of many short-term observational or experimental "snapshots" that can obscure long-term trends (NRC 2005). Finally, the variety of dating techniques available and their continuously improving accuracy and precision have correspondingly improved the ability of conservation paleobiologists to detect and account for biases, such as time averaging, and to constrain the ages of fossil material (NRC 2005).

How conservation paleobiology can help

Although baseline information extending back a few centuries could be useful, survey responses indicated that precolonial baseline information is rarely used in oyster restoration (Figure 1.2). Most written accounts and other historical records in the United States are no more than two or three centuries old, but conservation paleobiologists are capable of providing additional local geohistorical baseline information for restoration practitioners on centennial to millennial timescales. Increasing the available information for baseline development may also help restoration professionals justify project success criteria. For instance, many respondents noted that a "successfully" restored reef should be similar to nearby natural reefs. Using natural living reefs to define restoration targets, however, leaves projects susceptible to the shifting baseline syndrome (Pauly 1995)—the masking of long-term environmental degradation by the tendency of each generation to consider the world they inhabit as "natural". Given the pervasive influences of stressors such as

eutrophication and coastal development on estuaries over decadal to centennial timescales, natural reefs surviving in an area may still be degraded relative to those that lived before the restoration. Evaluation of geohistorical records produced on matching time scales (decades or centuries), such as the death assemblages beneath natural oyster reefs, can offer insights into recent changes in reef structure and function to avoid shifting baselines and help restoration professionals either justify restoration targets based on living populations or indicate when such criteria are insufficient.

By improving baselines, documenting HRV in ecosystem attributes, and informing predictions of species, community, and ecosystem responses to change, geohistorical data can help restoration professionals adopt realistic success criteria. For instance, respondents overwhelmingly reported using structural criteria such as oyster density, reef height and areal extent, and oyster size frequency distributions to evaluate project outcomes, and both baseline values and HRV can be measured for these metrics using geohistorical records such as fossil reefs (e.g., reef area, Carbotte et al. 2004). Other success criteria, including functional characteristics and the values of related ecosystem services, can often be estimated geohistorically using proxies or the death assemblages themselves (e.g., filtration rate; zu Ermgassen et al. 2013). Geohistorical data may also help build stakeholder consensus for restoration criteria by informing narratives of degradation and shifting baselines to clarify the ecological and environmental changes that must be addressed by the restoration.

Finally, although many restored reefs may be too young to have produced a geohistorical record and some techniques, such as planting loose cultch, could make it difficult to identify shells produced by restored reefs, comparing restoration metrics between restored reefs and nearby natural death assemblages could help evaluate whether the restoration achieved its goals. This application was mentioned by only one

respondent, but given that monitoring has often been neglected in oyster restoration projects—for instance, only 43% of restoration datasets collected between 1990 and 2007 from over 1000 Chesapeake Bay oyster bars included both restoration and monitoring (Kennedy et al. 2011)—retroactive evaluation of restored reefs to help compensate for the scarcity of adequate monitoring and assessment is a use for geohistorical data that deserves further attention.

When it works: a restoration case study involving geohistorical data

As the survey results suggest, and others have learned from experience (Willis & Birks 2006; Flessa 2009; Davies et al. 2014), integrating geohistorical data into conservation and restoration practice is challenging. The few case studies that exist, however, demonstrate that geohistorical data can provide useful information for the planning and implementation of restoration projects. For instance, Volety et al. (2009) conducted a study of extant and past oyster reef distributions in southwest Florida and their influence on coastal geomorphology during the mid-to-late Holocene, in support of the Comprehensive Everglades Restoration Plan, a massive, ongoing water management and restoration program in southern Florida that began in 2000. Oysters are important indicators of past and present water quality in southwest Florida, so "understanding the historical, pre-modification distribution of oyster buildups is a critical baseline from which to guide Everglades freshwater flow restoration" (Volety et al. 2009, p. 11).

Using 26 cores from the Ten Thousand Islands (TTI) and the Everglades Estuarine Tract (EET), Volety et al. (2009) compared the stratigraphy of these two regions, and based on lithology and faunal assemblages, including fossil oyster reefs, they determined that the TTI and EET experienced very different geological histories. These geohistorical data allowed Volety et al. (2009) to understand past hydrological

conditions before widespread freshwater channelization and flood control, and are helping to facilitate a coordinated restoration of freshwater flow and oyster populations in the TTI and EET.

This case study is noteworthy because of the influence geohistorical data have had on restoration practices within the Comprehensive Everglades Restoration Plan. Similar benefits are likely possible for most restoration projects that consider geohistorical data, but making their use in conservation and restoration more common will depend on closer collaboration among conservation paleobiologists and restoration professionals so that integration challenges can be addressed and geohistorical data can begin contributing directly to restoration practices (Willis et al. 2007; Flessa 2009).

Evidence of shifting paradigms

Responses to the survey may reflect some shifting paradigms in oyster restoration and the restoration field in general. For instance, "restoration to deliver ecosystem services" is an emerging paradigm in ecological restoration (Suding 2011) that has influenced oyster restoration. Historically, oyster restoration maintained one ecosystem service—the fishery. In the past two decades, however, appreciation for the ecological importance of oysters and the variety of ecosystem services they provide has increased (Coen & Luckenbach 2000; Grabowski & Peterson 2007). This priority shift may be reflected in the survey results by the small number of respondents that explicitly mentioned the ability of a restored reef to support harvest as a success criterion (4%, n = 4) relative to those that mentioned functional habitat characteristics (36%, n = 35) and ecosystem services other than harvest (9%, n = 9).

Interestingly, only three responses were indicative of another emerging paradigm in ecological restoration: "restoration to ensure resilience" (Suding 2011).

One respondent wrote that "a restored population is one that exhibits resistance and resilience to disturbance." Another said, "restoration is going to depend on the ability of species to… adapt to not only current conditions, but ever changing conditions." Resilience—the amount of disturbance a system can accommodate before exhibiting changes in fundamental characteristics, such as structure and function (Walker et al. 2004)—has the potential to make restoration sustainable through disturbances (Suding 2011), making it an important goal for coastal restoration, including oyster restoration, in the face of climate change (Bernhardt & Leslie 2013). Similarly, the capacity of species to evolve and adapt to disturbance is becoming an important focus of restoration, both because of its influence on resilience (e.g., Sgrò et al. 2011) and an increasing recognition that contemporary evolution often happens on short enough timescales to affect restoration outcomes (Ashley et al. 2003).

Whereas successful oyster restoration used to mean increasing harvest yields for the fishing industry, the broader ecological processes and services that characterize the newer restoration paradigms are more difficult to quantify and operationalize (Coen & Luckenbach 2000; Suding 2011; Bernhardt & Leslie 2013). Geohistorical data can offer insights into both resilience (Willis et al. 2010a; CPW 2012; Dietl et al. 2015) and evolutionary adaptation (Willis & MacDonald 2011; Dietl 2013) to disturbances, which are increasingly important goals for ecological restoration in the face of growing anthropogenic pressures, such as climate change.

1.4 Conclusions

This survey approach obtained valuable information about how collaboration between conservation paleobiologists and oyster restoration professionals can progress. In particular, the positive responses about the utility of geohistorical data suggested that collaborations would be productive, and responses that detailed

restoration professionals' reservations surrounding geohistorical data will help focus future education and outreach.

Collaboration between paleobiologists and restoration professionals must be the first step in overcoming the knowledge gaps and misunderstandings apparent from the survey responses (Willis et al. 2007; Flessa 2009). Crossing disciplinary boundaries will take time and patience, but the potential rewards are great. Geohistorical data can improve baselines for many structural and functional oyster ecosystem attributes and be used to reconstruct their HRV, which can in turn be applied to: (1) examine responses of oysters to environmental changes in the past and thus improve understanding of how oysters may respond to similar environmental changes in the future; (2) investigate oyster responses to anthropogenic disturbance, including both ecological and evolutionary responses; (3) develop more detailed information on the local history of oyster populations to inform decisions about restoration project designs and goals; and (4) evaluate "completed" restoration projects relative to their stated objectives and retroactively compare between restoration projects, even in the absence of sufficient monitoring.

Acknowledgments

We thank M. Hare and W. Allmon for their helpful comments on drafts of the manuscript. We also thank B. Gollands for help with technical aspects of hosting the survey on the Paleontological Research Institution server, and M. Aldridge for help navigating the Cornell University Institutional Review Board process. Finally, we also thank T. Butler, K. Durham, T. Durham, L. Eierman, D. Friend, C. Rose, J. Smith, and J. Spector, whose survey testing and comments improved the final version. This study is based on work supported by a National Science Foundation Graduate Research Fellowship to S. Durham (NSF DGE 1144153).

CHAPTER 2

RAPID DETERMINATION OF OYSTER LIFESPANS AND GROWTH RATES USING LA-ICP-MS LINE SCANS OF SHELL MG/CA RATIOS[2]

Abstract

Retrospective estimates of life-history traits (e.g., growth rate, lifespan, phenology) of mollusks are valuable data for a number of fields, including paleontology, archaeology, and fisheries science. The best option for obtaining these data for species such as oysters that lack reliable morphological indicators of annual accretionary growth (e.g., growth lines) is to use time consuming and expensive stable isotope analyses. However, laser ablation analyses of Mg/Ca are faster and less expensive than stable isotope analyses, and although several studies have shown Mg/Ca ratios in bivalve shells do not reflect water temperature, there is often a weak correlation that may allow annual cycles to be detected. Here, we explore the utility of line scan analyses of Mg/Ca ratios using laser ablation-inductively coupled plasma-mass spectrometry (LA-ICP-MS) as a more rapid and less expensive method for obtaining ontogenetic age estimates of mollusk shells than more traditional oxygen stable isotope analyses. We tested this method by measuring Mg/Ca ratios from 21 fossil and modern specimens of two oyster species, *Crassostrea virginica* and *Magallana gigas* (formerly *Crassostrea gigas*), collected across a wide geographic area along the coast of the United States. We compared Mg/Ca growth profiles with either known lifespans or with growth characteristics estimated from $\delta^{18}O$ profiles.

[2] Reprinted from *Palaeogeography, Palaeoclimatology, Palaeoecology*, in press, Durham, S. R., Gillikin, D. P., Goodwin, D. H., Dietl, G. P., Rapid determination of oyster lifespans and growth rates using LA-ICP-MS line scans of shell Mg/Ca ratios, Copyright (2017), with permission from Elsevier. Available from https://doi.org/10.1016/j.palaeo.2017.06.013.

These analyses showed that Mg/Ca profiles from laser ablation analyses reliably reproduced the annual features of the more widely used $\delta^{18}O$ profiles. In total, 97% (n = 102) of all seasonal peaks and troughs, including both those from the $\delta^{18}O$ profiles and the expected patterns in the shells of known age, were detectable in the Mg/Ca profiles. We conclude that laser ablation analysis of Mg/Ca ratios is a rapid and cost effective alternative to stable isotope analysis for retrospective estimation of the growth characteristics of oysters and potentially other taxa with shells lacking reliable annual morphological features.

2.1 Introduction

Determination of life-history traits (e.g., growth rate, lifespan, phenology) of mollusks is an important task for researchers in a number of fields, including paleontology, archaeology, fisheries science, and marine biology for myriad research purposes, such as studies of species' responses to environmental change and evaluations of the fishing behaviors of past human populations (Kirby et al. 1998; Andrus & Crowe 2000; Kirby 2001; Mann et al. 2009; Harding et al. 2010; Lartaud et al. 2010; Andrus 2011; Thomas 2015; Rick et al. 2016; Savarese et al. 2016; Twaddle et al. 2016). This information is usually gathered by analyzing shells or parts of shells exhibiting regular accretionary growth, the characteristics of which often display seasonal periodicities. For instance, shell growth rates and lifespans of the venerid clam *Mercenaria mercenaria* can be estimated by counting growth bands in polished shell cross-sections under a microscope (e.g., Jones et al., 1989). However, determination of life-history traits from the shells of other mollusk groups that in many cases lack simple-to-interpret morphological features, such as oysters, is more challenging.

A variety of methods has been used to estimate the growth characteristics of oyster shells retrospectively, such as tracking cohorts using population size-frequency distributions (e.g., Mann et al., 2009), counting growth lines or undulations of the surface of the resilifer (hinge plate) of left valves (Custer & Doms 1990; Richardson et al. 1993; Kirby et al. 1998; Johnson et al. 2007; Kraeuter et al. 2007; Fan et al. 2011; Savarese et al. 2016), cathodoluminescence imaging to reveal seasonal Mn^{2+} variations (Langlet et al. 2006; Lartaud et al. 2010), and sclerochemical analyses (sensu Gröcke & Gillikin 2008) of stable isotopes or trace elements in the shell (e.g., Bougeois et al., 2014; Fan et al., 2011; Goodwin et al., 2013, 2010; Kirby et al., 1998; Surge and Lohmann, 2008). Although some studies have found that morphological features of oyster shells, such as growth lines or undulations on the surface of the resilifer, are annual (e.g., Fan et al., 2011; Kirby et al., 1998; Kraeuter et al., 2007), others have found that estimation of oyster growth characteristics from such features is inaccurate (e.g., Andrus and Crowe, 2000; Hong et al., 1995; Surge et al., 2001). By contrast, geochemical analyses are arguably the most accurate and reliable methods of retrospective age determination, but can be expensive and time consuming. For instance, the ^{18}O:^{16}O ratio in shell carbonate, expressed as $\delta^{18}O$ values, is a common and trusted method of estimating a wide range of growth-related characteristics from mollusk shells (e.g., size-at-age relationships, lifespan, growth rate, and season of recruitment or death), including oysters (Kirby et al. 1998; Goodwin et al. 2010, 2013). Stable oxygen isotope analysis, however, often requires hours of sample collection followed by a lengthy analysis procedure (or weeks of waiting for results if the samples are sent to a commercial lab) and analyzing large numbers of specimens is usually cost-prohibitive.

An alternative geochemical proxy, whose applications to assessing mollusk growth characteristics have yet to be widely explored, is the magnesium to calcium

(Mg/Ca) ratio in shell carbonate. The Mg/Ca ratio of biogenic minerals has been intensely studied as a temperature proxy in a variety of calcifying taxa (e.g., sponges: (Swart et al. 2002; Fabre & Lathuiliere 2007); corals: (Watanabe et al. 2001; Sherwood et al. 2005); and mollusks: (Dodd 1965; Klein et al. 1996; Vander Putten et al. 1999; Wanamaker Jr et al. 2008; Freitas et al. 2012), including oysters (Surge & Lohmann 2008; Mouchi et al. 2013; Bougeois et al. 2014, 2016; Tynan et al. in press). Although evidence shows that Mg/Ca ratios are not reliable paleothermometers in the case of mollusks due to vital effects associated with Mg^{2+} incorporation into shell carbonate (coefficient of determination typically <0.5; e.g., Lorrain et al. 2005; Surge & Lohmann 2008; Wanamaker Jr et al. 2008; Poulain et al. 2015; Graniero et al. 2017), the sensitivity of Mg/Ca ratios to seasonally correlated environmental forcings or shell microstructural patterns (e.g., Marali et al. in press) may be sufficient as an alternative to $\delta^{18}O$ values for estimation of growth characteristics such as lifespan and growth rate (e.g., Richardson et al. 2004, 2005; Bougeois et al. 2014; but see Graniero et al. 2017).

The major potential advantage of using Mg/Ca ratios for estimating growth characteristics is that they can be analyzed more rapidly and are less expensive than $\delta^{18}O$ analyses. Mg/Ca ratios are most often measured using laser ablation-inductively coupled plasma-mass spectrometry (LA-ICP-MS). This technique uses one of several kinds of lasers to ablate small amounts of shell that are then swept into an ICP-MS by a stream of helium and/or argon (Durrant & Ward 2005). Trace element concentrations are measured in real time and, depending on the scan speed and specimen size, entire specimens can be analyzed in minutes. Our experiences suggest that around 10–15 specimens can be analyzed in one day by LA-ICP-MS, and per-specimen costs are currently approximately 1/10 those of stable isotope analysis.

Here, we test Mg/Ca ratios measured from LA-ICP-MS line scans as a rapid and cost-effective method of estimating growth characteristics of oysters. We used the eastern oyster, *Crassostrea virginica*, because they lack reliable morphological indicators of annual accretionary growth (e.g., distinct annual growth lines; Hong et al. 1995; Andrus & Crowe 2000; Surge et al. 2001), leaving few alternatives to sclerochemical approaches for obtaining accurate retrospective estimates of life-history traits from their shells. Oysters are also a group for which growth data are frequently needed—information on growth rates and population dynamics of *C. virginica*, mostly gathered from cohort analyses using size-frequency distributions, is important for the conservation, restoration, and management of oyster populations (e.g., Harding et al. 2010; Levinton et al. 2013; Baggett et al. 2015). Accurate estimates of oyster lifespans and growth rates from geochemical analyses of shells could complement these data by, for instance, allowing verification of cohort identifications and making rapid and inexpensive investigations of growth characteristics in the past possible through retrospective analysis of dead shells.

2.2 Material and methods

Sixteen *C. virginica* specimens were analyzed for both Mg/Ca ratios and $\delta^{18}O$ values: one live-collected specimen from Connecticut; one live-collected specimen and six modern dead-collected shells from South Carolina; seven fossil shells from the Pleistocene Canepatch Formation in South Carolina; and one modern dead-collected specimen from Louisiana (Table 2.1). Additionally, Mg/Ca was analyzed from three hatchery-reared specimens of known age (nine months; Dec. to Aug.) from North Carolina (Table 2.1). Together, these specimens represent wide geographic and temporal range, including most of the North American portion of *C. virginica*'s geographic range (Gulf of St. Lawrence

Table 2.1
Information on the specimens used in the study.

Species	Collection location	Collection type	Specimen ID	Collection date	Mg/Ca evaluation	Resilifer height (mm)	Resilifer width (mm)	Valve height (mm)	Valve width (mm)	*n* ($\delta^{18}O$, $\delta^{13}C$)	*n* (Mg/Ca)	Mean $\delta^{18}O$ (VPDB)	SD $\delta^{18}O$ (VPDB)	Mean $\delta^{13}C$ (VPDB)	SD $\delta^{13}C$ (VPDB)	Mean Mg/Ca (mmol/mol)	SD Mg/Ca (mmol/mol)
Crassostrea virginica	Madison, Connecticut	Live	CT-L-01	9/6/2014	$\delta^{18}O$, $\delta^{13}C$	29	37	177	89	36	1326	-2.71	0.81	-1.51	0.27	1.91	0.61
	Grand Terre Island, Louisiana	Dead	LA-D-01	1/25/2013	$\delta^{18}O$, $\delta^{13}C$	10	13	64	38	13	225	-2.65	0.95	-3.05	0.72	2.71	1.14
	Watie's Island, South Carolina	Dead	SC-D-01	2/20/2014	$\delta^{18}O$, $\delta^{13}C$	23	16	118	36	40	494	-1.41	1.01	-1.73	0.69	2.31	0.69
		Dead	SC-D-02	2/20/2014	$\delta^{18}O$, $\delta^{13}C$	13	13	59	29	15	274	-1.42	0.98	-2.11	0.42	2.44	0.80
		Dead	SC-D-03	2/20/2014	$\delta^{18}O$, $\delta^{13}C$	27	14	120	28	38	648	-1.75	1.12	-2.05	0.51	3.01	0.93
	Cherry Grove, South Carolina	Dead	SC-D-04	5/16/2015	$\delta^{18}O$, $\delta^{13}C$	37	22	127	49	52	905	-0.44	1.19	-0.94	0.27	2.90	0.89
		Dead	SC-D-05	5/16/2015	$\delta^{18}O$, $\delta^{13}C$	31	21	92	41	41	705	-0.50	1.07	-0.99	0.27	2.52	0.75
		Dead	SC-D-06	5/16/2015	$\delta^{18}O$, $\delta^{13}C$	15	12	63	28	20	352	-0.42	0.72	-1.12	0.29	1.53	0.62
	North Myrtle Beach, South Carolina	Fossil	SC-F-01	7/20/2013	$\delta^{18}O$, $\delta^{13}C$	14	10	61	24	18	328	-0.24	1.12	-0.45	0.81	2.00	0.47
		Fossil	SC-F-02	7/20/2013	$\delta^{18}O$, $\delta^{13}C$	28	15	111	31	37	634	-0.64	0.93	0.15	0.62	2.15	0.51
		Fossil	SC-F-03	7/21/2013	$\delta^{18}O$, $\delta^{13}C$	22	16	127	41	30	529	-0.34	1.14	-0.48	0.54	3.00	0.92
		Fossil	SC-F-04	7/21/2013	$\delta^{18}O$, $\delta^{13}C$	35	17	130	41	54	912	-0.07	1.22	-0.11	0.37	3.01	1.06
		Fossil	SC-F-05	7/21/2013	$\delta^{18}O$, $\delta^{13}C$	20	14	88	27	26	470	-1.03	0.98	-0.76	0.49	2.72	0.90
		Fossil	SC-F-06	7/21/2013	$\delta^{18}O$, $\delta^{13}C$	14	10	75	30	15	587	-0.64	1.16	-0.20	0.24	1.93	0.76
		Fossil	SC-F-07	7/21/2013	$\delta^{18}O$, $\delta^{13}C$	11	15	53	25	13	252	-0.36	1.06	-0.78	0.49	2.68	0.78
	Watie's Island, South Carolina	Live	SC-L-01	2/20/2014	$\delta^{18}O$, $\delta^{13}C$	18	12	80	26	27	390	-0.71	0.90	-1.87	0.57	2.71	0.62
	Jarrett Bay, North Carolina	Live	NC-L-01	8/7/2015	Known age	12	20	89	61	n/a	245	n/a	n/a	n/a	n/a	2.51	0.96
		Live	NC-L-02	8/7/2015	Known age	14	22	94	57	n/a	312	n/a	n/a	n/a	n/a	2.87	0.93
		Live	NC-L-03	8/7/2015	Known age	14	21	88	62	n/a	250	n/a	n/a	n/a	n/a	2.88	1.23
Magallana gigas	San Francisco Bay, California	Live	CA-L-01	7/28/2006	$\delta^{18}O$, $\delta^{13}C$			126	42	39	2352	-2.08	1.24	-4.79	1.04	0.80	0.21
		Live	CA-L-02	7/28/2006	$\delta^{18}O$, $\delta^{13}C$			71	39	45	1598	-2.01	0.93	-4.95	1.13	0.48	0.18

to the Gulf of Mexico; Carriker & Gaffney 1996) and approximately 350,000 years of geological history. We also tested the method on two specimens of *Magallana gigas* (formerly *Crassostrea gigas*, see Salvi & Mariottini 2016), collected from San Francisco Bay in California, in order to examine the utility of Mg/Ca profiles in a different oyster taxon, as well as the performance of the method in a location with lower-amplitude seasonal temperature variability (Figure 2.1). Stable isotope and LA-ICP-MS analyses for the California specimens were performed as part of previous work by a subset of the authors, but the Mg/Ca data were not previously reported (see Goodwin et al. 2010, 2013 for details). Thus, our analysis was designed to incorporate environmental and geographic variability, representing

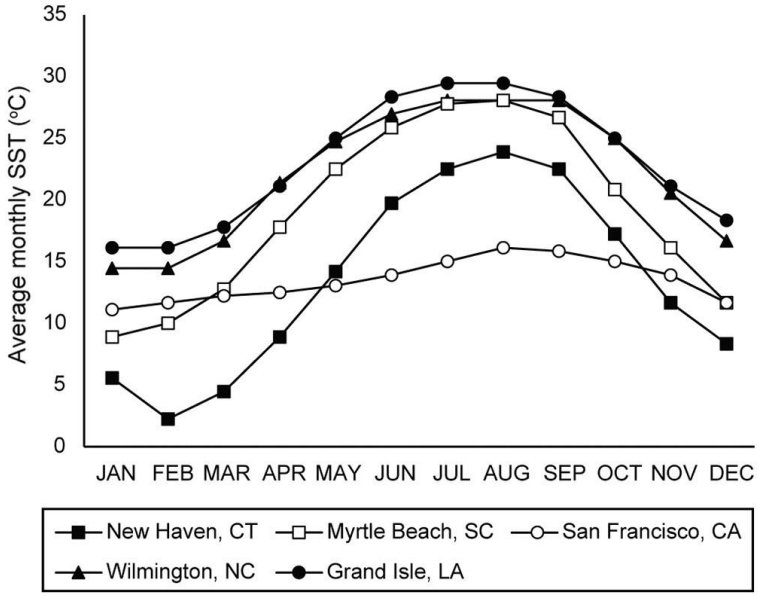

Figure 2.1 | Plots of average monthly temperature for areas near our sample locations. Data are from the National Oceanic and Atmospheric Administration (NOAA) Coastal Water Temperature Guide (https://www.nodc.noaa.gov/dsdt/cwtg/all_meanT.html; Accessed 11/3/2016). Data are averages of several years to decades, depending on the duration of monitoring records at each location, as reported by NOAA. CT = Connecticut; NC = North Carolina; SC = South Carolina; LA = Louisiana; CA = California.

coastal intertidal marsh environments with a variety of seasonal patterns in temperature (Figure 2.1) from four different ecoregions (Virginian, Carolinian, Northern Gulf of Mexico, and Northern California; sensu Spalding et al. 2007).

We followed Goodwin et al. (2010, 2013) in analyzing cross-sections of the hinge plate (resilifer) of the left valve for each specimen (Figure 2.2). All specimens were prepared by cutting a cross-section through the resilifer parallel to the direction of growth and perpendicular to the anteroposterior axis with a low-speed

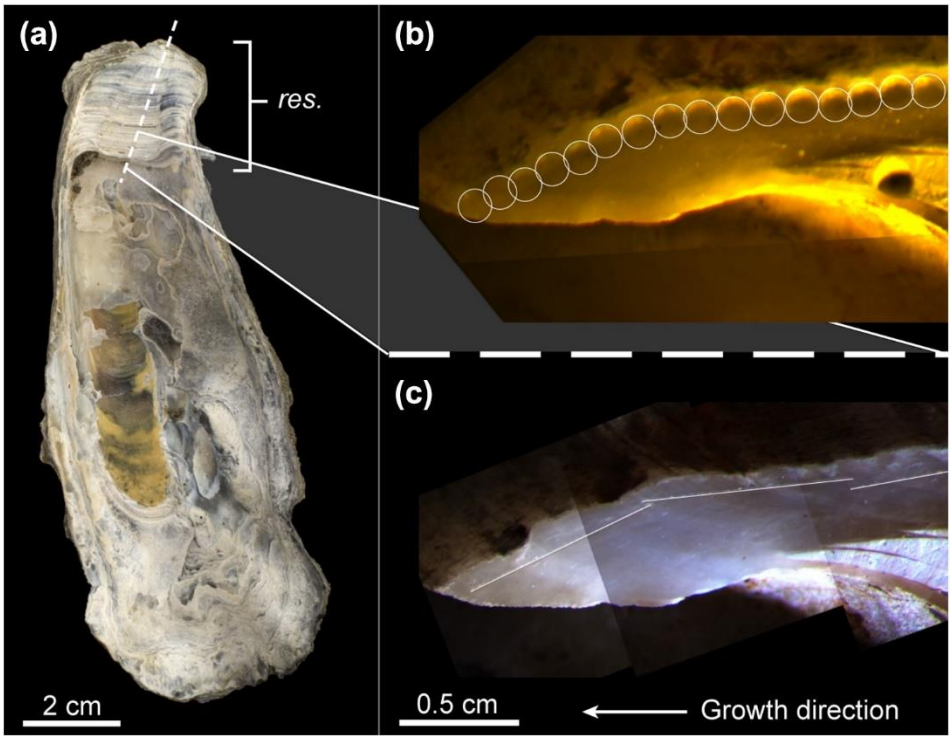

Figure 2.2 | (a) Images of a fossil *C. virginica* left valve highlighting the resilifer (res.) and the plane cut to produce the cross-sections used in our geochemical analyses. The composite images on the right show the growth margin of the resilifer cross-section for specimen SC-F-04. The foliated calcite layer at the resilifer surface was sampled with (b) a micromill and (c) by laser ablation. Micromill point samples (b) and laser lines (c) are highlighted with circles and lines, respectively. Images for panels (b) and (c) were taken with different cameras and lighting. Note: the 0.5 cm scale bar and growth direction label apply to both (b) and (c).

diamond saw (Figure 2.2a). One of the resilifer halves of each specimen was then polished using a series of fine-grit silicon carbide sandpapers (up to P4000 grit) and mounted on a glass slide such that the polished cross-section was horizontal and level.

Following O'Neil & Gillikin (2014), each specimen was analyzed for Mg/Ca ratios by ablating overlapping line patterns along the foliated calcite layer of each resilifer (avoiding the alternating chalky and foliated calcite mineralogy that characterizes the umbonal cavity), parallel to the direction of growth (Figure 2.2c), with a CETAC LSX-213 frequency quintupled Nd:YAG laser ablation unit (λ = 213 nm) connected to a Perkin Elmer Elan 6100 ICP-MS at Union College in Schenectady, New York. A 50 μm spot size was used with a shot frequency of 10 Hz. Each line was pre-ablated at a scan rate of 150 μm/s to remove contaminants before being scanned again at a scan rate of 50 μm/s, resulting in an approximate sampling resolution of 50 μm. For all line scans, a 15 s shutter delay was used so that each series of sample data was preceded by gas blank data. The gas blank values were subtracted from the sample values in order to remove the gas signal from the specimen data. ^{43}Ca was used as an internal standard and all Mg/Ca intensity values were calibrated using the United States Geological Survey MACS-3 carbonate standard[3] (values from USGS 2012). The average calibrated MACS-3 Mg concentration had a relative standard deviation (%RSD) of 2.4% (n = 32 over eight analytical days), showing excellent precision. The calibration was checked using the non-matrix-matched NIST 610 glass standard, yielding an average Mg concentration of 445 ± 20 ppm—within 5% of the recommended value (465 ppm; Pearce et al. 1997)—and 4.5%RSD (n = 24 over eight analytical days). Details on the analyses and calibrations

[3] Although we present our data in molar units to allow comparison with other studies, this step is not necessary to estimate growth characteristics from the Mg/Ca profiles; ratios of blank-subtracted raw counts of Mg and Ca (i.e., units of counts/counts) are generally sufficient for these analyses.

for the California specimens can be found in Goodwin et al. (2013), which were analyzed on the same LA-ICP-MS.

Each *C. virginica* resilifer specimen, excluding the hatchery-raised individuals of known age from North Carolina, was then re-polished and a series of carbonate powder samples was drilled along the same foliated calcite layer, parallel to the direction of growth (from the umbo to the growth margin; Figure 2.2b), using a Merchantek micromill at Syracuse University in Syracuse, New York. The carbonate samples were analyzed for $\delta^{18}O$ and $\delta^{13}C$ values using a Finnigan MAT 251 coupled to a Finnigan Kiel automated preparation device at the University of Michigan's stable isotope laboratory in Ann Arbor, Michigan or a Thermo Gas Bench II connected to a Thermo Delta Advantage mass spectrometer in continuous flow mode at the stable isotope laboratory at Union College. Analyses from the University of Michigan and Union College both had an analytical uncertainty for $\delta^{18}O$ and $\delta^{13}C$ values of <0.1‰ (VPDB) based on 22 and 13 NBS-19 standards, respectively. Details on the $\delta^{18}O$ and $\delta^{13}C$ analyses for the California specimens can be found in Goodwin et al. (2010, 2013).

The resulting Mg/Ca and $\delta^{18}O$ and $\delta^{13}C$ profiles were matched by measuring sample distances for both the laser line scans and the micromill samples from digital photographs, using a single scale, with the ImageJ 1.51f image processing software (Rasband 1997). Sample distances for the North Carolina hatchery specimens were estimated using the same method. The Mg/Ca, $\delta^{18}O$, and $\delta^{13}C$ values were then plotted against the sample distances from the umbo in order to compare the profiles.

To aid in distinguishing the lower-frequency annual variability from the higher-frequency intra-annual variability in the high-resolution laser ablation line-scan data, each Mg/Ca profile was centered around zero by subtracting the linear trendline values from the raw data to remove ontogenetic trends and applying running medians

to the data. Linear detrending is commonly used in sclerochronology and is among the simplest detrending methods available (e.g., Cook and Holmes, 1986; Cook and Krusic, 2005), but we also tested two alternative detrending methods with variance-stabilizing properties on a subset of the Mg/Ca profiles (measured/predicted ratios and the adaptive power transformation, Cook & Peters 1997). The choice of detrending method did not impact our interpretations of annual peaks and troughs in the test profile (Appendix 2.1), so we used the simple, widely used linear detrending method. Note that detrending was inappropriate for specimens < 1 year old, because in such cases the trend lines would track intra-annual variation in Mg/Ca, obscuring the incomplete annual pattern (e.g., Figure A2.2-16). Thus, the Mg/Ca profiles of the three nine-month-old North Carolina specimens were not adjusted for ontogenetic trends (Figure A2.2-17).

Running medians with adaptive median windows based on oyster growth data were plotted to help distinguish annual variability in the Mg/Ca profiles from intra-annual variability. We used "adaptive" median windows because oyster growth rate slows during ontogeny—meaning more intra-annual Mg/Ca variation must be discounted in earlier parts of the profiles than in later portions. This correction was achieved by having the median windows decrease in width with increasing distance from the umbo according to regressions of oyster growth rate against specimen age (size-at-age relationships were estimated from the $\delta^{18}O$ profiles). Further, because oyster growth patterns vary with latitude (e.g., Shumway 1996), we plotted separate medians based on growth data from three geographical and temporal subsets of our oyster specimens. The three geographic and temporal subsets were 1) the Connecticut specimen, 2) the modern South Carolina specimens, and 3) the fossil South Carolina specimens (Figure 2.3). All three medians were plotted on each profile in order to test whether local oyster growth data are needed to use this method—if the same life-

history interpretations were given by all three medians, this result would indicate that regional oyster growth data would be sufficient for future uses of the method. The windows for the running medians were all scaled so that a growth distance of 40 mm would result in a median window width of five data points. A fourth running median was calculated for each specimen individually—using the growth data from the live-collected South Carolina specimens—that scaled the median window widths to five data points at the maximum growth distance for each specimen. These trendlines were then compared with the $\delta^{18}O$ profiles to evaluate the ability of Mg/Ca to capture annual signals. Peaks and troughs in the $\delta^{18}O$ profiles were matched visually to the closest peak in the corresponding Mg/Ca profile based on the following criteria. A $\delta^{18}O$ peak was considered detectable in the Mg/Ca profile if all running medians substantially crossed zero in the direction corresponding to the $\delta^{18}O$ peak or trough. In cases where features of the $\delta^{18}O$ profile were visible in the Mg/Ca profile, but one or

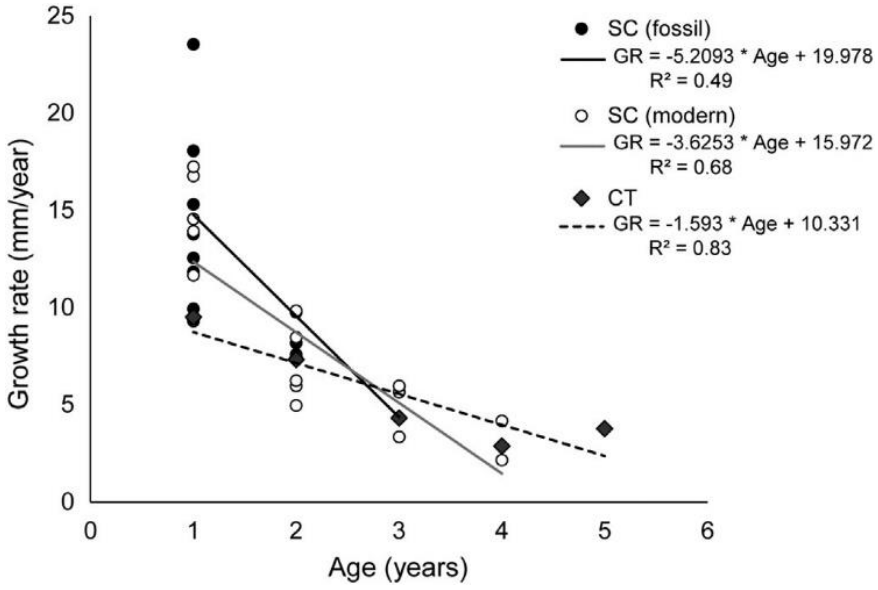

Figure 2.3 | Regressions of resilifer growth rate (GR) against age in years for the specimen from Connecticut (CT) and modern and fossil dead specimens from South Carolina (SC; determined from $\delta^{18}O$ profiles). The regressions were used to determine the window widths of the running medians to aid in Mg/Ca profile interpretations (see text for details).

more running medians did not substantially cross zero, the peak was considered present but ambiguous. Undetectable $\delta^{18}O$ peaks were those that would have been missed in the Mg/Ca profile in the absence of the $\delta^{18}O$ profiles.

2.3 Results and discussion

Annual peaks in the $\delta^{18}O$ profiles were identifiable in the majority of Mg/Ca profiles (The raw Mg/Ca and stable isotope values are available online as Appendix 2 to the published version of this paper; Durham et al. in press). Further, our results agree with those of previous studies reporting that the foliated calcite growth lines in the oyster hinge cross-sections may not always form with annual periodicity (e.g., Hong et al. 1995; Andrus & Crowe 2000; Surge et al. 2001; Figure 2.4), highlighting the importance of geochemical analyses for evaluating growth characteristics in this taxonomic group. Collectively, out of 105 total peaks and troughs in the $\delta^{18}O$ profiles of the Connecticut, South Carolina, and California oyster specimens, 97% (n = 102) were detectable in the Mg/Ca profiles, 9% (n = 9) of which would have been ambiguous in the Mg/Ca profiles in the absence of the $\delta^{18}O$ profiles. Three percent (n = 3) of the $\delta^{18}O$ profile peaks and troughs were undetectable in the Mg/Ca profiles (see Figure 2.5 for an example; profiles for all specimens can be found in Appendix 2.2). The specimen from Louisiana was not included in these totals because the geochemical results suggested it was less than a year old[4] (Figure A2.2-16).

[4] This conclusion was based on three factors: 1) the raw Mg/Ca profile had a prominent positive slope, similar to the nine-month-old specimens from North Carolina; 2) the only major positive excursion in the $\delta^{18}O$ profile corresponded to a large positive excursion in the $\delta^{13}C$ profile and was not visible in the Mg/Ca profile, suggesting that it may not have been a winter seasonal signal; and 3) the Louisiana specimen was from a lower latitude than the South Carolina specimens (so would likely have grown as fast or faster than them), several of which grew 10–20 mm in their first year (Appendix 2.2). Finally, the match between the median patterns and the $\delta^{18}O$ profile for the Louisiana specimen is poor (Figure A2.2-16).

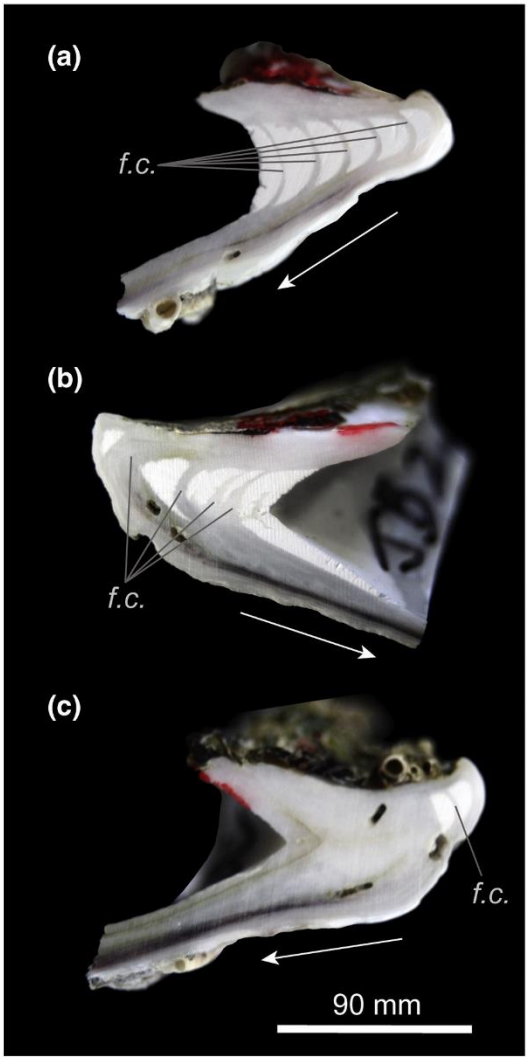

Figure 2.4 | Resilifer cross-sections of the three North Carolina specimens included in our study: (a) NC-L-01, (b) NC-L-02, and (c) NC-L-03. These specimens were live-collected in August 2015 at the same time from the same hatchery at nine months of age, yet show highly variable numbers of foliated calcite growth lines (examples are labeled f.c.), demonstrating that the lines are not annual morphological features in these specimens. Scale bar applies to all images. White arrows indicate direction of growth.

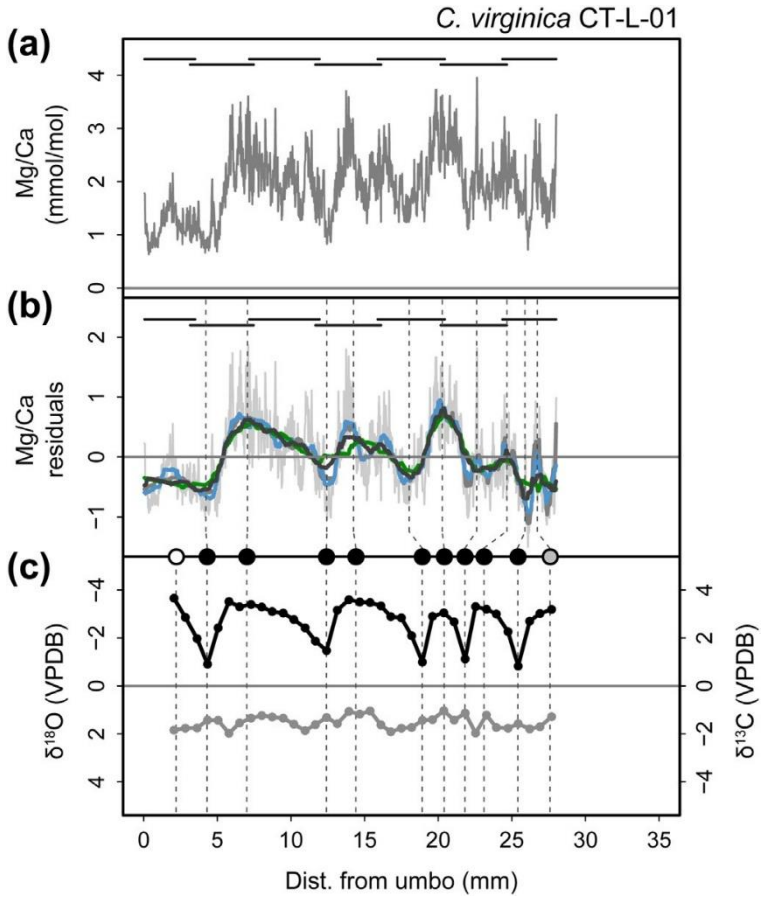

Figure 2.5 | Plots showing (a) the raw Mg/Ca ratio data, (b) the Mg/Ca profile centered around zero with four running medians, and (c) the $\delta^{18}O$ (black line, axis inverted) and $\delta^{13}C$ (grey line) profiles for the C. virginica specimen CT-L-01. Dark grey lines above the profile in panels (a) and (b) represent the distances covered by individual laser ablation line scans. Mean-subtracted data (i.e., residuals) in panel (b) are in light grey. The four running median trendlines in panel (b) have median windows based on growth rate/ age relationships for: 1. the live-collected Connecticut specimen (blue); 2. the fossil South Carolina specimens (green); 3. the modern South Carolina specimens (dark grey); and 4. the modern South Carolina specimens, but with window widths scaled to the individual specimen (grey). See text for details. Vertical dashed lines that cross panels (b) and (c) correspond with peaks and troughs in the $\delta^{18}O$ profile. Shaded circles in between the two panels indicate whether the corresponding peak or trough in the $\delta^{18}O$ profile is detectable in the Mg/Ca profile (black = detectable; grey = present but ambiguous; white = undetectable).

The Mg/Ca profiles matched all $\delta^{18}O$ peaks in nine of the 17 shells analyzed that were more than one year old, and only three specimens had $\delta^{18}O$ peaks that were undetectable in the Mg/Ca profiles (Appendix 2.2).[5] Lifespan estimates based on each of the four medians were equal for six of the 17 specimens (35%) that were over one year old and were within one year or less of each other for 14 of the 17 specimens (82%). The medians based on Connecticut growth data and the individually scaled modern dead South Carolina data tended to overestimate the corresponding $\delta^{18}O$ profile lifespan estimates, and the medians based on the growth data from fossil dead South Carolina specimens and the modern dead South Carolina data (with windows scaled to 40 mm) more frequently underestimated the corresponding $\delta^{18}O$ profile lifespan estimates. Overall, lifespan estimates based on 67 out of the 68 medians (98.5%) were within ±1 year of the corresponding $\delta^{18}O$ profile estimates, and the average differences between Mg/Ca profile and $\delta^{18}O$ profile lifespan estimates were 0.21 ± 0.41 years, -0.18 ± 0.52 years, -0.18 ± 0.47 years, and 0.46 ± 0.81 years, for the medians based on growth data from the Connecticut specimen, the South Carolina fossil dead specimens, and the South Carolina modern dead specimens with windows scaled to 40 mm and to the maximum growth distance of each specimen, respectively. Further, the Mg/Ca profiles accurately represented the lifespans of the three nine-month-old *C. virginica* specimens from North Carolina (Figure A2.2-17), and all present but ambiguous and undetectable peaks occurred at the beginning and/or end of growth profiles, areas in which the annual pattern is often not clear, even for $\delta^{18}O$ profiles (e.g., Goodwin et al. 2003). Altogether, these results suggest that Mg/Ca

[5] It should be noted that the Mg/Ca peaks and troughs were occasionally offset from the corresponding distance position of their counterparts in the $\delta^{18}O$ profiles. We consider these offsets to be related to the difference in spatial and temporal averaging between the LA-ICP-MS and stable isotope sampling methods and the fact that we matched the $\delta^{18}O$ peaks and troughs to the running median trendlines rather than the Mg/Ca profiles themselves.

profiles are useful alternatives to $\delta^{18}O$ profiles for determination of growth characteristics, such as lifespan and growth rate,[6] in oysters.

These encouraging results for oysters also suggest that this method is likely to be useful for many other molluscan taxa. The oysters studied here produce calcite shells, which are expected to incorporate Mg relatively easily due to the similar crystal structures of $MgCO_3$ and $CaCO_3$ (Oomori et al. 1987), suggesting that this method is likely to work well for analyzing the shells of other calcitic mollusk species. Further, although the Mg partition coefficient is about 100 times lower in aragonite than in calcite (Oomori et al. 1987; Poulain et al. 2015)—suggesting that there should be relatively low Mg incorporation in aragonitic mollusk shells—seasonally correlated Mg/Ca ratios have been reported for a number of aragonitic mollusk taxa (e.g., Takesue & van Geen 2004; Richardson et al. 2005; Schöne et al. 2011; Marali et al. in press; but see also Foster et al. 2008). The Mg/Ca ratio values reported in some of these studies are also very similar to those of the calcite shells reported here (e.g., Takesue & van Geen 2004; Schöne et al. 2011). This similarity despite the differences in Mg/Ca ratios between inorganic aragonite and calcite is likely due to the vital effects associated with biogenic carbonates. Thus, LA-ICP-MS analysis of Mg/Ca ratios is likely applicable to a wide variety of molluscan taxa, including both aragonitic and calcitic species.

[6] Note that because our analyses were performed on the resilifer, the growth rate reflected in the $\delta^{18}O$ and Mg/Ca profiles is that of the resilifer, and not necessarily that of the whole shell. A linear regression of resilifer height against whole-valve height for 256 left valves from the modern South Carolina samples, however, shows the two dimensions are well correlated (whole shell height = $3.08 * \text{resilifer height} + 17.09$; $R^2 = 0.75$; $F_{1,253} = 743.3$; $p \leq 0.0001$).

Effects of species, seasonality, geography, and growth rate on Mg/Ca profile interpretations

The age estimates from Mg/Ca profiles largely agree with those from the $\delta^{18}O$ profiles of all specimens analyzed, including both *C. virginica* and *M. gigas* and across all localities. This result demonstrates that Mg/ Ca profiles can be used to estimate growth characteristics even when seasonal variability in temperature is relatively low, as is the case in San Francisco Bay (Figure 2.1). Despite the overall agreement among the medians and with the corresponding $\delta^{18}O$ profiles, growth variability between specimens from different locations did influence the performance of the running medians. For instance, the growth differences between localities in our study qualitatively corresponded to expectations based on differences in temperature (Shumway 1996): the Connecticut specimen, from our northernmost locality, grew most slowly and its growth rate decreased the least between years, and the fossil South Carolina specimens, from a lower latitude, grew most rapidly and decreased their growth fastest with age (Figure 2.3). The modern South Carolina *C. virginica* specimens were intermediate in their growth rate and the rate of decline in growth rate over ontogeny (Figure 2.3). This pattern also fits with interpretations of the Pleistocene Canepatch Formation that suggest it was deposited during a warm interglacial period (although exactly which one is uncertain; e.g., Wehmiller et al. 1988).

These variations in growth characteristics were evident in the performance of the running medians because they determined the patterns of median window widths over the Mg/Ca profile distances. For instance, because the Connecticut specimen grew relatively slowly and had a relatively small decrease in growth rate over time, the median windows based on this relationship were narrow and did not change very much with shell distance. The result was an increased sensitivity in this running

median to intra-annual variation in the Mg/Ca profiles for specimens from warmer locations (e.g., South Carolina) that had a greater difference in growth rate between early and late ontogeny (Figure 2.6). The opposite was true of the running median based on growth of the fossil South Carolina specimens, which showed the most rapid growth early in ontogeny and the steepest decline in growth rate with time (Figure 2.3). This running median tended to have windows that began very wide and narrowed rapidly with shell distance, which sometimes resulted in insensitivity to inter-annual variability in the Mg/Ca profiles, especially the ontogenetically early sections (Figure 2.6).

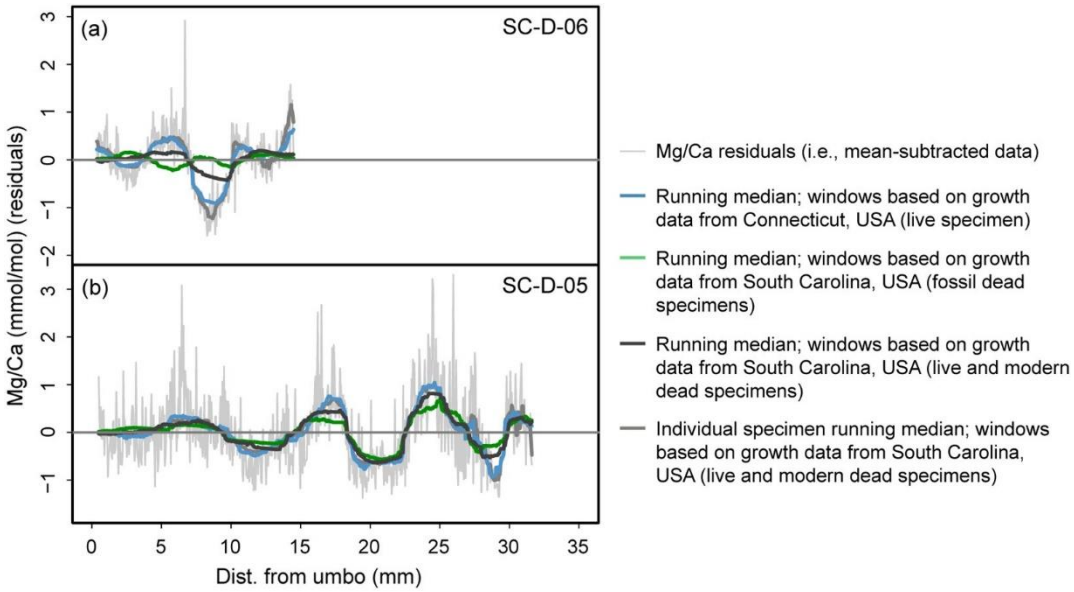

Figure 2.6 | Mg/Ca profiles for two modern *C. virginica* specimens from South Carolina: (a) SC-D-06 and (b) SC-D-05, demonstrating the decrease in the match between the running medians in smaller specimens (i.e., SC-D-06 in this case) because of the way the median window widths were calculated. See text for details.

The variability in patterns of growth rate also affected the performance of the running median scaled for each specimen individually versus the one scaled to 40 mm growth distance. Interestingly, the individually scaled median often matched the

running median based on the Connecticut specimen growth characteristics fairly closely because they both tended to have relatively narrow median windows (though in the former the narrow windows were the result of scaling to shorter shell distances, whereas the latter had narrow windows because of the slow growth rate of the Connecticut specimen). Although this sensitivity made both medians, especially the individually scaled median, susceptible to overestimating the $\delta^{18}O$ profile lifespan estimates (e.g., Figures A2.2-13 to A2.2-15), in other cases they captured important variation towards the ends of the Mg/Ca profiles that was missed by the other medians (e.g., Figures A2.2-1, A2.2-2, A2.2-5). Thus, basing our interpretations of oyster lifespans from the Mg/Ca data on multiple running medians helped account for the effects of geographic and environmental variations in growth.

Sources of variation between Mg/Ca and $\delta^{18}O$ profiles

Potential sources of variation between the Mg/Ca and $\delta^{18}O$ profiles could include variation in insoluble organic matrix content of the shell with growth rate, differential effects of salinity variations on the Mg/Ca and $\delta^{18}O$ profiles, and the distance of the samples from the edge of the resilifer cross-section. For instance, it has been shown that the concentration of insoluble organic matrix (IOM) increases at growth lines in the aragonitic bivalve *Arctica islandica* (i.e., when shell growth slows; Schöne et al. 2010), leading to errors in the measured Mg/Ca ratios by LA-ICP-MS. This variation in IOM concentration could effectively decrease the amplitude of seasonal variation in Mg/Ca profiles. For instance, growth lines in bivalve shells are often produced during winter months at mid to high latitudes, which tend to be characterized by low Mg/Ca ratios in the shell, but the increased concentrations of Mg-enriched IOM at these growth lines might dampen that pattern. Thus, if such heterogeneous distribution of IOM is also characteristic of the oysters analyzed here,

then this effect could contribute to difficulties in interpreting some annual cycles in the Mg/Ca profiles in our study by decreasing the amplitude of annual cycles relative to the often noisy intra-annual Mg/Ca patterns. Mg-enriched IOM associated with nonannual growth lines formed in response to other disturbances such as reproduction, temperature, or osmotic stress, may also complicate Mg/ Ca profile interpretations. However, the intertidal, estuarine oysters used in this study likely experience a wider range of environmental stresses than mollusks living in full marine conditions, suggesting that this may not be a very common impediment to analyzing Mg/Ca profiles.

Salinity variations are another potential source of disagreement because Mg/Ca ratios have low sensitivity to salinity fluctuations above about 10 (Dodd & Crisp 1982), but $\delta^{18}O$ and $\delta^{13}C$ values are typically both positively correlated with salinity (Epstein & Mayeda 1953; Mook & Tan 1991). Although *C. virginica* can survive salinities of 5 or lower for short periods, optimal salinities are typically 14–28 and populations inhabiting waters with average salinities around 10 tend to be sparse (Shumway 1996), thus it is unlikely that the oysters used in our study—all of which were collected from areas with dense oyster populations—regularly experienced salinities below 10. Indeed, a regression of the $\delta^{18}O$ and $\delta^{13}C$ values measured from our specimens showed they were positively correlated overall ($\delta^{18}O = 0.61 * \delta^{13}C - 0.93$; $R^2 = 0.23$; $p \leq 0.0001$), and thus likely reflect salinity variations (cf. Gillikin et al. 2006b) given the coastal marsh environments inhabited by *C. virginica* and *M. gigas* (see also Goodwin et al. 2010). We consider it unlikely that salinity variations influenced the match between the Mg/Ca and $\delta^{18}O$ profiles for most specimens, however, because there were few large excursions in the $\delta^{13}C$ profiles and there was generally a good correspondence between the Mg/Ca profiles and the $\delta^{18}O$ profiles. Two potential exceptions were specimens SC-L-01 and LA-D-01 (Figures A2.2-2 and

A2.2-16), both of which showed prominent, simultaneous, positive excursions in the $\delta^{18}O$ and $\delta^{13}C$ profiles that were not reflected in the Mg/Ca profiles (i.e., consistent with short-term increases in salinity).

Finally, Mg concentration has been shown to vary with distance from the edge of shell cross-sections in the calcitic bivalve *Pecten maximus* (Freitas et al. 2012). Specifically, Freitas et al. (2012) found that Mg/Ca ratios increased in magnitude and variability within ~200 μm of the exterior edge of the shell cross-section. Because the laser lines are straight but the shell layer in cross-section often is not (the reason multiple overlapping laser lines are required to construct the Mg/Ca profile), the distances from the laser lines to the exterior edges of the resilifer cross-sections were not constant. For instance, laser lines frequently were <200 μm from the cross-section edge at the ends of line scans and in the resilifer sections from early in ontogeny, when the foliated calcite layer is often very thin. We tested this relationship in *C. virginica* by regressing the distances of the laser lines from the edge of the cross-section against the variance in Mg/Ca values from the South Carolina *C. virginica* specimens (Appendix 2.3). Surprisingly, there was a weak but statistically significant positive correlation between distance from the exterior edge of the cross-section and the mean (Mg/Ca mean = 0.73 ∗ Dist. + 2.3; $R^2 = 0.02$; $p = 0.0019$; Figure A2.3-1) and variance (Mg/Ca variance = 0.31 ∗ Dist. + 0.13; $R^2 = 0.05$; $p \leq 0.0001$; Figure A2.3-2) of Mg/Ca ratios, suggesting that the mean and variability of ratios increase with distance from the exterior edge of the resilifer cross-section in *C. virginica* (Appendix 2.3), counter to previous findings in *Pecten*. These weak relationships, however, make it unlikely that the distance of the laser lines from the cross-section edge affected the Mg/Ca profile interpretations for the specimens in our study.

Advantages of Mg/Ca ratios over $\delta^{18}O$ values for sclerochronology

There are a few major potential advantages to choosing Mg/Ca-based sclerochronological analyses over stable isotope analyses for at least some applications, including the relative ease of higher resolution sampling that is possible with the LA-ICP-MS technique, as well as its lower time and financial costs. For instance, an interesting possibility is that the high-resolution sampling afforded by laser ablation line scans (~50 μm in this case, but LA-ICP-MS resolution can be easily adjusted by changing the laser scan rate and involves little additional sampling effort or cost) may out-perform $\delta^{18}O$ profiles for detecting some late-ontogeny annual cycles, because each LA-ICP-MS measurement is less time-averaged than the typical point samples milled for stable isotope analyses (resolution usually ~300 μm; see Goodwin et al. 2003). A potential example of this advantage is specimen CT-L-01, the longest-lived specimen in our study. There is an additional trough and peak at the distal end of the Mg/Ca profile for CT-L-01, relative to the $\delta^{18}O$ profile, thus possibly capturing almost an additional year of growth missed by the $\delta^{18}O$ profile (Figure 2.5). This example highlights the fact that although life-history trait estimates from $\delta^{18}O$ profiles are generally considered reliable, they are not always completely accurate or easily interpretable (e.g., Goodwin et al. 2003).

In addition, the lower time and financial costs of LA-ICP-MS relative to stable isotope analyses allow for more shells to be analyzed. The benefits of larger sample sizes may outweigh the costs associated with the occasionally challenging profile interpretations, particularly for life history studies of populations. To illustrate this point, for the present study we completed stable isotope sampling for no more than three specimens per day and there was a turnaround time of at least one week to acquire the data, whereas we sampled up to ~10–15 specimens per day by LA-ICP-MS and the results were available in real time.

Finally, interpretation of $\delta^{18}O$ analyses of estuarine taxa, such as *C. virginica* and *M. gigas*, is sometimes challenging due to the combined influence of temperature and salinity on $\delta^{18}O$ water values (e.g., Surge et al. 2003). Thus, another potential advantage of using Mg/Ca profiles measured by LA-ICP-MS for characterizing mollusk shell growth characteristics is the low sensitivity of Mg/Ca ratios to salinity fluctuations relative to $\delta^{18}O$ values (Dodd & Crisp 1982).

Conclusions

Our results suggest that Mg/Ca ratios measured from LA-ICP-MS line scans are a viable alternative to more traditional stable oxygen isotope analyses for estimating lifespans and growth rates of oysters and other mollusks that lack reliable annual morphological shell features. We also found that running medians with median windows based on shell growth data can capture annual cycles in the Mg/Ca profiles, making them easier to interpret. Further, plotting multiple running medians based on different sets of growth data or scaled to different maximum growth distances can aid the interpretation of ambiguous peaks and troughs in the Mg/Ca profiles. Although $\delta^{18}O$ profiles have been used extensively for sclerochronological applications for decades, the lower time and financial costs and increased sampling resolution of LA-ICPMS analyses are potentially significant advantages over stable oxygen isotope analyses, particularly for studies requiring analysis of large numbers of specimens. Future research should further investigate the reasons for mismatches between the Mg/Ca and $\delta^{18}O$ profiles, particularly in ontogenetically early and late sections.

Acknowledgments

We thank A. Cohen for providing access to the *M. gigas* specimens from California, the Jarrett Bay Oyster Company (www. jarrettbayoysters.com) for

supplying the hatchery reared *C. virginica* specimens from North Carolina, and Indian River Shellfish (www. indianrivershellfish.com) and the Madison Shellfish Commission for allowing us to collect *C. virginica* from Madison, Connecticut. We also thank J. Smith, A. Tweitmann, T. Butler, and M. Durham for assistance with fieldwork; A. Verheyden-Gillikin, M. Manon, S. Katz, and M. King for lab assistance at Union College; E. Mosier and C. Sweeney for lab assistance at Cornell University; and L. Ivany (Syracuse University) for micromill use. We also gratefully acknowledge funding support from the Atkinson Center for a Sustainable Future's Sustainable Biodiversity Fund (award to SRD) and the U.S. National Science Foundation for graduate research fellowship support to SRD (NSF-DGE #1144153). We also thank the U.S. National Science Foundation for providing funding for Union College's Perkin Elmer ICP-MS (NSF-CCLI #9952410), CETAC LSX-213 (NSF-MRI #1039832), and isotope ratio mass spectrometer and peripherals (NSF-MRI #1229258). Finally, we thank W. Allmon, M. Hare, J. Wehmiller, and I. Montanez (editor) for comments that helped improve the manuscript, as well as one anonymous reviewer, D. Surge, and S. Finnegan, for excellent reviews of the manuscript.

1

CHAPTER 3

METABOLIC THEORY OF ECOLOGY EXPLAINS LIFESPAN DIFFERENCES IN THE EASTERN OYSTER (*CRASSOSTREA VIRGINICA*) BETWEEN A PAST INTERGLACIAL AND TODAY

Abstract

Our ability to anticipate biotic responses to future climate change depends in part on our understanding of the effects of changes in major climate change variables (such as temperature) on the life history of individual species. Further, because multiple variables (and multiple species' responses) are likely to have interactive effects, a general modeling framework capable of making quantitative predictions of the responses of species, communities, and ecosystems to climate change is needed. Here we provide a test of the metabolic theory of ecology for explaining the scaling of lifespan with temperature over millennial timescales in the eastern oyster, *Crassostrea virginica*, using fossil and modern reef assemblages. Our study demonstrates that lifespans measured from Pleistocene fossil oysters from South Carolina were shorter than they are today, and that this difference is consistent with the predictions of the metabolic theory of ecology for the scaling of lifespan with the effect of temperature on metabolic rate. This result has potentially important implications for management of this economically and ecologically important species in the future, and demonstrates the potential utility of fossils and other geohistorical records for evaluating the biotic effects of slow, long-term processes, such as climate change, that are difficult to examine with monitoring records and experimental studies.

3.1 Introduction

Climate change has the potential to alter the structure and function of marine environments in the near future via a variety of influences, including increasing temperatures, decreasing pH, rising sea levels, and changes to ocean circulation patterns (Hoegh-Guldberg & Bruno 2010; Doney et al. 2012). These physical changes will significantly impact marine species, communities, and ecosystems through myriad direct and indirect effects. For instance, fundamental aspects of the life history of many species vary with temperature, including growth rate, lifespan, egg size, and body size (e.g., Atkinson 1996; Blackburn et al. 1999; Angilletta et al. 2004; Angilletta Jr 2009; Zuo et al. 2012). Our ability to anticipate and respond to the impacts of climate change on marine resources depends on our ability to understand these basic biological responses.

One of the most successful theoretical frameworks to date for describing the impact of temperature on life history is the Metabolic Theory of Ecology (MTE), which attempts to explain a wide variety of ecological patterns through first-principles based on the scaling relationships between temperature, mass, and metabolism (Brown et al. 2004). Although some of the mechanistic assumptions of the MTE are still being debated, it has performed remarkably well at predicting patterns in aspects of life history, animal behavior, community ecology, and more across a broad range of taxonomic groups (see Sibly et al. 2012 for a recent, wide-ranging treatment of current research in metabolic ecology).

The patterns that have been successfully predicted by the MTE include variation in lifespan with temperature (Gillooly 2001; O'Connor et al. 2007; Munch & Salinas 2009). For instance, Munch and Salinas (2009) conducted a global meta-analysis of intraspecific lifespan variation with latitude in 95 ectothermic species representing 4 phyla and 23 orders, including taxa from terrestrial, aquatic, and marine

habitats. Using data gathered from laboratory studies (30 species) and field observations of wild populations (67 species), Munch and Salinas (2009) showed that intraspecific ectotherm lifespans tend to increase with latitude, and that temperature is the primary variable driving this pattern. Moreover, the relationship between log lifespan and inverse temperature fit the MTE-predicted range (slope = 0.2–1.2) for most of the species analyzed, consistent with the theory that metabolic rate is a fundamental mechanism linking latitudinal temperature and lifespan within ectothermic species. Munch and Salinas (2009) ended by suggesting that, given the effects of temperature on intraspecific ectotherm lifespans with latitude, populations living at a single location may see reductions in lifespan of 3-42% within the next century, depending on the climate change scenario (1.1 – 2.9^{o}C increase over the next century; IPCC 2007). Such an impact could have important effects on marine species and habitats already under pressure from anthropogenic activities, such as pollution, coastal development, and overfishing.

Predicting the magnitude of lifespan reduction of particular species over time as the climate changes is difficult, however, because synergistic or antagonistic effects associated with the responses of other species to the warming temperatures or to other climatic variables that may change along with temperature (e.g., pH, salinity, production) are difficult to replicate experimentally, and models necessarily rely on modern data of limited temporal and climatic scope (Willis & MacDonald 2011; Byrne & Przeslawski 2013; Dietl et al. 2015). A third option that integrates other ecosystem and climatic effects is to make a comparison with a climate analogue from the geological past (e.g., Williams & Jackson 2007; Willis & Bhagwat 2009; Willis et al. 2010; Willis & MacDonald 2011). These tests are also imperfect because they require assumptions about similarities between climatic intervals and ecosystem types separated by long durations of time, perhaps the most obvious difference being that

past climate change was not driven by human activity and many anthropogenic impacts may interact with current climate change effects in a way that prevents species from responding in the same ways as in the past (Harris et al. 2006; Hobbs et al. 2006; Williams & Jackson 2007). However, fossil evidence suggests that many coastal marine habitats have persisted through multiple glacial-interglacial cycles with essentially the same communities of species present, and geohistorical studies can demonstrate actualistic species responses to past climate change (i.e., "natural experiments") and are often the only sources of data on a host of other long term ecological dynamics that are not covered by monitoring data or historical records (Dietl et al. 2015).

The consequences of climate change for lifespans of the eastern oyster, *Crassostrea virginica*, may be of particular interest. *Crassostrea virginica* is a reef-forming oyster that is an economically and ecologically important species in estuaries across the East and Gulf Coasts of North America—they provide fishery resources, water filtration, shoreline stabilization, wave energy buffering, and habitat for other economically important species, such as fish and crabs (e.g., Coen et al. 2007; Grabowski & Peterson 2007; Beck et al. 2011). Further, the habitat structure that *C. virginica* reefs provide may be a temperate analogue of coral reefs (Harding & Mann 1999), and the biodiversity they harbor can number hundreds of species (e.g., 303 species from multiple reefs in North Carolina, Wells 1961; 105 species in Florida, Boudreaux et al. 2006; 107 species in Louisiana, Humphries & La Peyre 2015). Anthropogenic impacts have already caused an estimated 85% decline in oyster reef habitat globally within the last 130 years (including *C. virginica*), making oyster reefs one of the most threatened marine habitats on Earth (Beck et al. 2011). Finally, the pattern of increasing lifespan with latitude appears to be an ubiquitous pattern in the marine Bivalvia (Moss et al. 2016), suggesting that oyster lifespan is likely to vary

with temperature as found by Munch and Salinas (2009). Thus, understanding how *C. virginica* may respond to the warming climate in the coming decades is critical to ongoing efforts to manage and protect this species.

Fortunately, *C. virginica* populations leave dense geohistorical records in coastal sediments (i.e., death assemblages; DA) that can be studied to reconstruct an enormous amount of information about their history (e.g., Kirby et al. 1998; Surge et al. 2003; Kirby & Miller 2005; Rick et al. 2016; Savarese et al. 2016). *Crassostrea virginica* reefs grow by accretion as new recruits settle and grow on the reef surface, entombing the shells of previous generations of oysters and other calcifying reef inhabitants within the reef structure in the process. These buried assemblages can persist in the sedimentary record for millions of years under the right conditions (e.g., Lawrence 1968), making comparisons between oyster populations separated by centuries to millennia possible.[7]

Here, we compare lifespans measured from fossil and modern shells of *C. virginica* from South Carolina to test whether oyster lifespans during a warmer interglacial climate in the Pleistocene were shorter than they are today, and whether this variation agrees with predictions of the MTE. We show that the average lifespans of oysters from modern reefs are slightly longer than those of their fossil counterparts,

[7] An additional, potentially advantageous feature of oyster assemblages is that the reef framework may reduce the degree of time averaging and spatial averaging in the assemblage (e.g., by resisting mixing processes such as bioturbation and transport by currents or waves). This assertion requires more supporting research, but some studies show sub-millennial age distributions in oyster reef assemblages (e.g., Lindland et al. 2001; Surge et al. 2003), which is less time averaging than has been documented from other types of shell beds (e.g., Flessa et al. 1993; Kowalewski et al. 1998; Kosnik et al. 2013; Kidwell 2013; Dominguez et al. 2016), although non-reef molluscan DAs sometimes also exhibit sub-millennial scales of time averaging (e.g., Kosnik et al. 2015; Dominguez et al. 2016). Assuming oyster reef accretion proceeds more or less gradually—rather than in short, rapid pulses separated by relatively long periods of static reef height or erosion—centennial-scale time averaging could cause oyster reef assemblages to preserve a finer-resolution record of environmental history than many non-reef molluscan DAs, while maintaining the benefit of time averaging's tendency to smooth out short term temporal variability (i.e., inter-annual or inter-decadal variability) that can obscure long term patterns (Kowalewski et al. 1998).

and that the differences are consistent with the latitudinal patterns in ectotherm lifespans observed by Munch and Salinas (2009) and the predictions of the MTE.

3.2 Methods

Sample collection and processing

Four fossil and four modern oyster assemblages were sampled in northeast South Carolina (SC). Live oysters were collected under scientific collection permit #3279 issued to SRD by the South Carolina Department of Natural Resources. The fossil assemblages were sampled from the banks of the Intracoastal Waterway (ICW) in North Myrtle Beach, SC. All of the fossil assemblages occurred at the base of the banks of the ICW, extending above and below the ground level by up to ~1m (i.e., ranging from a maximum of ~1m high in the outcrop to a minimum elevation of ~1m below ground level; Table 3.1). The assemblages were nearly submerged at high tide, so all sampling was conducted at low tide. At each site, a fresh surface of outcrop was exposed, and excavated below ground level as necessary, to expose the entire stratigraphic height of each oyster assemblage (~1m). Then, beginning at the top of the oyster assemblage, sequential bulk samples 20cm x 20cm x 15cm (L x W x H) in size were extracted until the bottom of the oyster assemblage was reached. Three replicate series of bulk samples were taken. A 15cm depth interval was chosen because it was wide enough to accommodate relatively large oysters, but narrow enough that multiple stratigraphic layers in each assemblage could be sampled.

The oyster assemblages sampled occur in an unconsolidated sedimentary unit composed predominantly of bluish-grey clay and silt with variable amounts of fine sand and/or peat (interpreted as a back barrier facies, e.g., McCartan et al. 1982) that falls within the middle Pleistocene Canepatch Formation, as defined by DuBar (1971) (see Appendix 3.1 for discussion). There is general agreement that the Canepatch units

Table 3.1 | Locality information for the fossil and modern oyster assemblages.

Age	Site ID	Coordinates	Description
Pleistocene	P2	33°49'59.20"N, 78°41'19.90"W	North bank, Intracoastal Waterway, between Robert Edge Parkway bridge and Grand Strand Airport (North Myrtle Beach, South Carolina)
Pleistocene	P4	33°49'41.70"N, 78°42'8.40"W	South bank, Intracoastal Waterway, between Robert Edge Parkway bridge and Grand Strand Airport (North Myrtle Beach, South Carolina)
Pleistocene	P5	33°50'0.60"N, 78°41'17.70"W	North bank, Intracoastal Waterway, between Robert Edge Parkway bridge and Grand Strand Airport (North Myrtle Beach, South Carolina)
Pleistocene	P6	33°51'59.92"N, 78°34'32.13"W	West bank, Little River, just south of Intracoastal Waterway (North Myrtle Beach, South Carolina)
Recent	R1	33°51'10.90"N, 78°35'37.20"W	Dunn Sound, just northeast of access bridge to Watie's Island (North Myrtle Beach, South Carolina)
Recent	R5	33°50'11.10"N, 78°38'0.00"W	House Creek, near Cherry Grove (North Myrtle Beach, South Carolina)
Recent	R11	33°19'34.70"N, 79°10'35.10"W	Sixty Bass Creek, near outlet to North Inlet, North Inlet/Winyah Bay National Estuarine Research Reserve (Georgetown, South Carolina)
Recent	R12	33°16'48.00"N, 79°11'14.60"W	South/east bank, Jones Creek, North Inlet/Winyah Bay National Estuarine Research Reserve (Georgetown, South Carolina)

reflect climatic conditions that were as warm as or warmer than the present based on geochronologic, lithostratigraphic, and fossil evidence (DuBar 1971; Cronin et al. 1981), suggesting these assemblages are appropriate for testing MTE predictions of lifespan variation with temperature.

The modern oyster reefs were sampled at four locations: near Watie's Island, SC, in the marsh adjacent to Cherry Grove, SC, and at two sites in the North Inlet/Winyah Bay National Estuarine Research Reserve in Georgetown, SC—Sixty Bass Creek and Jones Creek. Each reef was sampled by hand at low tide by randomly positioning a 20cm x 20cm quadrat on top of each reef and extracting bulk samples by hand at ~15cm depth intervals (replicating the fossil assemblage bulk sample sizes). Sampling continued until we reached either the bottom of the reef assemblage or the maximum depth that could be dug by hand (~60cm). The first bulk sample always consisted of the living layer of oysters, so did not often extend further than ~6-8cm

below the sediment surface, but also included the full height of unburied living oysters. The depth intervals were necessarily approximate because cemented clumps of oysters often crossed these arbitrary sampling interval boundaries. One series of bulk samples was collected from each living reef. Although only densely populated oyster reefs were sampled to match the fossil assemblages, an effort was made to sample oyster populations representing a range of microhabitat conditions such as salinity, proximity to the marsh mouth, and the amount and character of sediment on and around the reef (i.e., firmer/sandier vs. softer/muddier) in order to increase our chance of capturing environments similar to those represented in the fossil assemblages (Appendices 3.1, 3.2).

The bulk samples from 30-45cm below the top of each fossil assemblage and below the living layer of each modern reef were processed for this study. All bulk samples were washed over a ~3mm screen (after setting aside an archival subsample in the case of the fossil bulks) and all specimens >5mm—mostly mollusks and crustaceans—were sorted, with paired oyster valves kept together, unpaired oyster specimens separated by valve type (i.e., left or right) and completeness, and non-oyster specimens separated and sorted by species where possible. Either all of the material in the size fraction between 3-5mm or a representative subsample was sorted in the same manner. After washing and initial processing, the unpaired oyster specimens >5mm from each sample were checked for matches that may have separated during collection, transport, or washing.

Oyster measurements

For each sample, all oyster specimens that were >5mm and at least ~80% complete were numbered (paired valves were given the same number) and five measurements were collected using digital calipers: total left valve height (the longest

distance from the umbo to the growth margin), left valve attachment scar height (the longest dimension of the left valve attachment area), resilifer height (the straight line distance from the umbo to the center of the resilifer growth margin), right valve height (the longest dimension from the umbo to the growth margin), and right valve width (the widest distance between anterior and posterior edges of the right valve). If any of these dimensions seemed significantly broken for a given specimen, it was not measured.

LA-ICP-MS and stable isotope analyses

Following the methods reported in Chapter 2 (Durham et al., 2017), an additional 92 specimens were analyzed by laser ablation-inductively coupled plasma-mass spectrometry (LA-ICP-MS) in order to gather Mg/Ca ratio data for estimating oyster lifespans. Because these analyses were carried out on the resilifers, a minimum of 10 specimens were analyzed from each fossil and modern oyster assemblage, selected to represent as much of the left valve size range present in each sample as possible. All but one specimen chosen for LA-ICP-MS analysis had paired valves, and all specimens had relatively straight resilifers that could be bisected with a single, straight cut. Paired valve specimens were favored because we considered them unlikely to have been reworked and their completeness could be gauged more precisely. It was occasionally necessary to include specimens from other bulk samples from the same assemblage (i.e., stratigraphically higher or lower) if too few specimens from the 30-45cm depth interval met these criteria (Appendix 3.3).

Oyster lifespan and body size analysis

Lifespan estimates derived using the method of Durham et al. (2017) were plotted against the size of each specimen analyzed to create size-at-age plots. A power

function was applied to the data for each assemblage, and the resulting equations were used to estimate lifespans for all of the other resilifer specimens in each sample. Average lifespans were then calculated for each assemblage and these were averaged to produce single average lifespan values for the fossil and modern oyster assemblages. Specimens with estimated lifespans <1 year were excluded from these averages to avoid potential biases associated with the variable abundance of small specimens (i.e., spat), which can vary due to taphonomic loss or irregular recruitment (see Dietl & Durham, 2016 for a similar standardization based on size). These average lifespan values were compared using a Wilcoxon rank-sum test in order to test the prediction that oyster lifespans were lower during the past interglacial.

Testing fit with the metabolic theory of ecology

Finally, to test the fit of lifespan differences between fossil and modern oyster assemblages with the metabolic theory of ecology (MTE), we followed Munch and Salinas (2009) by plotting ln(average lifespan) against inverse temperature (1/kT, where k is Boltzmann's constant [8.62×10^{-5} eV/K] and T is temperature in Kelvin). The fossil-modern lifespan differences were considered consistent with MTE predictions if the slope of this relationship fell between 0.2-1.2 eV (Munch & Salinas 2009).

Temperature estimates for the modern sites were based on an average of monthly temperature measurements collected by the South Carolina Department of Health and Environmental Control (SCDHEC) between 1999 and 2006 from stations very near our collection sites (SCDHEC monitoring locations 21SCSHL-01-06, 21SCSHL-01-17, 21SCSHL-05-08, 21SCSHL-05-01 were the closest to our sites R1, R5, R11 and R12, respectively; data archived by the National Water Quality Monitoring Council, accessed from www.waterqualitydata.us/portal/ on 6/28/2017).

Only months with average temperatures above 10°C were included because oysters cease to calcify when water temperatures fall below ~10°C (Kirby et al. 1998), yielding an average modern temperature across all of our sites of 20.19°C.

Dubar (1971) suggested that the Canepatch Fm. reflects a slightly warmer climate than present, but did not estimate the magnitude of the temperature difference. Unfortunately, empirical estimates of paleotemperature differences from our oyster stable isotope and trace element data were inconclusive due to the effects of diagenesis and the confounding influence of salinity on $\delta^{18}O_{water}$ values (Appendix 3.2). A subsequent search for literature values of the temperature difference between the present and possible interglacials represented in the Canepatch Fm. revealed widely varying estimates from essentially zero up to ~2°C warmer than present (Cronin 1991; McManus et al. 2003; Rodrigues et al. 2011; McKay et al. 2011). Cronin (1991) found very similar paleotemperatures to today for MIS 5e based on ostracodes from South Carolina, although it is unclear if any of his samples came from the Canepatch Fm.(Cronin 1979). In contrast, McKay et al. (2011) found that global average temperatures were warmer by 0.7C ± 0.6°C during MIS 5e based on a meta-analysis of published paleotemperature records. McManus et al. (2003) also found similar paleotemperatures to modern values for MIS 11 based on stable oxygen isotopes from planktonic foraminifera preserved in deep sea cores from the North Atlantic. Finally, Rodrigues et al. (2011) found that paleotemperatures during MIS 9 were ~2°C warmer than present based on biomarker analyses of deep sea cores from the western Iberian Margin. Given that Dubar (1971) thought the Canepatch Fm. fossil assemblages represented a warmer climate than present, we examined two possible scenarios based on the non-zero paleotemperature difference values from the literature: 1) the fossil oyster assemblages formed in waters ~0.7°C warmer than present (i.e., 20.89°C), based on the estimate from McKay et al. (2011) and 2) the fossil oyster assemblages

grew during a time that was ~2^{o}C warmer than present (i.e., 22.19^{o}C), based on the estimate from Rodrigues et al. (2011).

3.3 Results

A total of 634 fossil and 367 modern oyster resilifer specimens had estimated lifespans of ≥ 1 year (Table 3.2), after converting their height measurements to estimated age using the oyster growth equations for each assemblage (Figure 3.1; see Appendix 3.3 for the Mg/Ca data used to construct the growth curves). The median lifespan of the Pleistocene *C. virginica* was about 12.4% shorter than the median lifespan of the modern oyster specimens (1.54 and 1.76 years, respectively; Wilcoxon rank-sum test; W = 139600, n_{fossil} = 634, n_{modern} = 367, p = <0.0001). Consistent with the findings of Munch and Salinas (2009) that lifespan varied with temperature independent of mass, the difference in median resilifer height between fossil and modern assemblages was not significant (16.62 and 16.98 mm, respectively; Wilcoxon rank-sum test; W = 119700, n_{fossil} = 634, n_{modern} = 367, p = 0.4458).

Table 3.2 | Average sizes and lifespan estimates for each fossil and modern oyster assemblage.

			Resilifer height (mm)		Lifespan (years)	
Age	Site	n	Avg.	SD	Avg.	SD
Pleistocene	P2	340	18.27	5.55	1.63	0.47
Pleistocene	P4	127	17.61	5.65	1.5	0.42
Pleistocene	P5	60	17.55	4.2	1.65	0.53
Pleistocene	P6	107	16.73	5.39	2.15	1.02
Recent	R1	87	17.42	4.96	1.75	0.57
Recent	R5	160	18.05	6.72	2.21	0.82
Recent	R11	52	19.12	7.08	1.95	1.1
Recent	R12	68	18.83	5.4	1.7	0.6

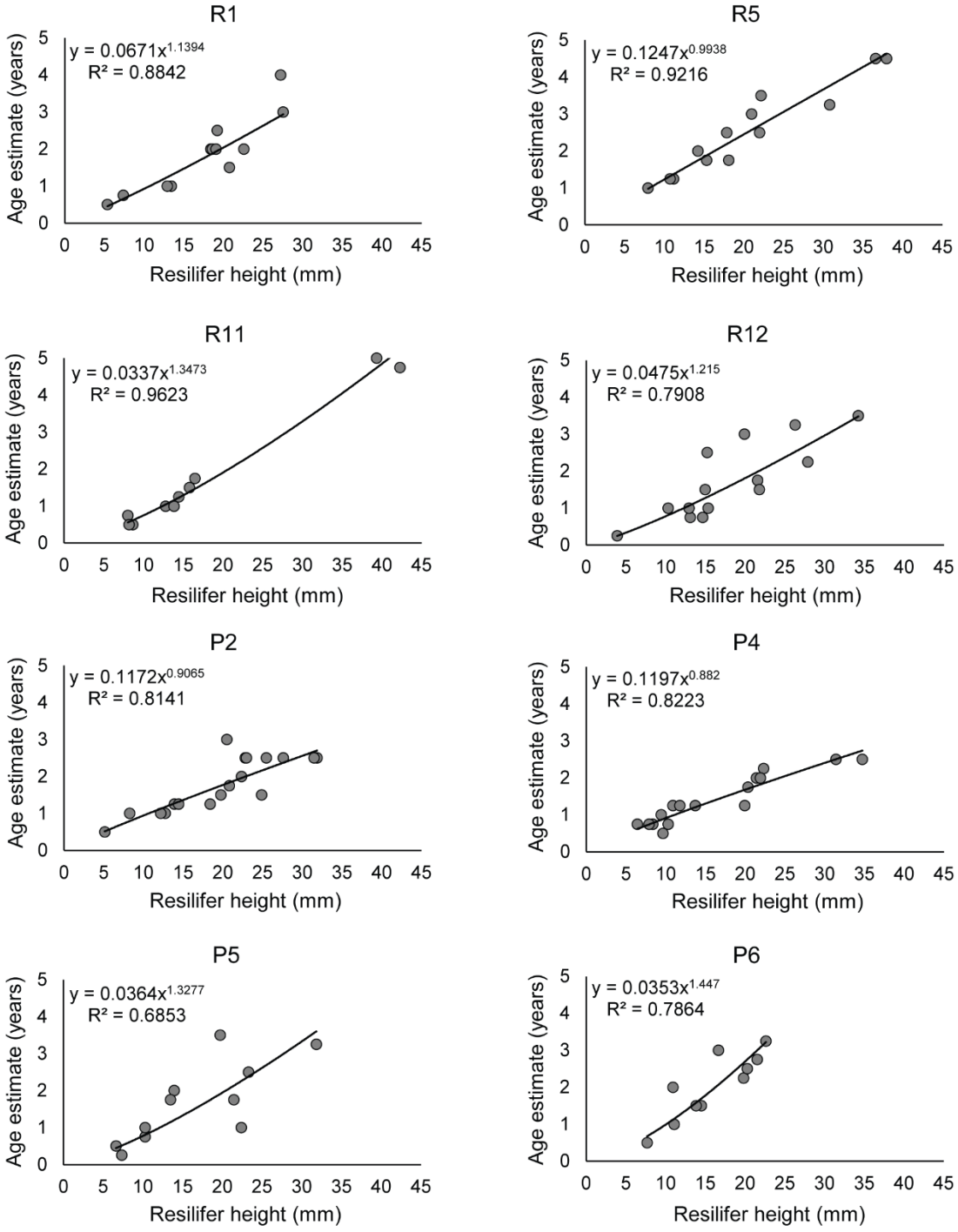

Figure 3.1 | Plots of lifespan (age) estimates against resilifer heights for a minimum of 10 specimens per assemblage. Lifespan estimates were based on Mg/Ca profiles (Appendix 3.3). Equations were used to convert other resilifer heights to estimated ages for each assemblage.

The MTE predicts that plots of ln(lifespan) against inverse temperature (1/kT, where k is Boltzmann's constant, 8.62 x 10^{-5} eV/K, and T is temperature in Kelvin) should have slopes approximating the average activation energy of respiratory metabolism (~0.65eV; Gillooly 2001; Brown et al. 2004; Brown & Sibly 2012), though as stated earlier, this value is expected to range between 0.2-1.2eV (Munch & Salinas 2009). Plotting our ln(lifespan) values for fossil and modern oyster samples against inverse temperature based on our modern average value for northeastern South Carolina (20.19 ^{o}C) and the two relative paleotemperature estimates (+0.7^{o}C for MIS 5e and +2^{o}C for MIS 9) yielded regressions with slopes of 0.93 and 0.33, respectively (Table 3.3; Fig 3.2). These slope values fit the MTE-predicted range for both MIS 5e and MIS 9 estimated temperature differences, but neither regression was significant (Table 3.3).

Table 3.3 | Information on regressions of ln(lifespan) (LS in regression equations) against 1/kT (T in regression equations) for two different paleotemperature estimates.

	Temperature				Regression: Ln(lifespan) ~ 1/kT		
Age	Difference	^{o}C	K	1/kT	Equation	R^2	*p*
Recent	0	20.19	293.34	39.55			
Pleistocene (MIS 5e estimate)	+0.70	20.89	294.04	39.45	LS = 0.929 * T - 36.114	0.12	0.407
Pleistocene (MIS 9 estimate)	+2.00	22.19	295.34	39.28	LS = 0.3266 * T - 12.2897	0.12	0.407

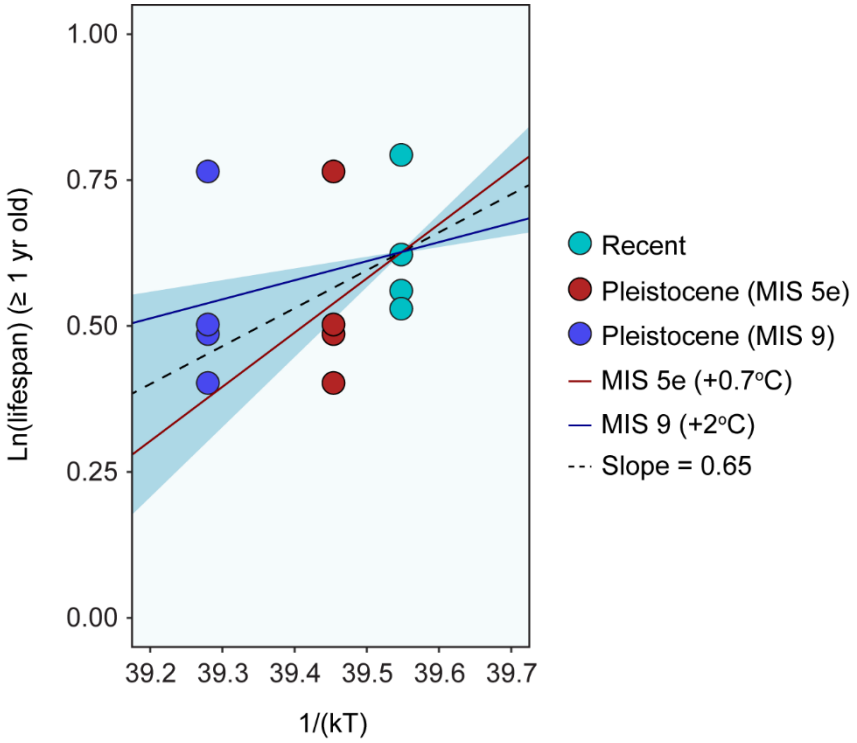

Figure 3.2 | Plot of ln(lifespan) against inverse temperature (k=Boltzmann's constant, T=temperature in K) for oysters (≥1 year old) from our four modern (i.e., Recent) and four fossil assemblages. The fossil oyster lifespan data are plotted twice, based on temperature differences between the Recent and two potential ages of our fossil sites for comparison (MIS5e and MIS9, see Appendix 3.1). The blue shaded area reflects the MTE-predicted range of slope values: 0.2-1.2 (these values correspond to temperature differences between Pleistocene and Recent of 0.55°C and 3.28°C, respectively). The average activation energy for respiratory metabolism (~0.65eV) is plotted as well for reference.

3.4 Discussion

The lifespans estimated from the fossil oysters were significantly shorter than those measured from the modern oysters, with a reduction in median lifespan between the fossil and modern assemblages of 12.4%. This value fits within the range of lifespan reductions predicted by Munch and Salinas (2009) of 3-42%. Further, given estimates of temperature differences between previous interglacial climates and today

of ~0-2ºC above modern (Cronin 1991; McManus et al. 2003; Rodrigues et al. 2011; McKay et al. 2011), this lifespan difference also fits the MTE-predicted range of slope values for the relationship between ln(lifespan) and inverse temperature expressed as 1/kT (i.e., 0.2-1.2eV). Although neither slope was significantly different from zero, meaning our interpretations about the explanatory power of the MTE must be regarded as preliminary, the close fit of the slope values with MTE predictions and with the findings of Munch and Salinas (2009), combined with the fact that the environments represented in the fossil and modern assemblages appear to have been very similar (Appendix 3.1), is consistent with our interpretation that the primary driver of this difference in average oyster lifespan was a difference in water temperature. Further, 61% of the slope values calculated by Munch and Salinas (2009) were also not significantly different from zero, but they pointed out that obtaining positive slopes for 85% of the species they examined in the absence of a latitudinal lifespan gradient was extremely unlikely. Particularly given the fact that we had multiple replicates of only two temperatures (i.e., time periods), the lack of a significant regression was not surprising. The addition of more fossil and modern data to this relationship in the future, as well as the addition of samples from other temperature conditions (either from other geographic locations or time periods) will be needed to clarify this relationship.

Our results, however, are consistent with the findings of Munch and Salinas (2009) that the MTE is a useful theoretical framework for predicting the responses of individual species to warming temperatures. Given that average ocean temperatures in the western Atlantic Ocean at mid-latitudes of the northern hemisphere are predicted to rise by as much as 0.5-0.75ºC by 2035, and perhaps 1-3ºC by the end of the century (Collins et al. 2013; Kirtman et al. 2013), if we assume that average oyster lifespans in South Carolina will respond to warming temperatures as predicted by the MTE, they

would be expected to decrease by a minimum of 2-6% (0.5ºC warming) or a maximum of 12-31% (3ºC warming) depending on whether the MIS 9 or MIS 5e paleotemperature estimate is used.

Alternatives to temperature

Although Munch and Salinas (2009) found that temperature explained the majority of the variation in ectotherm lifespan with latitude, alternative hypotheses have been put forward to explain this pattern in bivalves, such as predation and food limitation (Moss et al. 2016, 2017). Predation and disease intensity tend to be positively correlated with temperature and salinity in oyster habitats (Shumway 1996), so it is possible that these variables contributed to reduced lifespan in Pleistocene oysters. Predation by mollusks and crustaceans can be estimated in fossil and death assemblages by analyzing the frequencies of traces, such as scars and drill holes, left on the shells of their prey (Dietl & Alexander 2003; Kelley & Hansen 2003). For instance, one of the most conspicuous indicators of predation in many bivalve assemblages are circular holes drilled by predatory gastropods such as *Eupleura* sp. and *Urosalpinx* sp. (e.g., Harding et al. 2007). These traces—along with the shells of predatory gastropods—were exceedingly rare, however, with only a few examples found in the eight assemblages examined (i.e., >4000 shells). Still, other indicators of predation, such as repair scars, must be assessed and compared between assemblages before predation can be more safely dismissed as a driver of oyster lifespan difference.

Disease and parasitism both also are positively correlated with temperature, so would be expected to have qualitatively similar impacts to those of predation on lifespans in *C. virginica* (Ford & Tripp 1996; White & Wilson 1996). First, although most disease epizootics were not documented until the mid-twentieth century, there is evidence that the presence of some modern oyster diseases, such as *Perkinsus*

marinus, pre-date their recognition by scientists, and even low-level infections can have sublethal effects on growth and condition (Ford & Tripp 1996). Most oyster diseases do not leave diagnostic traces in the shell morphology, however, so estimating their occurrence in the fossil and death assemblages is difficult or impossible. Second, parasites such as the pyramidellid snail *Boonea impressa*, specimens of which occur in many of the fossil and modern oyster assemblages we examined, can also negatively impact oyster condition and growth, potentially shortening lifespans (White & Wilson 1996).

Importantly, however, the impacts of predation, disease, and parasitism are all likely to reduce average shell size in an assemblage, for instance, by selecting for earlier maturation at a smaller size, decreasing growth rates, increasing early mortality, etc. (Ford & Tripp 1996; Abrams & Rowe 1996; Coen & Bishop 2015; although size-selective predation may produce either increases or decreases in size at maturity in snails, Crowl & Covich 1994). This expectation was not met in the case of our comparison of fossil and modern oyster assemblages, because although there was a significant difference in lifespan between fossil and modern oysters, there was no difference in size. By contrast, a decrease in lifespan with no difference in size implies an increase in growth rate, a pattern which is consistent with expectations based on an increase in temperature between modern and fossil assemblages. Thus, the likely impacts of predation, disease, and parasitism on oyster growth suggests that they are not as likely as temperature to be drivers of the reduced oyster lifespan in the fossil assemblages relative to the modern assemblages.

A difference in food availability is another variable that warrants investigation, because primary production also tends to increase with temperature and has been a suggested driver of life history differences in other studies (Kirby & Miller 2005; Anderson-Teixeira & Vitousek 2012; Litchman 2012; Moss et al. 2017). For instance,

Moss et al. (2017) found that lifespans of long-lived Cretaceous and Eocene bivalves from Antarctica were comparable to those of modern high-latitude bivalve species, despite the fact that Antarctica experienced a climate during that time at least ~7-8^{o}C warmer than similar latitudes today. They hypothesized that this striking result is best explained by food limitation at high latitudes related to reduced insolation (and therefore lower primary production; Moss et al. 2017). Also, a modest eutrophication increase in Chesapeake Bay in the past has been correlated with increased growth rate in *C. virginica* (Kirby & Miller 2005), suggesting that food availability can have important influences on oyster life history. Thus, it is possible that higher metabolisms, and the resulting lower average lifespans, of fossil specimens were at least partially related to greater food availability in the warmer climate.

However, several lines of reasoning suggest food availability was not likely to be the primary driver of the lifespan pattern. First, given that filtration rates of bivalves are correlated with temperature (Dame 2012) and metabolic rate scales exponentially with temperature (Gillooly 2001), the effect of temperature on metabolism is likely much more important than fluctuations in food availability at lower latitudes (Dillon et al. 2010; Anderson-Teixeira et al. 2012). For instance, Dillon et al. (2010) found that although temperature increases in recent decades have been larger at higher latitudes, changes in ectotherm metabolism have been greater at tropical and northern temperate latitudes than in the arctic. Second, there is evidence that increasing temperatures have differential effects on heterotrophs versus autotrophs because of different scaling relationships between temperature and respiration versus photosynthesis (O'Connor et al. 2009). Such differential scaling could potentially lead to *increased* food limitation for filter feeders at higher temperatures despite increases in primary production (i.e., an inverted food web, O'Connor et al. 2009), again leading us to conclude that temperature is the most likely driver of decreased lifespan in

Pleistocene oysters. Finally, although the longevity of high latitude bivalves may be related to adaptation to food limitation as suggested by Moss et al. (2017), it is not necessarily linked to metabolic rate. Studies of the impact of food limitation on metabolic rates in other marine invertebrates have not found an effect (e.g., Cowles et al. 1991; Seibel & Drazen 2007), and there is some evidence that very long lifespans in bivalves at high latitudes may be related to selection for elevated antioxidant production in food-limited conditions (i.e., as a trade-off for decreased tissue maintenance costs and lower metabolism), rather than as a direct result of metabolic scaling.

Considerations for oyster management in a warming world

Our study results suggest that the MTE is a useful theoretical framework for making predictions about life history changes in oysters through time, justifying the space-for-time approximation offered by Munch and Salinas (2009). This is important, because MTE-based models have not been widely applied in conservation, but offer potentially valuable insights for setting research directions and conservation/restoration priorities (Boyer & Jetz 2012). For instance, as mentioned above, the exponential scaling of metabolic rate with body temperature leads to the somewhat counterintuitive conclusion that lower latitude species, particularly tropical species, may experience greater increases in metabolism even though the absolute temperature change expected at these latitudes is lower than that expected at high latitudes (Deutsch et al. 2008; Tewksbury et al. 2008; Dillon et al. 2010). Given that many tropical species likely already live near their thermal optima the large physiological consequences of even modest warming could have very serious consequences for these species (Dillon et al. 2010; Boyer & Jetz 2012).

These thermal patterns may also have the potential to significantly impact *C. virginica* reefs. Although it is certainly true that their large geographic range and fossil record dating back millions of years suggests that *C. virginica* has been resilient to past climate changes, their long history does not mean that oyster reefs were equally abundant or geographically distributed throughout the past, and so climate change could still pose difficulties for managers, whose job it is to maintain or increase oyster populations. For instance, *C. virginica* populations throughout the South Atlantic Bight are predominantly intertidal, and during the summer in the southern part of their range oyster body temperatures can reach 49^{o}C (Galtsoff 1964). These temperatures are capable of killing some oysters within minutes to hours, and lethal temperatures and survivability vary depending on the rate of increase and the acclimation temperature (Shumway 1996). Given that average air temperatures in the southeast United States are projected to increase by 2.5-5^{o}C over the next 70 years, with concomitant increases in the frequency of daily high temperatures $\geq$ 38^{o}C, the exposure of intertidal oysters to temperature extremes at low tide is likely to become more frequent in the coming decades (SCDNRCCTWG 2013). Multiple studies support the general pattern that the frequency of extreme high temperatures will increase as mean temperature increases, though there is substantial regional variability (e.g., Mearns et al. 1984; Griffiths et al. 2005; Kirtman et al. 2013). Although mutual shading among reef oysters can attenuate extreme air temperatures (Bahr & Lanier 1981), the impact of modest warming on oyster metabolism could mean that oyster reefs experiencing these conditions will need to migrate lower into the intertidal. This scenario could lead to a reduction of suitable habitat area for intertidal oysters. For instance, as mentioned above, rising temperatures are likely to increase disease and predation pressures on oyster populations (e.g., Shumway 1996), but potentially could also make long periods of exposure at low tide—presently a refuge from less

eurythermal or less exposure-tolerant predators, parasites, and possibly some diseases (Bahr & Lanier 1981; Brown & Stickle 2002; La Peyre et al. 2015)—intolerable. Further, oyster reefs that lose living oysters along the top and upper flanks to heat stress may also be more vulnerable to smothering by sedimentation or subsidence because reef height is thought to be an important variable in this regard (Coen & Humphries 2017). Considering potential impacts of climate warming such as these in the context of known latitudinal and temperature patterns in oyster growth (e.g., the parabolic relationship of oyster growth rate with latitude; Dame 2012) and MTE could help predict which populations of oysters are most vulnerable.

This scenario-building capacity of models such as MTE is likely to become important for making management decisions, as the importance of anticipating and explicitly managing natural populations for climate change is increasingly recognized. For instance, "climate smart conservation" (Hansen et al. 2010; Stein et al. 2014; Nadeau et al. 2015) is a relatively new framework for conservation, restoration, and management decision making in the face of climate change that advocates deliberate, anticipatory management actions based on scientific evidence to help ecological systems adapt to climate change. It is based on the recognition that traditional management approaches may be inadequate or misguided without taking into consideration the expected future impacts of environmental change. Currently, oyster restoration and management is focused on quantitative metrics of reef success and habitat suitability measured over very short timeframes (often only 1-3 years, if at all; Kennedy et al. 2011; Coen & Humphries 2017). Monitoring of these variables in real time is critically important to recognizing restoration success or failure and implementing adaptive management (e.g., NRC 2017), but studies such as ours suggest long term conservation and restoration success may depend on incorporating expected near-future changes in organism life history and ecology into planning.

Integrating more forward-looking modeling into conservation and restoration planning will be particularly important given the complexity of biological responses to climate change that must be integrated to build realistic scenarios. For instance, the impacts of temperature increases and acidification tend to be negative on their own, but may interact additively or antagonistically (Waldbusser et al. 2011; Talmage & Gobler 2011; Byrne & Przeslawski 2013; Speights et al. 2017). Further, the degree and direction of impact varies depending on the developmental stage of the oysters considered (Waldbusser et al. 2011; Parker et al. 2012; Byrne & Przeslawski 2013; Parker et al. 2017), and when contemporaneous impacts of elevated activity among oyster predators (e.g., mud crabs) with increasing temperature are considered, negative impacts to oyster populations may be increased (Speights et al. 2017). Thus, it is clear that modeling approaches capable of deriving general conclusions based on the integration of multiple variables, as MTE is capable of doing, will be important for identifying areas of conservation, restoration, and management policy and practice that might need to be adjusted in anticipation of climate impacts.

The importance of geohistorical records

Lastly, this study demonstrates how geohistorical records can be used to test ecological models and enhance our understanding of the responses of organisms and ecosystems to a wide range of climate change scenarios (e.g., Dietl et al. 2015). There is evidence that information from geohistorical records may be particularly valuable for addressing conservation issues in the face of climate change (Smith et al. in press). Studies using a variety of geohistorical data from sediment cores to archeological middens and oyster shells themselves have yielded abundant new sources of baseline information that is enhancing our understanding of the responses of *C. virginica* reefs to anthropogenic and natural environmental change (Surge et al. 2003; Kirby & Miller

2005; Rick et al. 2016; Brandon et al. 2016; Dietl & Durham 2016; Savarese et al. 2016). More broadly, geohistorical data are increasingly being applied to conservation-relevant investigations, such as tracking and identifying invasive species (van Leeuwen et al. 2008; Smith & Dietl 2016), assessing contributions of molluscan habitats to carbon cycling (Smith et al. 2016), disentangling the effects of multiple anthropogenic stressors (Casey et al. 2014), and assessing trajectories of coastal ecosystem health through time (Dietl & Smith in press; Kidwell 2007; Dietl et al. 2016; Tomašových & Kidwell 2017). Considering insights such as these in conjunction with those from field and experimental studies of extant species, communities, and ecosystems, which contribute to a more detailed mechanistic understanding of many short-term, modern ecological processes, are likely to enhance our ability to adapt to climate change and mitigate harmful impacts to the natural systems on which human society ultimately depends.

3.5 Conclusions and future work

The average lifespans of modern *C. virginica* in northeastern South Carolina are longer than those of the fossil specimens, but none of the regressions of ln(lifespan) against inverse temperature (i.e., 1/kT) were significant. We must therefore interpret the results with regard to the MTE with caution, particularly given that the paleotemperature of the Canepatch Fm. is not precisely known. However, the broad support for the variation of lifespan with temperature according to the MTE found by Munch and Salinas (2009) across a wide variety of ectothermic taxa combined with the fact that the reduction in oyster lifespans between the modern and Pleistocene assemblages in our study fit the predicted range from Munch and Salinas (2009) is consistent with the interpretation that oyster lifespan variation with temperature through time is also predicted by the MTE.

As discussed above, there are potentially important implications for oyster management if oysters respond to warming temperatures according to the MTE, so future work should focus on adding new lifespan data from additional oyster assemblages that grew in different temperature environments using additional fossil assemblages and/or modern assemblages from different climates in the past and/or latitudes, respectively. For instance, the addition of preliminary data from a single reef in Connecticut (~1.5^{o}C cooler average growth temperatures than those in northeastern South Carolina) strengthened the regression of ln(lifespan) versus inverse temperature (1/kT), though it still is not significant (Appendix 3.4).

In addition to adding data to clarify whether oyster lifespans vary with temperature through time according to the MTE, improving our understanding of how temperature effects will interact with the impacts of the numerous other natural and anthropogenic stressors of oysters (such as ocean acidification, as discussed above) will be critical for deriving the best possible management recommendations. Although geohistorical data that predate the complicated multi-stressor combinations facing anthropogenically influenced coastal habitats today can help isolate specific variables—such as temperature, as we have done in the present study—their utility as a direct analog for species' responses to future warming is likely limited (Dietl 2016). Our conclusions must therefore be considered as only a starting point on which to layer the impacts of additional stressors in order to produce realistic scenarios of species' responses to ongoing climate change.

REFERENCES

Abrams PA, Rowe L. 1996. The effects of predation on the age and size of maturity of prey. Evolution **50**:1052–1061.

Alexander RR, Dietl GP. 2003. The fossil record of shell-breaking predation on marine bivalves and gastropods. Pages 141–176 in P. H. Kelley, M. Kowalewski, and T. A. Hansen, editors. Predator-prey interactions in the fossil record. Kluwer Academic/Plenum Publishers, New York.

Anderson TF, Arthur MA. 1983. Stable isotopes of oxygen and carbon and their application to sedimentologic and paleoenvironmental problems. Pages 1-1 to 1-151 Stable Isotopes in Sedimentary Geology. SEPM.

Anderson-Teixeira KJ, Smith FA, Ernest SKM. 2012. Climate change. Pages 280–292 in R. M. Sibly, J. H. Brown, and A. Kodric-Brown, editors. Metabolic Ecology. John Wiley & Sons, Ltd, West Sussex, UK. Available from http://onlinelibrary.wiley.com.proxy.library.cornell.edu/doi/10.1002/9781119968535.ch23/summary.

Anderson-Teixeira KJ, Vitousek PM. 2012. Ecosystems. Pages 99–111 in R. M. Sibly, J. H. Brown, and A. Kodric-Brown, editors. Metabolic Ecology. John Wiley & Sons, Ltd, West Sussex, UK. Available from http://onlinelibrary.wiley.com.proxy.library.cornell.edu/doi/10.1002/9781119968535.ch9/summary.

Andrus CFT. 2011. Shell midden sclerochronology. Quaternary Science Reviews **30**:2892–2905.

Andrus CFT, Crowe DE. 2000. Geochemical analysis of *Crassostrea virginica* as a method to determine season of capture. Journal of Archaeological Science **27**:33–42.

Angilletta Jr MJ. 2009. Thermal Adaptation: A Theoretical and Empirical Synthesis. Oxford University Press, New York.

Angilletta MJ, Steury TD, Sears MW. 2004. Temperature, growth rate, and body size in ectotherms: fitting pieces of a life-history puzzle. Integrative and Comparative Biology **44**:498–509.

Ashley MV, Willson MF, Pergams ORW, O'Dowd DJ, Gende SM, Brown JS. 2003. Evolutionarily enlightened management. Biological Conservation **111**:115–123.

Atkinson D. 1996. Ectotherm life-history responses to developmental temperature. Pages 183–204 in I. A. Johnston and A. F. Bennett, editors. Animals and temperature: phenotypic and evolutionary adaptation. Cambridge University Press, New York.

Baggett LP et al. 2015. Guidelines for evaluating performance of oyster habitat restoration. Restoration Ecology **23**:737–745.

Baggett LP, Powers SP, Brumbaugh RD, Coen LD, DeAngelis B, Green J, Hancock B, Morlock S. 2014. Oyster Habitat Restoration Monitoring and Assessment Handbook. The Nature Conservancy, Arlington, VA.

Bahr LM, Lanier WP. 1981. The ecology of intertidal oyster reefs of the South Atlantic coast: a community profile. U.S. Fish and Wildlife Service, Office of Biological Services, Washington, D.C.

Beck MW et al. 2011. Oyster reefs at risk and recommendations for conservation, restoration, and management. BioScience **61**:107–116.

Bernhardt JR, Leslie HM. 2013. Resilience to climate change in coastal marine ecosystems. Annual Review of Marine Science **5**:371–392.

Blackburn TM, Gaston KJ, Loder N. 1999. Geographic gradients in body size: a clarification of Bergmann's rule. Diversity and Distributions **5**:165–174.

Boudreaux ML, Stiner JL, Walters LJ. 2006. Biodiversity of sessile and motile macrofauna on intertidal oyster reefs in Mosquito Lagoon, Florida. Journal of Shellfish Research **25**:1079–1089.

Bougeois L, de Rafélis M, Reichart G-J, de Nooijer LJ, Dupont-Nivet G. 2016. Mg/Ca in fossil oyster shells as palaeotemperature proxy, an example from the Palaeogene of Central Asia. Palaeogeography, Palaeoclimatology, Palaeoecology **441**:611–626.

Bougeois L, de Rafélis M, Reichart G-J, de Nooijer LJ, Nicollin F, Dupont-Nivet G. 2014. A high resolution study of trace elements and stable isotopes in oyster shells to estimate Central Asian Middle Eocene seasonality. Chemical Geology **363**:200–212.

Boyer AG, Jetz W. 2012. Conservation biology. Pages 271–279 in R. M. Sibly, J. H. Brown, and A. Kodric-Brown, editors. Metabolic Ecology. John Wiley & Sons, Ltd, West Sussex, UK. Available from http://onlinelibrary.wiley.com.proxy.library.cornell.edu/doi/10.1002/9781119968535.ch22/summary.

Brandon CM, Woodruff JD, Orton PM, Donnelly JP. 2016. Evidence for elevated coastal vulnerability following large-scale historical oyster bed harvesting. Earth Surface Processes and Landforms **41**:1136–1143.

Brown JH, Gillooly JF, Allen AP, Savage VM, West GB. 2004. Toward a metabolic theory of ecology. Ecology **85**:1771–1789.

Brown JH, Sibly RM. 2012. The metabolic theory of ecology and its central equation. Pages 21–33 in R. M. Sibly, J. H. Brown, and A. Kodric-Brown, editors. Metabolic Ecology. John Wiley & Sons, Ltd, West Sussex, UK. Available from http://onlinelibrary.wiley.com.proxy.library.cornell.edu/doi/10.1002/9781119968535.ch2/summary.

Brown KM, Stickle WB. 2002. Physical constraints on the foraging ecology of a predatory snail. Marine and Freshwater Behaviour and Physiology **35**:157–166.

Brumbaugh RD, Beck MW, Coen LD, Craig L, Hicks P. 2006. A Practitioner's Guide to the Design and Monitoring of Shellfish Restoration Projects: An Ecosystem Services Approach. The Nature Conservancy, Arlington, VA.

Burrows F, Harding JM, Mann R, Dame RF, Coen LD. 2005. Restoration monitoring of oyster reefs. Page 4.1-4.73 in G. W. Thayer, T. A. McTigue, R. J. Salz, D. H. Merkey, F. M. Burrows, and P. F. Gayaldo, editors. Science-Based Restoration Monitoring of Coastal Habitats, Volume Two: Tools for Monitoring Coastal Habitats. NOAA National Centers for Coastal Ocean Science, Silver Spring, MD.

Byrne M, Przeslawski R. 2013. Multistressor impacts of warming and acidification of the ocean on marine invertebrates' life histories. Integrative and Comparative Biology **53**:582–596.

Carbotte SM, Bell RE, Ryan WBF, McHugh C, Slagle A, Nitsche F, Rubenstone J. 2004. Environmental change and oyster colonization within the Hudson River estuary linked to Holocene climate. Geo-Marine Letters **24**:212–224.

Carriker MR, Gaffney PM. 1996. A catalogue of selected species of living oysters (*Ostreacea*) of the world. Pages 1–18 in V. S. Kennedy, R. I. E. Newell, and A. F. Eble, editors. The Eastern Oyster, *Crassostrea virginica*. Maryland Sea Grant College, College Park, MD.

Casey MM, Dietl GP, Post DM, Briggs DEG. 2014. The impact of eutrophication and commercial fishing on molluscan communities in Long Island Sound, USA. Biological Conservation **170**:137–144.

Coen LD, Bishop MJ. 2015. The ecology, evolution, impacts and management of host–parasite interactions of marine molluscs. Journal of Invertebrate Pathology **131**:177–211.

Coen LD, Brumbaugh RD, Bushek D, Grizzle R, Luckenbach MW, Posey MH, Powers SP, Tolley SG. 2007. Ecosystem services related to oyster restoration. Marine Ecology Progress Series **341**:303–307.

Coen LD, Humphries AT. 2017. Oyster generated marine habitats: their services, enhancement, restoration and monitoring. Pages 274–294 in S. K. Allison and Murphy, editors. Routledge Handbook of Ecological and Environmental Restoration. Routledge, New York, NY.

Coen LD, Luckenbach MW. 2000. Developing success criteria and goals for evaluating oyster reef restoration: ecological function or resource exploitation? Ecological Engineering **15**:323–343.

Collins M et al. 2013. Long-term climate change: projections, commitments and irreversibility. Pages 1029–1136 in T. F. Stocker, D. Qin, G.-K. Plattner, M. Tignor, S. K. Allen, J. Boschung, A. Nauels, Y. Xia, V. Bex, and P. M. Midgley, editors. Climate Change 2013: The Physical Science Basis. Contribution of Working Group I to the Fifth Assessment Report of the Intergovernmental Panel on Climate Change. Cambridge University Press, New York, NY.

CPW (Conservation Paleobiology Workshop). 2012. Conservation paleobiology: opportunities for the earth sciences. Page 32. Report to the Division of Earth Sciences, National Science Foundation. Paleontological Research Institution, Ithaca, NY.

Cook, E.R., Holmes, R.L., 1986. User's manual for program ARSTAN. In: Holmes, R.L., Adams, R.K., Fritts, H.C. (Eds.), Tree-ring Chronologies of Western North America: California, Eastern Oregon and Northern Great Basin with Procedures Used in the Chronology Development Work Including Users Manuals for Computer Programs COFECHA and ARSTAN. University of Arizona, Tucson, AZ, Laboratory of Tree-Ring Research, pp. 50–65.

Cook, E.R., Krusic, P.J., 2005. ARSTAN v. 41d: A Tree-Ring Standardization Program Based on Detrending and Autoregressive Time Series Modeling, with Interactive Graphics. Tree-Ring Laboratory, Lamont-Doherty Earth Observatory of Columbia University, Palisades, New York, USA.

Cook ER, Peters K. 1997. Calculating unbiased tree-ring indices for the study of climatic and environmental change. The Holocene **7**:361–370.

Corrado JC, Weems RE, Hare PE, Bambach RK. 1986. Capabilities and limitations of applied aminostratigraphy as illustrated by analyses of *Mulinia lateralis* from the late Cenozoic marine beds near Charleston, South Carolina. South Carolina Geology **30**:19–46.

Cowles DL, Childress JJ, Wells ME. 1991. Metabolic rates of midwater crustaceans as a function of depth of occurrence off the Hawaiian Islands: food availability as a selective factor? Marine Biology **110**:75–83.

Cronin TM. 1979. Late Pleistocene marginal marine ostracodes from the southeastern Atlantic coastal plain and their paleoenvironmental implications. Géographie physique et Quaternaire **33**:121.

Cronin TM. 1991. Pliocene shallow water paleoceanography of the North Atlantic Ocean based on marine ostracodes. Quaternary Science Reviews **10**:175–188.

Cronin TM, Szabo BJ, Ager TA, Hazel JE, Owens JP. 1981. Quaternary climates and sea levels of the U.S. Atlantic Coastal Plain. Science **211**:233–240.

Crowl TA, Covich AP. 1994. Responses of a freshwater shrimp to chemical and tactile stimuli from a large decapod predator. Journal of the North American Benthological Society **13**:291–298.

Custer JF, Doms KR. 1990. Analysis of microgrowth patterns of the American oyster (*Crassostrea virginica*) in the middle Atlantic region of eastern North America: archaeological applications. Journal of Archaeological Science **17**:151–160.

Dame RF. 2012. Ecology of Marine Bivalves: An Ecosystem Approach. Second edition. CRC Press, Boca Raton, FL.

Davies AL, Colombo S, Hanley N. 2014. Improving the application of long-term ecology in conservation and land management. Journal of Applied Ecology **51**:63–70.

Deutsch CA, Tewksbury JJ, Huey RB, Sheldon KS, Ghalambor CK, Haak DC, Martin PR. 2008. Impacts of climate warming on terrestrial ectotherms across latitude. Proceedings of the National Academy of Sciences **105**:6668–6672.

Dietl GP. 2013. The great opportunity to view stasis with an ecological lens. Palaeontology **56**:1239–1245.

Dietl GP. 2016. Ecology: Different worlds. Nature **529**:29–30.

Dietl GP, Alexander RR. 2003. The fossil record of shell-breaking predation on marine bivalves and gastropods. Pages 141–176 in P. H. Kelley, M. Kowalewski, and T. A. Hansen, editors. Predator-Prey Interactions in the Fossil Record. Kluwer Academic/Plenum Publishers, New York.

Dietl GP, Durham SR. 2016. Geohistorical records indicate no impact of the Deepwater Horizon oil spill on oyster body size. Royal Society Open Science **3**:160763.

Dietl GP, Durham SR, Smith JA, Tweitmann A. 2016. Mollusk assemblages as records of past and present ecological status. Frontiers in Marine Science **3**:Article 169.

Dietl GP, Flessa KW. 2011. Conservation paleobiology: putting the dead to work. Trends in Ecology & Evolution **26**:30–37.

Dietl GP, Kidwell SM, Brenner M, Burney DA, Flessa KW, Jackson ST, Koch PL. 2015. Conservation paleobiology: leveraging knowledge of the past to inform conservation and restoration. Annual Review of Earth and Planetary Sciences **43**:79–103.

Dietl GP, Smith JA. in press. Live-dead analysis reveals long-term response of the estuarine bivalve community to water diversions along the Colorado River. Ecological Engineering. Available from http://www.sciencedirect.com/science/article/pii/S0925857416305249 (accessed December 4, 2016).

Dillon ME, Wang G, Huey RB. 2010. Global metabolic impacts of recent climate warming. Nature **467**:704–706.

Doar WR. 2014. The Geologic Implications of the Factors that Affected Relative Sea-level Positions in South Carolina During the Pleistocene and the Associated Preserved High-stand Deposits. Ph.D. dissertation, University of South Carolina, United States -- South Carolina. Available from http://search.proquest.com.proxy.library.cornell.edu/docview/1651954547/abstract/80611B0BA05A428FPQ/1.

Doar WR, Kendall CGSC. 2014. An analysis and comparison of observed Pleistocene South Carolina (USA) shoreline elevations with predicted elevations derived from Marine Oxygen Isotope Stages. Quaternary Research **82**:164–174.

Dodd JR. 1965. Environmental control of strontium and magnesium in *Mytilus*. Geochimica et Cosmochimica Acta **29**:385–398.

Dodd JR, Crisp EL. 1982. Non-linear variation with salinity of Sr/Ca and Mg/Ca ratios in water and aragonitic bivalve shells and implications for paleosalinity studies. Palaeogeography, Palaeoclimatology, Palaeoecology **38**:45–56.

Dominguez JG, Kosnik MA, Allen AP, Hua Q, Jacob DE, Kaufman DS, Whitacre K. 2016. Time-averaging and stratigraphic resolution in death assemblages and Holocene deposits: Sydney Harbour's molluscan record. PALAIOS **31**:563–574.

Doney SC et al. 2012. Climate change impacts on marine ecosystems. Annual Review of Marine Science **4**:11–37.

DuBar JR. 1971. Neogene stratigraphy of the Lower Coastal Plain of the Carolinas. South Carolina Geological Survey, Myrtle Beach, South Carolina.

Dubar JR, Johnson HS, Thom B, Hatchell WO. 1974. Neogene stratigraphy and morphology, south flank of the Cape Fear Arch, North and South Carolina. In: Oaks Jr., Robert W., DuBar, Jules R. (Eds.), Post-Miocene Stratigraphy Central and Southern:139–173.

Durham SR, Gillikin DP, Goodwin DH, Dietl GP. in press. Rapid determination of oyster lifespans and growth rates using LA-ICP-MS line scans of shell Mg/Ca ratios. Palaeogeography, Palaeoclimatology, Palaeoecology. Available from http://www.sciencedirect.com/science/article/pii/S0031018217300421.

Durrant SF, Ward NI. 2005. Recent biological and environmental applications of laser ablation inductively coupled plasma mass spectrometry (LA-ICP-MS). Journal of Analytical Atomic Spectrometry **20**:821–829.

Epstein S, Mayeda T. 1953. Variation of O^{18} content of waters from natural sources. Geochimica et Cosmochimica Acta **4**:213–224.

Fabre C, Lathuiliere B. 2007. Relationships between growth-bands and paleoenvironmental proxies Sr/Ca and Mg/Ca in hypercalcified sponge: a micro-laser induced breakdown spectroscopy approach. Spectrochimica Acta Part B: Atomic Spectroscopy **62**:1537–1545.

Fan C, Koeniger P, Wang H, Frechen M. 2011. Ligamental increments of the mid-Holocene Pacific oyster *Crassostrea gigas* are reliable independent proxies for seasonality in the western Bohai Sea, China. Palaeogeography, Palaeoclimatology, Palaeoecology **299**:437–448.

Fisher B, Turner RK, Morling P. 2009. Defining and classifying ecosystem services for decision making. Ecological Economics **68**:643–653.

Flessa KW. 2009. Putting the dead to work: translational paleoecology. Pages 275–281 in G. P. Dietl and K. W. Flessa, editors. Conservation Paleobiology: Using the Past to Manage for the Future. The Paleontological Society, Yale University Printing and Publishing Services.

Flessa KW, Cutler AH, Meldahl KH. 1993. Time and taphonomy: quantitative estimates of time-averaging and stratigraphic disorder in a shallow marine habitat. Paleobiology **19**:266–286.

Ford SE, Tripp MR. 1996. Diseases and defense mechanisms. Pages 581–660 in V. S. Kennedy, R. I. E. Newell, and A. F. Eble, editors. The Eastern Oyster, *Crassostrea virginica*. Maryland Sea Grant College, College Park, MD.

Foster LC, Finch AA, Allison N, Andersson C, Clarke LJ. 2008. Mg in aragonitic bivalve shells: Seasonal variations and mode of incorporation in *Arctica islandica*. Chemical Geology **254**:113–119.

Freitas PS, Clarke LJ, Kennedy H, Richardson CA. 2012. The potential of combined Mg/Ca and $\delta^{18}O$ measurements within the shell of the bivalve *Pecten maximus* to estimate seawater $\delta^{18}O$ composition. Chemical Geology **291**:286–293.

Galtsoff PS. 1964. The American oyster *Crassostrea virginica* (Gmelin). U.S. Fish and Wildlife Service Fisheries Bulletin **64**:1–480.

Gillikin DP, Dehairs F, Baeyens W, Navez J, Lorrain A, André L. 2005. Inter- and intra-annual variations of Pb/Ca ratios in clam shells (*Mercenaria mercenaria*): a record of anthropogenic lead pollution? Marine Pollution Bulletin **50**:1530–1540.

Gillikin DP, Dehairs F, Lorrain A, Steenmans D, Baeyens W, André L. 2006a. Barium uptake into the shells of the common mussel (*Mytilus edulis*) and the potential for estuarine paleo-chemistry reconstruction. Geochimica et Cosmochimica Acta **70**:395–407.

Gillikin DP, Lorrain A, Bouillon S, Willenz P, Dehairs F. 2006b. Stable carbon isotopic composition of *Mytilus edulis* shells: relation to metabolism, salinity, $\delta^{13}C_{DIC}$ and phytoplankton. Organic Geochemistry **37**:1371–1382.

Gillooly JF. 2001. Effects of size and temperature on metabolic rate. Science **293**:2248–2251.

Goodwin DH, Cohen AN, Roopnarine PD. 2010. Forensics on the half shell: a sclerochronological investigation of a modern biological invasion in San Francisco Bay, United States. PALAIOS **25**:742–753.

Goodwin DH, Gillikin DP, Roopnarine PD. 2013. Preliminary evaluation of potential stable isotope and trace element productivity proxies in the oyster *Crassostrea gigas*. Palaeogeography, Palaeoclimatology, Palaeoecology **373**:88–97.

Goodwin DH, Schöne BR, Dettman DL. 2003. Resolution and fidelity of oxygen isotopes as paleotemperature proxies in bivalve mollusk shells: models and observations. Palaios **18**:110–125.

Grabowski JH, Peterson CH. 2007. Restoring oyster reefs to recover ecosystem services. Pages 281–298 in K. Cuddington, J. E. Byers, W. G. Wilson, and A. Hastings, editors. Ecosystem Engineers: Concepts, Theory and Applications. Elsevier-Academic Press, Amsterdam.

Graniero LE, Surge D, Gillikin DP, Briz i Godino I, Álvarez M. 2017. Assessing elemental ratios as a paleotemperature proxy in the calcite shells of patelloid limpets. Palaeogeography, Palaeoclimatology, Palaeoecology **465**, **Part B**:376–385.

Griffiths GM et al. 2005. Change in mean temperature as a predictor of extreme temperature change in the Asia–Pacific region. International Journal of Climatology **25**:1301–1330.

Gröcke DR, Gillikin DP. 2008. Advances in mollusc sclerochronology and sclerochemistry: tools for understanding climate and environment. Geo-Marine Letters **28**:265–268.

Grossman EL. 2012. Applying oxygen isotope paleothermometry in deep time. Pages 39–67 Reconstructing Earth's Deep-Time Climate--The State of the Art in 2012. Paleontological Society. Available from http://geoweb.tamu.edu/grossman/Grossman_2012_PaleoShortCourse.pdf (accessed June 22, 2015).

Hansen L, Hoffman J, Drews C, Mielbrecht E. 2010. Designing climate-smart conservation: guidance and case studies. Conservation Biology **24**:63–69.

Harding JM, Kingsley-Smith P, Savini D, Mann R. 2007. Comparison of predation signatures left by Atlantic oyster drills (*Urosalpinx cinerea* Say, Muricidae) and veined rapa whelks (*Rapana venosa* Valenciennes, Muricidae) in bivalve prey. Journal of Experimental Marine Biology and Ecology **352**:1–11.

Harding JM, Mann R. 1999. Fish species richness in relation to restored oyster reefs, Piankatank River, Virginia. Bulletin of Marine Science **65**:289–300.

Harding JM, Mann R, Southworth MJ, Wesson JA. 2010. Management of the Piankatank River, Virginia, in support of oyster (*Crassostrea virginica*, Gmelin 1791) fishery repletion. Journal of Shellfish Research **29**:867–888.

Hargis WJ, Haven DS. 1999. Chesapeake oyster reefs, their importance, destruction and guidelines for restoring them. Pages 329–358 in M. W. Luckenbach, R. Mann, and J. A. Wesson, editors. Oyster Reef Habitat Restoration: A Synopsis and Synthesis of Approaches. Virginia Institute of Marine Science Press, Gloucester Point, Virginia. Available from http://web.vims.edu/mollusc/pdffiles/HargisHaven.PDF (accessed June 25, 2014).

Harris JA, Hobbs RJ, Higgs E, Aronson J. 2006. Ecological restoration and global climate change. Restoration Ecology **14**:170–176.

Hobbs RJ et al. 2006. Novel ecosystems: theoretical and management aspects of the new ecological world order. Global Ecology and Biogeography **15**:1–7.

Hoegh-Guldberg O, Bruno JF. 2010. The impact of climate change on the world's marine ecosystems. Science **328**:1523–1528.

Hollin JT, Hearty PJ. 1990. South Carolina interglacial sites and stage 5 sea levels. Quaternary Research **33**:1–17.

Hong W, Keppens E, Nielsen P, van Riet A. 1995. Oxygen and carbon isotope study of the Holocene oyster reefs and paleoenvironmental reconstruction on the northwest coast of Bohai Bay, China. Marine Geology **124**:289–302.

Humphries AT, La Peyre MK. 2015. Oyster reef restoration supports increased nekton biomass and potential commercial fishery value. PeerJ **3**:e1111.

IPCC (Intergovernmental Panel on Climate Change). 2007. Synthesis Report. Contribution of Working Groups I, II, and III to the Fourth Assessment Report of the Intergovernmental Panel on Climate Change. IPCC, Geneva, Switzerland.

Jackson JB, Kirby MX, Berger WH, Bjorndal KA, Botsford LW, Bourque BJ, Bradbury RH, Cooke R, Erlandson J, Estes JA. 2001. Historical overfishing and the recent collapse of coastal ecosystems. Science **293**:629–637.

Jackson ST, Hobbs RJ. 2009. Ecological restoration in the light of ecological history. Science **325**:567–569.

Johnson ALA, Liquorish MN, Sha J. 2007. Variation in growth-rate and form of a Bathonian (Middle Jurassic) oyster in England, and its environmental implications. Palaeontology **50**:1155–1173.

Jones DS, Arthur MA, Allard DJ. 1989. Sclerochronological records of temperature and growth from shells of *Mercenaria mercenaria* from Narragansett Bay, Rhode Island. Marine Biology **102**:225–234.

Kelley PH, Hansen TA. 2003. The fossil record of drilling predation on bivalves and gastropods. Pages 113–139 in P. H. Kelley, M. Kowalewski, and T. A. Hansen, editors. Predator-Prey Interactions in the Fossil Record. Kluwer Academic/Plenum Publishers, New York.

Kennedy VS, Breitburg DL, Christman MC, Luckenbach MW, Paynter K, Kramer J, Sellner KG, Dew-Baxter J, Keller C, Mann R. 2011. Lessons learned from efforts to restore oyster populations in Maryland and Virginia, 1990 to 2007. Journal of Shellfish Research **30**:719–731.

Kent BW. 1992. Making Dead Oysters Talk: Techniques for Analyzing Oysters from Archaeological Sites. Maryland Historical & Cultural Publications, Crownsville, MD.

Kidwell SM. 2007. Discordance between living and death assemblages as evidence for anthropogenic ecological change. Proceedings of the National Academy of Sciences **104**:17701–17706.

Kidwell SM. 2013. Time-averaging and fidelity of modern death assemblages: building a taphonomic foundation for conservation palaeobiology. Palaeontology **56**:487–522.

Kirby MX. 2001. Differences in growth rate and environment between Tertiary and Quaternary *Crassostrea* oysters. Paleobiology **27**:84–103.

Kirby MX, Miller HM. 2005. Response of a benthic suspension feeder (*Crassostrea virginica* Gmelin) to three centuries of anthropogenic eutrophication in Chesapeake Bay. Estuarine, Coastal and Shelf Science **62**:679–689.

Kirby MX, Soniat TM, Spero HJ. 1998. Stable isotope sclerochronology of Pleistocene and Recent oyster shells (*Crassostrea virginica*). PALAIOS **13**:560–569.

Kirtman B et al. 2013. Near-term climate change: projections and predictability. Pages 953–1028 in T. F. Stocker, G.-K. Plattner, M. Tignor, S. K. Allen, J. Boschung, A. Nauels, Y. Xia, V. Bex, and P. M. Midgley, editors. Climate Change 2013: The Physical Science Basis. Contribution of Working Group I to the Fifth Assessment Report of the Intergovernmental Panel on Climate Change. Cambridge University Press, New York, NY. Available from http://pure.iiasa.ac.at/10550 (accessed July 17, 2017).

Klein RT, Lohmann KC, Thayer CW. 1996. Bivalve skeletons record sea-surface temperature and $\delta^{18}O$ via Mg/Ca and $^{18}O/^{16}O$ ratios. Geology **24**:415–418.

Kosnik MA, Hua Q, Kaufman DS, Zawadzki A. 2015. Sediment accumulation, stratigraphic order, and the extent of time-averaging in lagoonal sediments: a comparison of ^{210}Pb and ^{14}C/amino acid racemization chronologies. Coral Reefs **34**:215–229.

Kosnik MA, Kaufman DS. 2008. Identifying outliers and assessing the accuracy of amino acid racemization measurements for geochronology: II. Data screening. Quaternary Geochronology **3**:328–341.

Kosnik MA, Kaufman DS, Hua Q. 2013. Radiocarbon-calibrated multiple amino acid geochronology of Holocene molluscs from Bramble and Rib Reefs (Great Barrier Reef, Australia). Quaternary Geochronology **16**:73–86.

Kowalewski M, Flessa KW, Hallman DP. 1995. Ternary taphograms: triangular diagrams applied to taphonomic analysis. PALAIOS **10**:478–483.

Kowalewski M, Goodfriend GA, Flessa KW. 1998. High-resolution estimates of temporal mixing within shell beds: the evils and virtues of time-averaging. Paleobiology **24**:287–304.

Kraeuter JN, Ford S, Cummings M. 2007. Oyster growth analysis: a comparison of methods. Journal of Shellfish Research **26**:479–491.

Kurlansky M. 2006. The Big Oyster: History on the Half Shell. Ballantine Books, New York.

La Peyre MK, Serra K, Joyner TA, Humphries A. 2015. Assessing shoreline exposure and oyster habitat suitability maximizes potential success for sustainable shoreline protection using restored oyster reefs. PeerJ **3**:e1317.

Langlet D, Alunno-Bruscia M, Rafélis M, Renard M, Roux M, Schein E, Buestel D. 2006. Experimental and natural cathodoluminescence in the shell of *Crassostrea gigas* from Thau lagoon (France): ecological and environmental implications. Marine Ecology Progress Series **317**:143–156.

Lartaud F, de Rafelis M, Ropert M, Emmanuel L, Geairon P, Renard M. 2010. Mn labelling of living oysters: artificial and natural cathodoluminescence analyses as a tool for age and growth rate determination of *C. gigas* (Thunberg, 1793) shells. Aquaculture **300**:206–217.

Lawrence DR. 1968. Taphonomy and information losses in fossil communities. Geological Society of America Bulletin **79**:1315–1330.

Levinton J, Doall M, Allam B. 2013. Growth and mortality patterns of the eastern oyster *Crassostrea virginica* in impacted waters in coastal waters in New York, USA. Journal of Shellfish Research **32**:417–427.

Lindland E, Burt C, Edlin J, Elkins M, Leavor J, Mallon J, Myers M, Obley S, Savarese M, Goodfriend GA. 2001. Time averaging on oyster reefs: implications for environmental reconstruction and historical change. 50th Annual Meeting of the Southeastern Section of the Geological Society of America, April 5-6, 2001, Raleigh, NC.

Litchman E. 2012. Phytoplankton. Pages 154–163 in R. M. Sibly, J. H. Brown, and A. Kodric-Brown, editors. Metabolic Ecology. John Wiley & Sons, Ltd, West Sussex, UK. Available from http://onlinelibrary.wiley.com.proxy.library.cornell.edu/doi/10.1002/9781119968535.ch13/summary.

Lorrain A, Gillikin DP, Paulet Y-M, Chauvaud L, Mercier AL, Navez J, André L. 2005. Strong kinetic effects on Sr/Ca ratios in the calcitic bivalve *Pecten maximus*. Geology **33**:965–968.

Lotze HK, Lenihan HS, Bourque BJ, Bradbury RH, Cooke RG, Kay MC, Kidwell SM, Kirby MX, Peterson CH, Jackson JBC. 2006. Depletion, degradation, and recovery potental of estuaries and coastal seas. Science **312**:1806–1809.

Mann R, Harding JM, Southworth MJ. 2009. Reconstructing pre-colonial oyster demographics in the Chesapeake Bay, USA. Estuarine, Coastal and Shelf Science **85**:217–222.

Marali S, Schöne BR, Mertz-Kraus R, Griffin SM, Wanamaker Jr. AD, Butler PG, Holland HA, Jochum KP. in press. Reproducibility of trace element time-series (Na/Ca, Mg/Ca, Mn/Ca, Sr/Ca, and Ba/Ca) within and between specimens of the bivalve *Arctica islandica* – a LA-ICP-MS line scan study. Palaeogeography, Palaeoclimatology, Palaeoecology:20pp.

McCartan L, Owens JP, Blackwelder BW, Szabo BJ, Belknap DF, Kriausakul N, Mitterer RM, Wehmiller JF. 1982. Comparison of amino acid racemization geochronometry with lithostratigraphy, biostratigraphy, uranium-series coral dating, and magnetostratigraphy in the Atlantic Coastal Plain of the southeastern United States. Quaternary Research **18**:337–359.

McKay NP, Overpeck JT, Otto-Bliesner BL. 2011. The role of ocean thermal expansion in Last Interglacial sea level rise. Geophysical Research Letters **38**:L14605.

McManus J, Oppo D, Cullen J, Healey S. 2003. Marine Isotope Stage 11 (MIS 11): analog for Holocene and future climate? Pages 69–85 in A. W. Droxler, R. Z. Poore, and L. H. Burckle, editors. Geophysical Monograph Series. American Geophysical Union, Washington, D. C. Available from http://doi.wiley.com/10.1029/137GM06 (accessed November 10, 2014).

Mearns LO, Katz RW, Schneider SH. 1984. Extreme high-temperature events: changes in their probabilities with changes in mean temperature. Journal of Climate and Applied Meteorology **23**:1601–1613.

Mook WG, Tan FC. 1991. Stable carbon isotopes in rivers and estuaries. Pages 245–264 in E. T. Degens, S. Kempe, and J. E. Richey, editors. Biogeochemistry of Major World Rivers. John Wiley & Sons, Ltd, New York.

Moss DK, Ivany LC, Judd EJ, Cummings PW, Bearden CE, Kim W-J, Artruc EG, Driscoll JR. 2016. Lifespan, growth rate, and body size across latitude in marine Bivalvia, with implications for Phanerozoic evolution. Proc. R. Soc. B **283**:20161364.

Moss DK, Ivany LC, Silver RB, Schue J, Artruc EG. 2017. High-latitude settings promote extreme longevity in fossil marine bivalves. Paleobiology **43**:365–382.

Mouchi V, de Rafélis M, Lartaud F, Fialin M, Verrecchia E. 2013. Chemical labelling of oyster shells used for time-calibrated high-resolution Mg/Ca ratios: A tool for estimation of past seasonal temperature variations. Palaeogeography, Palaeoclimatology, Palaeoecology **373**:66–74.

Muhs DR, Wehmiller JF, Simmons KR, York LL. 2003. Quaternary sea-level history of the United States. Pages 147–183 Developments in Quaternary Sciences. Elsevier. Available from http://linkinghub.elsevier.com/retrieve/pii/S157108660301008X (accessed June 27, 2017).

Munch SB, Salinas S. 2009. Latitudinal variation in lifespan within species is explained by the metabolic theory of ecology. Proceedings of the National Academy of Sciences **106**:13860–13864.

Nadeau CP, Fuller AK, Rosenblatt DL. 2015. Climate-smart management of biodiversity. Ecosphere **6**:1–17.

NRC (National Research Council). 2005. The Geological Record of Ecological Dynamics: Understanding the Biotic Effects of Future Environmental Change. The National Academies Press, Washington, D.C. Available from http://www.nap.edu/catalog.php?record_id=11209 (accessed June 5, 2014).

NRC (National Research Council). 2017. Effective Monitoring to Evaluate Ecological Restoration in the Gulf of Mexico. National Academies Press, Washington, D.C. Available from https://www.nap.edu/catalog/23476/effective-monitoring-to-evaluate-ecological-restoration-in-the-gulf-of-mexico (accessed July 15, 2017).

NOAA FOHC (Fisheries Office of Habitat Conservation). 2013, August 19. Oyster Habitat Restoration Monitoring Factsheet. NOAA. Available from http://www.habitat.noaa.gov/partners/toolkits/restoration_center_toolkits/forms_and_guidance_documents/oyster_restoration_monitoring_factsheet.pdf (accessed July 8, 2014).

NOAA ORR (Office of Response and Restoration). 2013, February 14. About DARRP. Available from http://www.darrp.noaa.gov/about/ (accessed July 9, 2014).

O'Connor MI, Bruno JF, Gaines SD, Halpern BS, Lester SE, Kinlan BP, Weiss JM. 2007. Temperature control of larval dispersal and the implications for marine ecology, evolution, and conservation. Proceedings of the National Academy of Sciences **104**:1266–1271.

O'Connor MI, Piehler MF, Leech DM, Anton A, Bruno JF. 2009. Warming and resource availability shift food web structure and metabolism. PLoS Biology **7**:e1000178.

O'Neil DD, Gillikin DP. 2014. Do freshwater mussel shells record road-salt pollution? Scientific Reports **4**:srep07168.

Oomori T, Kaneshima H, Maezato Y, Kitano Y. 1987. Distribution coefficient of Mg^{2+} ions between calcite and solution at 10–50°C. Marine Chemistry **20**:327–336.

Parker LM, O'Connor WA, Byrne M, Coleman RA, Virtue P, Dove M, Gibbs M, Spohr L, Scanes E, Ross PM. 2017. Adult exposure to ocean acidification is maladaptive for larvae of the Sydney rock oyster *Saccostrea glomerata* in the presence of multiple stressors. Biology Letters **13**:20160798.

Parker LM, Ross PM, O'Connor WA, Borysko L, Raftos DA, Pörtner H-O. 2012. Adult exposure influences offspring response to ocean acidification in oysters. Global Change Biology **18**:82–92.

Pauly D. 1995. Anecdotes and the shifting baseline syndrome of fisheries. Trends in Ecology & Evolution **10**:430.

Pearce NJG, Perkins WT, Westgate JA, Gorton MP, Jackson SE, Neal CR, Chenery SP. 1997. A compilation of new and published major and trace element data for NIST SRM 610 and NIST SRM 612 glass reference materials. Geostandards Newsletter **21**:115–144.

Penkman KEH, Kaufman DS, Maddy D, Collins MJ. 2008. Closed-system behaviour of the intra-crystalline fraction of amino acids in mollusc shells. Quaternary Geochronology **3**:2–25.

Pilkey OH, Goodell HG. 1964. Comparison of the composition of fossil and recent mollusk shells. GSA Bulletin **75**:217–228.

Poulain C, Gillikin DP, Thébault J, Munaron JM, Bohn M, Robert R, Paulet Y-M, Lorrain A. 2015. An evaluation of Mg/Ca, Sr/Ca, and Ba/Ca ratios as environmental proxies in aragonite bivalve shells. Chemical Geology **396**:42–50.

Railsback LB, Anderson TF, Ackerly SC, Cisne JL. 1989. Paleoceanographic modeling of temperature-salinity profiles from stable isotopic data. Paleoceanography **4**:585–591.

Rasband WS. 1997. ImageJ. U. S. National Institutes of Health, Bethesda, Maryland, USA. Available from http://imagej.nih.gov/ij/ (accessed June 12, 2016).

Richardson CA, Collis SA, Ekaratne K, Dare P, Key D. 1993. The age determination and growth rate of the European flat oyster, *Ostrea edulis*, in British waters determined from acetate peels of umbo growth lines. ICES Journal of Marine Science: Journal du Conseil **50**:493–500.

Richardson CA, Peharda M, Kennedy H, Kennedy P, Onofri V. 2004. Age, growth rate and season of recruitment of *Pinna nobilis* (L) in the Croatian Adriatic determined from Mg:Ca and Sr:Ca shell profiles. Journal of Experimental Marine Biology and Ecology **299**:1–16.

Richardson CA, Saurel C, Barroso CM, Thain J. 2005. Evaluation of the age of the red whelk *Neptunea antiqua* using statoliths, opercula and element ratios in the shell. Journal of Experimental Marine Biology and Ecology **325**:55–64.

Rick TC et al. 2016. Millennial-scale sustainability of the Chesapeake Bay Native American oyster fishery. Proceedings of the National Academy of Sciences:201600019.

Rodrigues T, Voelker AHL, Grimalt JO, Abrantes F, Naughton F. 2011. Iberian Margin sea surface temperature during MIS 15 to 9 (580–300 ka): glacial suborbital variability versus interglacial stability. Paleoceanography **26**:PA1204.

Salvi D, Mariottini P. 2016. Molecular taxonomy in 2D: a novel ITS2 rRNA sequence-structure approach guides the description of the oysters' subfamily Saccostreinae and the genus *Magallana* (Bivalvia: Ostreidae). Zoological Journal of the Linnean Society:13pp.

Savarese M, Walker KJ, Stingu S, Marquardt WH, Thompson V. 2016. The effects of shellfish harvesting by aboriginal inhabitants of Southwest Florida (USA) on productivity of the eastern oyster: implications for estuarine management and restoration. Anthropocene **16**:28–41.

Schöne BR, Freyre Castro AD, Fiebig J, Houk SD, Oschmann W, Kröncke I. 2004. Sea surface water temperatures over the period 1884–1983 reconstructed from oxygen isotope ratios of a bivalve mollusk shell (*Arctica islandica*, southern North Sea). Palaeogeography, Palaeoclimatology, Palaeoecology **212**:215–232.

Schöne BR, Zhang Z, Jacob D, Gillikin DP, Tütken T, Garbe-Schönberg D, McConnaughey T, Soldati A. 2010. Effect of organic matrices on the determination of the trace element chemistry (Mg, Sr, Mg/Ca, Sr/Ca) of aragonitic bivalve shells (*Arctica islandica*)—comparison of ICP-OES and LA-ICP-MS data. Geochemical Journal **44**:23–37.

Schöne BR, Zhang Z, Radermacher P, Thébault J, Jacob DE, Nunn EV, Maurer A-F. 2011. Sr/Ca and Mg/Ca ratios of ontogenetically old, long-lived bivalve shells (*Arctica islandica*) and their function as paleotemperature proxies. Palaeogeography, Palaeoclimatology, Palaeoecology **302**:52–64.

Seibel BA, Drazen JC. 2007. The rate of metabolism in marine animals: environmental constraints, ecological demands and energetic opportunities. Philosophical Transactions of the Royal Society of London B: Biological Sciences **362**:2061–2078.

Sgrò CM, Lowe AJ, Hoffmann AA. 2011. Building evolutionary resilience for conserving biodiversity under climate change. Evolutionary Applications **4**:326–337.

Sherwood OA, Heikoop JM, Sinclair DJ, Scott DB, Risk MJ, Shearer C, Azetsu-Scott K. 2005. Skeletal Mg/Ca in *Primnoa resedaeformis*: relationship to temperature? Pages 1061–1079 in A. Freiwald and J. M. Roberts, editors. Cold-Water Corals and Ecosystems. Springer Berlin Heidelberg, New York. Available from http://link.springer.com/10.1007/3-540-27673-4_53 (accessed September 23, 2016).

Shumway SE. 1996. Natural environmental factors. Pages 467–513 in V. S. Kennedy, R. I. E. Newell, and A. F. Eble, editors. The Eastern Oyster, *Crassostrea virginica*. Maryland Sea Grant College, College Park, MD.

Sibly RM, Brown JH, Kodric-Brown A, editors. 2012. Metabolic Ecology: A Scaling Approach. Wiley-Blackwell, West Sussex, UK.

Smith JA, Auerbach DA, Flessa KW, Flecker AS, Dietl GP. 2016. Fossil clam shells reveal unintended carbon cycling consequences of Colorado River management. Royal Society Open Science **3**:160170.

Smith JA, Dietl GP. 2016. The value of geohistorical data in identifying a recent human-induced range expansion of a predatory gastropod in the Colorado River delta, Mexico. Journal of Biogeography **43**:791–800.

Smith JA, Durham SR, Dietl GP. in press. Conceptions of long-term data among marine conservation biologists and what conservation paleobiologists need to know. Marine Conservation Paleobiology. Springer-Verlag, New York.

SCDNRCCTWG (South Carolina Department of Natural Resources Climate Change Technical Working Group). 2013. Climate Change Impacts to Natural Resources in South Carolina. 101 pp. South Carolina Department of Natural Resources, Columbia, SC.

Spalding MD et al. 2007. Marine ecoregions of the world: a bioregionalization of coastal and shelf areas. BioScience **57**:573–583.

Speights CJ, Silliman BR, McCoy MW. 2017. The effects of elevated temperature and dissolved ρCO2 on a marine foundation species. Ecology and Evolution **7**:3808–3814.

Stein BA, Glick P, Edelson N, Staudt A, editors. 2014. Climate-Smart Conservation: Putting Adaptation Principles into Practice. National Wildlife Federation, Washington, D.C.

Suding KN. 2011. Toward an era of restoration in ecology: successes, failures, and opportunities ahead. Annual Review of Ecology, Evolution, and Systematics **42**:465–487.

Surge D, Lohmann KC. 2008. Evaluating Mg/Ca ratios as a temperature proxy in the estuarine oyster, *Crassostrea virginica*. Journal of Geophysical Research: Biogeosciences **113**:G02001.

Surge D, Lohmann KC, Dettman DL. 2001. Controls on isotopic chemistry of the American oyster, *Crassostrea virginica*: implications for growth patterns. Palaeogeography, Palaeoclimatology, Palaeoecology **172**:283–296.

Surge DM, Lohmann KC, Goodfriend GA. 2003. Reconstructing estuarine conditions: oyster shells as recorders of environmental change, Southwest Florida. Estuarine, Coastal and Shelf Science **57**:737–756.

Swart PK, Thorrold S, Rosenheim B, Eisenhauer A, Harrison CGA, Grammer M, Latkoczy C. 2002. Intra-annual variation in the stable oxygen and carbon and trace element composition of sclerosponges. Paleoceanography **17**:1045.

Szabo BJ. 1985. Uranium-series dating of fossil corals from marine sediments of southeastern United States Atlantic Coastal Plain. GSA Bulletin **96**:398–406.

Takesue RK, van Geen A. 2004. Mg/Ca, Sr/Ca, and stable isotopes in modern and Holocene *Protothaca staminea* shells from a northern California coastal upwelling region. Geochimica et Cosmochimica Acta **68**:3845–3861.

Talmage SC, Gobler CJ. 2011. Effects of elevated temperature and carbon dioxide on the growth and survival of larvae and juveniles of three species of northwest Atlantic bivalves. PLOS ONE **6**:e26941.

Tewksbury JJ, Huey RB, Deutsch CA. 2008. Putting the heat on tropical animals. Science **320**:1296–1297.

Thomas KD. 2015. Molluscs emergent, Part I: themes and trends in the scientific investigation of mollusc shells as resources for archaeological research. Journal of Archaeological Science **56**:133–140.

Tomašových A, Kidwell SM. 2017. Nineteenth-century collapse of a benthic marine ecosystem on the open continental shelf. Proc. R. Soc. B **284**:20170328.

Twaddle RW, Ulm S, Hinton J, Wurster CM, Bird MI. 2016. Sclerochronological analysis of archaeological mollusc assemblages: methods, applications and future prospects. Archaeological and Anthropological Sciences **8**:359–379.

Tynan S, Opdyke BN, Walczak M, Eggins S, Dutton A. in press. Assessment of Mg/Ca in *Saccostrea glomerata* (the Sydney rock oyster) shell as a potential temperature record. Palaeogeography, Palaeoclimatology, Palaeoecology. Available from http://www.sciencedirect.com/science/article/pii/S003101821630308X (accessed March 7, 2017).

United States Geological Survey. 2012. United States Geological Survey Preliminary Certificate of Analysis, Microanalytical Carbonate Standard, MACS-3. United States Geological Survey.

Vachon RW, Welker JM, White JWC, Vaughn BH. 2010. Monthly precipitation isoscapes ($\delta^{18}O$) of the United States: connections with surface temperatures, moisture source conditions, and air mass trajectories. Journal of Geophysical Research: Atmospheres **115**:D21126.

van Leeuwen JF, Froyd CA, Van der Knaap WO, Coffey EE, Tye A, Willis KJ. 2008. Fossil pollen as a guide to conservation in the Galápagos. Science **322**:1206–1206.

Vander Putten E, Dehairs F, André L, Baeyens W. 1999. Quantitative in situ microanalysis of minor and trace elements in biogenic calcite using infrared laser ablation – inductively coupled plasma mass spectrometry: a critical evaluation. Analytica Chimica Acta **378**:261–272.

Volety AK, Savarese M, Hoye B, Loh AN. 2009. Landscape Pattern: Present and Past Distribution of Oysters in South Florida Coastal Complex (Whitewater Bay/Oyster Bay/Shark to Robert's Rivers). 192 pp. Report to the South Florida Water Management District. Florida Gulf Coast University, Fort Myers, FL.

Waldbusser GG, Voigt EP, Bergschneider H, Green MA, Newell RIE. 2011. Biocalcification in the eastern oyster (*Crassostrea virginica*) in relation to long-term trends in Chesapeake Bay pH. Estuaries and Coasts **34**:221–231.

Walker B, Holling CS, Carpenter SR, Kinzig A. 2004. Resilience, adaptability and transformability in social–ecological systems. Ecology and society **9**:5.

Walker SE. 2007. Traces of gastropod predation on molluscan prey in tropical reef environments. Pages 324–344 in W. Miller, III, editor. Trace Fossils: Concepts, Problems, Prospects. Elsevier, New York.

Wanamaker Jr AD, Kreutz KJ, Wilson T, Borns Jr HW, Introne DS, Feindel S. 2008. Experimentally determined Mg/Ca and Sr/Ca ratios in juvenile bivalve calcite for *Mytilus edulis*: implications for paleotemperature reconstructions. Geo-Marine Letters **28**:359–368.

Watanabe T, Winter A, Oba T. 2001. Seasonal changes in sea surface temperature and salinity during the Little Ice Age in the Caribbean Sea deduced from Mg/Ca and $^{18}O/^{16}O$ ratios in corals. Marine Geology **173**:21–35.

Wehmiller JF. 2013a. United States Quaternary coastal sequences and molluscan racemization geochronology – What have they meant for each other over the past 45 years? Quaternary Geochronology **16**:3–20.

Wehmiller JF. 2013b. Interlaboratory comparison of amino acid enantiomeric ratios in Pleistocene fossils. Quaternary Geochronology **16**:173–182.

Wehmiller JF, Belknap DF. 1982. Amino acid age estimates, Quaternary Atlantic coastal plain: comparison with U-series dates, biostratigraphy, and paleomagnetic control. Quaternary Research **18**:311–336.

Wehmiller JF, Belknap DF, Boutin BS, Mirecki JE, Rahaim SD, York LL. 1988. A review of the aminostratigraphy of Quaternary mollusks from United States Atlantic Coastal Plain sites. Geological Society of America Special Papers **227**:69–110.

Wehmiller JF, Miller GH. 2000. Aminostratigraphic dating methods in Quaternary geology. Pages 187–222 in J. S. Noller, J. M. Sowers, and W. R. Lettis, editors. Quaternary Geochronology: Methods and Applications. American Geophysical Union. Available from http://onlinelibrary.wiley.com.proxy.library.cornell.edu/doi/10.1029/RF004p0187/summary (accessed February 23, 2015).

Wells HW. 1961. The fauna of oyster beds, with special reference to the salinity factor. Ecological Monographs **31**:239.

White ME, Wilson EA. 1996. Predators, pests, and competitors. Pages 581–660 in V. S. Kennedy, R. I. E. Newell, and A. F. Eble, editors. The Eastern Oyster, *Crassostrea virginica*. Maryland Sea Grant College, College Park, MD.

Wiens JA, Hayward GD, Safford HD, Giffen CM, editors. 2012. Historical Environmental Variation in Conservation and Natural Resource Management. Wiley-Blackwell, West Sussex, UK.

Williams JW, Jackson ST. 2007. Novel climates, no-analog communities, and ecological surprises. Frontiers in Ecology and the Environment **5**:475–482.

Willis KJ, Araujo MB, Bennett KD, Figueroa-Rangel B, Froyd CA, Myers N. 2007. How can a knowledge of the past help to conserve the future? Biodiversity conservation and the relevance of long-term ecological studies. Philosophical Transactions of the Royal Society B: Biological Sciences **362**:175–187.

Willis KJ, Bailey RM, Bhagwat SA, Birks HJB. 2010a. Biodiversity baselines, thresholds and resilience: testing predictions and assumptions using palaeoecological data. Trends in Ecology & Evolution **25**:583–591.

Willis KJ, Bennett KD, Bhagwat SA, Birks HJB. 2010b. 4 °C and beyond: what did this mean for biodiversity in the past? Systematics and Biodiversity **8**:3–9.

Willis KJ, Bhagwat SA. 2009. Biodiversity and climate change. Science **326**:806–807.

Willis KJ, Birks HJB. 2006. What is natural? The need for a long-term perspective in biodiversity conservation. Science **314**:1261–1265.

Willis KJ, MacDonald GM. 2011. Long-term ecological records and their relevance to climate change predictions for a warmer world. Annual Review of Ecology, Evolution, and Systematics **42**:267–287.

Wingard GL, Hudley JW. 2012. Application of a weighted-averaging method for determining paleosalinity: a tool for restoration of South Florida's estuaries. Estuaries and Coasts **35**:262–280.

zu Ermgassen PSE, Spalding MD, Grizzle RE, Brumbaugh RD. 2013. Quantifying the loss of a marine ecosystem service: filtration by the eastern oyster in US estuaries. Estuaries and Coasts **36**:36–43.

Zuo W, Moses ME, West GB, Hou C, Brown JH. 2012. A general model for effects of temperature on ectotherm ontogenetic growth and development. Proceedings of the Royal Society B: Biological Sciences **279**:1840–1846.

APPENDIX 1.1

A1.1.1 Survey questions

The following are the survey questions used to assess restorationprofessionals perspectivesongeohistoricaldataandtheiruse in oyster restoration. The questions and answer choices are listed in the order in which they appeared on the web survey, and are split into three categories: research background, perspectives on geohistorical data, and demographic information.

Research Background

1. Please indicate your primary oyster species of interest:
    a. Crassostrea virginica
    b. Crassostrea gigas
    c. Ostrea conchaphila
    d. Ostrea lurida
    e. Other:_____
2. If you work in the United States, which state(s) does yourwork primarily affect?
3. If you work outside the United States, which country doesyour work primarily affect?
4. How many years of experience do you have in your field?
    a. <5 y
    b. 5–10 y
    c. 10–15 y
    d. 15–20 y
    e. 20–25 y
    f. >25 y

5. Please list at least three sources that you read and/orpublish in for your oyster work. (Please name specific scientific journal titles, government documents, technical reports, conference proceedings, etc.)
6. Please provide a brief description of your work as it relatesto oyster restoration (e.g., research, constructing living shorelines, disease prevention, depositing cultch, etc.). (1 paragraph max.)
7. How do you define success for an oyster restorationproject? In other words, what goal(s) must be accomplished before restoration is considered complete?

Perspectives on Geohistorical Data

8. Lotze et al. (2006) used the following cultural periods toexamine changing human impacts on estuaries and coastal seas through time. Which of the following best defines the timeframeofthebaseline conditionsusedinyourrestoration work? Check all that apply. Dates are approximate ranges based on Chesapeake Bay, MD (from Lotze et al. 2006).
   a. Baselines dont apply to my work
   b. Global market 2 (1950 CE to present)
   c. Global market 1 (1900 CE to 1950 CE)
   d. Market-colonial development (1700 CE to 1900 CE)
   e. Market-colonial establishment (1600 CE to 1700 CE)
   f. Agricultural (1200 CE to 1600 CE)
   g. Hunter-gatherer (8000 BCE to 1200 CE)
   h. Prehuman (before 8000 BCE)

9a. How informative do you think geohistorical data are for conservation/restoration practice? (Please select one.)
   a. Very informative
   b. Sometimes informative

c. Not informative

d. Unsure

e. Other: _____

9b. Please comment on your answer to 9a: why are or why aren't geohistorical data informative for conservation/ restoration practice in your opinion?

10a. Do you know of any successful applications of geohistorical data in oyster restoration?

a. Yes

b. No

10b. If your answer was Yes to Question 10a, please briefly describe the success story. If possible, please provide a citation.

11a. The NOAA Fisheries Office of Habitat Conservation defines the following universal metrics (UM), universal environmental variables (UEV), and restoration variables (RV) as important to track for oyster restoration. In your opinion, which of these values can be accurately assessed in the past using geohistorical data? (Please check all that apply.)

a. Reef areal dimension (UM)

b. Reef height (UM

c. Oyster density (UM)

d. Oyster size-frequency distribution (UM)

e. Water temperature (UEV)

f. Salinity (UEV)

g. Dissolved oxygen (UEV)

h. Disease and pathogens (RV)

i. Predation and competition (RV)

j. Oyster reproductive status (RV)

k. None

l. Unsure

11b. How would you use these geohistorical data if you had them? (1 paragraph max.)

Demographic Information

12. Please select the race/ethnicity with which you identify.

a. Asian

b. Black

c. Hispanic

d. White

e. Other: _____

13. Please select your sex.

a. Male

b. Female

14. Select the option below that best describes your highest level of education.

a. High school diploma

b. Bachelors degree

c. Masters degree

d. Doctorate

e. Other: _____

15. Select the option(s) below that best describe(s) your job type. (Please select all that apply.)

a. Fisheries/resource manager

b. Research

c. Policy developer

d. Other: _____

16. Select the option(s) below that best describe(s) your workplace. (Please select all that apply.)

    a. Government

    b. Nongovernmental organization

    c. University/academia

    d. Museum

    e. Environmental consulting

    f. Industry

    g. Other: _____

17. Please enter an E-mail address at which you can be reached if you would like to receive the results of this survey. E-mail addresses provided here will not be distributed.

APPENDIX 1.2

A1.2.1 Population selection and survey methods

The population of 396 oyster biologists and restoration professionals was collected using: the literature; the member list of the Oyster Restoration Workgroup, a web-based community of researchers and restoration professionals working to "address questions related to shellfish restoration success" (www.oyster-restoration.org); online searches of state and federal government agencies (e.g., NOAA), academic institutions, and nongovernmental organizations (e.g., The Nature Conservancy); and recommendations from personal contacts with professionals via E-mail. The population included professionals working in 22 coastal states in the United States and a total of 14 countries; however, only nine respondents work internationally, so for the purposes of this paper, analysis was restricted to respondents working in the United States (Figure A1.2-1).

The password-protected survey was hosted on the servers of the Paleontological Research Institution in Ithaca, NY from June 20to July 31, 2013. The link to the survey was embedded in a website that contained background information on conservation paleobiology and this project, and definitions of important terms, such as baselines and geohistorical records. During the survey period, three reminder E-mails were sent and 97 responses were received from workers in the United States. The last question asked respondents to provide an E-mail address if they wanted to receive the survey results directly. Responses were otherwise anonymous and all E-mail addresses provided with survey responses were stored in a separate file on an external hard drive. This file was deleted after the results were distributed.

A1.2.2 Geographical categorization and data analysis

Respondents were categorized using the DARRP regions (NOAA ORR 2013) because oyster species and ecology differ geographically, potentially influencing the restoration and conservation practices used in any particular location, and many restoration professionals work in multiple states (Figure A1.2-1). The DAARP regions used were the following: (1) the northeast region, which encompasses East Coast states from Maine to Virginia; (2) the southeast region, which includes the East Coast and Gulf Coast states from North Carolina to Texas; and (3) the northwest and southwest regions, which together include all of the contiguous West Coast states, as well as Alaska and Hawaii. Responses from individuals whose work affects the northwest and southwest DARRP regions were combined because no respondents work only in the southwest region.

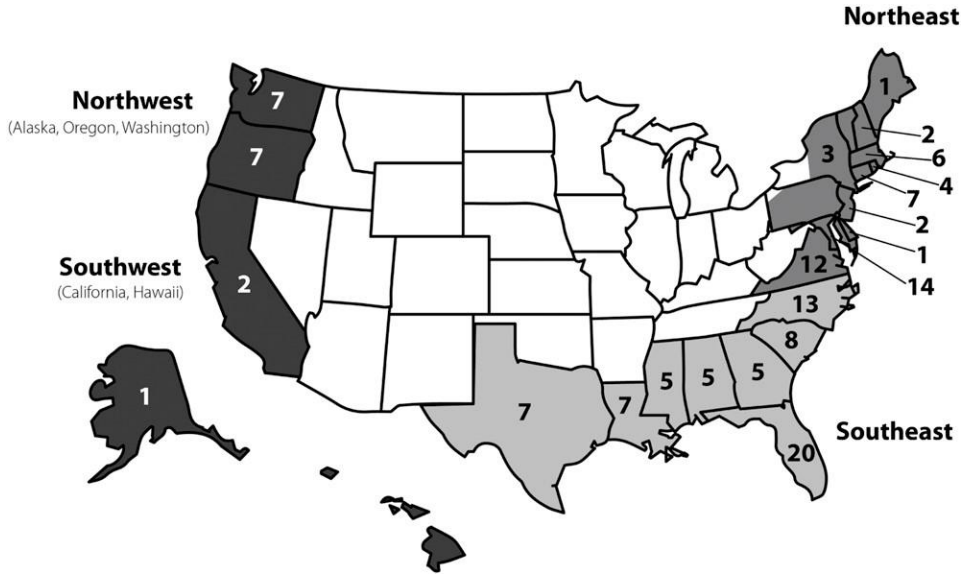

Figure A1.2-1 | Map showing the four DARRP regions covered by the respondent population. The number of respondents who indicated their work affects each state is denoted by the numbers on the map. The sum of the numbers exceeds the total number of respondents because many respondents work affected multiple states.

A1.2.3 Response categorization criteria for short answer questions

- Question 5 (sources): Respondents mentioned a wide variety of sources that they read and in which they publish. Responses ranged in specificity from individual journal articles to entire organizations; therefore all responses were categorized as either peer-reviewed literature, including books and journals, such as the Journal of Shellfish Research and Marine Ecology Progress Series, or non-peer-reviewed gray literature, such as conference proceedings and technical reports. Two of the most general responses, the World Aquaculture Society and the National Shellfisheries Association, were grouped into both categories because they are organizations that publish both peer-reviewed journals and host conferences or contribute in other ways to the non-peer-reviewed gray literature.
- Question 6 (job description): Respondents descriptions of their own jobs as they relate to oyster restoration were grouped into five categories: administration, aquaculture, education, research, and restoration. These categories were not mutually exclusive. Responses grouped into the administration category described the respondents' roles in oyster restoration as primarily supporting or managerial, e.g., coordination of training programs or regulation implementation. Responses falling into the aquaculture category mentioned involvement in activities specifically related to controlled rearing of oysters as distinct from restoration of wild populations. To be grouped into the education category respondents must have been involved in outreach or training related to oyster research and restoration. Respondents whose work was considered in the research category needed to be involved in answering research questions related to oyster biology, restoration techniques, etc. This category was distinct from the restoration category, which required that respondents discuss direct involvement in restoration practice (e.g., seeding and cultch planting operations or design, planning, and monitoring of

restoration projects), although many responses qualified for both the research and restoration categories (27%, n = 26).

- Question 7 (restoration success): Responses to Question 7 were categorized according to the groupings of oyster reef habitat characteristics outlined in Burrows et al. (2005). Other more recent restoration guides (e.g., Brumbaugh et al. 2006; Baggett et al. 2014) have updated information on oyster restoration methods and monitoring criteria, but Burrows et al. (2005) usefully divided reef habitat characteristics into two broad categories: structural characteristics (i.e., those aspects of a habitat that determine its physical organization), and functional characteristics, the ecological processes and products the habitat supports and provides, such as water filtration and foraging and breeding grounds for associated fauna. To these categories, stakeholder consensus and ecosystem services were added. These two additional categories were necessary because they are not encompassed in Burrows et al. (2005), which focused on the oyster reef habitat itself. Responses that fell into the stakeholder consensus category were those that discussed the importance of meeting the needs of multiple interest groups as a success metric. Ecosystem services, "the aspects of ecosystems utilized (actively or passively) to produce human well-being" (Fisher et al. 2009, p. 645), are distinct from functional characteristics of oyster reefs in that they are explicitly anthropocentric, thus although a respondent could have mentioned "water filtration" as a goal of their oyster restoration projects, unless they linked this goal to improving water quality for human benefit, this response was considered a "functional" criteria for restoration success and not an "ecosystem services" criteria. This distinction is not clear in Burrows et al. (2005), which defines functional characteristics of oyster habitat as "the ecological services a habitat provides" (p. 1.5). This difference was emphasized because many respondents discussed ecosystem function in their

responses without mentioning a benefit for human society. The structural and functional categories outlined by Burrows et al. (2005) include the following:

Structural characteristics

Biological

- Habitat created by animals (i.e., oysters)
- Diseases ₀ Oyster populations
- Natural recruitment levels
- Availability and integrity of substrate
- Spat abundance
- Spat survival
- Abundance and distribution of oysters on the reef

Physical

- Bathymetry/topography
- Sediment

Hydrological

- Tides/hydroperiod and currents
- Water sources
- Water temperature

Chemical

- Dissolved oxygen
- Salinity

Functional characteristics

Biological

-Provides habitat

-Complex trophic structure

-Biodiversity

-Benthic–pelagic coupling

-Provides breeding and nursery grounds

-Provides feeding grounds

-Provides substrate attachment

-Provides refuge from predation

-Supports carrying capacity/biomass production

Physical

-Reduces shoreline erosion

-Filters water and stabilizes sediments

Chemical

-Supports nutrient cycling

-Question 9b (why are/aren't geohistorical data useful?): Responses to Question 9b that discussed why geohistorical data are useful mostly focused on basic applications of geohistorical data to the production of baselines or quantifications of the HRV of aspects of oyster reef ecosystems. Some responses also included specific applications of the baseline and/or HRV to investigate research questions

related to anthropogenic changes or responses of oysters to natural disturbances such as climate change, or to applications of geohistorical data to planning or evaluating restoration projects. Thus, the positive responses fit into a spectrum from basic descriptive uses (e.g., what was it like in the past?) to applied uses in research and restoration. A two-level categorization was used for the general (baseline, HRV) and more specific (research and restoration applications) aspects of these responses because the baseline and HRV concepts are so fundamental to the use of geohistorical data (Dietl & Flessa 2011) that even specific uses for research or restoration must necessarily accept and use these concepts even if they were not explicitly mentioned in a given response.

The four general categories of responses were: baselines, HRV, other, and unsure. Most respondents were familiar with the baseline concept—the "reference conditions against which current changes can be assessed" (Dietl & Flessa 2011, p. 30). Any response that discussed using geohistorical data to reconstruct oyster reef attributes in the past qualified for this category. For a response to be grouped into the HRV category, it needed to mention using geohistorical data to reconstruct temporal variability of one or more oyster reef characteristics and/or environmental variables. Historical range of variation was defined following Wiens et al. (2012, p. 5): "the variation of ecological characteristics and processes over scales of time and space that are appropriate for a given management application". Responses categorized as other failed to answer the question, and no respondents replied that they were simply unsure.

Responses that went beyond the basic descriptive baseline and/or HRV concepts fell into one of four more specific categories: study the natural experiments of the past, research anthropogenic and non-anthropogenic change, plan/manage restoration or aquaculture projects, and evaluate restoration projects.

Responses in these categories discussed applying geohistorical data to specific research questions and/or restoration practice. Responses that described examining the responses of oysters or oyster reef ecosystems to past changes in environmental variables, such as climate change, were grouped into the study the natural experiments of the past category. Responses of species or ecosystems to natural environmental change in the past or over long timescales are often termed "natural experiments" because if the conditions are well understood, these intervals can yield information of similar quality to controlled experiments about processes that are impractical to study in a controlled laboratory or field environment (Willis & Birks 2006; Dietl & Flessa 2011). Any response that discussed researching anthropogenic impacts or distinguishing anthropogenic from natural influences on oyster reefs was grouped into the research anthropogenic and non-anthropogenic change category. Responses that involved using geohistorical data in the planning (e.g., site selection, goal development), managing, or monitoring phases of restoration projects fell into the plan/manage restoration or aquaculture projects category. Finally, the evaluate restoration projects category included responses that discussed using geohistorical data to study and evaluate "completed" restoration projects.

Responses that discussed why geohistorical data are not useful were grouped into two categories—the world has changed, so past conditions are less relevant, and geohistorical records are biased and incomplete. The first includes all responses that expressed doubt about the relevance of geohistorical data to oyster restoration because the world has changed dramatically in a very short period of time and humans have irrevocably altered much oyster reef habitat. The second category encompassed the responses that criticized the completeness and/or the biased nature of geohistorical records.

None of the positive or negative response categories were mutually exclusive, and responses frequently fell into multiple positive and/or negative categories.

-Question 10b (describe geohistorical success story): Responses to Question 10b were categorized based on the type of data described in the successful case studies being discussed. Many respondents who indicated they knew of successful applications of geohistorical data did not give sufficient detail of the case study to verify that they did, in fact, involve geohistorical data. Several responses that did give sufficient details about the case study being discussed revealed that they were not case studies involving geohistorical data. Thus, responses fell into three non-mutually exclusive categories: no details, non-geohistorical data, and geohistorical data depending on the detail level of the response and its content. Any response that mentioned the use of geohistorical data was grouped into the geohistorical data category, and those that discussed other types of data were grouped into the nongeohistorical data category. Responses that mentioned both geohistorical and nongeohistorical data were grouped into both categories. Geohistorical records were defined in the survey as "the sediment and fossil or death assemblages that provide temporal, environmental, and ecological information." This definition was based on the one from Dietl & Flessa (2011, p. 30).

-Question 11b (how would you use geohistorical data?): Responses to Question 11b were categorized using the same process that was used for Question 9b.

APPENDIX 2.1

A2.1.1 A comparison of detrending methods

This document contains plots comparing three methods of detrending the oyster shell Mg/Ca profiles produced for our study, using three examples. The first method shown (panel b in Figures A2.1-1 to A2.1-3) shows mean-subtracted data, produced by subtracting the linear regression-predicted values from the actual Mg/Ca values for each distance. This is a simple and commonly used method in sclerochronology (Cook and Holmes, 1986, Cook and Krusic, 2005). The scale remains the same as that for the raw data and there are no additional changes to the profile besides being reoriented around zero. The second method (panel c in Figures A2.1-1 to A2.1-3) shows dimensionless ratios of the actual Mg/Ca values to the linear regression-predicted values for each distance. This method results in a change of scale and a decrease in heteroscedasticity. The third detrending method (panel d in Figures A2.1-1 to A2.1-3) shows the data adjusted by the adaptive power transformation of Cook and Peters (1997). This method applies a power transformation to the data, the value of which is derived from the slope of the regression of local means against local standard deviations in logarithmic space. The power-transformed values are then detrended using mean subtraction. The adaptive power transformation homogenizes variance across the profile, thus decreasing heteroscedasticity, but is not susceptible to end-effect problems related to poor local goodness of fit and low predicted values that can bias results of the ratio method (see Cook and Peters, 1997 for further details).

Although we used the mean-subtraction detrending method for all of the profile interpretations (see Appendix 2.2), we tested the ratio and adaptive power tranformation methods because their impact on variance could be important for profile interpretations. For instance, interpreting annual cycles in the profiles would be made

easier if either or both intra-annual and higher-order annual variance was homogenized (particularly at the ends of the profiles, where interpretations were the most ambiguous). It is clear from Figures A2.1-1 to A2.1-3, however, that although these detrending methods improved the homoscedasticity of intra-annual variance slightly, they had little effect on the higher-order annual variance and did not affect the conclusions reached with regard to lifespan estimates using the mean-subtracted detrending method. Therefore, we used the simple mean-subtracted detrending method for all profiles. The alternative detrending methods likely would outperform the mean-subtraction method for profiles with greater heteroscedasticity, with higher magnitude ontogenetic trends (i.e., larger-magnitude slopes), or with less linear ontogenetic trends.

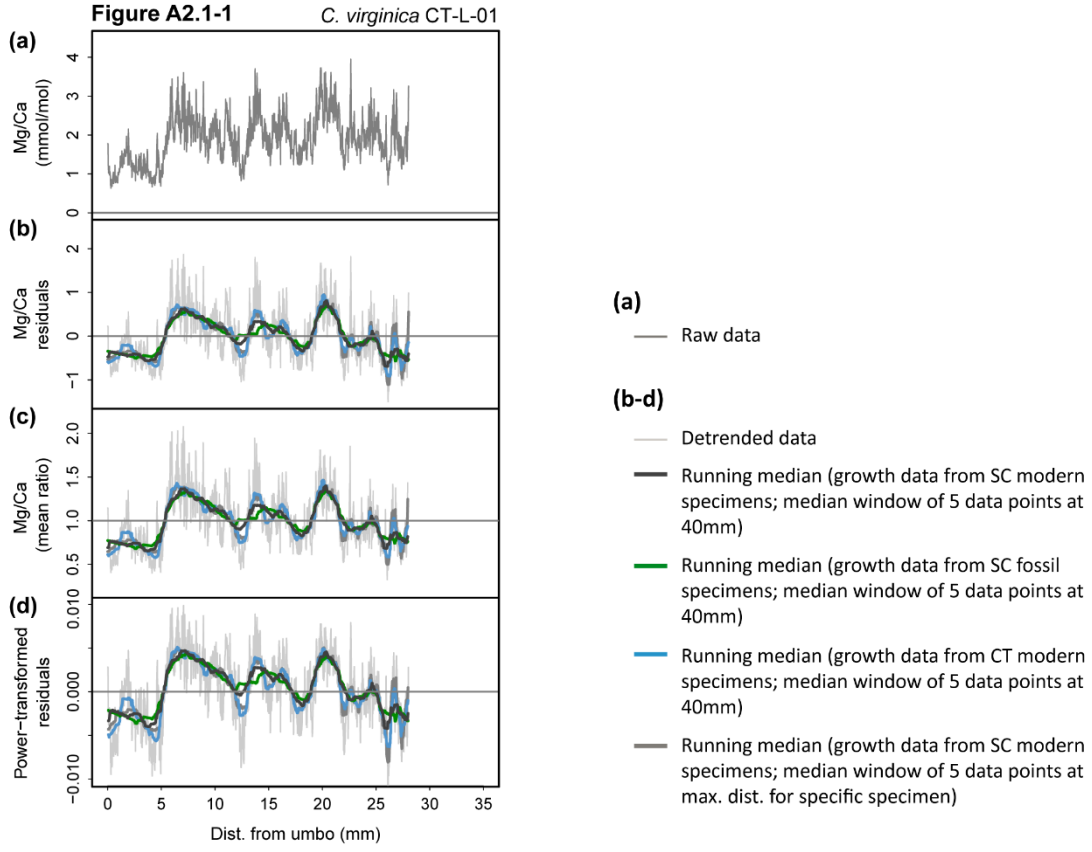

Figure A2.1-2 *C. virginica* SC-D-04

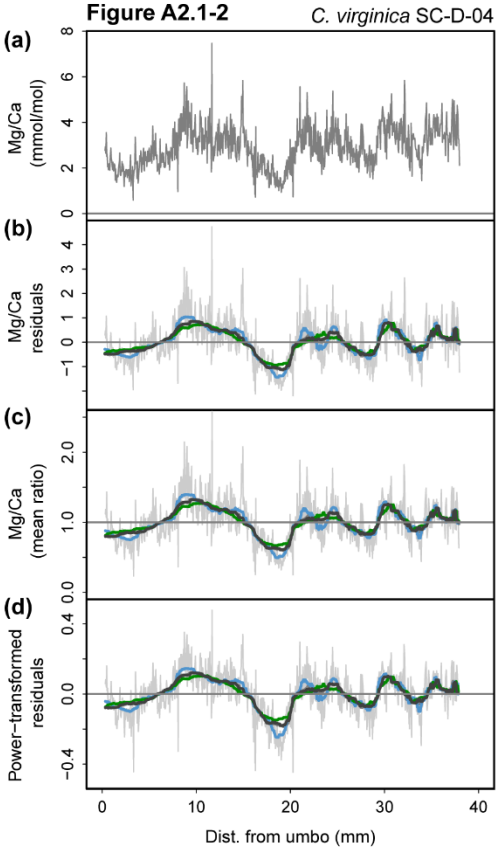

Figure A2.1-3 *C. virginica* SC-F-04

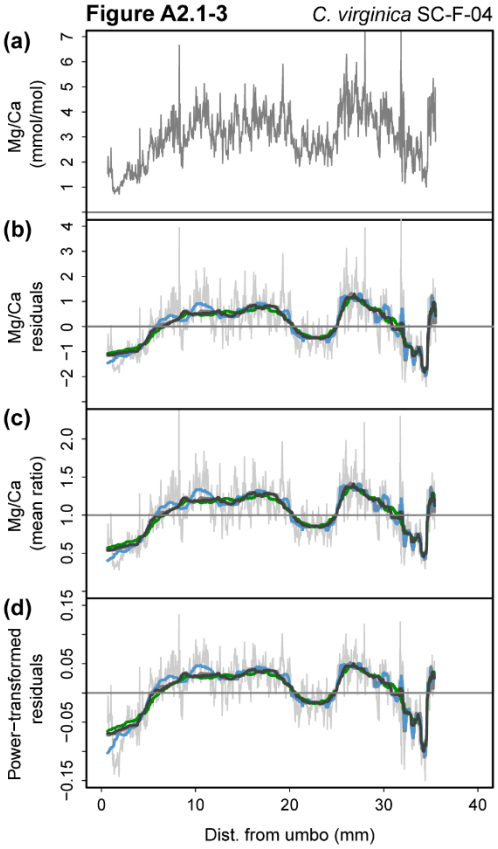

(a)

Raw data

(b-d)

Detrended data

Running median (growth data from SC modern specimens; median window of 5 data points at 40mm)

Running median (growth data from SC fossil specimens; median window of 5 data points at 40mm)

Running median (growth data from CT modern specimens; median window of 5 data points at 40mm)

Running median (growth data from SC modern specimens; median window of 5 data points at max. dist. for specific specimen)

APPENDIX 2.2

A2.2.1 Supplementary figures

This document contains plots showing the Mg/Ca profiles and the aligned $\delta^{18}O$ and $\delta^{13}C$ profiles (if applicable) for all 21 oyster specimens analyzed for our study. Each figure is composed of three panels:

(a) the raw Mg/Ca profile;

(b) the Mg/Ca profile with the linear trend subtracted and four different running medians plotted (see main text for details about the medians); and

(c) the $\delta^{18}O$ and $\delta^{13}C$ profiles.

Vertical dashed lines crossing panels (b) and (c) indicate the position of peaks and troughs in the $\delta^{18}O$ profiles, and circles at the boundary between the two panels are color-coded according to whether the oxygen profile features were considered annual and could be recognized in the Mg/Ca profiles (black = detectable, grey = present, but ambiguous without the $\delta^{18}O$ profile, white = undetectable). Peaks and troughs that were not considered annual are denoted with a white question mark inside a black square. The only exception to this labeling format is Figure A2.2-17, in which the three panels each correspond to the Mg/Ca profile for one of the North Carolina hatchery specimens. The North Carolina specimens were all of known age and under one year old, so the medians were plotted directly on the raw data for these specimens (the linear trend through these data would represent intra-annual variation in Mg/Ca, so subtracting the trend would be misleading).

A $\delta^{18}O$ peak was considered detectable in the Mg/Ca profile if all running medians crossed zero in the direction corresponding to the $\delta^{18}O$ peak. In cases where the $\delta^{18}O$ peak was visible in the Mg/Ca profile, but one or more running medians did not cross zero in the direction corresponding to the $\delta^{18}O$ peak, the peak was

considered present but ambiguous. Undetectable $\delta^{18}O$ peaks were those that would have been missed in the Mg/Ca profile in the absence of the $\delta^{18}O$ profiles. Non-annual peaks or troughs were those that, based on evidence such as the stable carbon isotope profile data or general knowledge about the specimen, were judged unlikely to be annual (and thus not informative for sclerochronology). For instance, the specimen from Louisiana (Figure A2.2-16) is most likely less than one year old based on a few lines of evidence: 1) The specimen is from the Gulf of Mexico, where oysters typically grow more rapidly compared with more northern locations (e.g., Shumway 1996) and several other specimens show resilifer growth in their first year of 10-20mm. 2) There are overall increasing and decreasing trends in the Mg/Ca and $\delta^{18}O$ profiles, respectively, over the specimen's ontogeny. 3) The one large, positive excursion in the $\delta^{18}O$ profile corresponds to a large positive excursion in the $\delta^{13}C$ profile and is not visible in the Mg/Ca profile, suggesting that this oxygen profile trough may not have been related to low temperatures (i.e., is not a winter seasonal signal).

Each plot has a title in the format:

Species XX - Y - ##

where "Species" is either *C. virginica* or *M. gigas*, "XX" is an abbreviation indicating the state in which the specimen was collected (CT = Connecticut, USA; SC = South Carolina, USA; LA = Louisiana, USA; CA = California, USA), "Y" is a letter indicating the type of specimen collected (L = live; D = modern dead; F = fossil dead), and "##" is a specimen number (unique within each state-type combination).

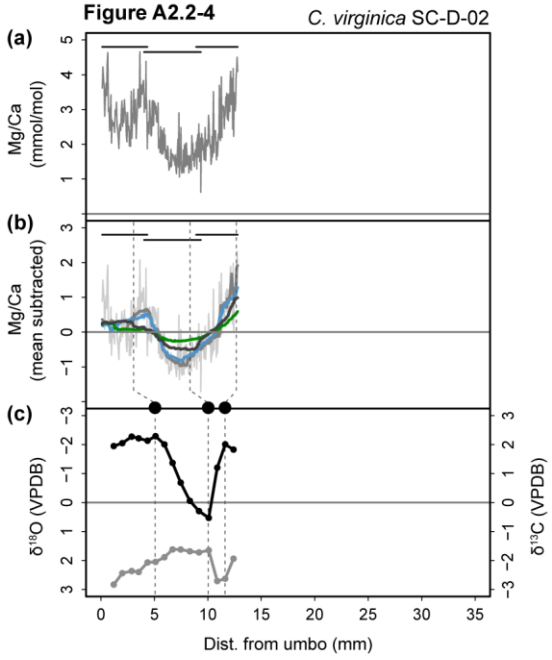
Figure A2.2-4
C. virginica SC-D-02
(a)
Mg/Ca (mmol/mol)
(b)
Mg/Ca (mean subtracted)
(c)
δ18O (VPDB)
δ13C (VPDB)
Dist. from umbo (mm)

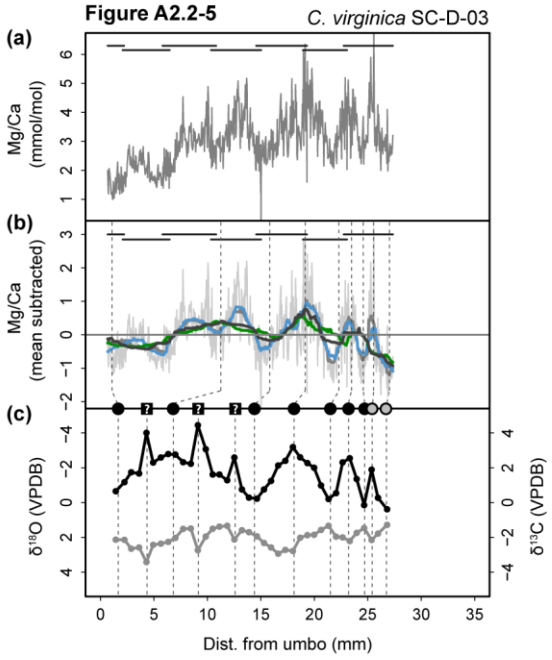
Figure A2.2-5
C. virginica SC-D-03
(a)
Mg/Ca (mmol/mol)
(b)
Mg/Ca (mean subtracted)
(c)
δ18O (VPDB)
δ13C (VPDB)
Dist. from umbo (mm)

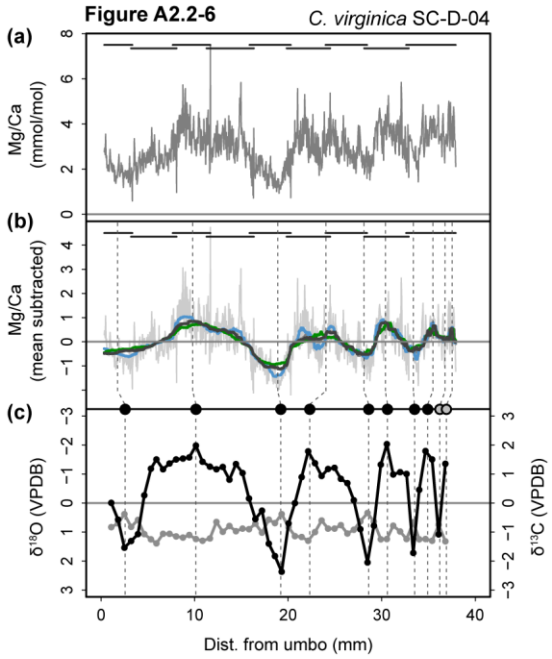
Figure A2.2-6
C. virginica SC-D-04
(a)
Mg/Ca (mmol/mol)
(b)
Mg/Ca (mean subtracted)
(c)
δ18O (VPDB)
δ13C (VPDB)
Dist. from umbo (mm)

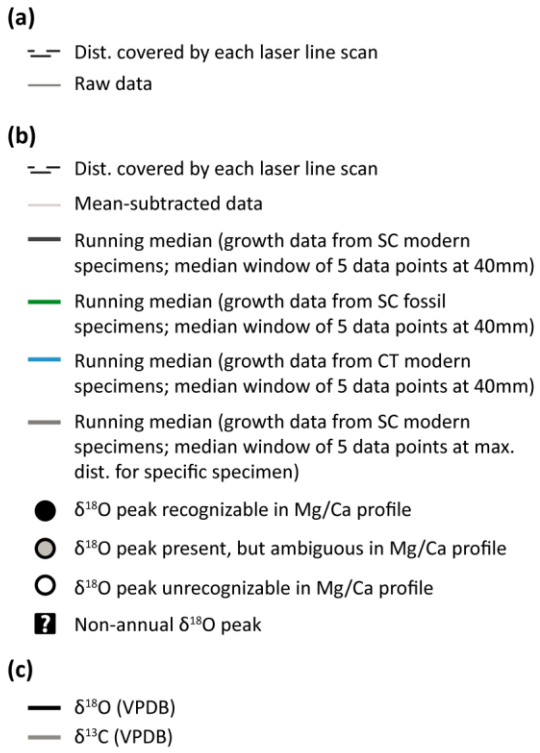
(a)
Dist. covered by each laser line scan
Raw data
(b)
Dist. covered by each laser line scan
Mean-subtracted data
Running median (growth data from SC modern specimens; median window of 5 data points at 40mm)
Running median (growth data from SC fossil specimens; median window of 5 data points at 40mm)
Running median (growth data from CT modern specimens; median window of 5 data points at 40mm)
Running median (growth data from SC modern specimens; median window of 5 data points at max. dist. for specific specimen)
δ18O peak recognizable in Mg/Ca profile
δ18O peak present, but ambiguous in Mg/Ca profile
δ18O peak unrecognizable in Mg/Ca profile
Non-annual δ18O peak
(c)
δ18O (VPDB)
δ13C (VPDB)

Figure A2.2-1 *C. virginica* CT-L-01

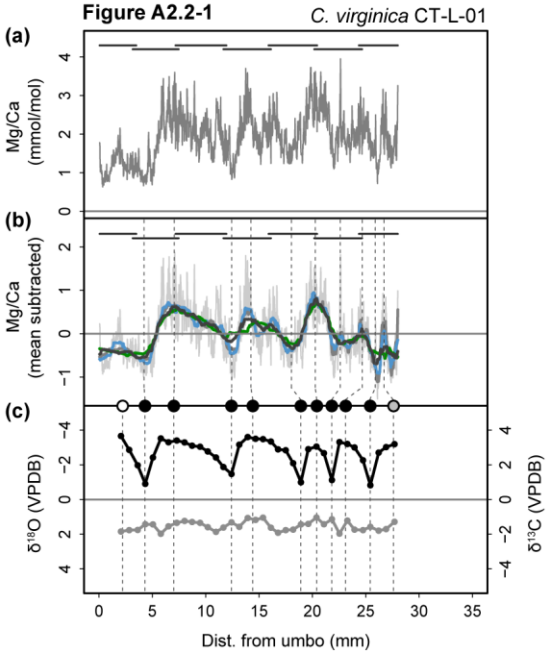

Figure A2.2-2 *C. virginica* SC-L-01

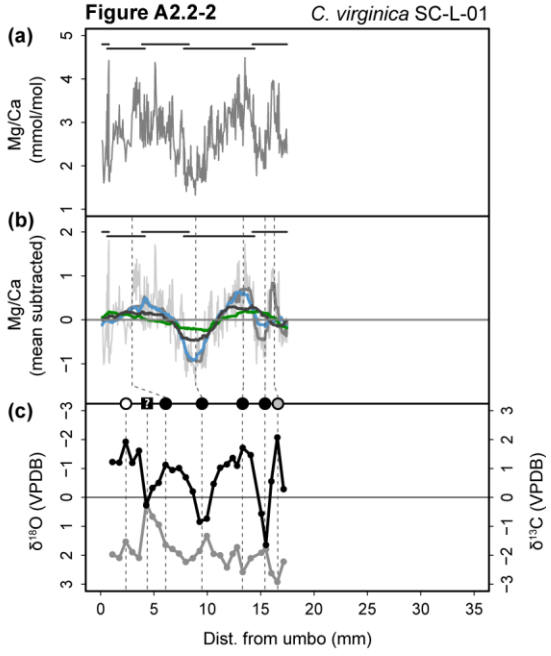

Figure A2.2-3 *C. virginica* SC-D-01

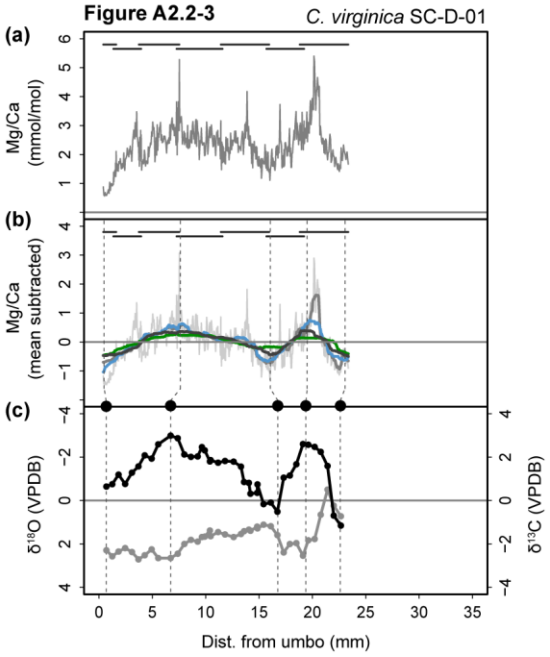

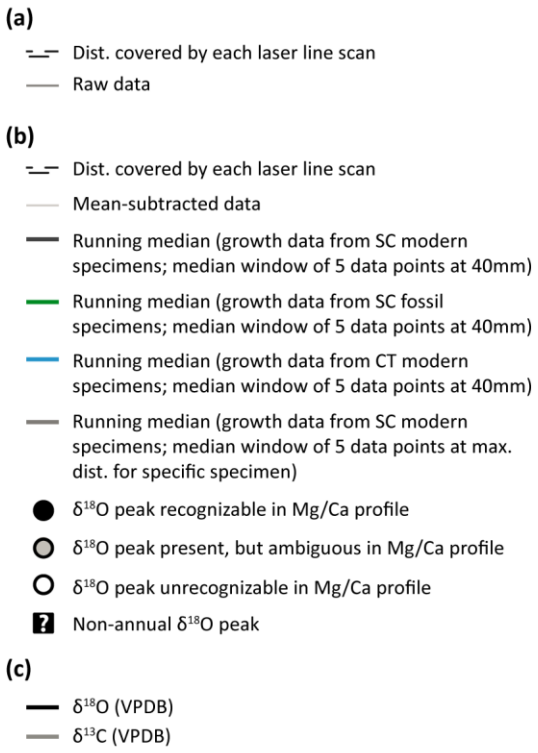

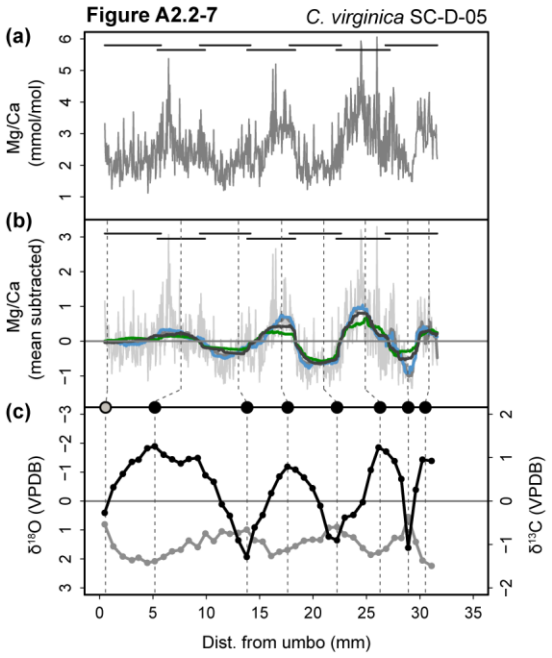
Figure A2.2-7
C. virginica SC-D-05
(a)
Mg/Ca (mmol/mol)
(b)
Mg/Ca (mean subtracted)
(c)
δ18O (VPDB)
δ13C (VPDB)
Dist. from umbo (mm)

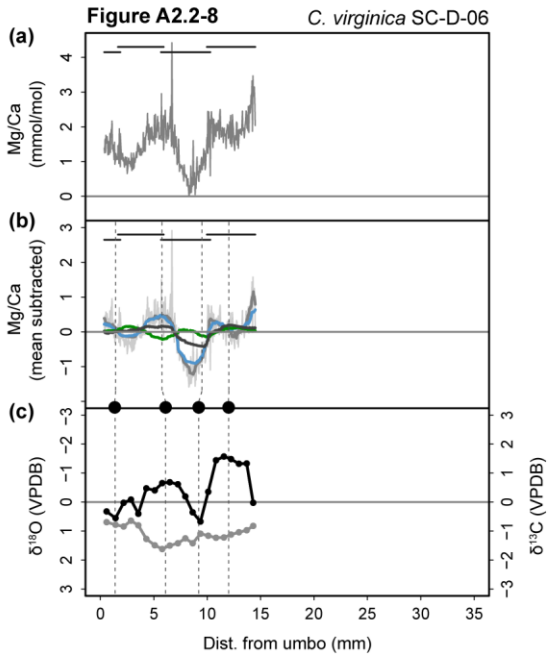
Figure A2.2-8
C. virginica SC-D-06
(a)
Mg/Ca (mmol/mol)
(b)
Mg/Ca (mean subtracted)
(c)
δ18O (VPDB)
δ13C (VPDB)
Dist. from umbo (mm)

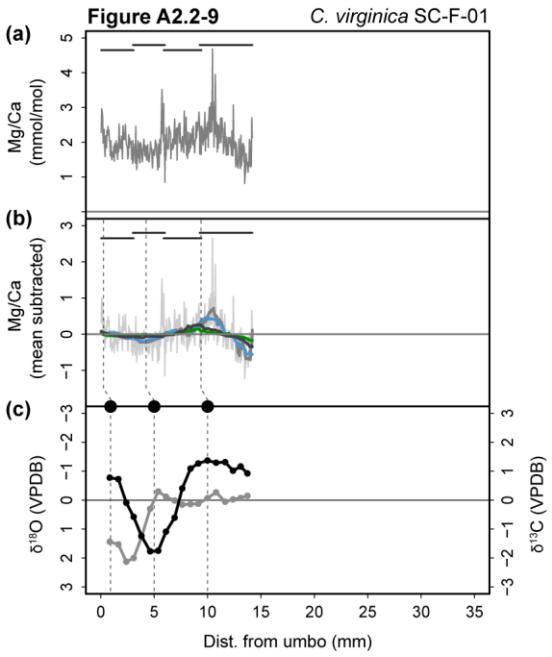
Figure A2.2-9
C. virginica SC-F-01
(a)
Mg/Ca (mmol/mol)
(b)
Mg/Ca (mean subtracted)
(c)
δ18O (VPDB)
δ13C (VPDB)
Dist. from umbo (mm)

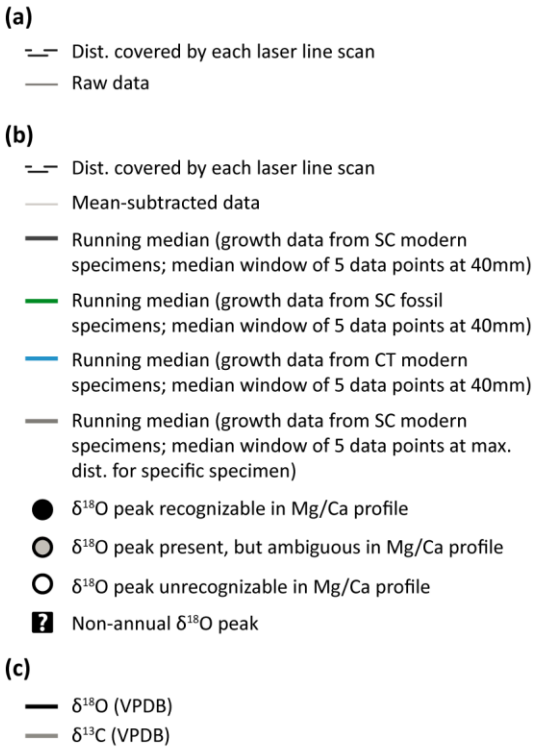
(a)
Dist. covered by each laser line scan
Raw data
(b)
Dist. covered by each laser line scan
Mean-subtracted data
Running median (growth data from SC modern specimens; median window of 5 data points at 40mm)
Running median (growth data from SC fossil specimens; median window of 5 data points at 40mm)
Running median (growth data from CT modern specimens; median window of 5 data points at 40mm)
Running median (growth data from SC modern specimens; median window of 5 data points at max. dist. for specific specimen)
δ18O peak recognizable in Mg/Ca profile
δ18O peak present, but ambiguous in Mg/Ca profile
δ18O peak unrecognizable in Mg/Ca profile
Non-annual δ18O peak
(c)
δ18O (VPDB)
δ13C (VPDB)

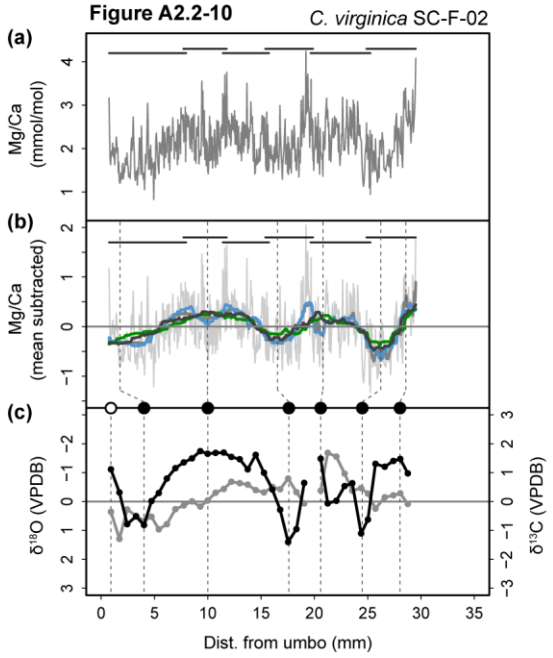
Figure A2.2-10
C. virginica SC-F-02
(a)
Mg/Ca (mmol/mol)
(b)
Mg/Ca (mean subtracted)
(c)
δ18O (VPDB)
δ13C (VPDB)
Dist. from umbo (mm)

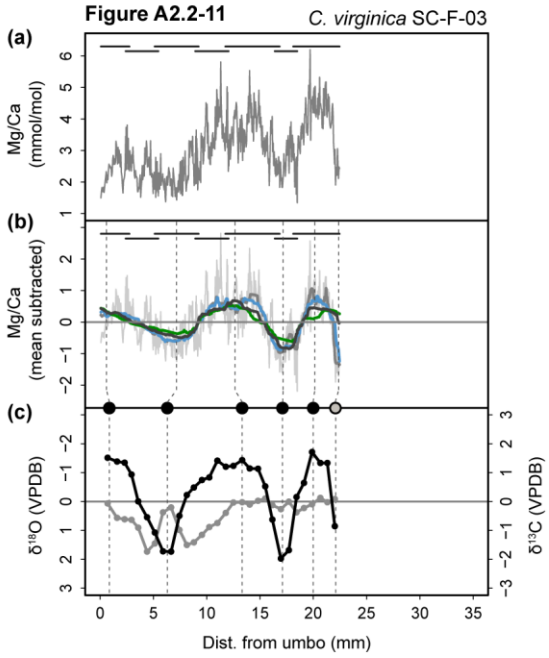
Figure A2.2-11
C. virginica SC-F-03
(a)
Mg/Ca (mmol/mol)
(b)
Mg/Ca (mean subtracted)
(c)
δ18O (VPDB)
δ13C (VPDB)
Dist. from umbo (mm)

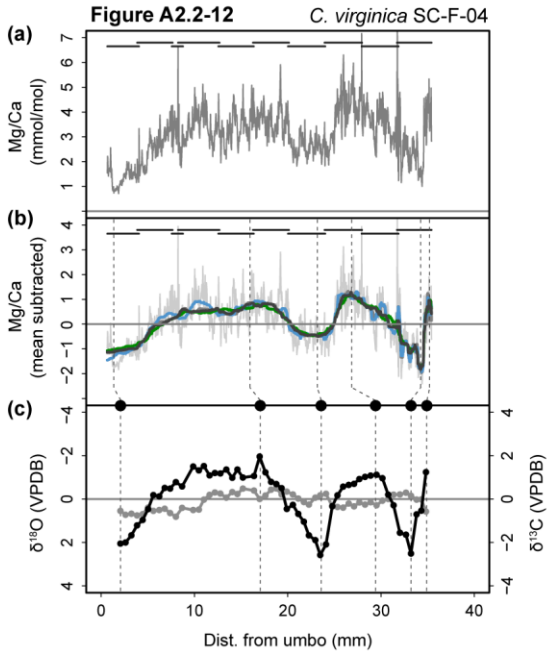
Figure A2.2-12
C. virginica SC-F-04
(a)
Mg/Ca (mmol/mol)
(b)
Mg/Ca (mean subtracted)
(c)
δ18O (VPDB)
δ13C (VPDB)
Dist. from umbo (mm)

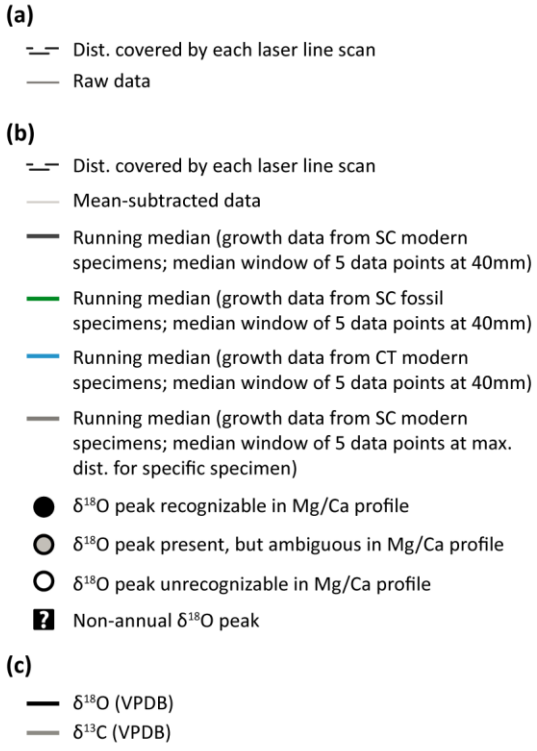
(a)
Dist. covered by each laser line scan
Raw data
(b)
Dist. covered by each laser line scan
Mean-subtracted data
Running median (growth data from SC modern specimens; median window of 5 data points at 40mm)
Running median (growth data from SC fossil specimens; median window of 5 data points at 40mm)
Running median (growth data from CT modern specimens; median window of 5 data points at 40mm)
Running median (growth data from SC modern specimens; median window of 5 data points at max. dist. for specific specimen)
δ18O peak recognizable in Mg/Ca profile
δ18O peak present, but ambiguous in Mg/Ca profile
δ18O peak unrecognizable in Mg/Ca profile
Non-annual δ18O peak
(c)
δ18O (VPDB)
δ13C (VPDB)

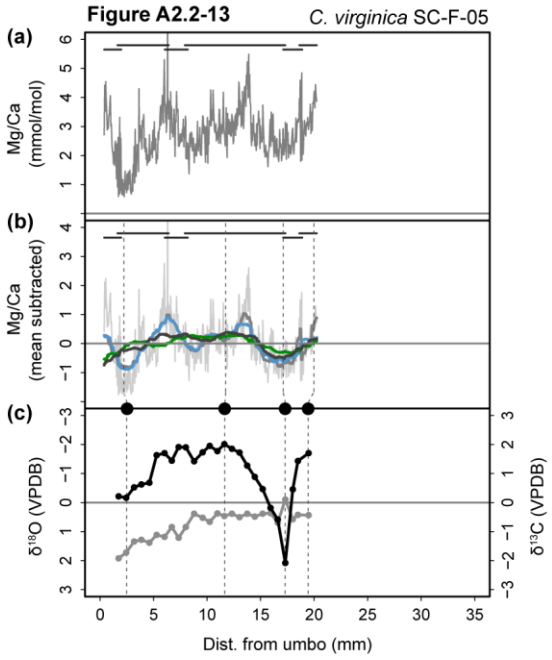
Figure A2.2-13
C. virginica SC-F-05
(a)
Mg/Ca (mmol/mol)
(b)
Mg/Ca (mean subtracted)
(c)
δ18O (VPDB)
δ13C (VPDB)
Dist. from umbo (mm)

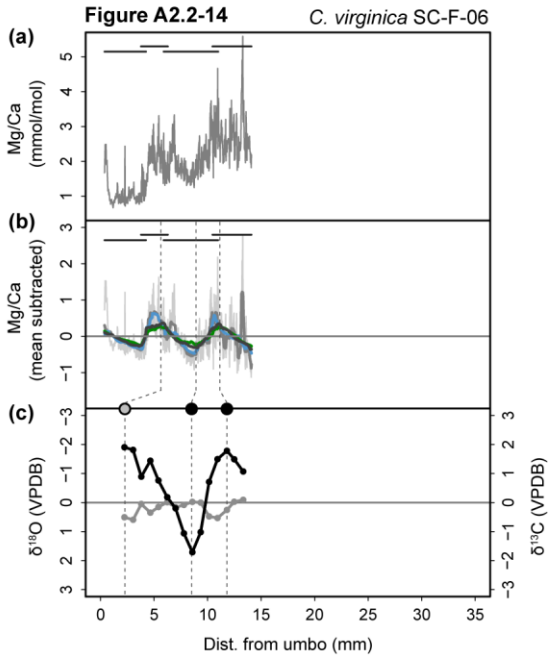
Figure A2.2-14
C. virginica SC-F-06
(a)
Mg/Ca (mmol/mol)
(b)
Mg/Ca (mean subtracted)
(c)
δ18O (VPDB)
δ13C (VPDB)
Dist. from umbo (mm)

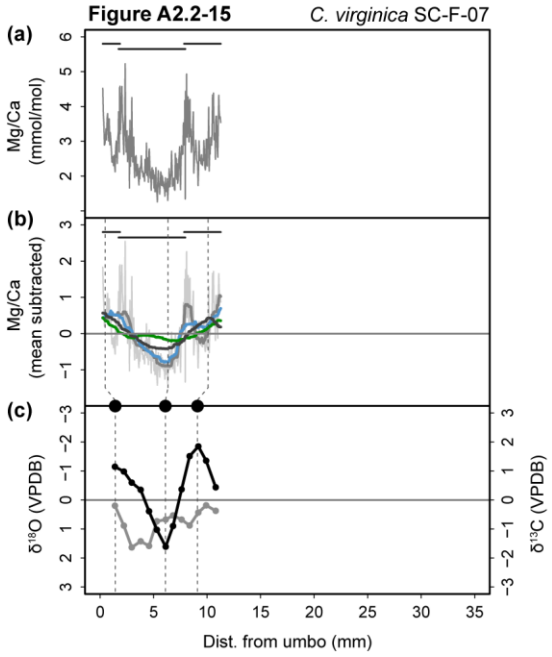
Figure A2.2-15
C. virginica SC-F-07
(a)
Mg/Ca (mmol/mol)
(b)
Mg/Ca (mean subtracted)
(c)
δ18O (VPDB)
δ13C (VPDB)
Dist. from umbo (mm)

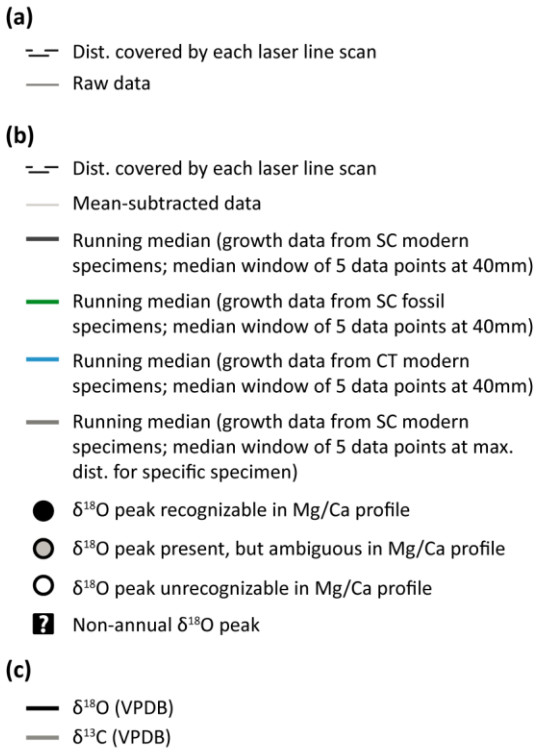
(a)
Dist. covered by each laser line scan
Raw data
(b)
Dist. covered by each laser line scan
Mean-subtracted data
Running median (growth data from SC modern specimens; median window of 5 data points at 40mm)
Running median (growth data from SC fossil specimens; median window of 5 data points at 40mm)
Running median (growth data from CT modern specimens; median window of 5 data points at 40mm)
Running median (growth data from SC modern specimens; median window of 5 data points at max. dist. for specific specimen)
δ18O peak recognizable in Mg/Ca profile
δ18O peak present, but ambiguous in Mg/Ca profile
δ18O peak unrecognizable in Mg/Ca profile
Non-annual δ18O peak
(c)
δ18O (VPDB)
δ13C (VPDB)

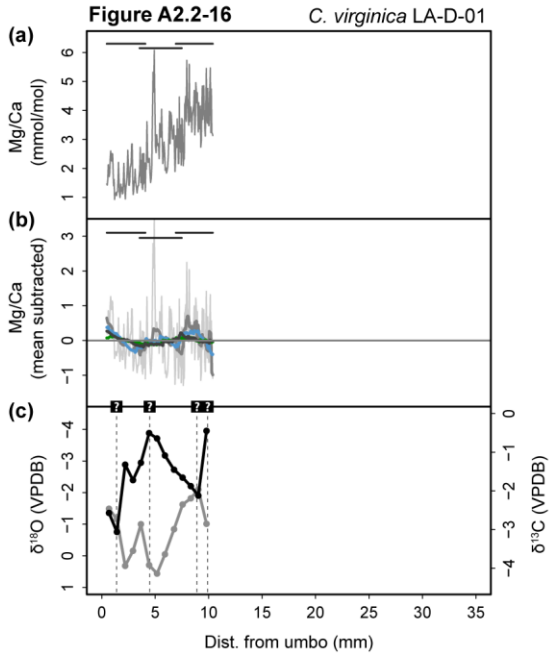

(a)

- Dist. covered by each laser line scan
- Raw data

(b)

- Dist. covered by each laser line scan
- Mean-subtracted data
- Running median (growth data from SC modern specimens; median window of 5 data points at 40mm)
- Running median (growth data from SC fossil specimens; median window of 5 data points at 40mm)
- Running median (growth data from CT modern specimens; median window of 5 data points at 40mm)
- Running median (growth data from SC modern specimens; median window of 5 data points at max. dist. for specific specimen)
- $\delta^{18}O$ peak recognizable in Mg/Ca profile
- $\delta^{18}O$ peak present, but ambiguous in Mg/Ca profile
- $\delta^{18}O$ peak unrecognizable in Mg/Ca profile
- Non-annual $\delta^{18}O$ peak

(c)

- $\delta^{18}O$ (VPDB)
- $\delta^{13}C$ (VPDB)

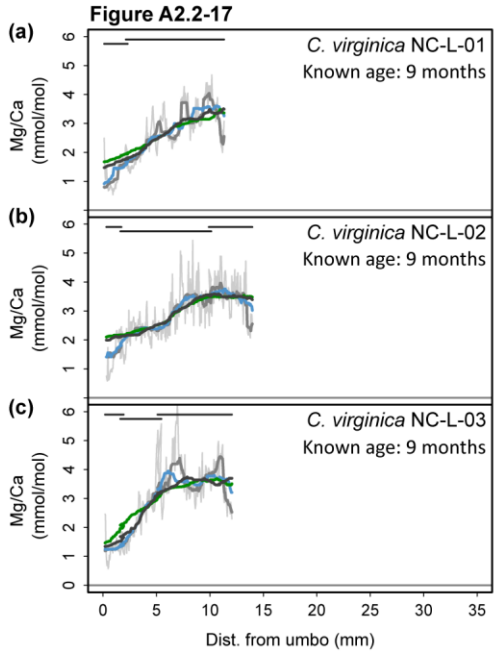

Fig. A3.17

- Dist. covered by each laser line scan
- Raw data
- Running median; windows based on growth data from Connecticut, USA (live specimen)
- Running median; windows based on growth data from South Carolina, USA (fossil specimens)
- Running median; windows based on growth data from South Carolina, USA (live specimens)
- Individual specimen running median; windows based on growth data from South Carolina, USA (live specimens)

Figure A2.2-18 *M. gigas* CA-L-01

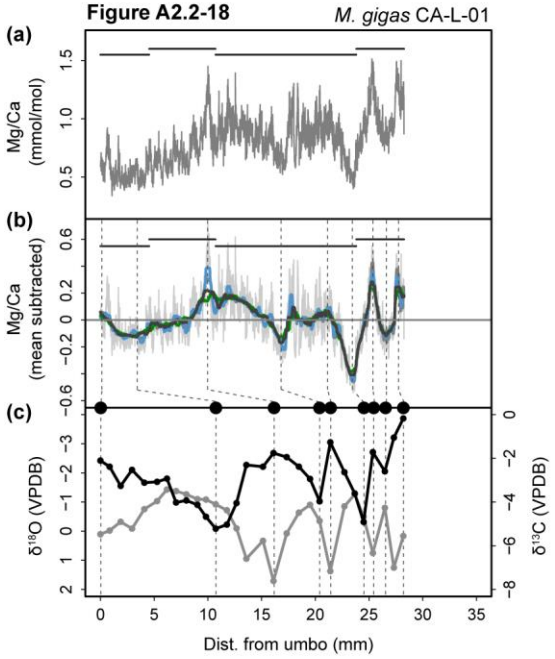

Figure A2.2-19 *M. gigas* CA-L-02

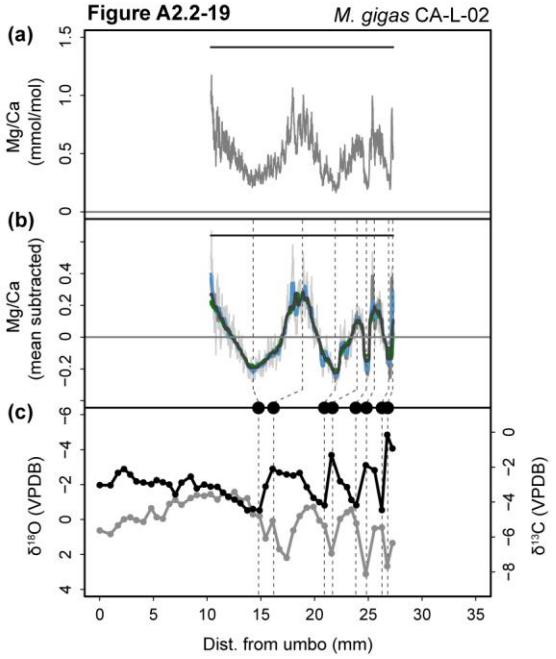

(a)

- Dist. covered by each laser line scan
- Raw data

(b)

- Dist. covered by each laser line scan
- Mean-subtracted data
- Running median (growth data from SC modern specimens; median window of 5 data points at 40mm)
- Running median (growth data from SC fossil specimens; median window of 5 data points at 40mm)
- Running median (growth data from CT modern specimens; median window of 5 data points at 40mm)
- Running median (growth data from SC modern specimens; median window of 5 data points at max. dist. for specific specimen)
- $\delta^{18}O$ peak recognizable in Mg/Ca profile
- $\delta^{18}O$ peak present, but ambiguous in Mg/Ca profile
- $\delta^{18}O$ peak unrecognizable in Mg/Ca profile
- ? Non-annual $\delta^{18}O$ peak

(c)

- $\delta^{18}O$ (VPDB)
- $\delta^{13}C$ (VPDB)

APPENDIX 2.3

A2.3.1 The effect of line scan position relative to the cross section edge on Mg/Ca ratios

Freitas et al. (2012) showed that Mg/Ca ratios vary depending on the distance of laser ablation-inductively coupled plasma-mass spectrometry (LA-ICP-MS) line scans from the exterior edge of the shell cross-section in *Pecten maximus*. We investigated the importance of this factor on our analyses of *Crassostrea virginica* specimens by measuring the distance between the laser line scans and the exterior edge of the resilifer cross-sections at the growth distance positions corresponding to each micromill point sample for the *C. virginica* specimens from South Carolina and Connecticut. The measurements were performed on the same images used to match the Mg/Ca and stable isotope profiles, again using ImageJ 1.51f image processing software (Rasband 1997). For each measurement, the mean and variance of Mg/Ca values from ± 0.3mm shell distance were calculated. These values were regressed against the distances of the line scans from the cross-section edges across all of the analyzed specimens to evaluate the effect of this distance on Mg/Ca ratios. The results show weak but statistically significant positive correlations between the mean ($F_{1,471}$ = 9.79, p = 0.0019; R^2 = 0.02; Figure A2.3-1) and variance ($F_{1,471}$ = 24.22, p = <0.0001; R^2 = 0.05; Figure A2.3-2) of Mg/Ca and distance of the laser lines from the cross-section edge.

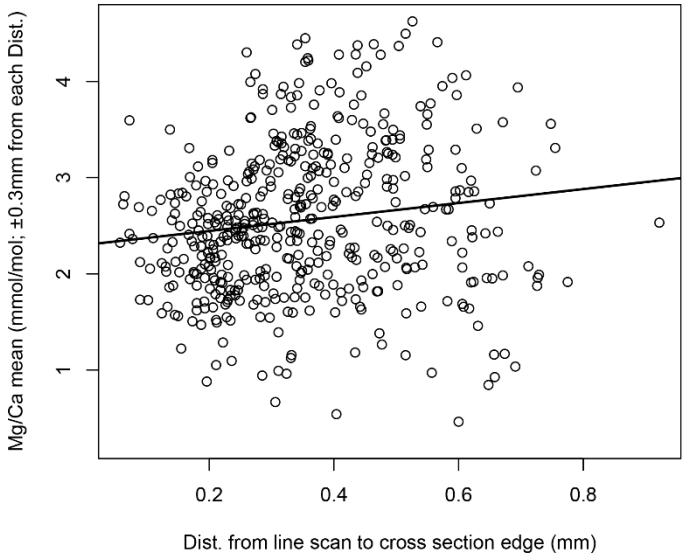

Figure A2.3-1 | Regression of mean Mg/Ca values (± 0.3mm growth distance from each edge distance measurement) against the distance between the line scans and the exterior edge of the resilifer cross sections (Mg/Ca mean = 0.73 * Dist. + 2.3; R^2 = 0.02).

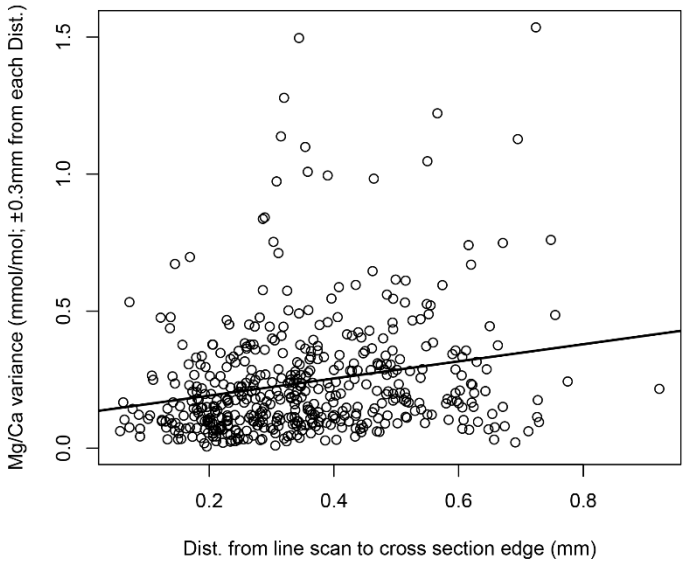

Figure A2.3-2 | Regression of Mg/Ca variance (± 0.3mm growth distance from each edge distance measurement) against the distance between the line scans and the exterior edge of the resilifer cross sections (Mg/Ca variance = 0.31 * Dist. + 0.13; R^2 = 0.05).

APPENDIX 3.1

Because preservational and environmental differences between assemblages could complicate our comparison of oyster lifespans and obscure the climate-related temperature effects we were interested in testing, we examined a number of environmental and taphonomic variables to justify the fossil versus modern oyster comparison in the main text. For instance, assemblage comparisons might be biased if all of the fossil and modern oyster assemblages were not from two relatively discrete time intervals or if there was evidence of particularly poor preservation in some assemblages relative to others. This appendix describes our efforts to document the similarity of the fossil and modern oyster assemblages and is divided into five sections: amino acid racemization geochronology, taphonomic analysis, oyster morphology, community composition, and salinity and temperature estimation.

A3.1.1 Amino acid racemization geochronology

Most of the geochronological work on the Canepatch Fm. has focused on the sandier units directly overlying the oyster facies, because the most useful fossils for geochronology (e.g., corals and venerid clams) are rare. This is a potential issue for our fossil/modern comparison because there is substantial disagreement on the age of the Canepatch Fm. and multiple studies have suggested it encompasses at least two transgressive cycles (e.g., DuBar 1971; Dubar et al. 1974; Wehmiller & Belknap 1982; McCartan et al. 1982; Szabo 1985; Corrado et al. 1986; Wehmiller et al. 1988; Hollin & Hearty 1990; Wehmiller 2013a; Doar 2014; Doar & Kendall 2014). Thus, we could not assume that the oyster facies and overlying sandier facies were from the same transgressive cycle based on lithostratigraphic evidence and pre-existing geochronology studies alone. If these two facies were not part of the same

transgressive sequence, then more in-depth geochronology work would likely be needed to ensure that the fossil oyster assemblages were approximately contemporaneous (i.e., at least from the same Marine Isotope Stage). We therefore checked the ages of the fossil oyster assemblages relative to dates in the literature using amino acid racemization geochronology—one of the most common dating methods used in studies of the Quaternary stratigraphy of the southeastern United States (Wehmiller 2013a).

Amino acid racemization geochronology is a relative dating method for biogenic carbonates that works by measuring the ratios of dextrorotatory (D-) and levorotatory (L-) isomers of several different amino acids in a sample. These D/L ratios are meaningful for geochronology because biogenic carbonates are produced with only L-amino acids, but after death L- and D-amino acid isomers gradually equilibrate in a predictable fashion (eventually reaching "infinite" age at D/L = 1, or 1.3 in the case of isoleucine/alloisoleucine), a process known as racemization (Wehmiller & Miller 2000). The racemization reaction is taxon- and temperature-dependent, but if the temperature history of a specimen can be estimated and the taxon-specific rate of the reaction can be tied to an absolute chronology using another dating method (e.g., radiocarbon dating or U-series dating), then D/L ratios of amino acids can be used to interpret sample ages (Wehmiller & Miller 2000).

A substantial portion of the previous aminostratigraphic work on the Quaternary of the Carolinas has focused on venerid clams (primarily *Mercenaria mercenaria*; e.g., Wehmiller et al. 1988; Wehmiller 2013a, 2013b), making them one of the best-understood taxa for this technique in this geographic and stratigraphic setting. Venerid shells are rare in the fossil oyster assemblages (though they are relatively common in the sandier facies directly overlying the oyster assemblages) and the four that we examined for the present study did not yield any suitable specimens

for dating. However, we collected a few well-preserved, articulated venerid specimens (*Mercenaria* sp. and *Chione* sp.) from other stratigraphically equivalent oyster assemblages in the same area of the Intracoastal Waterway. We therefore dated the oyster assemblages using one *Mercenaria* specimen and one *Chione* specimen in order to facilitate comparison of our results with previous studies.

We also report AAR results for 10 oyster specimens from our modern assemblages in order to estimate the age of the DA samples. There is no previous aminostratigraphic work on modern oyster reefs from South Carolina with which to compare these results, so we also analyzed two oyster specimens collected from comparable depths in intertidal oyster reef DAs in North Carolina that had been previously radiocarbon dated (Dietl, *unpublished data*).

All oyster specimen analyses were carried out on resilifers of articulated specimens (e.g., Surge et al. 2003). Each resilifer specimen was cut in half along the dorso-ventral axis and one half was prepared for AAR analysis while the other was saved. The venerid specimens were sectioned along their growth axes, and a chunk of shell was taken from the thickest portion of the cross section in the case of the *Mercenaria*, and a slice of the entire shell cross section was used from the *Chione* specimen because it was much smaller. The shell samples were sonicated for 2-5 minutes, then etched in dilute HCl to dissolve ~10% of the external surface, before being rinsed in distilled water and sonicated again for 2-5 minutes to remove all surface contamination. After initial cleaning, we ground and bleached each sample according to Penkman et al. (2008) in order to destroy intercrystalline organic material. This bleaching protocol has been shown to improve the precision of repeated analyses of Recent shells and to increase their enantiomeric ratio values slightly, but has progressively less impact on the AAR analysis results of older shells because more of the intercrystalline protein material is already lost from older specimens (Penkman

et al. 2008). We confirmed this pattern for our specimens with preliminary analyses of a series of bleached and unbleached laboratory standards of different ages ranging from early Pleistocene to late Pleistocene (ILC A, ILC B, and ILC C; Wehmiller 2013b; Table A3.1-1). The ILC A and ILC B standards were derived from late Pleistocene *Saxidomus* sp. shells and late Pleistocene *Mercenaria* sp. shells, respectively, and bleached samples of each showed elevated D/L ratios relative to unbleached samples, whereas the early Pleistocene ILC C (also derived from *Mercenaria* sp. shells) showed no systematic difference in the ratios from bleached and unbleached samples (Table A3.1-1). We therefore caution that the D/L ratios for our middle Pleistocene venerid samples may have slightly inflated D/L ratios relative to those of other studies that did not use the bleaching procedure.

Following preparation of the shell powder samples they were dissolved and hydrolyzed in 6N HCl for 22 hours at ~110^{o}C. Derivative preparation was conducted for gas chromatographic analysis according to Wehmiller & Miller (2000). All samples were analyzed on an Agilent 6890 gas chromatograph equipped with a flame ionization detector and using helium as the make-up gas at the Paleontological Research Institution in Ithaca, NY. Two injections per sample were conducted, and because peak heights tended to vary between samples, different injection volumes were used for each (1µl and 2µl). Every batch of samples included one preparation of interlaboratory comparison sample C (ILC C; Wehmiller 2013b) as a check for proper sample preparation and instrument function.

The enantiomeric (D/L) ratios for alanine (Ala), valine (Val), leucine (Leu), aspartic acid (Asx), phenylalanine (Phe), and glutamic acid (Glx) are reported in Table 3.1.1. Missing values were caused when peaks were not detected either because they were too small or there was an interfering peak that made estimation of the D/L ratio impossible. The repeated analysis of ILC C powder samples with each batch (n=16

over 8 analysis days) showed good precision (amino acid, %RSD in average D/L ratio, % difference from literature D/L value in Wehmiller 2013b): Ala, 6.9%, 10.7%; Val, 15.9%, 14.5%; Leu, 3.1%, 1.7%; Asx, 2.1%, -2.9%; Phe, 1.7%, 0.2%; Glx, 2.1%, -2.0%).

The ratios from the fossil venerids match previous results from the Intracoastal Waterway, though as mentioned above, the Penkman et al. (2008) bleaching procedure may have slightly inflated our D/L ratios (Wehmiller et al. 1988; Hollin & Hearty 1990; Muhs et al. 2003). For instance, the D/L Leu values from other fossil *Mercenaria* shells assigned to aminozone IVb by Wehmiller et al. (1988) range from 0.63 to 0.67, and the average (± SD) D/L Leu for our *Mercenaria* and *Chione* specimens were 0.66 ± 0.03 and 0.66 ± 0.02, respectively (the *Chione* value was increased by 10% as a correction to make it comparable to *Mercenaria*; Muhs et al. 2003). Also, Muhs et al. (2003) found that averages of the D/L values for Val, Leu, Phe, and Glx (called VLPG) ranged from 0.56-0.79 for the Canepatch Formation, and the average VLPG value for our *Mercenaria* specimen was 0.57 ± 0.01. These results suggest that the oyster assemblage facies and the overlying sandier facies (from which most of the dated *Mercenaria* from previous studies were collected) are indeed part of the same transgressive sequence, though as discussed above, the exact Marine Isotope Stage is uncertain[8].

The DA oyster specimens from North Carolina had AMS radiocarbon dates of ~400 and ~600 years for AA101243 and AA101244, respectively. Because they were collected from the Wilmington, NC area, which is not very far north of our sites in

[8] Age determinations from amino acid ratios depend on the kinetic model used to relate latitude/temperature history and age, as well as interpretations of the lithostratigraphy and the results of absolute dating methods (mostly U-series isotopic dating in this case). Therefore, our amino acid racemization results unfortunately do not help to clarify this long-running issue and are consistent with multiple age determinations from different authors using different interpretations, lines of evidence, and assumptions (e.g., MIS 9 - Wehmiller et al. 1988; MIS 7 - Corrado et al. 1986; or MIS 5e - Hollin & Hearty 1990).

South Carolina, we compared Asx and Glx D/L values between samples directly, with no temperature correction. Asx and Glx are the two most commonly analyzed amino acids for very young specimens (e.g., Surge et al. 2003; Kosnik et al. 2015; Dominguez et al. 2016) and are frequently plotted against one another to help screen for outliers (Kosnik & Kaufman 2008). From our plot of D/L Asx versus D/L Glu it is clear that the modern DA samples from SC are of the same general age, although some degree of time averaging is present. Further, they plot lower than both of the NC shells, suggesting the SC specimens are less than 400 years old (only the specimen from site R12 comes close; Figure A3.1-1). Further, the SC and NC shells show an approximately linear relationship between Asx and Glx D/L values, suggesting there are no outliers (Figure A3.1-1). Thus, the modern oyster samples likely represent an early or pre-industrial baseline that predates at least a substantial amount of the anthropogenic impacts of the late 19th and 20th Centuries.

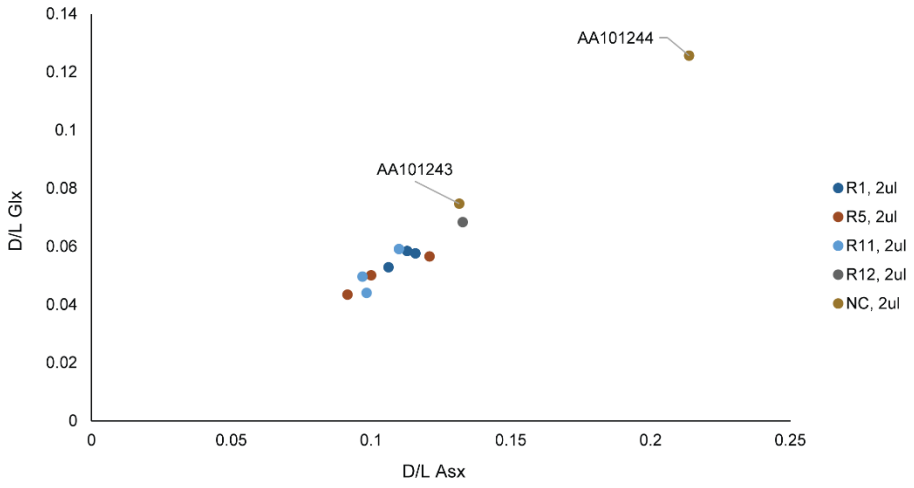

Figure A3.1-1 | Plot of Glx vs Asx D/L ratios for the 2ul injections of 12 modern oyster specimens from four modern reef DAs in South Carolina and two specimens from modern reef DAs of comparable depth in southern North Carolina (NC). Radiocarbon age estimates for the NC specimens were ~400 years old (AA101243) and ~600 years old (AA101244).

Table A3.1-1 | Data for all AAR analyses conducted on fossil and modern specimens, and interlaboratory comparison standards. NC=North Carolina, OR=Oregon, SC=South Carolina, Ala=Alanine, Val=Valine, Leu=Leucine, Asx=Aspartic acid, Phe=Phenylalanine, Glx=Glutamic acid, ILC=Interlaboratory comparison standard, ND=Not determined.

Genus	Site	Specimen ID	Injection ID	Bleached?	Injection vol. (µl)	D/L ratios					
						Ala	Val	Leu	Asx	Phe	Glx
Crassostrea	R5	L5.1-4_12	2017012a	1	1	ND	ND	ND	0.123	ND	0.057
Crassostrea	R5	L5.1-4_12	2017012b	1	2	0.083	0.036	0.047	0.121	0.047	0.057
Crassostrea	R5	L5.1-4_42	2017027a	1	1	ND	ND	ND	0.102	0.034	0.098
Crassostrea	R5	L5.1-4_42	2017027b	1	2	0.062	0.053	0.092	0.100	0.036	0.050
Crassostrea	R5	L5.1-4_90	2017028a	1	1	ND	ND	ND	0.116	ND	0.051
Crassostrea	R5	L5.1-4_90	2017028b	1	2	ND	ND	0.138	0.092	ND	0.043
Crassostrea	R1	L1.1-4_25	2017051a	1	1	ND	ND	ND	0.110	ND	0.052
Crassostrea	R1	L1.1-4_25	2017051b	1	2	ND	0.043	0.099	0.106	ND	0.053
Crassostrea	R1	L1.1-4_46	2017052a	1	1	ND	ND	ND	0.118	ND	0.060
Crassostrea	R1	L1.1-4_46	2017052b	1	2	ND	0.091	ND	0.113	ND	0.058
Crassostrea	R1	L1.1-4_52	2017053a	1	1	ND	ND	0.188	0.120	ND	0.062
Crassostrea	R1	L1.1-4_52	2017053b	1	2	0.126	0.076	0.371	0.116	0.065	0.058
Crassostrea	R11	L11.1-4_217	2017054a	1	1	ND	ND	0.080	0.112	ND	0.056
Crassostrea	R11	L11.1-4_217	2017054b	1	2	ND	0.064	0.165	0.110	0.052	0.059
Crassostrea	R11	L11.1-4_218	2017055a	1	1	ND	0.079	ND	0.099	ND	0.051
Crassostrea	R11	L11.1-4_218	2017055b	1	2	ND	0.110	0.183	0.097	ND	0.050
Crassostrea	R11	L11.1-4_25	2017056a	1	1	ND	0.229	ND	0.106	ND	0.048
Crassostrea	R11	L11.1-4_25	2017056b	1	2	ND	0.290	0.066	0.098	ND	0.044
Crassostrea	R12	L12.1-4_22	2017013a	1	1	ND	ND	0.318	0.132	0.079	0.068
Crassostrea	R12	L12.1-4_22	2017013b	1	2	ND	0.042	0.655	0.133	0.062	0.068
Crassostrea	NC	AA101244	2017041a	1	1	ND	0.072	0.182	0.211	0.145	0.108
Crassostrea	NC	AA101244	2017041b	1	2	ND	0.092	0.242	0.214	0.138	0.126
Crassostrea	NC	AA101243	2017042a	1	1	ND	ND	ND	0.128	0.075	0.070
Crassostrea	NC	AA101243	2017042b	1	2	ND	ND	ND	0.132	0.087	0.075
Chione	P3	3.1-3_Ch1	2017039a	1	1	ND	0.440	0.591	0.707	0.648	0.442
Chione	P3	3.1-3_Ch1	2017039b	1	2	ND	0.417	0.615	0.703	0.629	0.484
Mercenaria	P8	8.1-1_M1	2017037a	1	1	0.830	0.466	0.635	0.759	0.691	0.448
Mercenaria	P8	8.1-1_M1	2017037b	1	2	0.810	0.459	0.677	0.738	0.697	0.486
Saxidomus	OR	ILC A	2017001a	0	1	0.471	0.129	0.174	0.431	0.226	0.206
Saxidomus	OR	ILC A	2017001b	0	2	0.338	0.122	0.270	0.424	0.227	0.204
Saxidomus	OR	ILC A	2017002a	1	1	0.527	0.157	0.242	0.440	0.256	0.223
Saxidomus	OR	ILC A	2017002b	1	2	0.395	0.143	0.313	0.436	0.252	0.222
Mercenaria	SC	ILC B	2017003a	0	1	0.839	0.359	0.476	0.733	0.555	0.431
Mercenaria	SC	ILC B	2017003b	0	2	0.799	0.359	0.496	0.729	0.548	0.432
Mercenaria	SC	ILC B	2017004a	1	1	0.830	0.429	0.587	0.760	0.658	0.462
Mercenaria	SC	ILC B	2017004b	1	2	0.815	0.429	0.617	0.761	0.658	0.469
Mercenaria	SC	ILC C	2017005a	0	1	1.037	0.815	0.867	0.885	0.909	0.875
Mercenaria	SC	ILC C	2017005b	0	2	1.017	0.815	0.882	0.894	0.900	0.869
Mercenaria	SC	ILC C	2017006a	1	1	1.041	0.821	0.855	0.894	0.894	0.867
Mercenaria	SC	ILC C	2017006b	1	2	1.007	0.829	0.864	0.895	0.903	0.878
Mercenaria	SC	ILC C	2017016a	1	1	1.005	0.829	0.878	0.907	0.949	0.894
Mercenaria	SC	ILC C	2017016b	1	2	1.007	0.839	0.885	0.909	0.944	0.936
Mercenaria	SC	ILC C	2017024a	1	1	1.033	0.826	0.857	0.909	0.917	0.891
Mercenaria	SC	ILC C	2017024b	1	2	1.079	0.833	0.864	0.905	0.918	0.928
Mercenaria	SC	ILC C	2017029a	1	1	1.029	0.842	0.798	0.881	0.934	0.894
Mercenaria	SC	ILC C	2017029b	1	2	1.004	0.842	0.825	0.886	0.906	0.890
Mercenaria	SC	ILC C	2017030a	1	1	1.032	1.274	0.861	0.927	0.930	0.881
Mercenaria	SC	ILC C	2017030b	1	2	1.067	1.282	0.867	0.954	0.933	0.868
Mercenaria	SC	ILC C	2017031a	1	1	1.245	0.919	0.894	0.905	0.930	0.883
Mercenaria	SC	ILC C	2017031b	1	2	1.120	0.948	0.896	0.907	0.919	0.886
Mercenaria	SC	ILC C	2017031c	1	1	1.093	0.949	0.894	0.907	0.931	0.876
Mercenaria	SC	ILC C	2017031d	1	2	1.094	0.951	0.896	0.908	0.930	0.880
Mercenaria	SC	ILC C	2017032a	1	1	1.226	0.885	0.872	0.889	0.906	0.888
Mercenaria	SC	ILC C	2017032b	1	2	1.114	0.897	0.893	0.875	0.911	0.898

A3.1.2 Taphonomic analysis

Paleoenvironmental interpretations and comparisons between assemblages that differ substantially in taphonomic history could be misleading because the magnitude and types of information lost from an assemblage can vary substantially with taphonomic history (e.g., Lawrence 1968). For instance, because oysters are made mostly of calcite, the most stable polymorph of calcium carbonate, it is important to check whether aragonitic remains are preserved in the assemblage to ensure that the presence/absence of aragonitic taxa between assemblages is paleoecologically meaningful information (i.e., that they were not simply leached out of the assemblage).

Therefore, to check the comparability of taphonomic condition among our oyster assemblages we randomly selected 50 numbered oyster specimens and graded each for five characteristics: surface condition, fragmentation, color, encrustation, bioerosion, and aragonite preservation. We used a three-category grading system (0, 1, or 2), following Kowalewski et al. (1995), so that we could plot the characteristics on ternary diagrams to easily compare taphonomic condition between sites. Aragonite preservation was evaluated as averages of the grades for the five other taphonomic characteristics, scored based on all aragonitic bivalves and gastropods in each sample. Bivalves and gastropod components of the aragonitic taxa were scored separately because bivalve specimens tended to show a much higher incidence of fragmentation than gastropod specimens. Taphonomic grade values for each site reflect averages of three independent evaluations—by the author and two undergraduate lab assistants. The average taphonomic grades were assigned to the three discrete grade levels by rounding to the nearest grade (i.e., Grade 0 = average scores from 0-0.5, Grade 1 = average scores from 0.5-1.5, and Grade 2 = average scores from 1.5-2). Descriptions

of each taphonomic grade were as follows, and representative images of each can be found in Figure A3.1-2.

Surface condition

0: Natural luster with no obvious surface dissolution or other chemical alteration. Original shell texture present (e.g., growth lines visible, ornamentation not abraded).

1: Luster faded and/or original shell texture abraded or eroded. Shell may be beginning to become flakey or brittle.

2: Natural luster is gone or almost completely gone. Surface is obviously degraded chemically or physically such that original shell textures and features are difficult to recognize. The shell may be brittle and flakey or soft and chalky.

Fragmentation

0: Shell complete and unbroken. Edges intact.

1: Shell exhibits minor breakage that does not significantly interrupt the shell outline.

2: Shell obviously broken. Note: all of these specimens should have prompted a note in the measurement spreadsheet.

Color

0: Original colors present – shell exhibits white, yellow, and/or purple shades.

1: Some original color present (e.g., purple on muscle scar or shell exterior), but shell also beginning to bleach or have color alteration post-mortem (e.g., dark blue/grey colors or minor stains associated with diagenesis).

2: Original shell color not present. Shell may be bleached, stained, or the color may be completely altered.

Bioerosion

0: No bioerosion present.

1: Minor bioerosion present, affecting <50% of the shell

2: Significant bioerosion present, affecting >50% of the shell

Encrustation

0: No encrustation present.

1: Minor encrustation present, affecting <50% of the shell (e.g, one or a few scattered barnacles or worm tubes present).

2: Significant encrustation present, affecting >50% of the shell (e.g., a large portion of the shell covered in barnacles or worm tubes).

Aragonite preservation

Surface condition

Scored based on the same criteria used for the oyster specimens, but the sample score is determined by the majority taphonomic grade across all specimens/fragments in the sample.

Fragmentation

0: >50% of specimens/fragments are >50% complete

1: 10-50% of specimens/fragments are >50% complete

2: <10% of specimens/fragments are >50% complete

Color

0: >50% of specimens/fragments show original color or color pattern

1: 10-50% of specimens/fragments show original color or color pattern

2: <10% of specimens/fragments show original color or color pattern

Bioerosion

0: <10% of specimens/fragments show bioerosion

1: 10-50% of specimens/fragments show bioerosion

2: >50% of specimens/fragments show bioerosion

Encrustation

0: <10% of specimens/fragments show encrustation

1: 10-50% of specimens/fragments show encrustation

2: >50% of specimens/fragments show encrustation

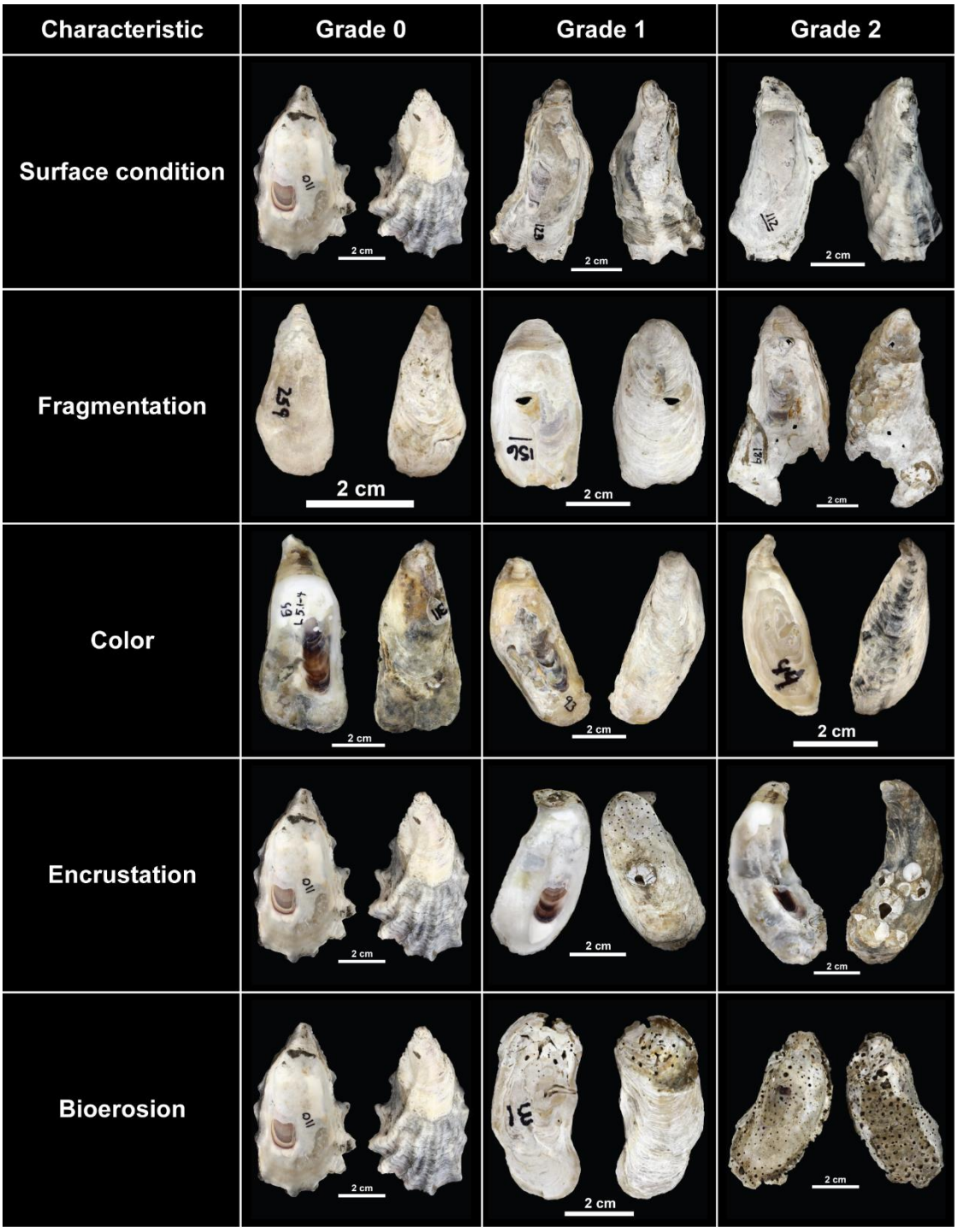

Figure A3.1-2 | Photographs of the interior (left) and exterior (right) surfaces of representative oyster specimens demonstrating the three taphonomic grades (0=best, 2=worst condition) for each of the five shell characteristics assessed.

From the ternary diagrams (Figure A3.1-3) and the plot of taphonomic grades for aragonitic bivalves and gastropods (Figure A3.1-4), it is clear that the fossil and modern oyster assemblages exhibit remarkably similar taphonomic condition. Fossil and modern site clusters in the ternary diagrams overlap for all shell characteristics examined (Figure A3.1-3) and aragonite preservation was largely consistent between assemblages, although the separation in taphonomic grade between bivalves and gastropods was higher in the fossil assemblages (Figure A3.1-4). Overall, these results suggest that the fossil and modern oyster assemblages reflect similar preservational environments, supporting the validity of our comparison between them.

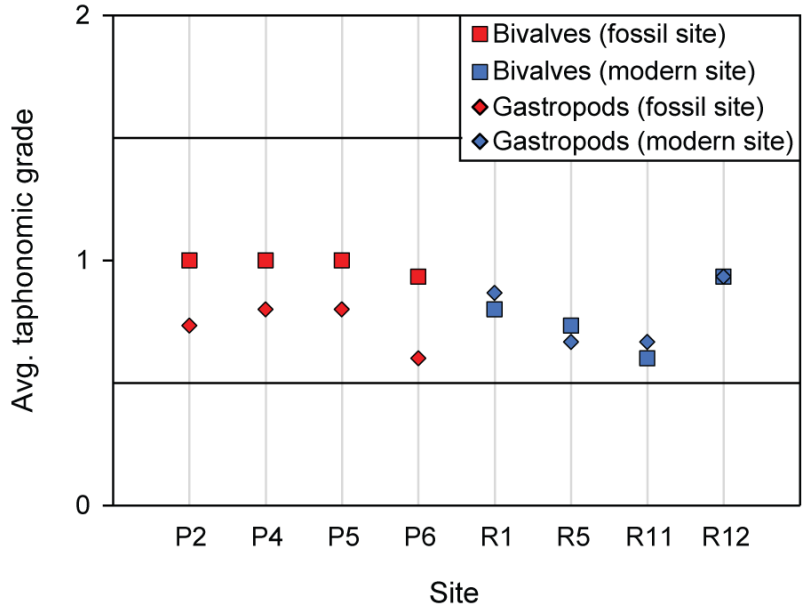

Figure A3.1-4 | Plot of average taphonomic grades for aragonitic bivalves and gastropods from each fossil and modern oyster assemblage. Lower grades indicate better condition. fossil assemblages = P2, P4, P5, P6; modern assemblages = R1, R5, R11, R12

Figure A3.1-3 | Ternary taphograms comparing the average taphonomic grades of five different shell characteristics and an overrall average score for each fossil and modern assemblage. Lower grades indicate better condition. fossil assemblages = P2, P4, P5, P6; modern assemblages = R1, R5, R11, R12

All avg.

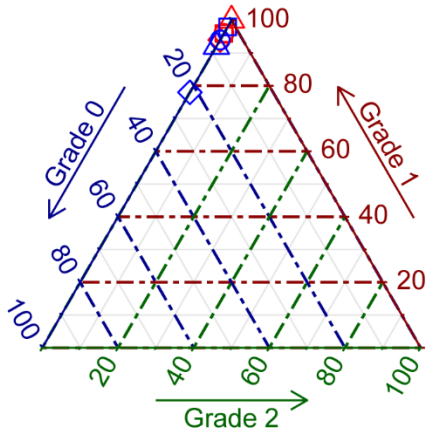

Surface condition

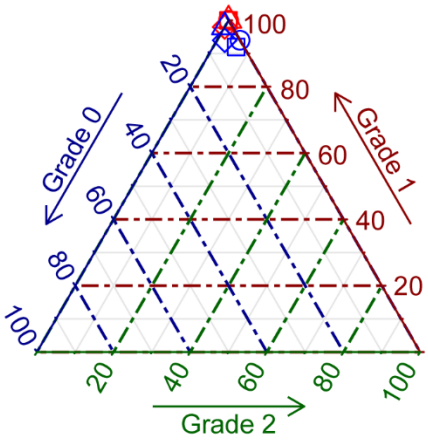

Fragmentation

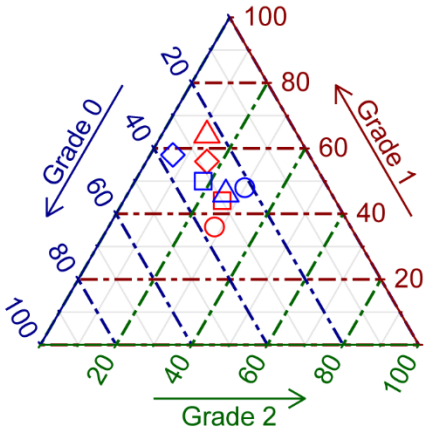

Color preservation

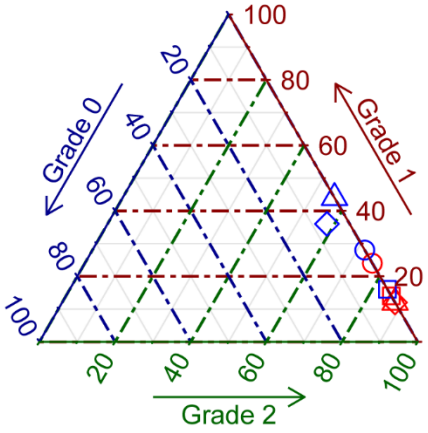

Encrustation

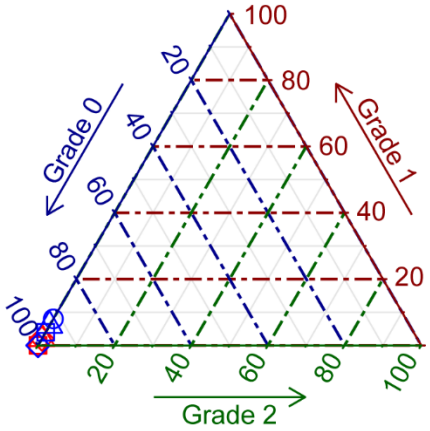

Bioerosion

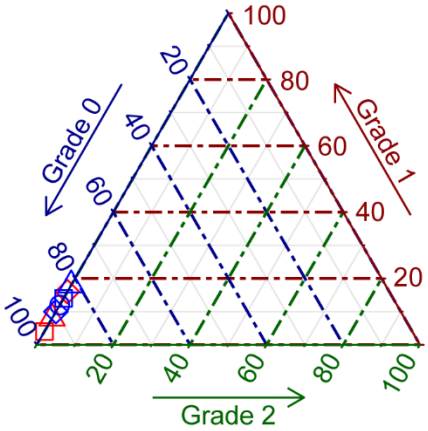

Site

P2 P5 R1 R11

P4 P6 R5 R12

A3.1.3 Oyster morphology

Crassostrea virginica displays a high degree of ecophenotypy, varying in shell form depending on their growth environment (e.g., Kent 1992). Thus, the shape of the oyster specimens themselves can yield useful information about the comparability of our fossil and modern assemblages. For instance, Kent (1992) describes general ranges of height:length ratios (HLR) for oysters growing in four different substrate categories: shallow, firm sandy environments (HLR ≤ 1.3); muddy sand substrates (HLR ≈ 1.3–2.0); deeper, soft mud channels (HLR ≥ 2.0); and crowded reefs (HLR ≥ 2.0). Reefs and deep channel environments are primarily distinguished based on size (oysters on reefs are generally smaller than those in channels) and the proportion of total shell height by which the oyster is attached to substrate (oysters from reefs are more crowded and the attachment scar tends to be at least half the height of the left valve, whereas attachment scars of less crowded, deeper channel oysters tend to be less than half of the total left valve height). We assessed average HLR, attachment length ratio (ALR), and size for each assemblage in order to check for evidence of different growth environments. In order to avoid variation related to irregular recruitment or differential preservation of small specimens, we restricted our analyses to specimens corresponding to approximate minimum lifespans of 1 year (right valves ≥ 21.19mm in height, left valves ≥ 21.43mm in height).

The results of an ANOVA carried out for average HLR by site was significant (Table A3.1-2), and post-hoc pairwise comparisons using Tukey's HSD show that this result was primarily driven by fossil sites P2 and P6 (Table A3.1-3), which had the highest and lowest HLR, respectively (Figure A3.1-5). There is no systematic difference between fossil and modern assemblages in HLR, however, and given the overlapping standard deviations and relatively small magnitude of the differences in

Table A3.1-2 | ANOVA table showing results from analysis of average oyster height:length ratio by site.

	Df	Sum Sq	Mean Sq	F value	Pr(>F)
Site	7	64.4	9.197	26.19	<2e-16***
Residuals	1473	517.3	0.351		
Signif. codes: 0 '***' 0.001 '**' 0.01 '*' 0.05 '.' 0.1 ' ' 1					
7 observations deleted due to missingness					

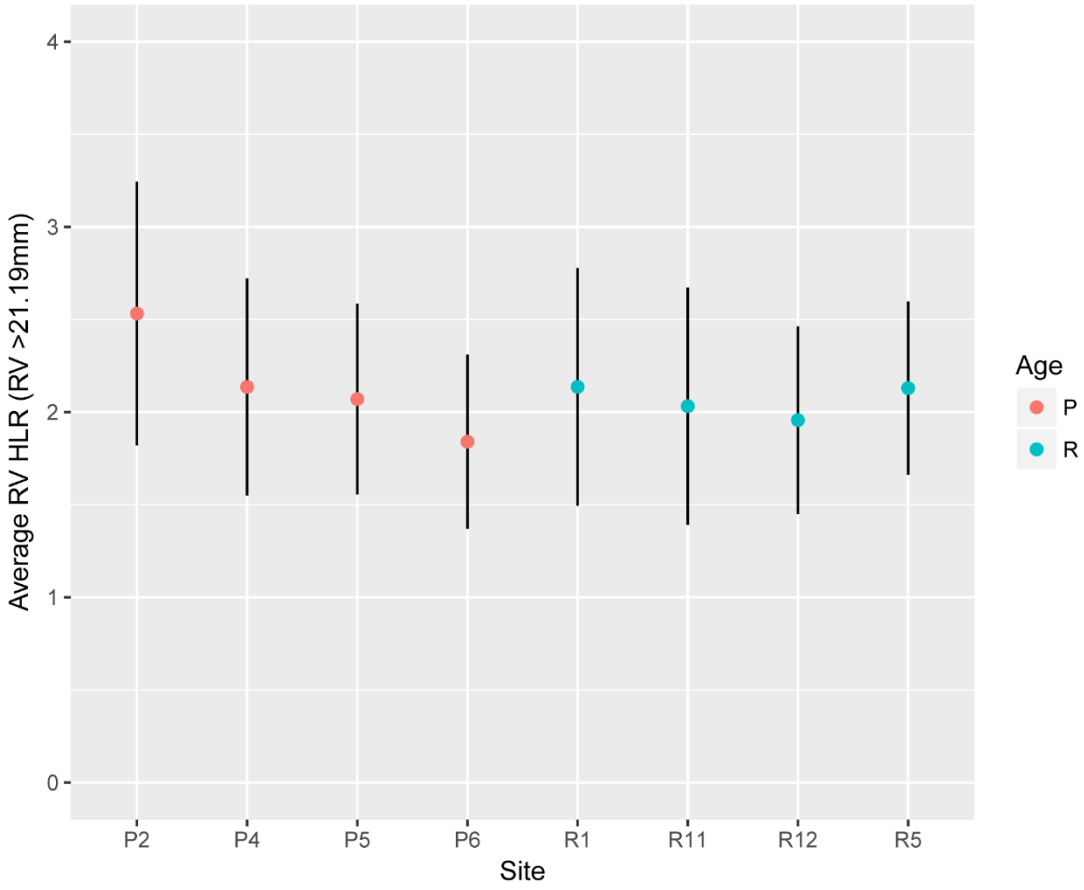

Figure A3.1-5 | Plot of average right valve (RV) height:length ratio (HLR) by site. P = fossil assemblages, R = modern assemblages; Error bars = 1SD.

Table A3.1-3 | Post-hoc pairwise comparisons of average oyster height:length ratio between assemblages. Significant comparisons are in bold.

Tukey multiple comparisons of means				
95% family-wise confidence level				
	diff	lwr	upr	p adj
P.4-P.2	**-0.396**	**-0.538**	**-0.255**	**0.000**
P.5-P.2	**-0.462**	**-0.652**	**-0.271**	**0.000**
P.6-P.2	**-0.692**	**-0.869**	**-0.514**	**0.000**
R.1-P.2	**-0.396**	**-0.566**	**-0.225**	**0.000**
R.11-P.2	**-0.500**	**-0.697**	**-0.304**	**0.000**
R.12-P.2	**-0.576**	**-0.785**	**-0.367**	**0.000**
R.5-P.2	**-0.403**	**-0.582**	**-0.223**	**0.000**
P.5-P.4	-0.065	-0.251	0.120	0.963
P.6-P.4	**-0.295**	**-0.468**	**-0.123**	**0.000**
R.1-P.4	0.001	-0.164	0.166	1.000
R.11-P.4	-0.104	-0.296	0.088	0.725
R.12-P.4	-0.179	-0.384	0.025	0.136
R.5-P.4	-0.006	-0.181	0.168	1.000
P.6-P.5	**-0.230**	**-0.444**	**-0.016**	**0.025**
R.1-P.5	0.066	-0.142	0.274	0.980
R.11-P.5	-0.038	-0.268	0.192	1.000
R.12-P.5	-0.114	-0.355	0.127	0.840
R.5-P.5	0.059	-0.157	0.275	0.991
R.1-P.6	**0.296**	**0.099**	**0.493**	**0.000**
R.11-P.6	0.192	-0.028	0.411	0.140
R.12-P.6	0.116	-0.115	0.347	0.793
R.5-P.6	**0.289**	**0.084**	**0.494**	**0.001**
R.11-R.1	-0.104	-0.318	0.110	0.818
R.12-R.1	-0.180	-0.405	0.045	0.231
R.5-R.1	-0.007	-0.205	0.192	1.000
R.12-R.11	-0.076	-0.321	0.170	0.983
R.5-R.11	0.097	-0.124	0.319	0.885
R.5-R.12	0.173	-0.059	0.405	0.316

HLR between individual assemblages, the variation in HLR we detected is unlikely to be biologically meaningful. All values are also close to 2, so are suggestive of reef or channel environments (Figure A3.1-5).

As expected based on the similar HLR values between fossil and modern assemblages, average ALR for each site was >0.5, indicative of a reef growth substrate (Figure A3.1-6). An ANOVA performed on ALR values by site was significant (Table A3.1-4), and a post-hoc TukeyHSD test showed the significant result was primarily driven by high average ALR at site R11 (Table A3.1-6). As was the case with HLR, however, none of the differences were very large in magnitude and standard deviations overlap substantially, so we consider them unlikely to be biologically meaningful.

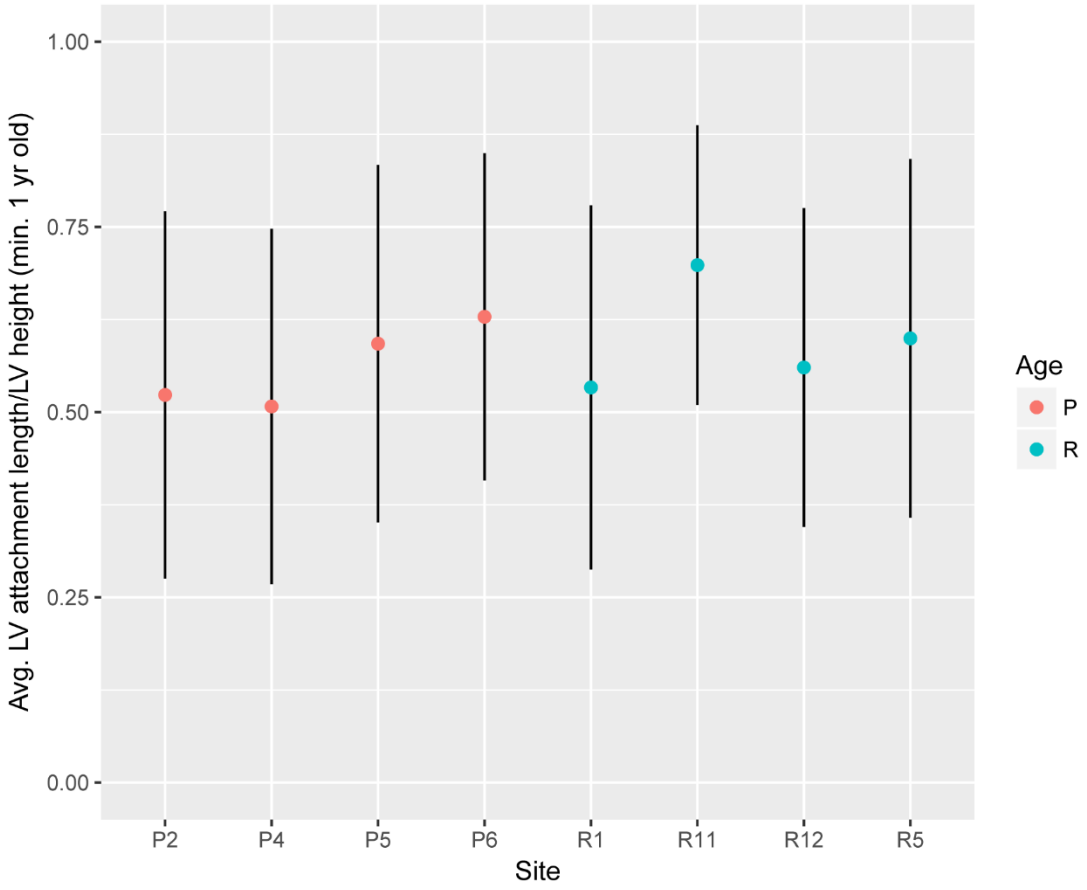

Figure A3.1-6 | Plot of average left valve (LV) attachment scar length:LV height ratio by site. P = fossil assemblages, R = modern assemblages; Error bars = 1SD.

Table A3.1-4 | ANOVA table showing results from analysis of average oyster left valve (LV) attachment scar length:LV height ratio by site.

	Df	Sum Sq	Mean Sq	F value	Pr(>F)
Site	7	1.68	0.24012	4.284	0.000124***
Residuals	575	32.23	0.05605		
Signif. codes: 0 '***' 0.001 '**' 0.01 '*' 0.05 '.' 0.1 ' ' 1					

Finally, there was not a large difference in resilifer heights among assemblages, again suggesting that the fossil oyster assemblages reflect crowded reef conditions, similar to the modern reef assemblages (Figure A3.1-7). An ANOVA of resilifer height by site was not significant (Table A3.1-6). Resilifer height was used as a proxy for overall specimen height in this analysis because many oyster valves were broken during collection of the fossil samples but most resilifers remained intact. There is a good correlation between resilifer height and total left valve height for both the fossil and modern oysters (fossil [n=705]: left valve height = 3.74 * resilifer height – 11.3, R^2=0.84, $p < 0.0001$; modern [n=909]: left valve height = 3.64 * resilifer height – 8.05, R^2=0.87, $p < 0.0001$).

Table A3.1-5 | Post-hoc pairwise comparisons of average left valve (LV) attachment scar length:LV height ratio between assemblages. Significant comparisons are in bold.

Tukey multiple comparisons of means				
95% family-wise confidence level				
	diff	lwr	upr	p adj
P.4-P.2	-0.016	-0.121	0.090	1.000
P.5-P.2	0.069	-0.051	0.190	0.656
P.6-P.2	0.105	-0.035	0.246	0.303
R.1-P.2	0.010	-0.098	0.118	1.000
R.11-P.2	**0.175**	**0.054**	**0.297**	**0.000**
R.12-P.2	0.037	-0.082	0.156	0.982
R.5-P.2	0.076	-0.010	0.163	0.128
P.5-P.4	0.085	-0.052	0.222	0.565
P.6-P.4	0.121	-0.034	0.276	0.254
R.1-P.4	0.026	-0.101	0.152	0.999
R.11-P.4	**0.191**	**0.053**	**0.329**	**0.001**
R.12-P.4	0.053	-0.084	0.189	0.939
R.5-P.4	0.092	-0.016	0.200	0.165
P.6-P.5	0.036	-0.129	0.201	0.998
R.1-P.5	-0.059	-0.198	0.080	0.901
R.11-P.5	0.106	-0.043	0.255	0.378
R.12-P.5	-0.032	-0.180	0.116	0.998
R.5-P.5	0.007	-0.115	0.130	1.000
R.1-P.6	-0.095	-0.252	0.061	0.583
R.11-P.6	0.070	-0.096	0.236	0.906
R.12-P.6	-0.068	-0.233	0.096	0.911
R.5-P.6	-0.029	-0.171	0.113	0.999
R.11-R.1	**0.165**	**0.025**	**0.305**	**0.008**
R.12-R.1	0.027	-0.111	0.165	0.999
R.5-R.1	0.066	-0.044	0.177	0.605
R.12-R.11	-0.138	-0.287	0.010	0.090
R.5-R.11	-0.099	-0.222	0.025	0.227
R.5-R.12	0.039	-0.082	0.161	0.977

Table A3.1-6 | ANOVA table showing results from analysis of average resilifer height by site.

	Df	Sum Sq	Mean Sq	F value	Pr(>F)
Site	7	385	54.94	1.684	0.109
Residual	993	32392	32.62		

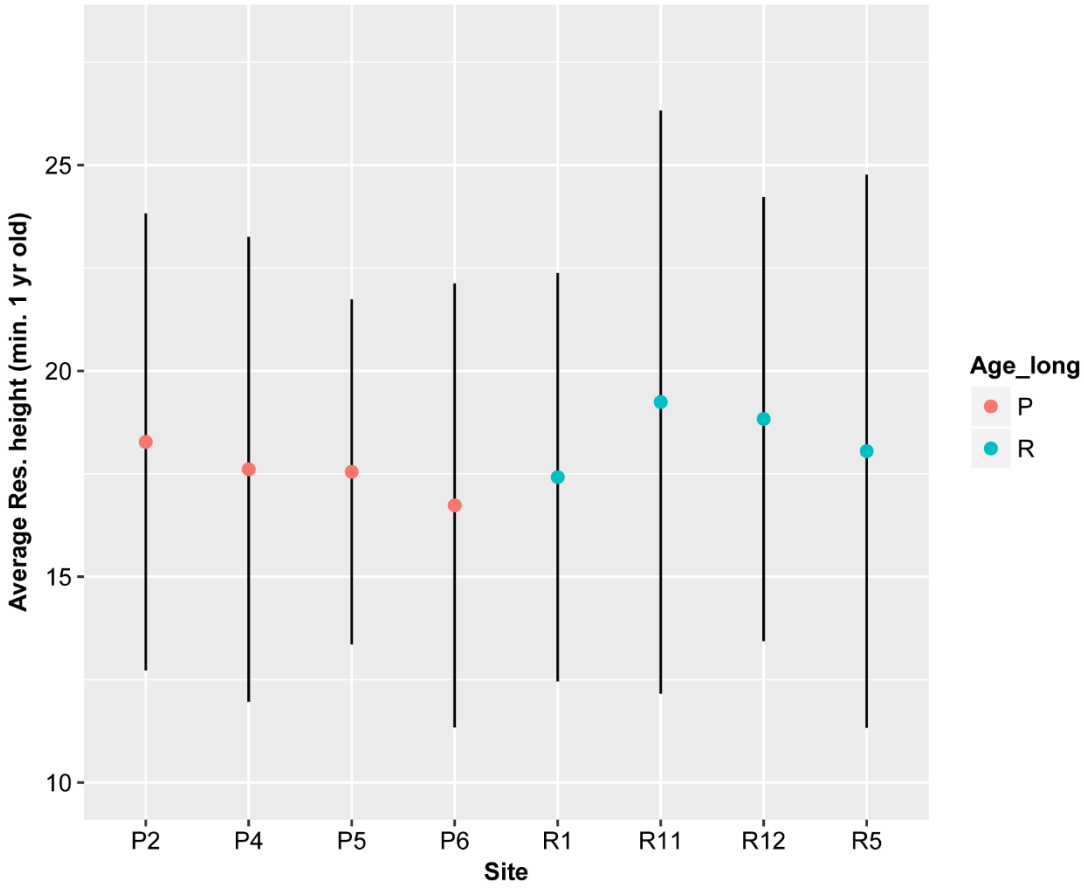

Figure A3.1-7 | Plot of average resilifer heights by site for specimens with lifespan estimates ≥1 year. P = fossil assemblages, R = modern assemblages; Error bars = 1SD.

A3.1.4 Community composition

As with oyster morphology, the associated fauna in an oyster assemblage can yield insights into the paleoenvironment (e.g., Wells 1961; Lawrence 1968; Wingard & Hudley 2012). For instance, Wells (1961) documented a positive correlation between macroinvertebrate diversity and salinity among multiple oyster reefs in North Carolina along a salinity gradient associated with the Newport River. He also found that reef communities at higher salinities did not simply have fewer species, but also had some different species from those found at higher salinities (Wells 1961). Thus, as

an additional check on the comparability between fossil and modern oyster assemblages, we composed species lists for each assemblage and then analyzed the community matrix using non-metric multidimensional scaling (NMDS).

In total, 43 different species were identified across all assemblages (including *Crassostrea virginica*; Table A3.1-7). This is a conservative estimate of total assemblage diversity because identification to the species level was not always possible. Eighteen of the species were found in both fossil and modern assemblages, and all of those found only in the fossil assemblages are still extant. An NMDS plot and PERMANOVA analysis of the fossil and modern species lists did not show systematic differences between the community compositions of the fossil and modern assemblages (Figure A3.1-8, Table A3.1-8). This result is further evidence of the similar environments in which the fossil and modern oyster assemblages formed, and supports our comparison of oyster lifespans from the fossil and modern assemblages.

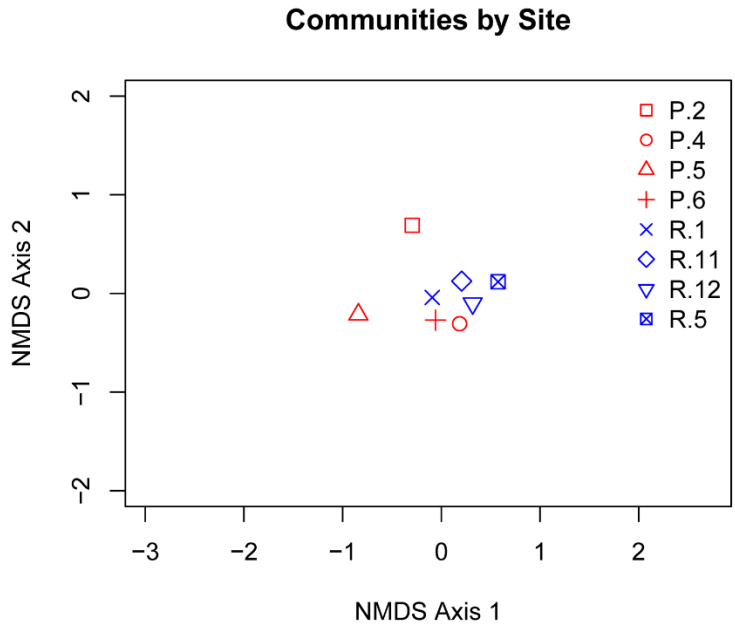

Figure A3.1-8 | Nonmetric multidimensional scaling (NMDS) plot comparing community composition among fossil (red symbols) and modern (blue symbols) assemblages.

Table A3.1-7 | Community composition of each oyster assemblage. Taxa that occur in both fossil and modern sites are in bold. Fossil sites = P2, P4, P5, P6; modern sites = R1, R5, R11, R12

Phylum	Taxon	P2	P4	P5	P6	R1	R5	R11	R12
Arthropoda	***Balanus* sp.**	**1**	**1**	**1**	**1**	**1**	**1**	**1**	**1**
Mollusca	***Crassostrea virginica***	**1**	**1**	**1**	**1**	**1**	**1**	**1**	**1**
Annelida	***Polydora* sp. (Ichnogenus = *Entobia*)**	**1**	**1**	**1**	**1**	**1**	**1**	**1**	**1**
Arthropoda	***Panopeus herbstii***	**1**	**1***	**1***	**1**	**1**	**0**	**1**	**1**
Mollusca	***Boonea impressa***	**1***	**0**	**0**	**1**	**1**	**1**	**1**	**1**
Mollusca	***Brachidontes exhustus***	**0**	**1**	**0**	**1**	**1**	**1**	**1**	**1**
Mollusca	***Geukensia demissa***	**0**	**1**	**1**	**1**	**1**	**1**	**0**	**1**
Arthropoda	***Eurypanopeus depressus***	**0**	**1**	**0**	**1**	**1**	**0**	**1**	**1**
Porifera	***Cliona* sp. (Ichnogenus = *Caulostrepsis*)**	**0**	**0**	**1**	**1**	**1**	**0**	**1**	**0**
Mollusca	***Mulinia lateralis***	**1**	**0**	**1**	**1***	**1**	**0**	**0**	**0**
Mollusca	***Tritia obsoleta***	**0**	**1**	**1**	**1**	**1***	**0**	**0**	**0**
Arthropoda	**Unknown crab species**	**0**	**1***	**1***	**1**	**0**	**0**	**0**	**1**
Mollusca	*Mercenaria mercenaria*	1	1*	1	0	0	0	0	0
Mollusca	***Parastarte triquetra***	**1**	**0**	**1**	**0**	**1**	**0**	**0**	**0**
Mollusca	***Pyrgocythara plicosa***	**0**	**0**	**1***	**1***	**1***	**0**	**0**	**0**
Annelida	**Serpulidae indet.**	**0**	**0**	**1**	**1**	**0**	**0**	**1**	**0**
Mollusca	*Acteocina canaliculata*	1	0	1	0	0	0	0	0
Mollusca	*Chione cancellata*	1*	0	1	0	0	0	0	0
Mollusca	***Crassinella lunulata***	**0**	**0**	**1**	**0**	**1***	**0**	**0**	**0**
Mollusca	***Crepidula fornicata***	**0**	**0**	**1**	**0**	**0**	**1**	**0**	**0**
Mollusca	*Littorina irrorata*	0	1*	0	1	0	0	0	0
Mollusca	*Nucula proxima*	1	0	1	0	0	0	0	0
Mollusca	*Odostomia* sp.	0	0	1	1*	0	0	0	0
Mollusca	***Sphenia fragilis***	**1**	**0**	**0**	**0**	**0**	**0**	**1**	**0**
Arthropoda	Alpheidae indet.	0	0	0	1	0	0	0	0
Mollusca	*Anachis obesa*	0	0	1	0	0	0	0	0
Mollusca	*Anadara transversa*	0	0	1	0	0	0	0	0
Mollusca	*Anomia simplex*	0	0	1	0	0	0	0	0
Mollusca	*Corbula contracta*	0	0	0	0	1*	0	0	0
Mollusca	*Eupleura caudata*	0	0	1*	0	0	0	0	0
Mollusca	*Kurtziella atrostyla*	0	0	1*	0	0	0	0	0
Mollusca	Lucinidae indet.	1*	0	0	0	0	0	0	0
Mollusca	*Martesia* sp.	0	0	1*	0	0	0	0	0
Mollusca	*Nassarius vibex*	0	0	1*	0	0	0	0	0
Mollusca	*Ostrea equestris*	0	0	0	0	0	0	1	0
Mollusca	*Seila adamsi*	0	0	1*	0	0	0	0	0
Mollusca	*Spisula* sp.	0	0	1*	0	0	0	0	0
Mollusca	*Tagelus* sp.	0	0	0	0	0	1	0	0
Mollusca	*Tellina* sp.	1*	0	0	0	0	0	0	0
Mollusca	*Trachycardium* sp.	0	0	1*	0	0	0	0	0
Mollusca	*Tucetona perctinata*	0	0	1*	0	0	0	0	0
Mollusca	*Turbonilla interrupta*	0	0	1	0	0	0	0	0
Mollusca	*Turbonilla* sp.	0	0	1*	0	0	0	0	0
Bryozoa	Bryozoa indet.	0	0	0	1*	0	0	0	0
Mollusca	*Cyrtopleura costata*	0	1*	0	0	0	0	0	0

*Presence in sample based on a single specimen

Table A3.1-8 | Results of a PERMANOVA test of community composition between assemblages grouped by age (i.e., fossil and modern).

Permutation test for adonis under reduced model
Terms added sequentially (first to last)
Permutation: free
Number of permutations: 999

adonis2(formula = nmds[1:7, 9:53] ~ nmds$Age, method = "bray")

	Df	SumOfSqs	F	Pr(>F)
nmds$Age	1	0.21058	1.8285	0.129
Residual	6	0.69098		

APPENDIX 3.2

A3.2.1 Salinity and temperature difference estimation

Previous studies have suggested that the Canepatch Formation was deposited during an interglacial period that was as warm as or warmer than the present (DuBar 1971; Cronin et al. 1981). However, in order to obtain a more specific estimate of the magnitude of temperature difference between the modern and fossil oyster assemblages we attempted to estimate water temperature from average $\delta^{18}O$ values for seven fossil and six modern oyster specimens from a subset of the assemblages (P2, P4, R1, R5; stable isotope profiles for each specimen analyzed are reported in Durham et al. in press). We estimated average salinity and temperature for the modern assemblages from monthly measurement data collected between 1999-2006 by the South Carolina Department of Health and Environmental Control (SCDHEC) at stations near each of our sampling locations (data archived by the National Water Quality Monitoring Council, accessed from www.waterqualitydata.us/portal/ on 6/28/2017).

This process required estimation of fossil-modern salinity differences as well, because to calculate temperature from $\delta^{18}O_{shell}$ values, an estimation of $\delta^{18}O_{water}$ value is required, and $\delta^{18}O_{water}$ varies with salinity. Background barium:calcium (Ba/Ca) ratios in mollusk shells have been shown to reflect average salinity (Gillikin et al. 2006a; Poulain et al. 2015). The Ba/Ca ratio is one of several elemental ratios that can be derived from the output of laser ablation-inductively coupled plasma-mass spectrometry (LA-ICP-MS) analyses of mollusk shells—the same technique used to obtain Mg/Ca ratios for our lifespan estimates (e.g., Durham et al. in press). Thus, we already had Ba/Ca data from 48 fossil and 44 modern oyster specimens from all eight assemblages (analyses described in Durham et al. in press). However, a preliminary

check of Mn and U values from the LA-ICP-MS data revealed elevated values of Mn/Ca and U/Ca in the fossil specimens relative to the modern specimens (Table A3.2-1; Figure A3.2-1); a result indicative of chemical diagenesis of the fossil shells (Pilkey & Goodell 1964; Gillikin et al. 2005). Because Ba concentrations in oyster shells are generally low, Ba/Ca is among the earlier elemental ratios to be affected by diagenesis. This fact combined with the probability that salinity differences were low between fossil and modern assemblages (e.g., based on community composition data, Appendix 3.1), suggested we should not interpret salinity from the oyster Ba/Ca ratios.

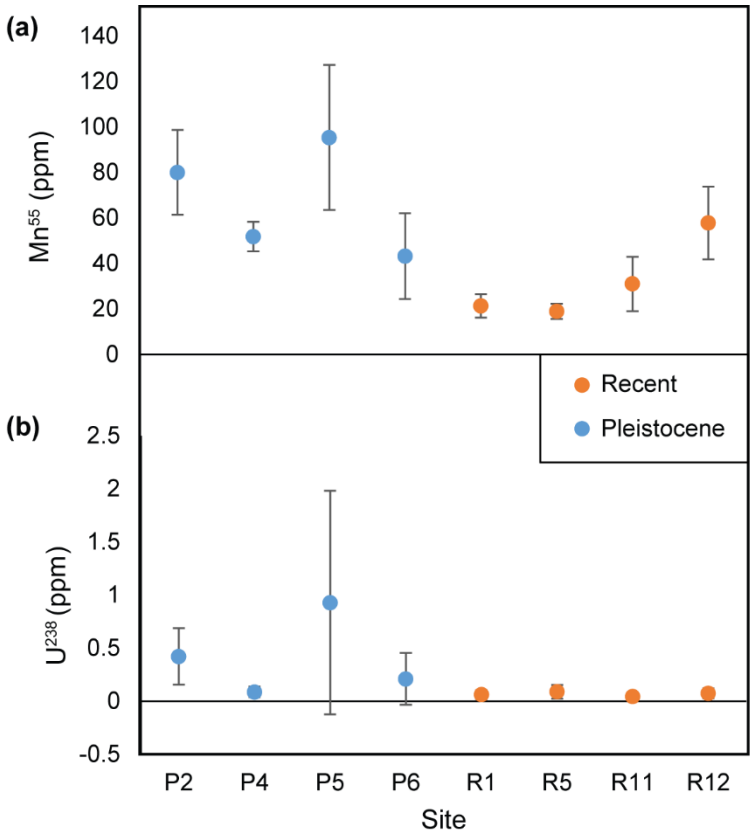

Figure A3.2-1 | Plots of (a) average Mn^{55} and (b) U^{238} concentrations for each fossil and modern site. Error bars = 1SD.

Table A3.2-1 | T-tests comparing fossil and modern values of Mn/Ca and U/Ca in order to assess levels of diagenesis in the fossil oysters.

Two-sample t-tests by age			
With/without P5	Element	t	p
With P5	Na23	0.8657	0.3903
With P5	Fe154	1.5761	0.1185
With P5	Fe256	1.2592	0.2127
With P5	Fe357	1.9115	0.0590
With P5	Mn55	7.2803	**<0.0001**
With P5	U238	4.0490	**0.0002**
Without P5	Na23	-1.8933	0.0635
Without P5	Fe154	0.2174	0.8284
Without P5	Fe256	0.5375	0.5923
Without P5	Fe357	1.2744	0.2058
Without P5	Mn55	6.3182	**<0.0001**
Without P5	U238	4.6022	**<0.0001**

An alternative, though less precise, paleosalinity proxy is $\delta^{13}C$, values for which are measured at the same time as the $\delta^{18}O$ (Durham et al. in press). However, $\delta^{13}C$ is unlikely to discriminate salinity differences less than ~5-10, and values within ~2‰ of each other are almost certainly the same within error (Gillikin et al. 2006b). Average $\delta^{13}C$ values for the fossil and modern sites (P2, P4 and R1, R5, respectively) are indeed within 2‰, suggesting that the most we can say about salinity in the fossil oyster assemblages is that it was most likely within 5-10 of modern values (i.e., ~30, Table A3.2-2).

We nevertheless tried calculating paleotemperature from our $\delta^{18}O$ data using the temperature equation from Anderson & Arthur (1983) for biogenic aragonite and calcite (equation listed in Table 1 in Grossman 2012), making the assumption that salinity was the same in the fossil and modern. For the $\delta^{18}O_{shell}$ values, we used average maximum $\delta^{18}O$ values, calculated by averaging the maximum values from each annual cycle in the $\delta^{18}O$ profiles for the South Carolina specimens from Durham et al. (in press). We estimated $\delta^{18}O_{water}$ from two end-member regressions of $\delta^{18}O$ values based on global mean ocean values for salinity and $\delta^{18}O$ of 34.7 and 0‰,

respectively, from Railsback et al. (1989) and the minimum and maximum estimated $\delta^{18}O$ of precipitation in northeastern South Carolina (-6.6‰ or -4.6‰; Vachon et al. 2010). Using precipitation $\delta^{18}O$ values to estimate the $\delta^{18}O$ of freshwater input is reasonable because precipitation is the primary source of freshwater input into the back barrier marsh environments where the oyster reefs we sampled grow (e.g., Bahr & Lanier 1981). The regression equations for calculating $\delta^{18}O_{water}$ assuming precipitation $\delta^{18}O$ values of -6.6‰ and -4.6‰ were [$\delta^{18}O_{water}$ = 0.1902 * salinity – 6.6] and [$\delta^{18}O_{water}$ = 0.1326 * salinity – 4.6], respectively. The resulting $\delta^{18}O_{water}$ estimates and our measured average $\delta^{18}O_{shell}$ values yielded temperature difference estimates (Pleistocene – Recent) of -3.48°C and -2.98°C (Table A3.2-2). These values are contrary to lithostratigraphic and fossil evidence that suggests the Canepatch Fm. was at least as warm or warmer than present (DuBar 1971; Cronin et al. 1981). This fact, combined with the large uncertainty in paleosalinity suggest that we should not interpret paleotemperature from the oyster shell $\delta^{18}O$ values.

Table A3.2-2 | Data used in paleosalinity and paleotemperature calculations.

Age	Site	Avg. Temp. (°C)[1]	Avg. Sal.[1]	Avg. max. $\delta^{18}O_{shell}$	Avg. $\delta^{13}C_{shell}$	Est. $\delta^{18}O_w$ A (Δfw =-4.6‰)[2]	Est. $\delta^{18}O_w$ B (Δfw =-6.6‰)[2]	Est. Temp (A)[3]	Est. Temp (B)[3]
Modern	R1	19.98	30.13	-2.81	-1.96	-0.61	-0.87	29.99	27.80
Modern	R5	19.96	30.29	-1.91	-1.02	-0.79	-1.13	21.91	19.83
Pleistocene	P2	n/a	n/a	-1.57	-0.15	n/a	n/a	20.99	19.48
Pleistocene	P4	n/a	n/a	-2.02	-0.47	n/a	n/a	23.94	22.19
Modern	All (Avg.)	19.97	30.21	-2.36	-1.49	-0.70	-1.00	25.95	23.81
Pleistocene	All (Avg.)	n/a	n/a	-1.80	-0.31	-0.59	-0.85	22.46	20.83
						Temp. difference (Pleistocene - Modern):		**-3.48**	**-2.98**

[1]Only including months with avg. temp. ≥ 10°C (minimum *C. virginica* calcification temp.)

[6]Pleistocene $\delta^{18}O_w$ calculated assuming paleosalinity equivalent to modern average salinity

[7]Calculated using temperature equation from Anderson and Arthur (1983), as listed in Grossman (2012)

APPENDIX 3.3

A3.3.1 Oyster lifespan estimates from Mg/Ca ratios

A total of 104 oyster specimens were prepared and analyzed by laser ablation-inductively couple plasma-mass spectrometry (LA-ICP-MS) at Union College in Schenectady, NY as described in Durham et al. (in press). The Mg/Ca data for the 13 South Carolina oyster specimens reported in Durham et al. (in press) are re-plotted here for convenience, along with the additional 91 specimens analyzed for this study (Figures A3.3-1 to A3.3-104).

Lifespans were estimated from the profiles using the following criteria. First, as described in Durham et al. (in press), if a peak or trough in the median in the detrended growth profile crossed the origin, this was considered a probable annual peak or trough. However, this was weighed against the degree of trend in the raw Mg/Ca data. If the median was either flat (i.e., uninformative) or the raw data showed a unidirectional slope with little obvious cyclicity in the profile, then the specimen was considered < 1 year old. Further, prominent peaks were occasionally missed by the median (most likely due to natural variability in growth rates among specimens), so a determination of whether to include the peak or trough was made based on: 1) comparisons with clearer age estimates of specimens from the same site and of similar size, and 2) the position of the peak or trough along the growth profile (missed peaks towards the beginning of profiles are less likely to be annual because the oysters tended to grow rapidly early in life). All lifespans were estimated to the nearest quarter of a year based on the apparent fraction of an entire annual cycle (i.e., one peak/trough pair) left over after all complete cycles were counted. The sizes and estimated lifespans for all specimens analyzed can be found in Table A3.3-1.

Table A3.3-1 | Sizes and estimated lifespans for each specimen analyzed by LA-ICP-MS. Lifespan estimates are interpreted from Mg/Ca profiles for each specimen (Figures AA3.3-1 to AA3.3-104).

Analysis date	Age	Site	Specimen ID	Right valve height (mm)	Resilifer height (mm)	Est. lifespan (years)
7/16/2015	Pleistocene	P2	F2.1-3_4	70.9	22.33	2
7/16/2015	Pleistocene	P2	F2.1-3_5	66.84	14.42	1.25
7/16/2015	Pleistocene	P2	F2.1-3_19	47.09	12.75	1
7/16/2015	Pleistocene	P2	F2.1-3_20	50.51	13.89	1.25
7/17/2015	Pleistocene	P2	F2.1-3_25	36.38	8.25	1
7/15/2015	Pleistocene	P2	F2.1-3_32	74.75	20.8	1.75
7/17/2015	Pleistocene	P2	F2.1-3_43	94.27	22.82	2.5
7/17/2015	Pleistocene	P2	F2.1-3_46	112.23	31.84	2.5
7/16/2015	Pleistocene	P2	F2.1-3_48	83.49	25.47	2.5
7/16/2015	Pleistocene	P2	F2.1-4_1	108.37	31.49	2.5
4/2/2015	Pleistocene	P2	F2.2-3_1	96.97	27.61	2.5
4/3/2015	Pleistocene	P2	F2.2-3_2	72.28	22.96	2.5
4/3/2015	Pleistocene	P2	F2.2-3_3	58.26	12.19	1
4/3/2015	Pleistocene	P2	F2.2-3_4	35.82	5.15	0.5
4/3/2015	Pleistocene	P2	F2.2-3_5	52.26	24.89	1.5
4/3/2015	Pleistocene	P2	F2.2-3_6	54.94	18.41	1.25
4/3/2015	Pleistocene	P2	F2.2-3_7	53.99	19.74	1.5
7/16/2015	Pleistocene	P2	F2.3-3_31	107.7	20.49	3
7/15/2015	Pleistocene	P4	F4.2-2_1	120.21	31.43	2.5
4/2/2015	Pleistocene	P4	F4.2-3_1	108.27	22.33	2.25
2/12/2015	Pleistocene	P4	F4.2-3_2	107.97	34.73	2.5
4/2/2015	Pleistocene	P4	F4.2-3_3	70.98	19.94	1.25
4/3/2015	Pleistocene	P4	F4.2-3_4	65.5	9.44	1
2/12/2015	Pleistocene	P4	F4.2-3_5	49.33	8.36	0.75
4/3/2015	Pleistocene	P4	F4.2-3_6	34.88	6.44	0.75
4/3/2015	Pleistocene	P4	F4.2-3_7	30.7	9.65	0.5
7/15/2015	Pleistocene	P4	F4.2-3_9	55.97	11.79	1.25
7/17/2015	Pleistocene	P4	F4.2-3_21	92.1	21.42	2
7/15/2015	Pleistocene	P4	F4.2-3_37	64.68	13.71	1.25
7/17/2015	Pleistocene	P4	F4.2-3_73	45.38	10.9	1.25
7/17/2015	Pleistocene	P4	F4.2-3_96	33.6	7.9	0.75
7/17/2015	Pleistocene	P4	F4.2-3_100	44.84	10.3	0.75
7/15/2015	Pleistocene	P4	F4.3-2_1	103.82	21.9	2
7/16/2015	Pleistocene	P4	F4.3-2_2	70.5	20.36	1.75
10/7/2015	Pleistocene	P5	F5.1-3_4	32.79	6.62	0.5
10/8/2015	Pleistocene	P5	F5.1-3_5	63.61	13.94	2
10/8/2015	Pleistocene	P5	F5.1-3_8	70.1	13.49	1.75
10/8/2015	Pleistocene	P5	F5.1-3_11	70.69	22.39	1
10/8/2015	Pleistocene	P5	F5.1-3_13	81.03	21.45	1.75
10/8/2015	Pleistocene	P5	F5.1-3_15	84.59	23.29	2.5

Table A3.3-1 (continued)

Analysis date	Age	Site	Specimen ID	Right valve height (mm)	Resilifer height (mm)	Est. lifespan (years)
10/8/2015	Pleistocene	P5	F5.1-3_16	34.98	10.28	0.75
10/8/2015	Pleistocene	P5	F5.1-3_18	26.6	7.35	0.25
10/8/2015	Pleistocene	P5	F5.1-3_20	49.87	10.28	1
10/8/2015	Pleistocene	P5	F5.1-3_25	98.81	31.83	3.25
10/8/2015	Pleistocene	P5	F5.1-3_26	84.69	19.72	3.5
10/7/2015	Pleistocene	P6	F6.1-3_2	87.47	19.82	2.25
10/8/2015	Pleistocene	P6	F6.2-3_1	102.49	22.63	3.25
10/7/2015	Pleistocene	P6	F6.2-3_11	51.77	14.5	1.5
10/8/2015	Pleistocene	P6	F6.2-3_12	26.46	7.66	0.5
10/7/2015	Pleistocene	P6	F6.2-4_1	92.83	21.54	2.75
10/8/2015	Pleistocene	P6	F6.2-4_2	55.97	16.64	3
10/8/2015	Pleistocene	P6	F6.3-3_1	54.18	13.84	1.5
10/7/2015	Pleistocene	P6	F6.3-3_4	78.44	20.28	2.5
10/7/2015	Pleistocene	P6	F6.3-4_1	75.96	10.91	2
10/7/2015	Pleistocene	P6	F6.3-4_2	43.47	11.09	1
2/12/2015	Recent	R1	L1.1-2_1	66.2	18.43	2
2/12/2015	Recent	R1	L1.1-2_4	20.28	5.39	0.5
4/3/2015	Recent	R1	L1.1-4_1	96.46	19.26	2.5
4/2/2015	Recent	R1	L1.1-4_2	99.21	22.6	2
7/17/2015	Recent	R1	L1.1-4_15	27.77	7.39	0.75
7/17/2015	Recent	R1	L1.1-4_23	82.56	27.54	3
7/17/2015	Recent	R1	L1.1-4_26	87.27	20.77	1.5
7/17/2015	Recent	R1	L1.1-4_35	49.37	13.44	1
7/16/2015	Recent	R1	L1.1-4_38	48.73	12.96	1
7/17/2015	Recent	R1	L1.1-4_42	75.38	18.61	2
7/17/2015	Recent	R1	L1.1-4_53	89.9	19.09	2
7/17/2015	Recent	R1	L1.1-4_57	94.67	27.24	4
7/16/2015	Recent	R5	L5.1-4_1	50.97	18.13	1.75
7/17/2015	Recent	R5	L5.1-4_4	59.23	17.88	2.5
7/17/2015	Recent	R5	L5.1-4_5	50.14	14.25	2
7/17/2015	Recent	R5	L5.1-4_6	102.02	36.6	4.5
7/17/2015	Recent	R5	L5.1-4_18	78.8	22.18	3.5
7/17/2015	Recent	R5	L5.1-4_19	33.14	7.95	1
7/17/2015	Recent	R5	L5.1-4_31	62.38	21.99	2.5
7/17/2015	Recent	R5	L5.1-4_32	67.59	21.01	3
7/17/2015	Recent	R5	L5.1-4_66	74.93	30.82	3.25
7/15/2015	Recent	R5	L5.1-4_79	31.69	11.18	1.25
7/17/2015	Recent	R5	L5.1-5_1	47.72	15.33	1.75
7/16/2015	Recent	R5	L5.1-5_2	105.1	38	4.5
7/16/2015	Recent	R5	L5.1-5_3	43.23	10.73	1.25
7/17/2015	Recent	R11	L11.1-2_1		39.33	5
10/7/2015	Recent	R11	L11.1-4_1	27.67	8.03	0.75
10/7/2015	Recent	R11	L11.1-4_2	43.58	12.77	1
10/7/2015	Recent	R11	L11.1-4_3	47.74	8.64	0.5
10/8/2015	Recent	R11	L11.1-4_4	45.77	8.17	0.5

Table A3.3-1 (continued)

Analysis date	Age	Site	Specimen ID	Right valve height (mm)	Resilifer height (mm)	Est. lifespan (years)
10/8/2015	Recent	R11	L11.1-4_5	61.81	14.44	1.25
10/7/2015	Recent	R11	L11.1-4_6	66.86	13.83	1
10/7/2015	Recent	R11	L11.1-4_7	81.13	16.48	1.75
10/8/2015	Recent	R11	L11.1-4_8	76.95	15.8	1.5
10/8/2015	Recent	R11	L11.1-4_9	123.06	42.28	4.75
10/26/2015	Recent	R12	L12.1-4_2	73.12	14.98	1.5
10/26/2015	Recent	R12	L12.1-4_5	66.11	12.94	1
10/26/2015	Recent	R12	L12.1-4_9	44.38	15.36	1
10/26/2015	Recent	R12	L12.1-4_12	71.61	27.91	2.25
10/26/2015	Recent	R12	L12.1-4_16	24.65	13.1	0.75
10/26/2015	Recent	R12	L12.1-4_17	18.46	3.89	0.25
10/26/2015	Recent	R12	L12.1-4_21	95.72	21.59	1.75
10/26/2015	Recent	R12	L12.1-4_28	118.6	26.29	3.25
10/26/2015	Recent	R12	L12.1-4_31	50.03	10.3	1
10/26/2015	Recent	R12	L12.1-4_35	66.21	14.67	0.75
10/26/2015	Recent	R12	L12.1-4_41	74.57	21.8	1.5
10/26/2015	Recent	R12	L12.1-4_43	81.61	15.22	2.5
10/26/2015	Recent	R12	L12.1-4_48	99.35	19.91	3
10/26/2015	Recent	R12	L12.1-4_57	107.64	34.25	3.5

Oyster Mg/Ca profiles | Plots of Mg/Ca ratios with growth distance for oyster specimens included in our study. Each figure includes (a) the raw Mg/Ca data in mmol/mol and (b) the detrended Mg/Ca profile with an adaptive running median plotted according to the method described in (Durham et al. in press). Overlapping horizontal lines at the top of each figure panel indicate the growth distance covered by each LA-ICP-MS line scan.

Figure A3.3-1

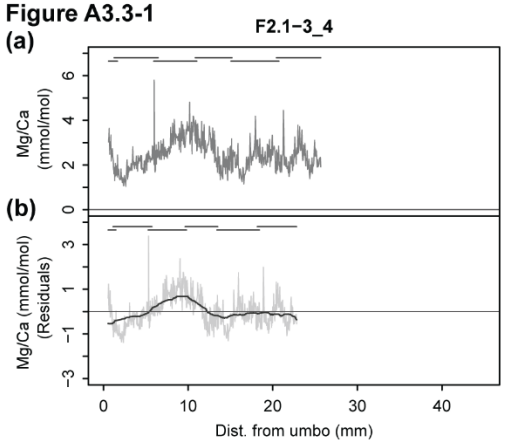

Figure A3.3-2

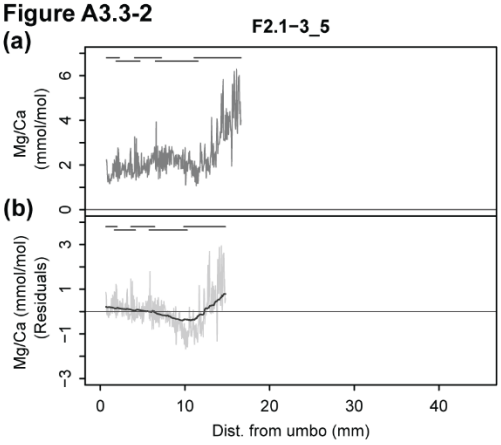

Figure A3.3-3

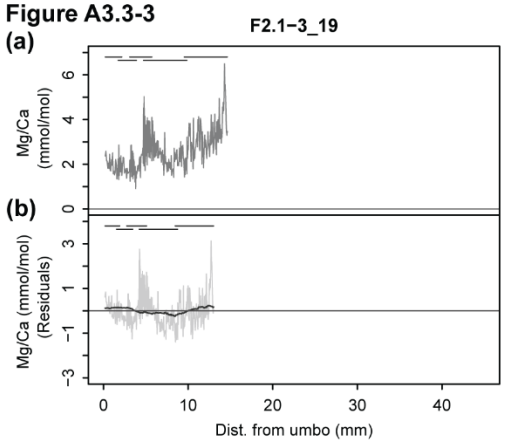

Figure A3.3-4

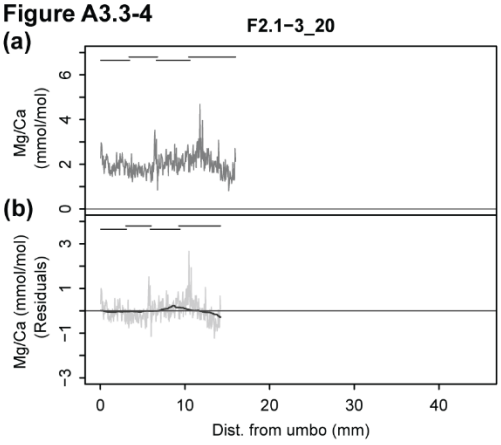

Figure A3.3-5

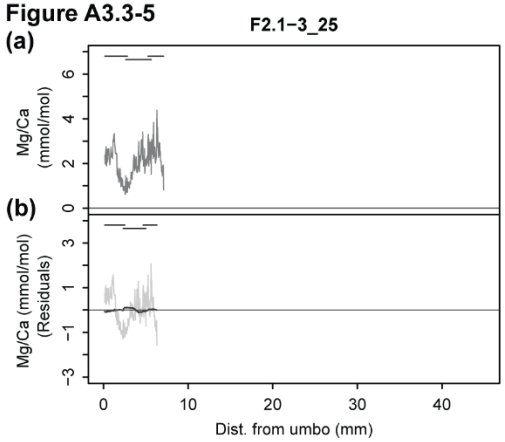

Figure A3.3-6

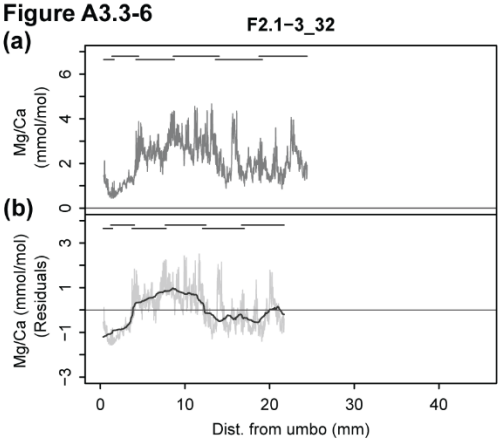

Oyster Mg/Ca profiles (continued) | Plots of Mg/Ca ratios with growth distance for oyster specimens included in our study. Each figure includes the (a) the raw Mg/Ca data in mmol/mol and (b) the detrended Mg/Ca profile with an adaptive running median plotted according to the method described in (Durham et al. in press). Overlapping horizontal lines at the top of each figure panel indicate the growth distance covered by each LA-ICP-MS line scan.

Figure A3.3-7

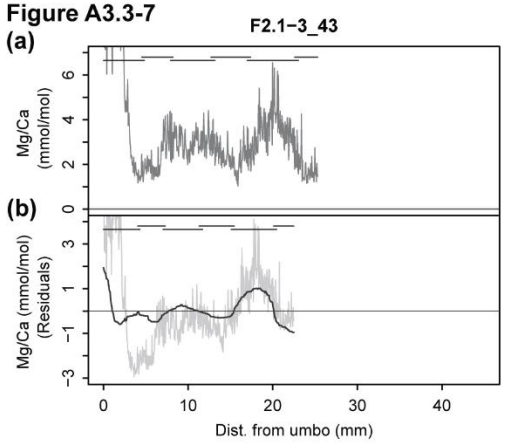

Figure A3.3-8

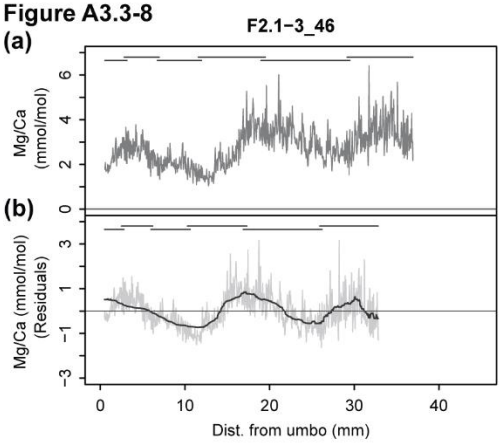

Figure A3.3-9

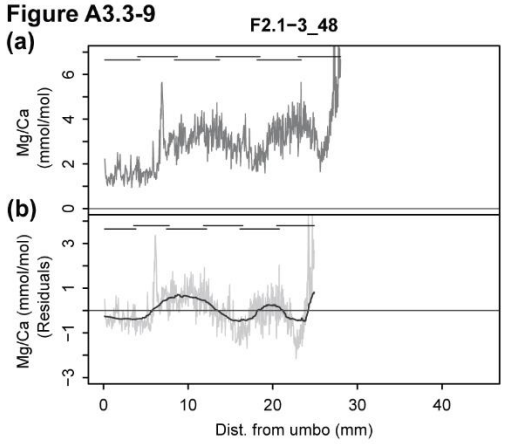

Figure A3.3-10

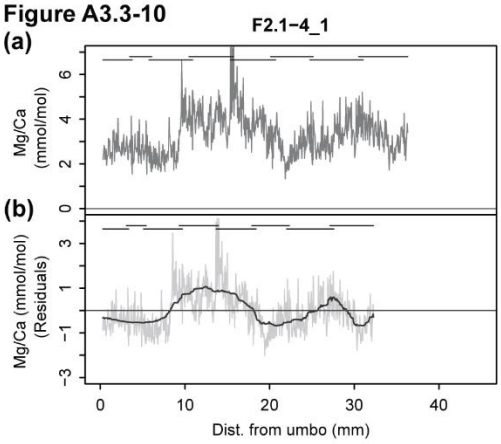

Figure A3.3-11

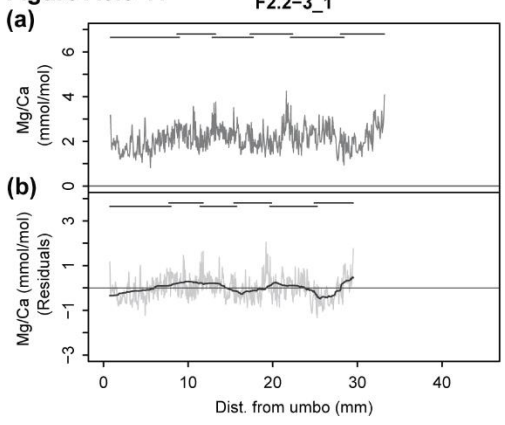

Figure A3.3-12

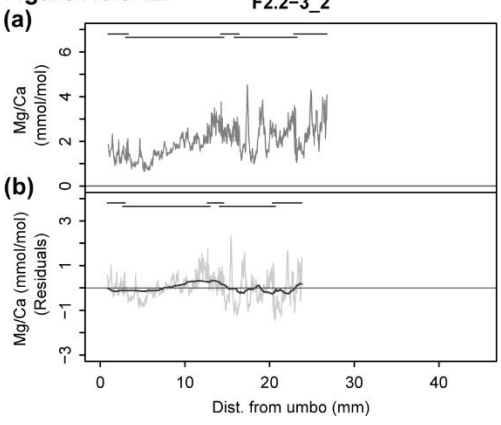

Oyster Mg/Ca profiles (continued) | Plots of Mg/Ca ratios with growth distance for oyster specimens included in our study. Each figure includes the (a) the raw Mg/Ca data in mmol/mol and (b) the detrended Mg/Ca profile with an adaptive running median plotted according to the method described in (Durham et al. in press). Overlapping horizontal lines at the top of each figure panel indicate the growth distance covered by each LA-ICP-MS line scan.

Figure A3.3-13

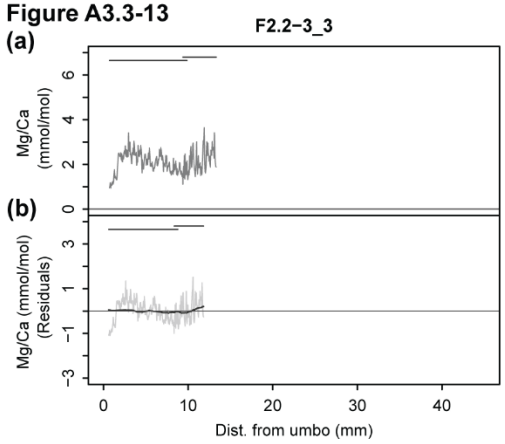

Figure A3.3-14

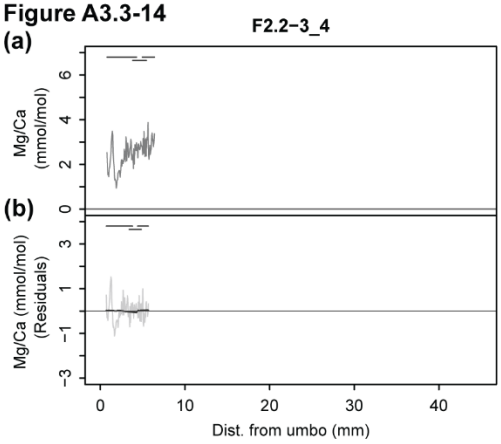

Figure A3.3-15

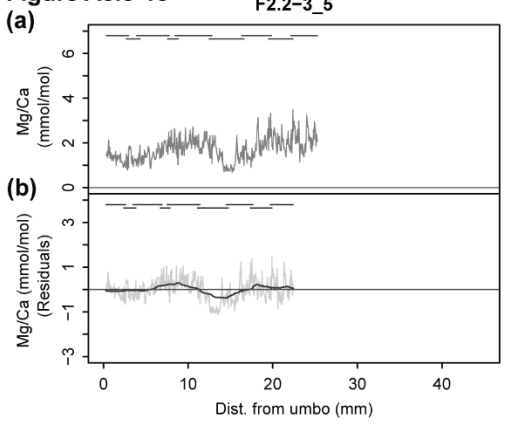

Figure A3.3-16

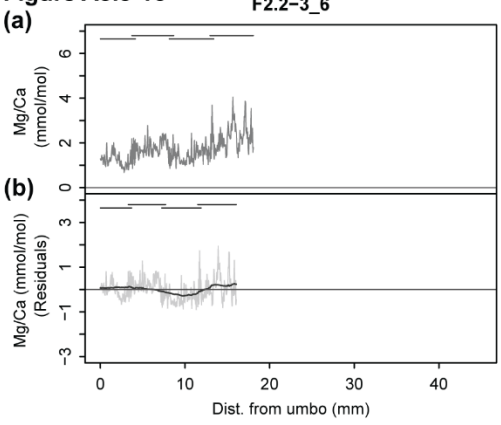

Figure A3.3-17

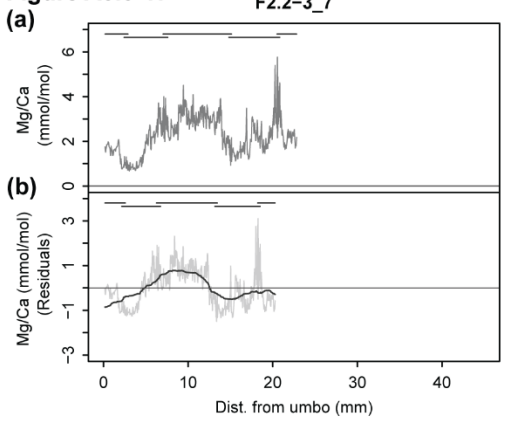

Figure A3.3-18

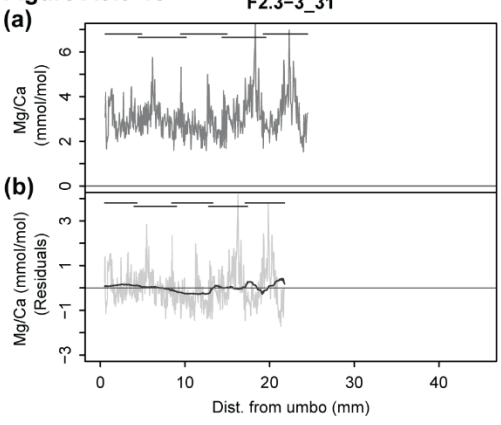

Oyster Mg/Ca profiles (continued) | Plots of Mg/Ca ratios with growth distance for oyster specimens included in our study. Each figure includes the (a) the raw Mg/Ca data in mmol/mol and (b) the detrended Mg/Ca profile with an adaptive running median plotted according to the method described in (Durham et al. in press). Overlapping horizontal lines at the top of each figure panel indicate the growth distance covered by each LA-ICP-MS line scan.

Figure A3.3-19

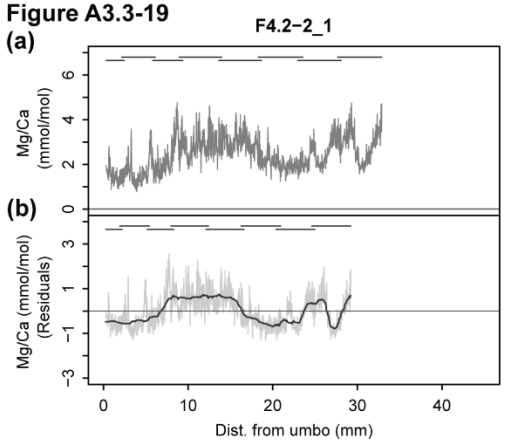

Figure A3.3-20

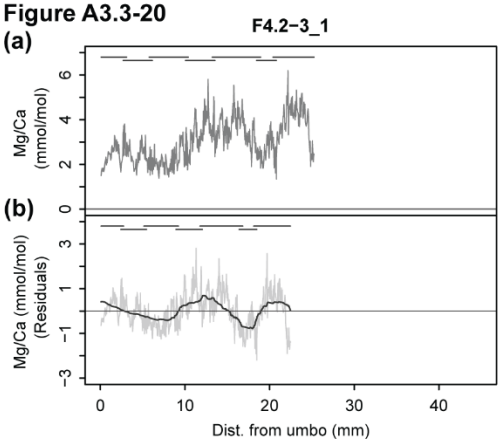

Figure A3.3-21

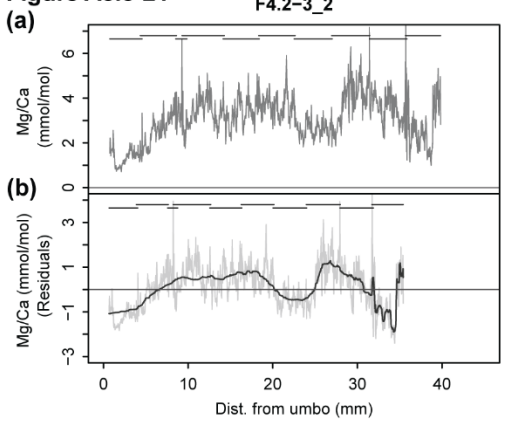

Figure A3.3-22

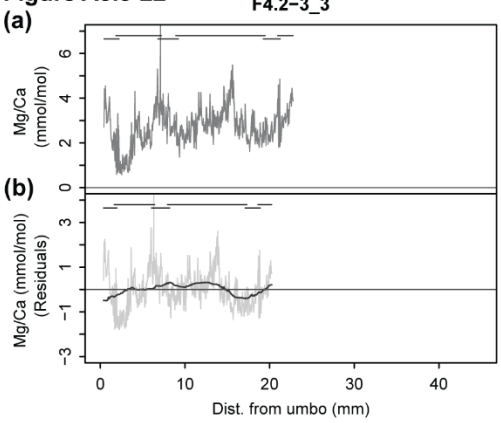

Figure A3.3-23

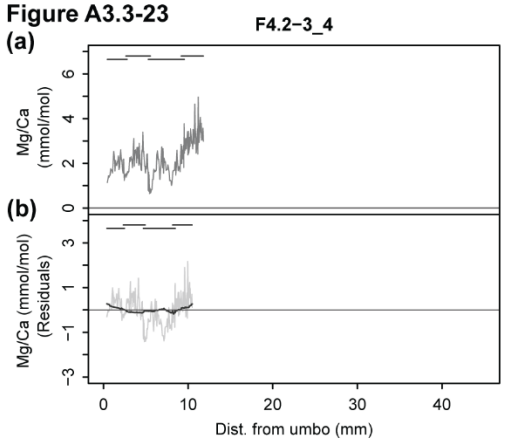

Figure A3.3-24

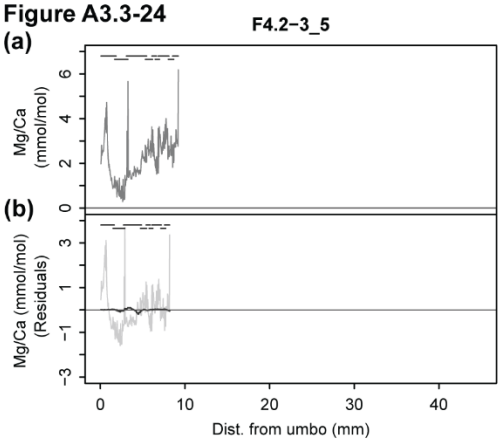

Oyster Mg/Ca profiles (continued) | Plots of Mg/Ca ratios with growth distance for oyster specimens included in our study. Each figure includes the (a) the raw Mg/Ca data in mmol/mol and (b) the detrended Mg/Ca profile with an adaptive running median plotted according to the method described in (Durham et al. in press). Overlapping horizontal lines at the top of each figure panel indicate the growth distance covered by each LA-ICP-MS line scan.

Figure A3.3-25

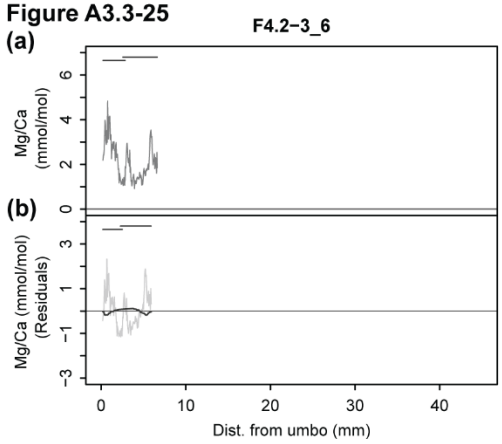

Figure A3.3-26

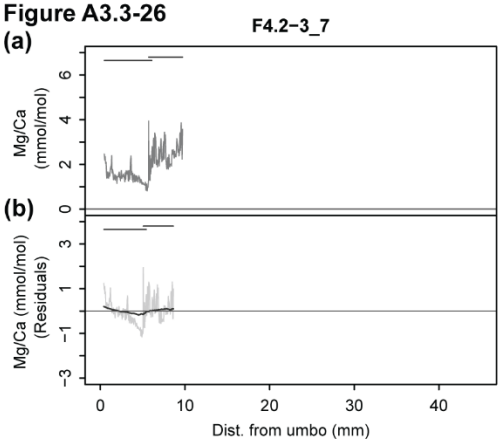

Figure A3.3-27

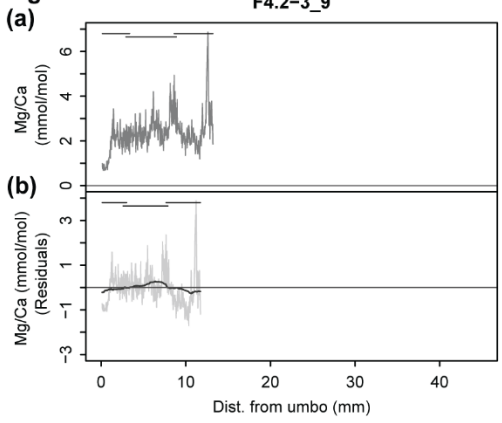

Figure A3.3-28

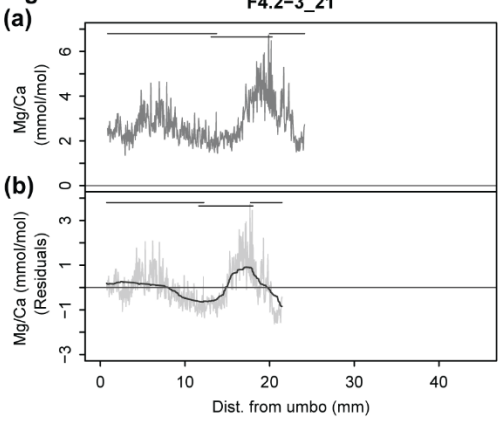

Figure A3.3-29

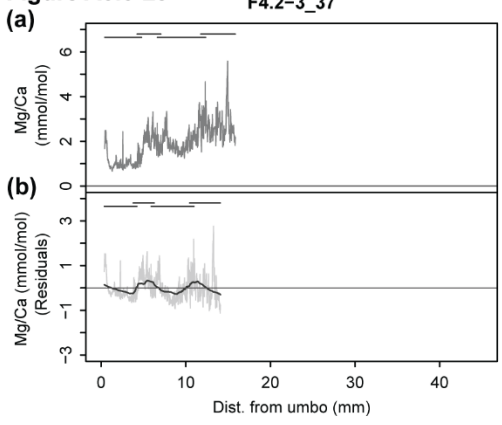

Figure A3.3-30

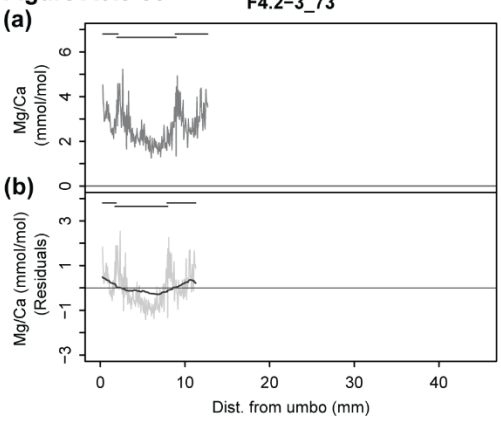

Oyster Mg/Ca profiles (continued) | Plots of Mg/Ca ratios with growth distance for oyster specimens included in our study. Each figure includes the (a) the raw Mg/Ca data in mmol/mol and (b) the detrended Mg/Ca profile with an adaptive running median plotted according to the method described in (Durham et al. in press). Overlapping horizontal lines at the top of each figure panel indicate the growth distance covered by each LA-ICP-MS line scan.

Figure A3.3-31

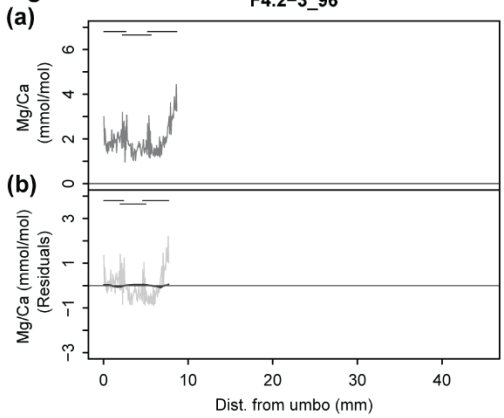

Figure A3.3-32

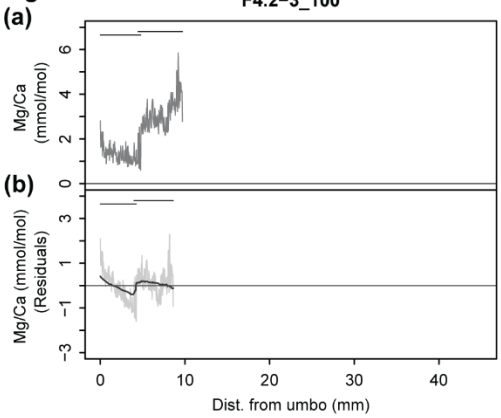

Figure A3.3-33

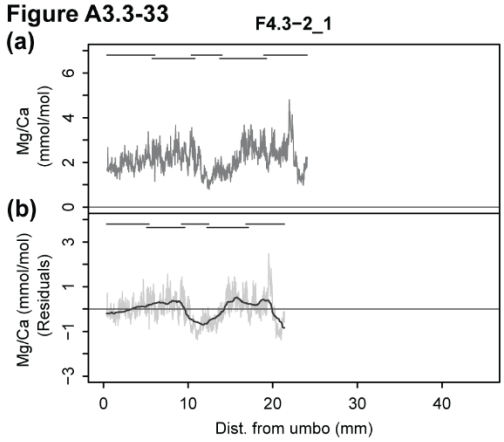

Figure A3.3-34

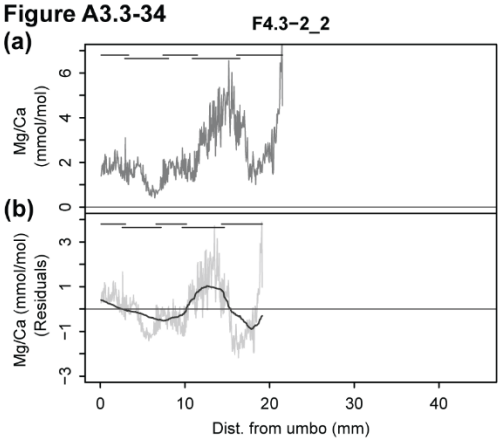

Figure A3.3-35

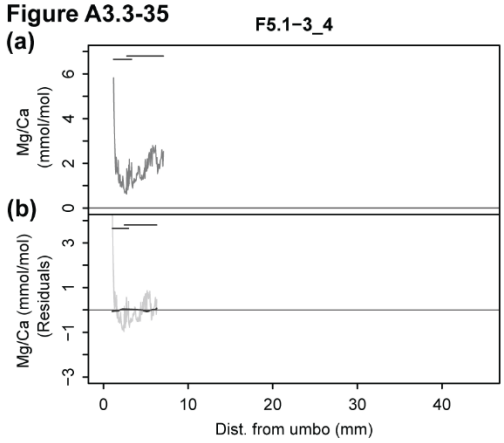

Figure A3.3-36

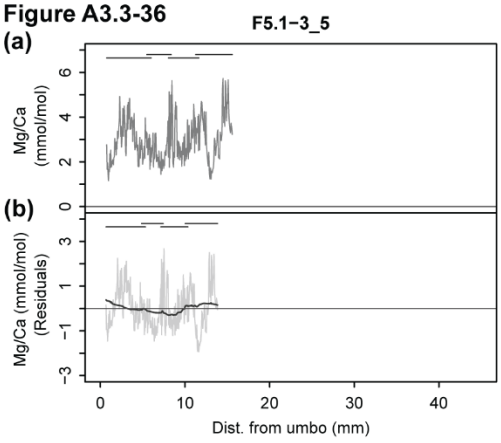

Oyster Mg/Ca profiles (continued) | Plots of Mg/Ca ratios with growth distance for oyster specimens included in our study. Each figure includes the (a) the raw Mg/Ca data in mmol/mol and (b) the detrended Mg/Ca profile with an adaptive running median plotted according to the method described in (Durham et al. in press). Overlapping horizontal lines at the top of each figure panel indicate the growth distance covered by each LA-ICP-MS line scan.

Figure A3.3-37

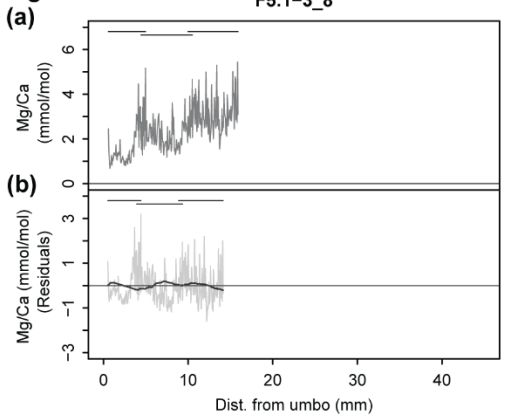

Figure A3.3-38

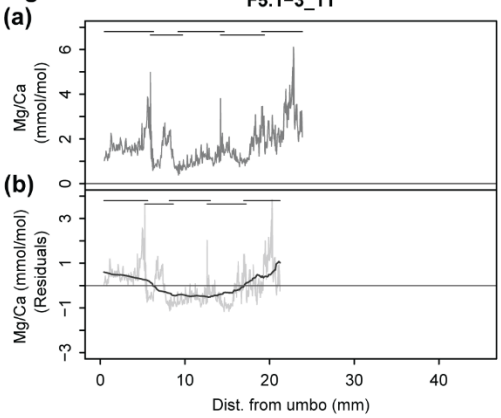

Figure A3.3-39

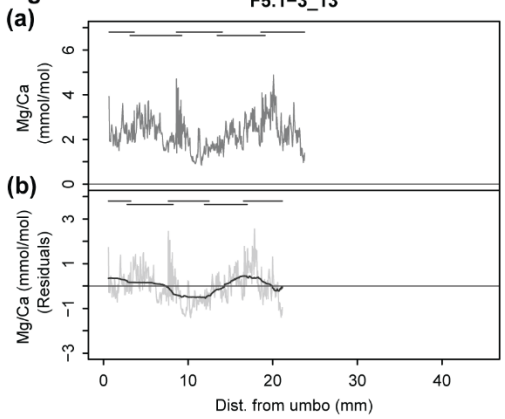

Figure A3.3-40

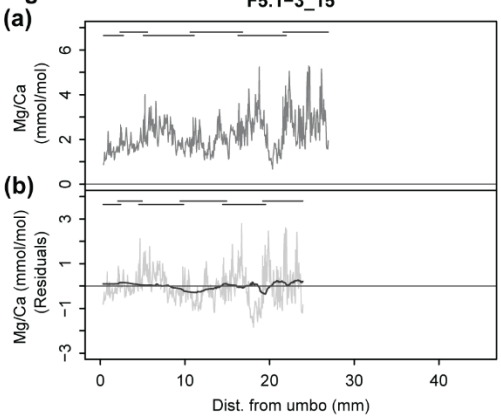

Figure A3.3-41

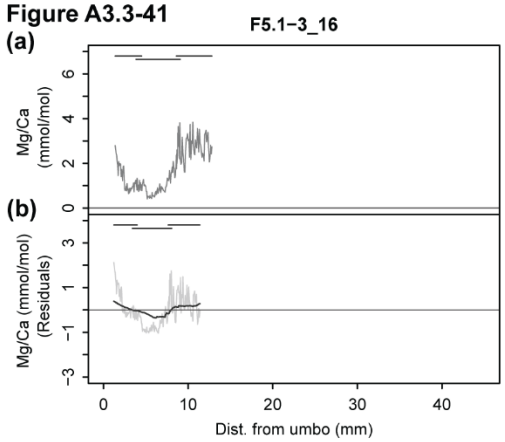

Figure A3.3-42

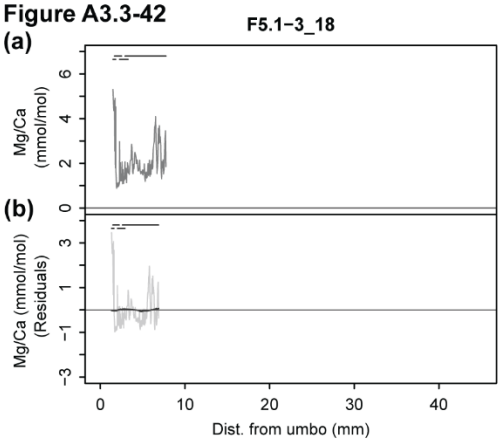

Oyster Mg/Ca profiles (continued) | Plots of Mg/Ca ratios with growth distance for oyster specimens included in our study. Each figure includes the (a) the raw Mg/Ca data in mmol/mol and (b) the detrended Mg/Ca profile with an adaptive running median plotted according to the method described in (Durham et al. in press). Overlapping horizontal lines at the top of each figure panel indicate the growth distance covered by each LA-ICP-MS line scan.

Figure A3.3-43

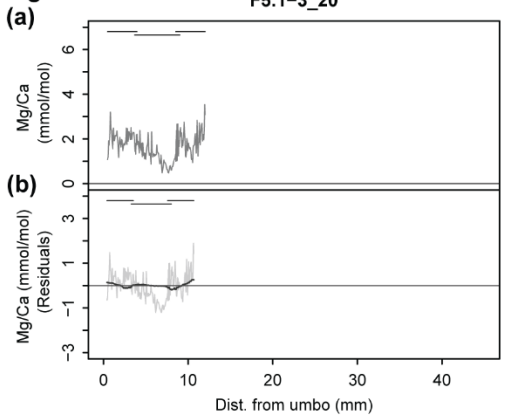

Figure A3.3-44

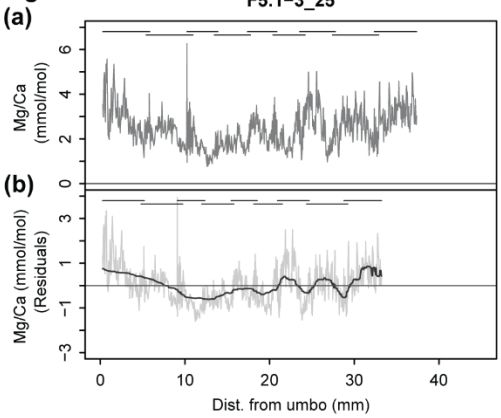

Figure A3.3-45

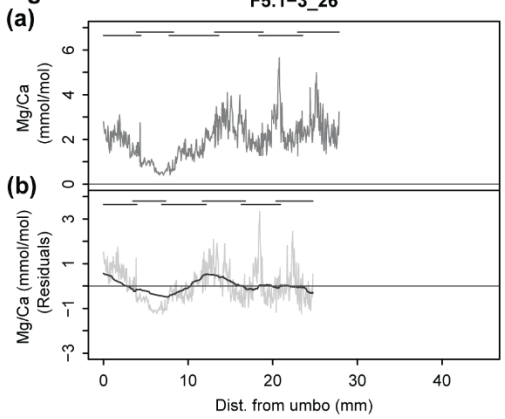

Figure A3.3-46

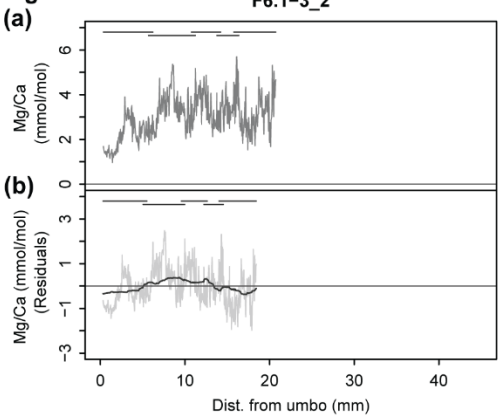

Figure A3.3-47

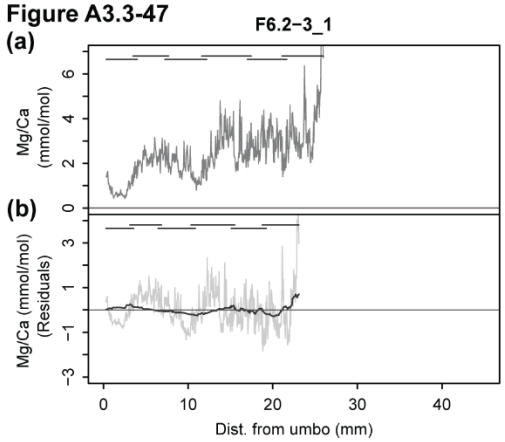

Figure A3.3-48

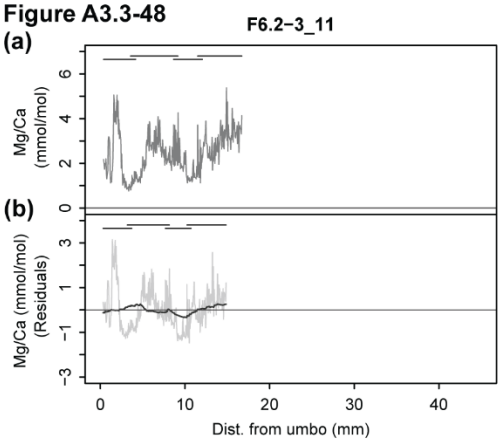

Oyster Mg/Ca profiles (continued) | Plots of Mg/Ca ratios with growth distance for oyster specimens included in our study. Each figure includes the (a) the raw Mg/Ca data in mmol/mol and (b) the detrended Mg/Ca profile with an adaptive running median plotted according to the method described in (Durham et al. in press). Overlapping horizontal lines at the top of each figure panel indicate the growth distance covered by each LA-ICP-MS line scan.

Figure A3.3-49

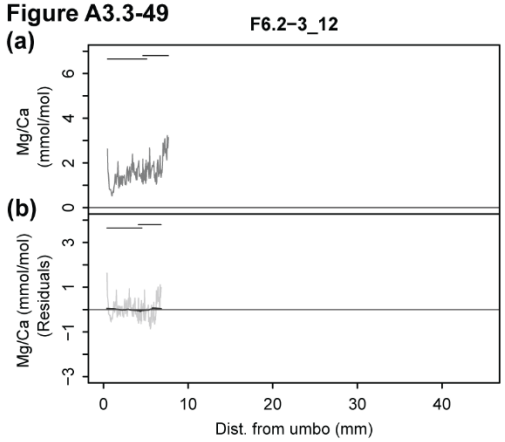

Figure A3.3-50

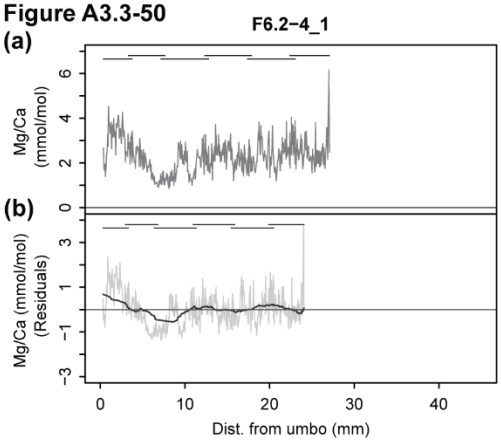

Figure A3.3-51

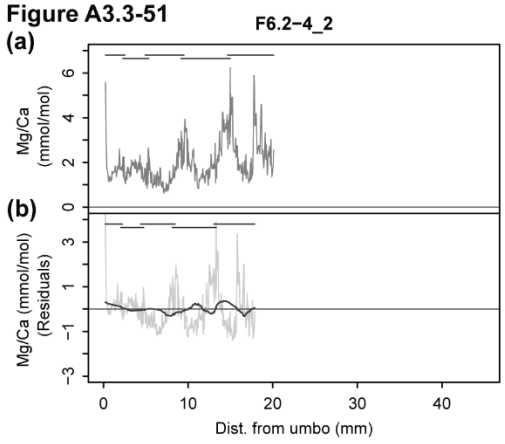

Figure A3.3-52

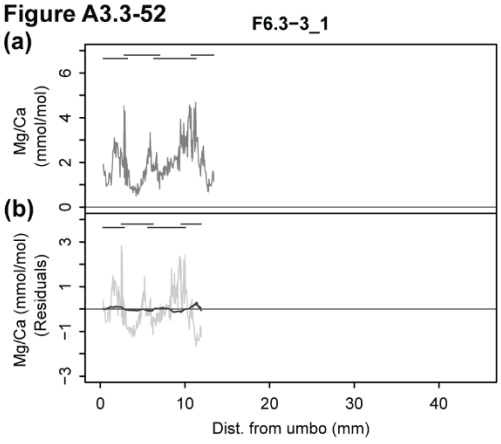

Figure A3.3-53

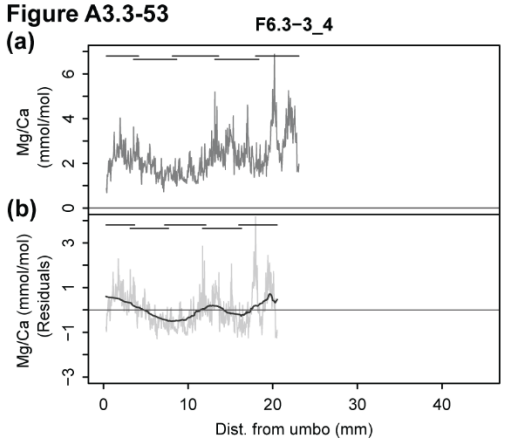

Figure A3.3-54

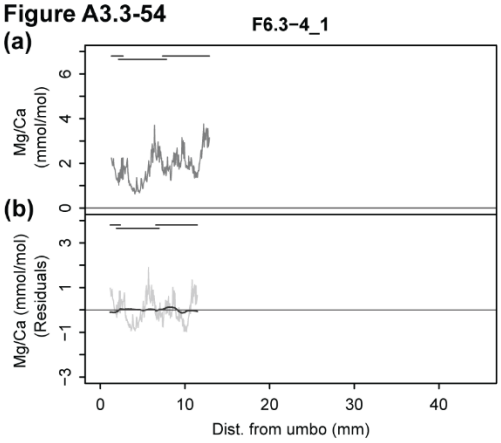

Oyster Mg/Ca profiles (continued) | Plots of Mg/Ca ratios with growth distance for oyster specimens included in our study. Each figure includes the (a) the raw Mg/Ca data in mmol/mol and (b) the detrended Mg/Ca profile with an adaptive running median plotted according to the method described in (Durham et al. in press). Overlapping horizontal lines at the top of each figure panel indicate the growth distance covered by each LA-ICP-MS line scan.

Figure A3.3-55

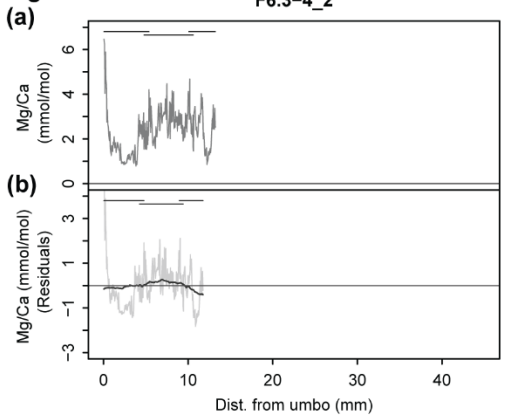

Figure A3.3-56

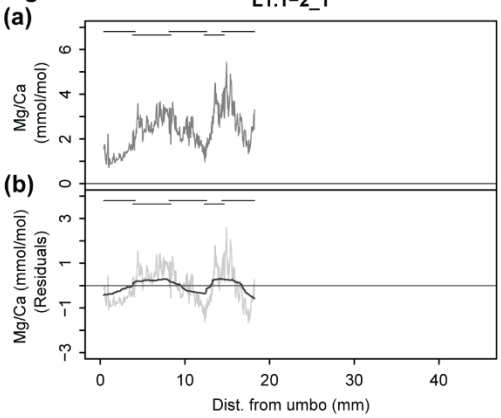

Figure A3.3-57

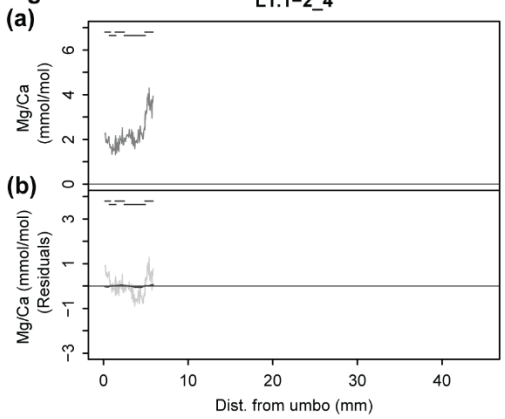

Figure A3.3-58

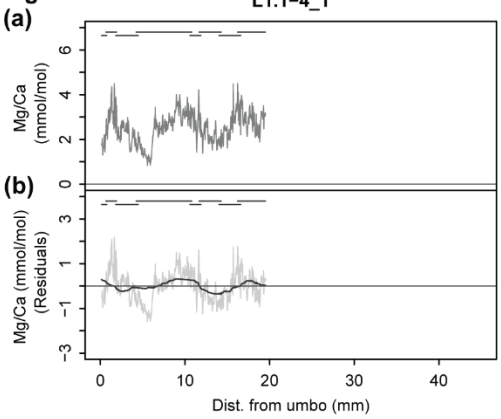

Figure A3.3-59

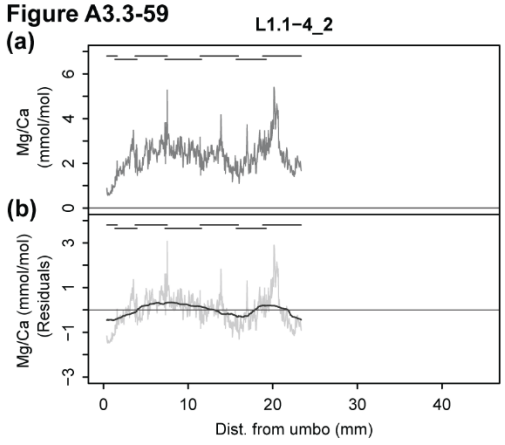

Figure A3.3-60

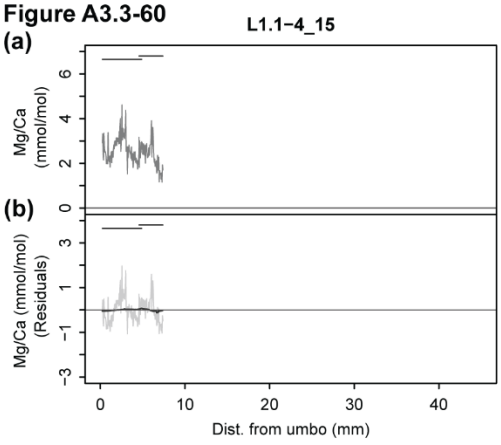

Oyster Mg/Ca profiles (continued) | Plots of Mg/Ca ratios with growth distance for oyster specimens included in our study. Each figure includes the (a) the raw Mg/Ca data in mmol/mol and (b) the detrended Mg/Ca profile with an adaptive running median plotted according to the method described in (Durham et al. in press). Overlapping horizontal lines at the top of each figure panel indicate the growth distance covered by each LA-ICP-MS line scan.

Figure A3.3-61

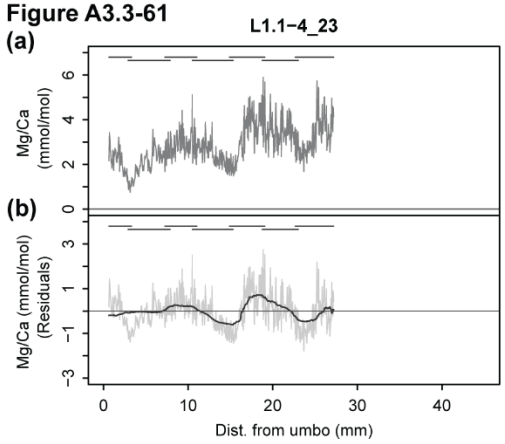

Figure A3.3-62

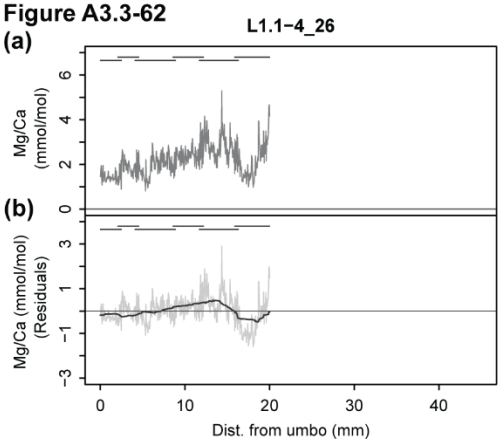

Figure A3.3-63

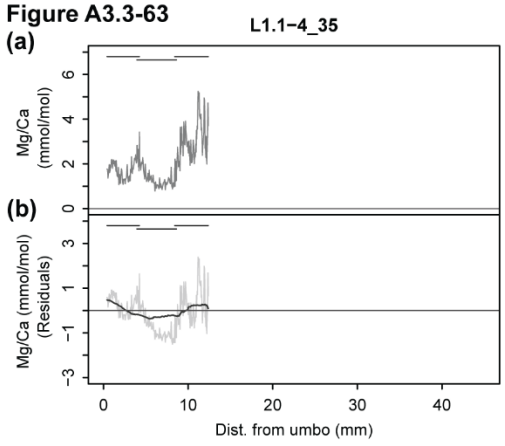

Figure A3.3-64

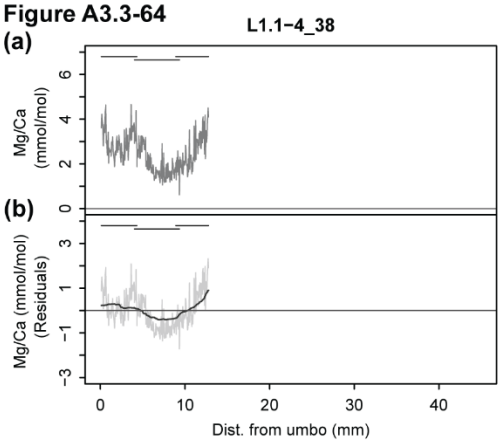

Figure A3.3-65

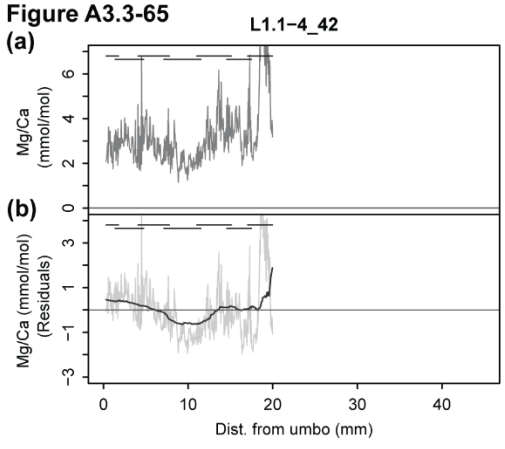

Figure A3.3-66

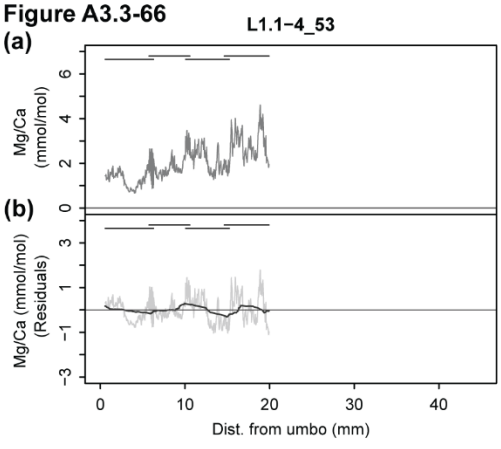

Oyster Mg/Ca profiles (continued) | Plots of Mg/Ca ratios with growth distance for oyster specimens included in our study. Each figure includes the (a) the raw Mg/Ca data in mmol/mol and (b) the detrended Mg/Ca profile with an adaptive running median plotted according to the method described in (Durham et al. in press). Overlapping horizontal lines at the top of each figure panel indicate the growth distance covered by each LA-ICP-MS line scan.

Figure A3.3-67

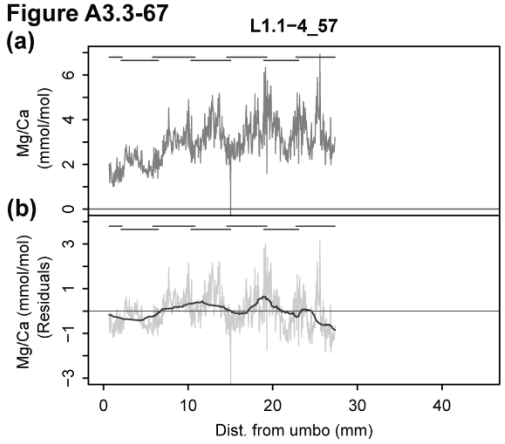

Figure A3.3-68

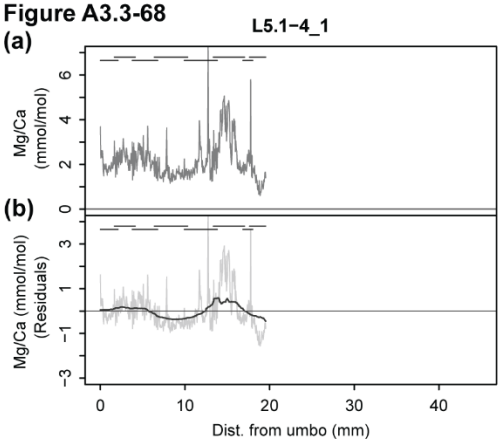

Figure A3.3-69

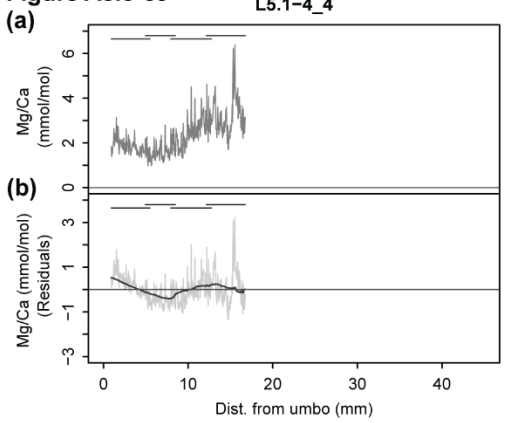

Figure A3.3-70

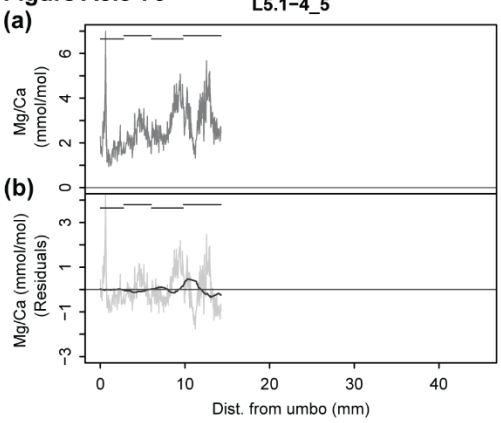

Figure A3.3-71

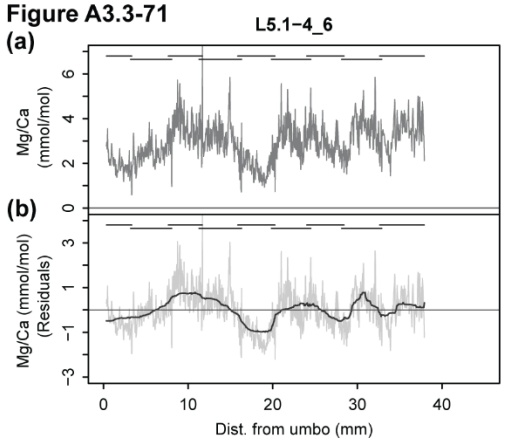

Figure A3.3-72

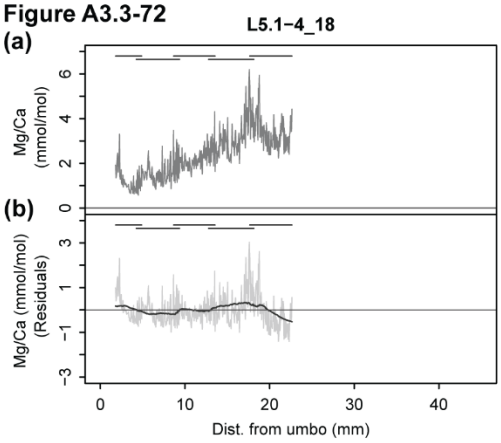

Oyster Mg/Ca profiles (continued) | Plots of Mg/Ca ratios with growth distance for oyster specimens included in our study. Each figure includes the (a) the raw Mg/Ca data in mmol/mol and (b) the detrended Mg/Ca profile with an adaptive running median plotted according to the method described in (Durham et al. in press). Overlapping horizontal lines at the top of each figure panel indicate the growth distance covered by each LA-ICP-MS line scan.

Figure A3.3-73

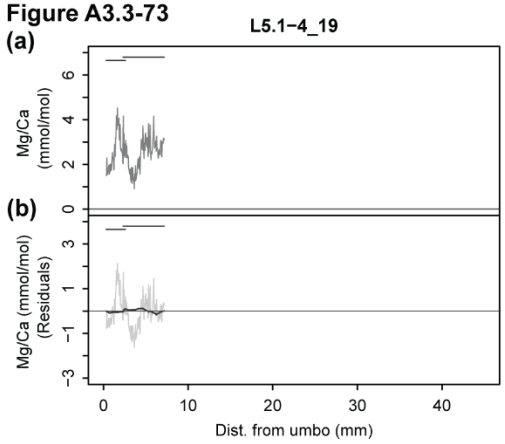

Figure A3.3-74

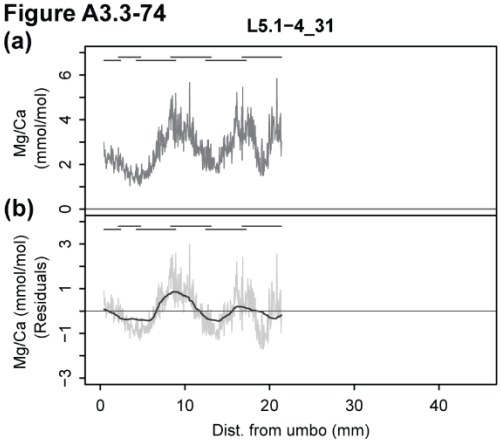

Figure A3.3-75

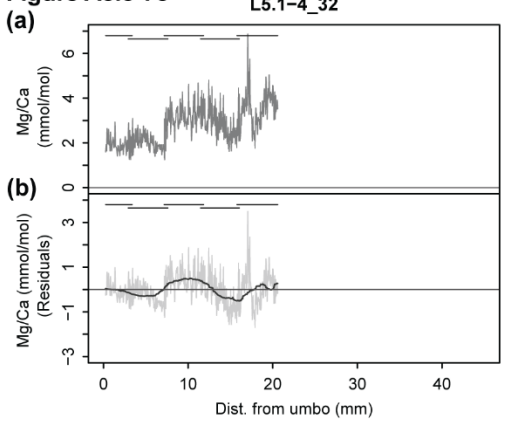

Figure A3.3-76

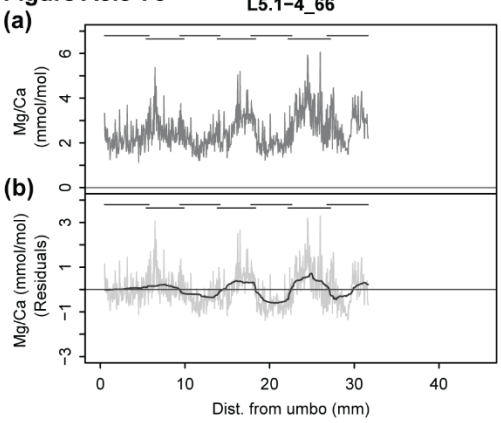

Figure A3.3-77

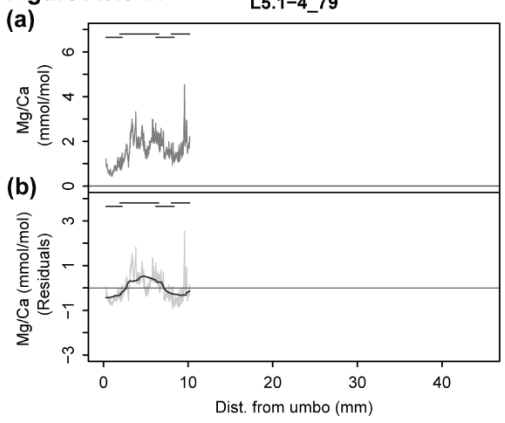

Figure A3.3-78

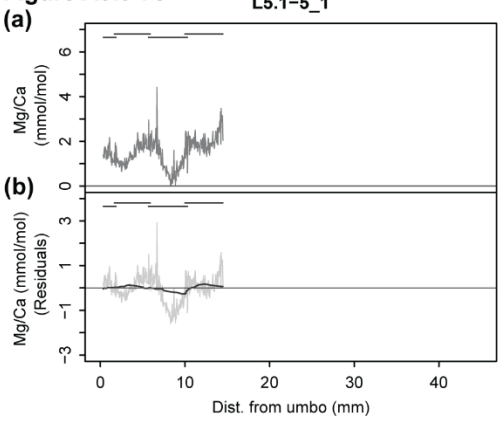

Oyster Mg/Ca profiles (continued) | Plots of Mg/Ca ratios with growth distance for oyster specimens included in our study. Each figure includes the (a) the raw Mg/Ca data in mmol/mol and (b) the detrended Mg/Ca profile with an adaptive running median plotted according to the method described in (Durham et al. in press). Overlapping horizontal lines at the top of each figure panel indicate the growth distance covered by each LA-ICP-MS line scan.

Figure A3.3-79

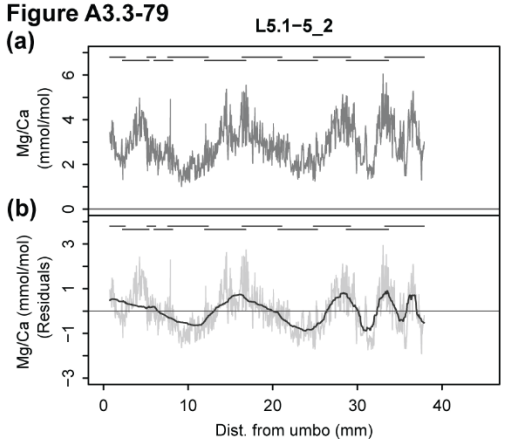

Figure A3.3-80

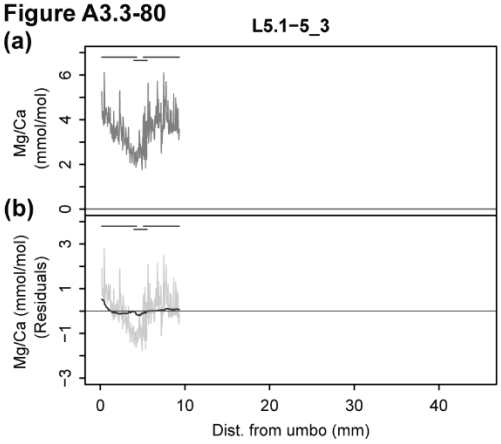

Figure A3.3-81

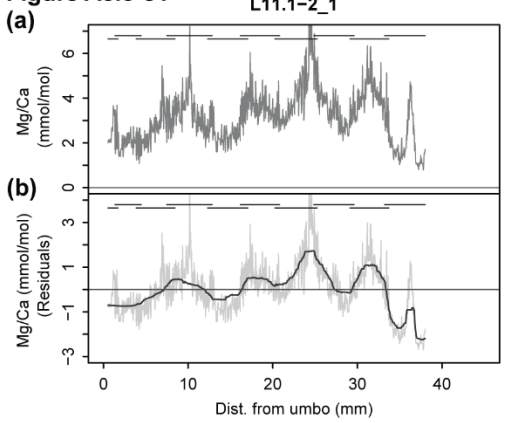

Figure A3.3-82

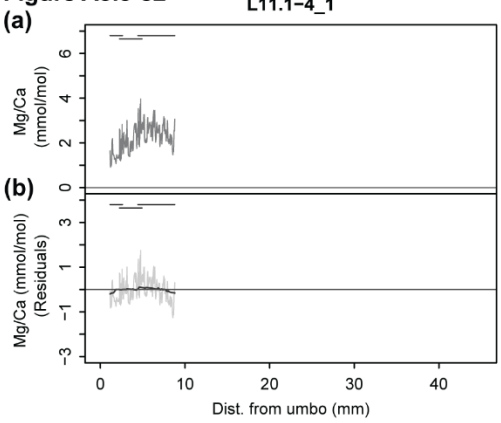

Figure A3.3-83

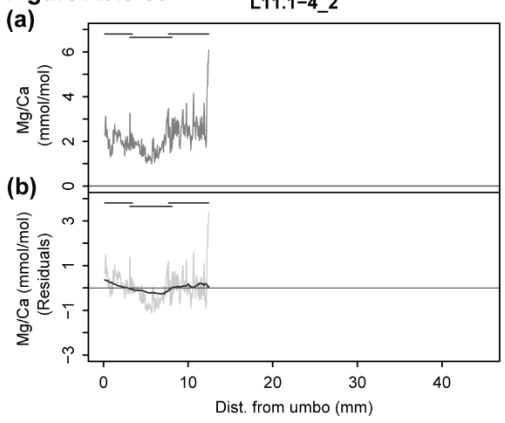

Figure A3.3-84

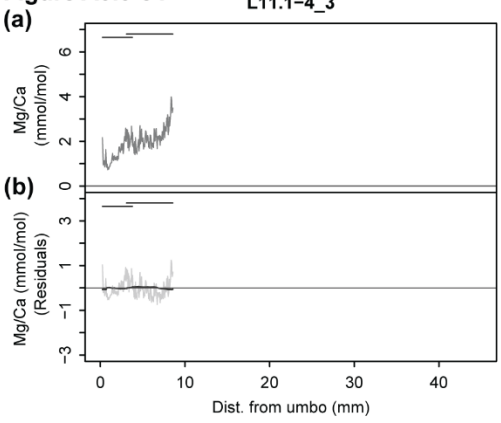

Oyster Mg/Ca profiles (continued) | Plots of Mg/Ca ratios with growth distance for oyster specimens included in our study. Each figure includes the (a) the raw Mg/Ca data in mmol/mol and (b) the detrended Mg/Ca profile with an adaptive running median plotted according to the method described in (Durham et al. in press). Overlapping horizontal lines at the top of each figure panel indicate the growth distance covered by each LA-ICP-MS line scan.

Figure A3.3-85

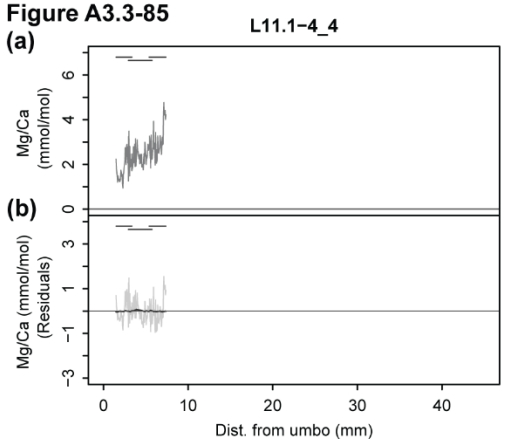

Figure A3.3-86

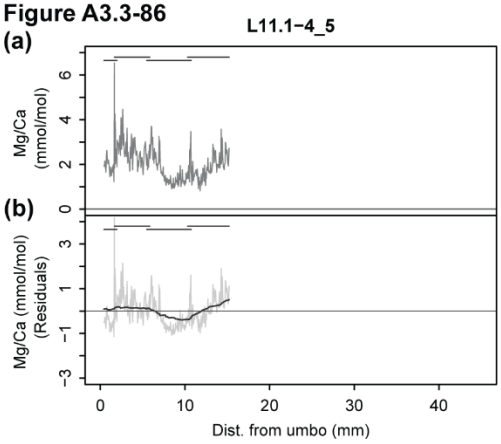

Figure A3.3-87

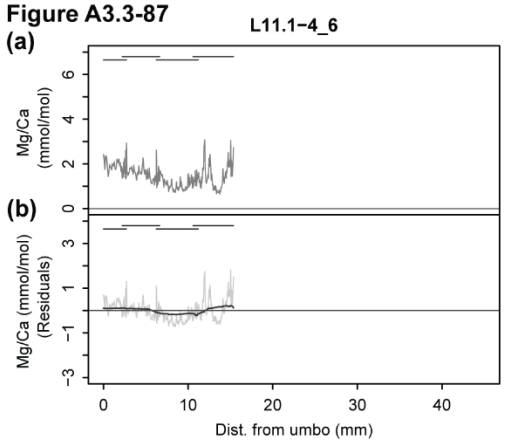

Figure A3.3-88

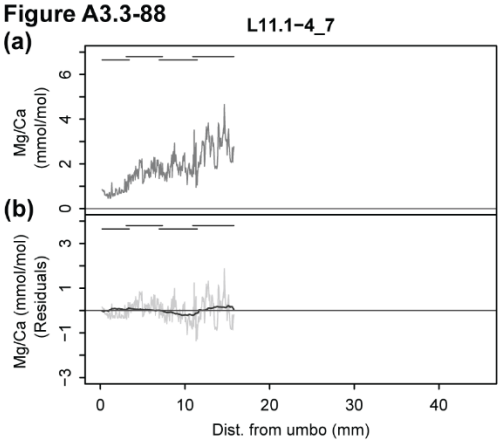

Figure A3.3-89

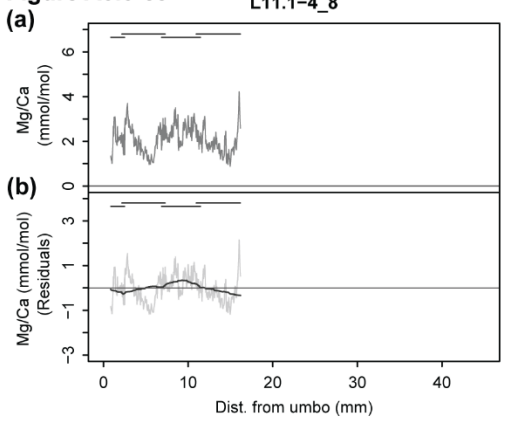

Figure A3.3-90

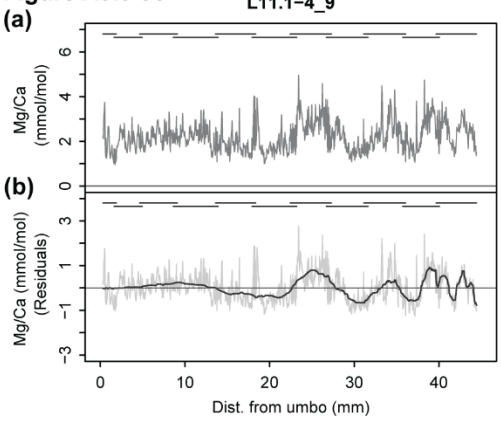

Oyster Mg/Ca profiles (continued) | Plots of Mg/Ca ratios with growth distance for oyster specimens included in our study. Each figure includes the (a) the raw Mg/Ca data in mmol/mol and (b) the detrended Mg/Ca profile with an adaptive running median plotted according to the method described in (Durham et al. in press). Overlapping horizontal lines at the top of each figure panel indicate the growth distance covered by each LA-ICP-MS line scan.

Figure A3.3-91

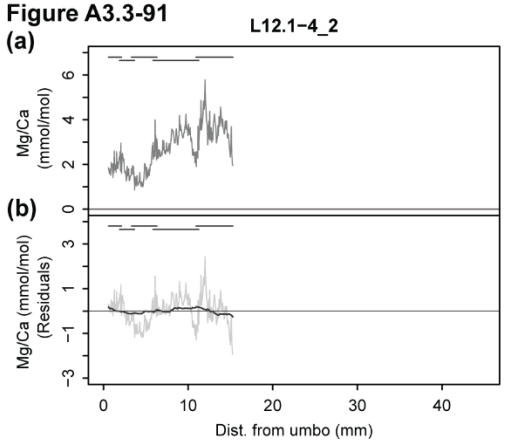

Figure A3.3-92

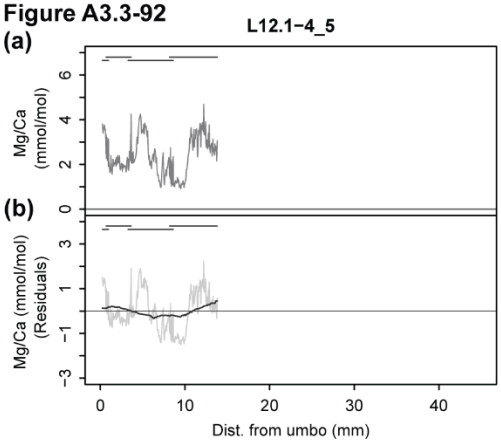

Figure A3.3-93

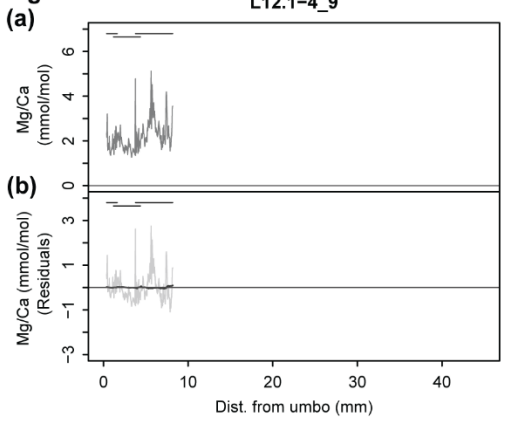

Figure A3.3-94

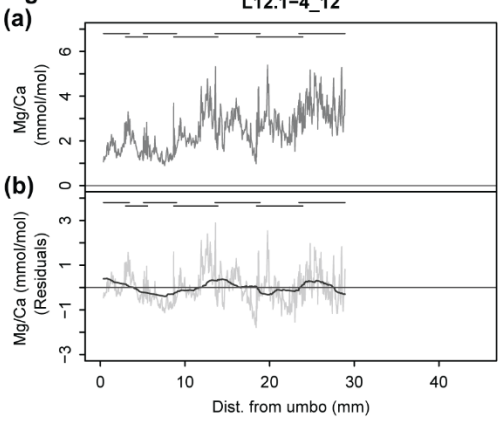

Figure A3.3-95

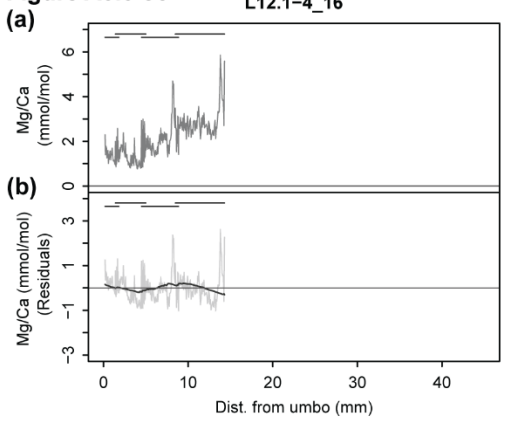

Figure A3.3-96

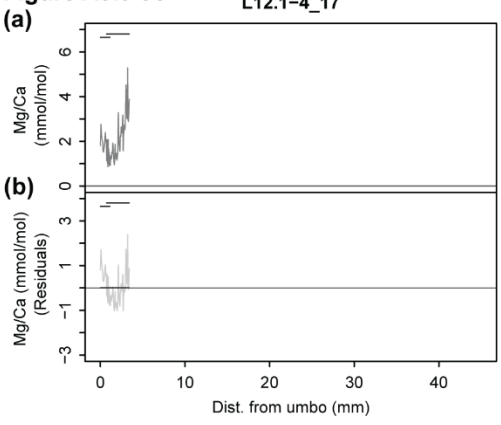

Oyster Mg/Ca profiles (continued) | Plots of Mg/Ca ratios with growth distance for oyster specimens included in our study. Each figure includes the (a) the raw Mg/Ca data in mmol/mol and (b) the detrended Mg/Ca profile with an adaptive running median plotted according to the method described in (Durham et al. in press). Overlapping horizontal lines at the top of each figure panel indicate the growth distance covered by each LA-ICP-MS line scan.

Figure A3.3-97

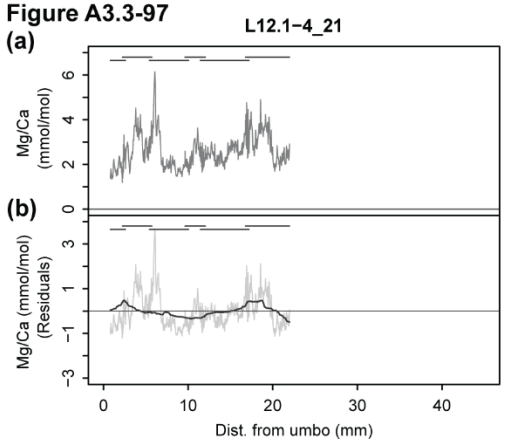

Figure A3.3-98

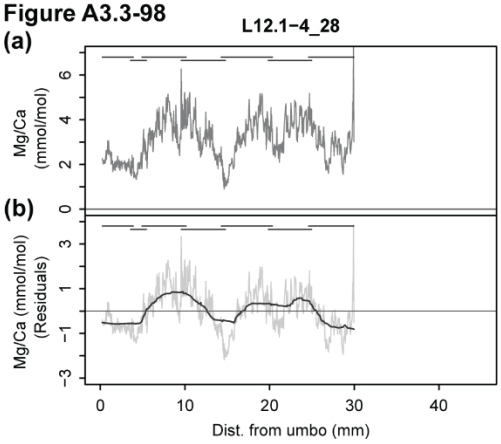

Figure A3.3-99

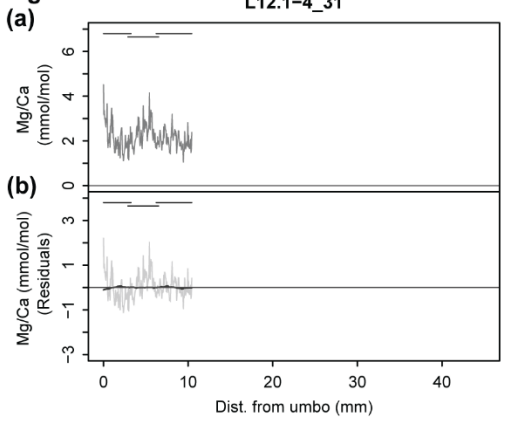

Figure A3.3-100

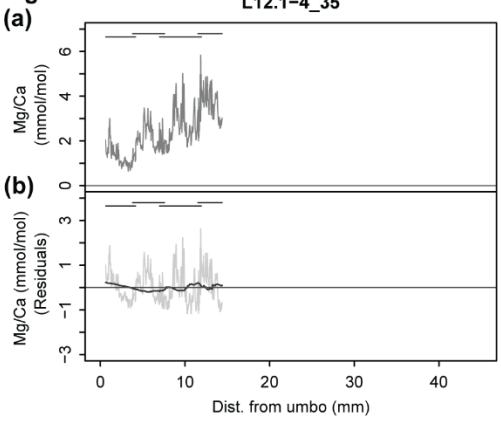

Figure A3.3-101

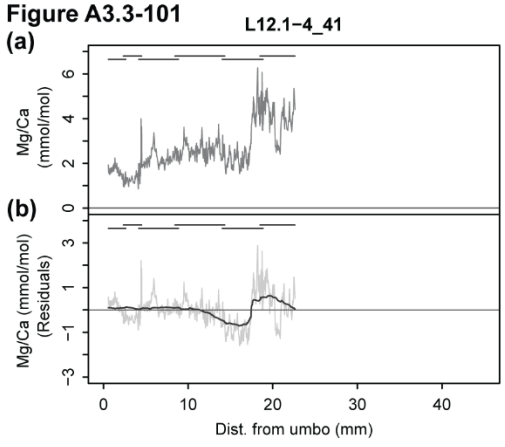

Figure A3.3-102

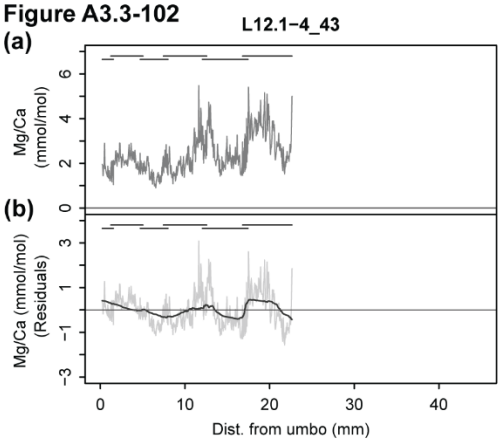

Oyster Mg/Ca profiles (continued) | Plots of Mg/Ca ratios with growth distance for oyster specimens included in our study. Each figure includes the (a) the raw Mg/Ca data in mmol/mol and (b) the detrended Mg/Ca profile with an adaptive running median plotted according to the method described in (Durham et al. in press). Overlapping horizontal lines at the top of each figure panel indicate the growth distance covered by each LA-ICP-MS line scan.

Figure A3.3-103

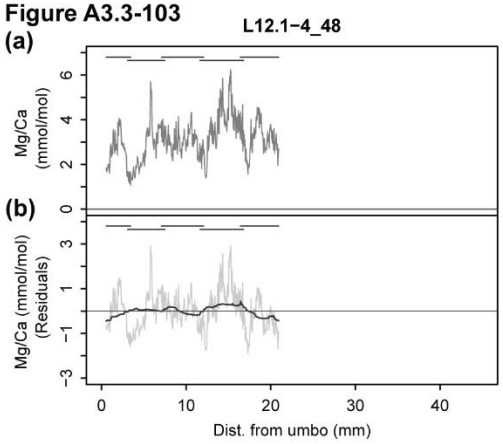

Figure A3.3-104

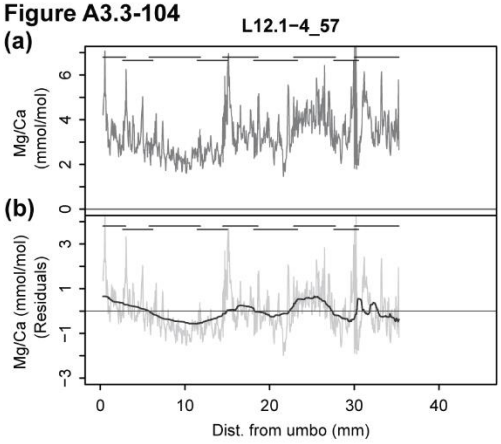

APPENDIX 3.4

A3.4.1 Addition of preliminary oyster lifespan data from Connecticut

If our conclusion that the variation in oyster lifespan with temperature through time fits the predictions of the metabolic theory of ecology (MTE) is accurate, we expect that adding lifespan estimates from oyster populations growing in different average temperature conditions (either alternative climates of the past or different latitudes in the present) should continue to fall within the MTE-predicted range of 0.2-1.2 as long as growth conditions remain similar except for temperature. To test this assertion we plotted estimated lifespans for three samples of live-collected oysters from an intertidal oyster reef in a tidal creek called Fence Creek in Madison, Connecticut (41°16'19.40"N, 72°35'10.80"W). The samples were collected from three different locations on the reef using the same 20cm x 20cm quadrat used to sample the oyster reefs in South Carolina. Lifespan estimates were made using the size-at-age relationship from the Mg/Ca profile in Figure A2.2-1 (Figure A3.4-1). A total of 151 specimens had lifespan estimates of at least 1 year (average ± SD = 2.19 ± 0.86 years). Connecticut coastal sea surface temperatures are approximately 1.5^{o}C cooler than the average for our South Carolina reefs (average annual temperature, including only months with average temperatures ≥10^{o}C, ± SD = 18.69 ± 4.78 ^{o}C, based on data for New Haven, Connecticut from the National Oceanic and Atmospheric Administration (NOAA) Coastal Water Temperature Guide: https://www.nodc.noaa.gov/dsdt/cwtg/all_meanT.html; Accessed 11/3/2016).

When the average lifespan of the Fence Creek oyster population was added to our plot of ln(lifespan) vs. inverse temperature (1/kT) for the fossil and modern South Carolina oysters, the slope was again within the MTE-predicted range of 0.2-1.2, whether the regression was performed using only the modern South Carolina values

(ln(lifespan) = 0.7834 * (1/kT) – 30.356; R^2 = 0.1045; p = 0.3126), the modern South Carolina and Pleistocene samples assuming the MIS5e paleotemperature difference (ln(lifespan) = 0.8393 * (1/kT) – 32.5725; R^2 = 0.2109; p = 0.1198), or the modern South Carolina and Pleistocene samples assuming the MIS9 paleotemperature difference (ln(lifespan) = 0.4404 * (1/kT) – 16.7699; R^2 = 0.1814; p = 0.1398), although as was the case with the South Carolina data alone, none of the regressions were statistically significant (Figure A3.4-2). This result is consistent with the interpretation that the lifespan differences between Pleistocene and modern oyster specimens can be explained by the MTE, but robust conclusions and confident interpretations of the regression model must await additional data.

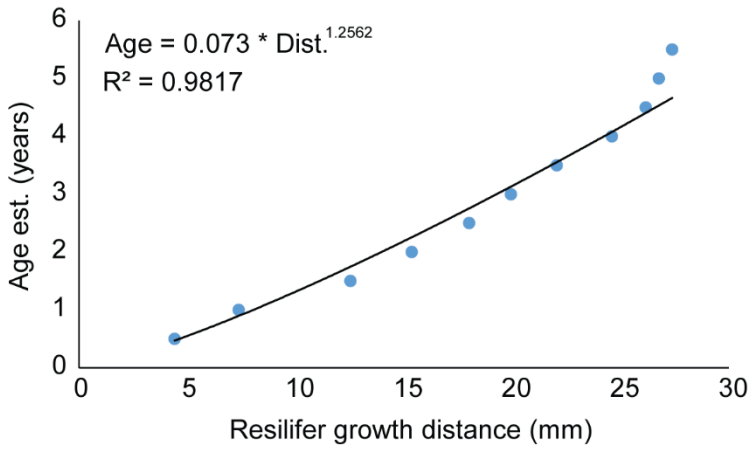

Figure A3.4-1 | Growth curve based on the Mg/Ca profile for specimen CT-L-01 from Chapter 2 (see Figure A2.2-1).

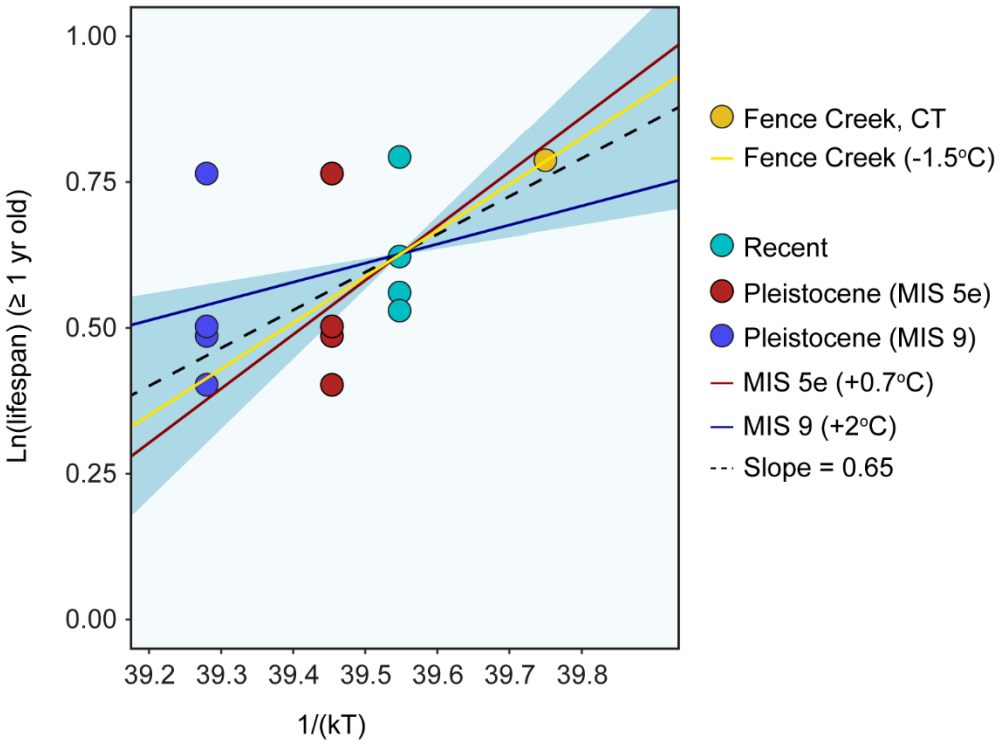

Figure A3.4-2 | Plot from Figure 3.2 of ln(lifespan) versus inverse temperature (1/kT, where k is Boltzmann's constant and T is temperature in Kelvin) updated to include the average lifespan estimate of live-collected oysters from Fence Creek in Madison, CT. The regression line shown for Fence Creek includes only the Recent South Carolina oyster samples, but regressions including the fossil data still fit the MTE-predicted range for both paleotemperature scenarios, though none of the regressions were significant (see text for details and regression equations).